E7.4-10.197
CR-136362

ERTS-1 VIRGIN ISLANDS EXPERIMENT 589

Determine Boundaries of ERTS and Aircraft Data within which Useful Water Quality Information Can Be Obtained

W. C. Coulbourn, Program Manager (Principal Investigator)
GRUMMAN ECOSYSTEMS CORPORATION
BETHPAGE, NEW YORK 11714

Dr. W. G. Egan, Co-Principal Investigator, Physicist
Grumman Aerospace Corporation

Dr. D. A. Olsen, Co-Principal Investigator, Biologist/Oceanographer
Marine Resources Development Foundation

G. B Heaslip, Data Manager
Grumman Data Systems Corporation

October, 1973
Final Report

Prepared for:

GODDARD SPACE FLIGHT CENTER
Greenbelt, Maryland 20771

ERTS-1 VIRGIN ISLANDS EXPERIMENT 589

Determine Boundaries of ERTS and Aircraft Data within which Useful Water Quality Information Can Be Obtained

W. C. Coulbourn, Program Manager (Principal Investigator)
GRUMMAN ECOSYSTEMS CORPORATION
BETHPAGE, NEW YORK 11714

Dr. W. G. Egan, Co-Principal Investigator, Physicist
Grumman Aerospace Corporation

Dr. D. A. Olsen, Co-Principal Investigator, Biologist/Oceanographer
Marine Resources Development Foundation

G. B Heaslip, Data Manager
Grumman Data Systems Corporation

E74-10197) ERTS-1 VIRGIN ISLANDS EXPERIMENT 589: DETERMINE BOUNDARIES OF ERTS AND AIRCRAFT DATA WITHIN WHICH (Grumman Ecosystems Corp., Bethpage, N.Y.) ~~255~~ p HC $14.75 CSCL 08H G3/13 — N74-15001 THRU N74-15005 Unclas 00197

247

October, 1973

Final Report

Prepared for:

GODDARD SPACE FLIGHT CENTER
Greenbelt, Maryland 20771

1. Report No. Final Report 2. Government Accession No. ---	3. Recipient's Catalog No.
4. Title and Subtitle: ERTS "A" Virgin Islands Experiment #589, Determine Boundaries of ERTS and Aircraft Data within which Useful Water Quality Information Can Be Obtained	5. Report Date October, 1973 6. Performing Organization Code: ---
7. Author(s): W. C. Coulbourn, Dr. W. G. Egan, G. Heaslip of Grumman, and Dr. A. Olsen of MRDF	8. Performing Organization Report No. ---
9. Performing Organization Name and Address: Grumman Ecosystems Corporation Bethpage, New York 11714	10. Work Unit No. --- 11. Contract or Grant No. NAS 5-21811
12. Sponsoring Agency Name and Address: Goddard Space Flight Center Greenbelt, Maryland 20771 Tech. Monitor: E. F. Szajna, Code 430	13. Type of Report and Period Covered: Final Report July 1972 - October 1973 14. Sponsoring Agency Code:

15. Supplementary Notes: Joint endeavor by W. C. Coulbourn, ________ Prog. Mgr. (P.I.), Grumman Ecosystems Corp.; Dr. W. G. Egan, Physicist Grumman Aerospace Corp.; Dr. D. A. Olsen, Bio/Oceanographer, Marine Resources Development Foundation; and G. B. Heaslip. Data Manager, Grumman Data Systems Corporation

16. Abstract:

The boundaries of application of ERTS and aircraft data are established for St. Thomas Harbor within which useful water quality information can be obtained. In situ physical, chemical and biological "water quality" and benthic data were collected. Moored current meters were employed. Optical measurements of solar irradiance, color test panel radiance and water absorption were taken. Procedures for correlating in situ optical, biological and chemical data with underflight aircraft I^2S data and ERTS-1 MSS scanner data are presented based on Grumman developed calibration techniques. Comparison of Bulk and Precision CCT computer print out data for this application is made, and a simple method for geometrically locating bulk data individual pixels based on land water interface is described. ERTS spacecraft data and I^2S aircraft imagery are correlated with optical in situ measurements of the harbor water, with the aircraft green photographic and ERTS-1 MSS-4 bands being the most useful. The biological pigments correlate inversely with the optical data for inshore areas and directly further seaward. Automated computer data processing facilitated analysis.

17. Key Words (Selected by Author(s)) Correlation spacecraft, aircraft and in situ data. Correlation water quality with water color. Expandable data base. Currents in harbor.	18. Distribution Statement ---

19. Security Classif. (of this report)	20. Security Classif. (of this page)	21. No. of Pages:	22. Price*
Unclassified	Unclassified		

PREFACE

OBJECTIVE

The primary objective of the ERTS-1 Virgin Islands Experiment, #589 was the determination of the boundaries of ERTS and aircraft data within which useful coastal zone water quality information could be obtained. A secondary objective was to provide an expandable water quality computer data base. This latter objective may become quite significant in the future by enabling scientists to measure the effect on the St. Thomas harbor waters of eliminating peak loads of approximately 3, 000, 000 gallons per day of raw sewage. (The primary sewage treatment plant is scheduled to come on line in the fall of 1973).

SCOPE OF WORK

- Calibrated color test panels, identifiable on the aircraft I^2S multiband photographic imagery were placed on Brewer's Bay Beach parking field. The parking field is composed of coral sand, has an area approximately 300 feet by 1200 feet and was detectable by the spacecraft MSS scanner. Ground optical photometric data were acquired of the color test panels and the coral sand. These measurements were recorded simultaneously with aircraft underflight passes and about one half hour preceding ERTS-1 pass. They enabled quantitative establishment of aircraft and ERTS-1 photometric levels. This accurate establishment of photometric levels provided the basis to precisely quantify the water radiance in relation to the biological and chemical parameters.

CONCLUSIONS

- Ground truth data is necessary to properly interpret ERTS-1 MSS Scanner Radiance Values, ie, to correlate turbidity with physical, chemical and biological water properties.
- There is a correlation between the optical in situ data, the aircraft I^2S green and red imagery and the ERTS-1 MSS band 4 and 5 data.

PRECEDING PAGE BLANK NOT FILMED

- The water characteristics of turbidity also correlate well with these data.
- Chlorophyll and carotenoid pigments inversely correlate with turbidity near the sewage effluent and directly correlate toward the seaward direction.
- Turbidity correlated inversely with benthic species diversity, furnishing an inferential tie between an easily sensed water quality variable and a sensitive indicator of average "water quality" conditions.
- Computer processing assisted in revealing correlation by calculating correlation matrices, performing factor analyses, producing graphical representations of data useful for first look analyses and producing print outs of MSS data for detail analysis of specific areas.
- Bulk CCT MSS, Band 4, computer print out quantum value contours of St. James Bay, St. Thomas match very closely the charted bathymetric contours where the bottom was visible, the water of uniform clarity, and depths approximately 30 feet or less. Bathymetric charting of coastal areas within these limitations appears to be a promising application of ERTS data.
- The need for high radiometric fidelity dictated the use of bulk rather than precision data. Further the necessity of accurately locating (within 2 pixels) the MSS data precluded the use of MSS imagery for this experiment.
- Bulk CCT print outs can be utilized in coastal zone investigations rather than precision data, even for those objectives requiring high positional accuracy, by constructing a grid scaled to match the computer print out to the reference chart being used. MSS band-7 delineated the land-water interface boundary used in constructing the grid.
- Registration of the 4 MSS spectral bands to each other was within one pixel as shown by comparing ERTS-1 bulk print outs with the aircraft I^2S imagery of the test site.
- The geographical location accuracy of the ERTS-1 bulk CCT data is ± 1 pixel (i.e. ± 80 m along the track and ± 57 M across the track) for the St. Thomas Harbor Area based upon initial area location using the scaled grid. The aircraft photographic I^2S resolution is about one foot. The optical in situ measurements have an accuracy of about ± 10%. The photometric resolution of the I^2S imagery is about 1% and the absolute accuracy is about 10% whereas, the photometric relative resolution of ERTS-1 MSS scanner, from NASA Data Users Handbook, is ± 1 digital level equivalent to about 1.5% based on the range of 63 levels.

- For the Virgin Islands area Band 4 radiances ranged from quantum levels of 20 to 30 for water to 80 to 90 for dry beach sand. To uniquely interpret the computer print out each character must designate a specific quantum value, not 2 values -- one high and one low as in the present system. (As an alternative we made a second print out which left blank all pixels in the high range; i.e. above the 53 quantum level - total range of 127).

RECOMMENDATIONS

We recommend our present program approach which, combines in situ optical, biological and chemical monitoring with similar calibrated aircraft I^2S and ERTS imagery to conduct the following:

- Large scale surveys of Northern Industrial Coastal areas for establishment of limits of utilization of ERTS-1 and aircraft for monitoring water quality in areas much more turbid than Carribean waters; in many areas certain industrial wastes darken the water, which effect is opposite to the brightening of St. Thomas harbor waters due to domestic wastes.
- Investigation of visible sea bottom bathymetry.

For future programs we suggest improvement in the following areas:

- Adapt rigid specifications to control the Kodak Versamat during processing of the film and prints; i.e., stability of illuminating lamp, constancy of developer strength and uniformity of contact pressure of negative on print during exposure.
- Conduct, on location, the biological and chemical measurements and analysis of water samples
- More detailed in situ optical measurements to establish the water spectral characteristics of the area of interest
- Operable internal calibration of ERTS sensors
- More digital radiance levels in high gain mode; i.e., increased relative resolution for darker areas, (water)
- Increase spectral resolution to detect discrete water characteristics; i.e., chlorophyll 645 and 665 nanometer bands, carotenoids 480 and 510 nanometer bands and others as appropriate.

- Incorporate capability to insert, by ground command, the filters required to obtain radiance data in specific spectral bands selected for the particular water or other target characteristics anticipated.
- Polarimetric capability should be incorporated in future ERTS sensor to increase the optical information acquisition in each spectral band.
- Thermal sensing capability would be desirable for detecting different water masses based on temperature differences.
- For coastal zone application retain MSS Band 7 for land water interface boundary determination.

TABLE OF CONTENTS

TABLE OF CONTENTS (Continued)

TABLE OF CONTENTS (Continued)

TABLE OF CONTENTS (Continued)

LIST OF ILLUSTRATIONS

LIST OF ILLUSTRATIONS (Continued)

LIST OF ILLUSTRATIONS (Continued)

LIST OF ILLUSTRATIONS (Continued)

LIST OF ILLUSTRATIONS (Continued)

LIST OF ILLUSTRATIONS (Continued)

LIST OF TABLES

LIST OF TABLES (Continued)

N74-15002

SECTION I

SUMMARY OF
ERTS-1 VIRGIN ISLANDS EXPERIMENT #589

1.0 INTRODUCTION

This final report on the ERTS-1 Experiment, #589 is divided into four sections as follows:

Section I is a summary of the entire program which is intended to provide the reader with a grasp of the experiment, the various procedures employed and the results obtained. It also refers the reader to various parts of the report where additional detail information will be found enabling the reader to delve more deeply into those particular aspects of interest.

Section II, prepared by Dr. W. G. Egan, Research Department, Grumman Aerospace Corporation describes the procedures used in the acquisition analysis and correlation of satellite, aircraft, surface and in situ optical data. The format of this section is that of an independent report in order to maintain the integrity of authorship.

Section III prepared by D.A. Olsen of Marine Resources Development Foundation describes the water quality parameters of the test site, the biological, chemical and physical water data acquisition program, and initial correlation of these data. The format of this section is also that of an independent report in order to maintain integrity of authorship.

Section IV, Data Processing prepared by Mr. G. Heaslip, Grumman Data Systems Corporation, describes the procedures used to log the data, the format of the data bank, various data presentation methods, procedure for geographically locating pixel elements of CCT bulk print outs, and computation by computer of correlation matrices and rotated factor analyses. Grumman Data Systems Corporation accomplished the computer operations on the data and supplied correlation matrices and factor analysis results used by Dr. Egan in Section II.

1.1 DESCRIPTION OF THE TEST SITE

The St. Thomas harbors as a water quality test site are unique in that they provide nearly laboratory conditions on a macro scale. Within a small area of three miles by seven miles are found three distinct types of polluting effluents, so separated that their dispersion plumes are virtually independent of each other. With reference to the chart Figure 1-1:

- Raw sewage effluent: a peak of 3×10^6 gallons per day flows into Charlotte Amalie Harbor. Major outfalls are located at Long Bay near West Indian dock, Kings Wharf, Charlotte Amalie, and at the juncture of East and West Grecerie channels. Organic discharge of 154,000 gallons per day peak from a black strap molasses plant also occurs.
- Combined desalinization/power plant discharge into Lindbergh Bay:
  - Coolant water, 21,000 gallons per minute at $38^{\circ}C$
  - Brine, 2,000 gallons per minute at 70 parts per thousand
- Solid waste ocean dump and fill off the western tip of Truman Airport

To the south of the harbor entrances the island platform slopes from 60 feet to 150 feet in a distance of about 7 miles. It then drops abruptly to deep ocean, several thousand feet. The normal set of the ocean current is from the S.E. to N.W., thus providing a source of ocean water which slowly flushes the harbors. Tides generally vary from diurnal to semi-diurnal over a lunar period with a height range of 6 inches to 12 inches. On October 17, 1972, the predicted tidal range was 6 1/2 inches, peak current recorded was 0.5 kts, and average current speed of all readings of all current meter stations for the 24 hour period was 0.14 kts. Water mass movement is quite slow for these harbors.

1.2 OPERATIONAL PLAN

The program operational plan included acquisition of aircraft multiband photography, optical measurements on the ground of calibration test panels and coral sand, optical in situ measurements of the water, and biological, chemical and physical data of the harbor water. The aircraft photography and ground optical data facilitated correlation of ERTS-1 data with water in situ data and established the limits of utility of the aircraft data. The steps followed in data acquisition, analysis and in determining the degree of correlation are set forth in the Flow Diagram, Figure 1-2, which was formulated by Dr. W.G. Egan. The following explanatory notes refer to the operations listed on Figure 1-2:

- Measurements of the sun on the ground enabled determination of the amount of atmospheric attenuation and scattering that occurs between the satellite and the ground at the solar elevation in blue, green and red spectral bands.

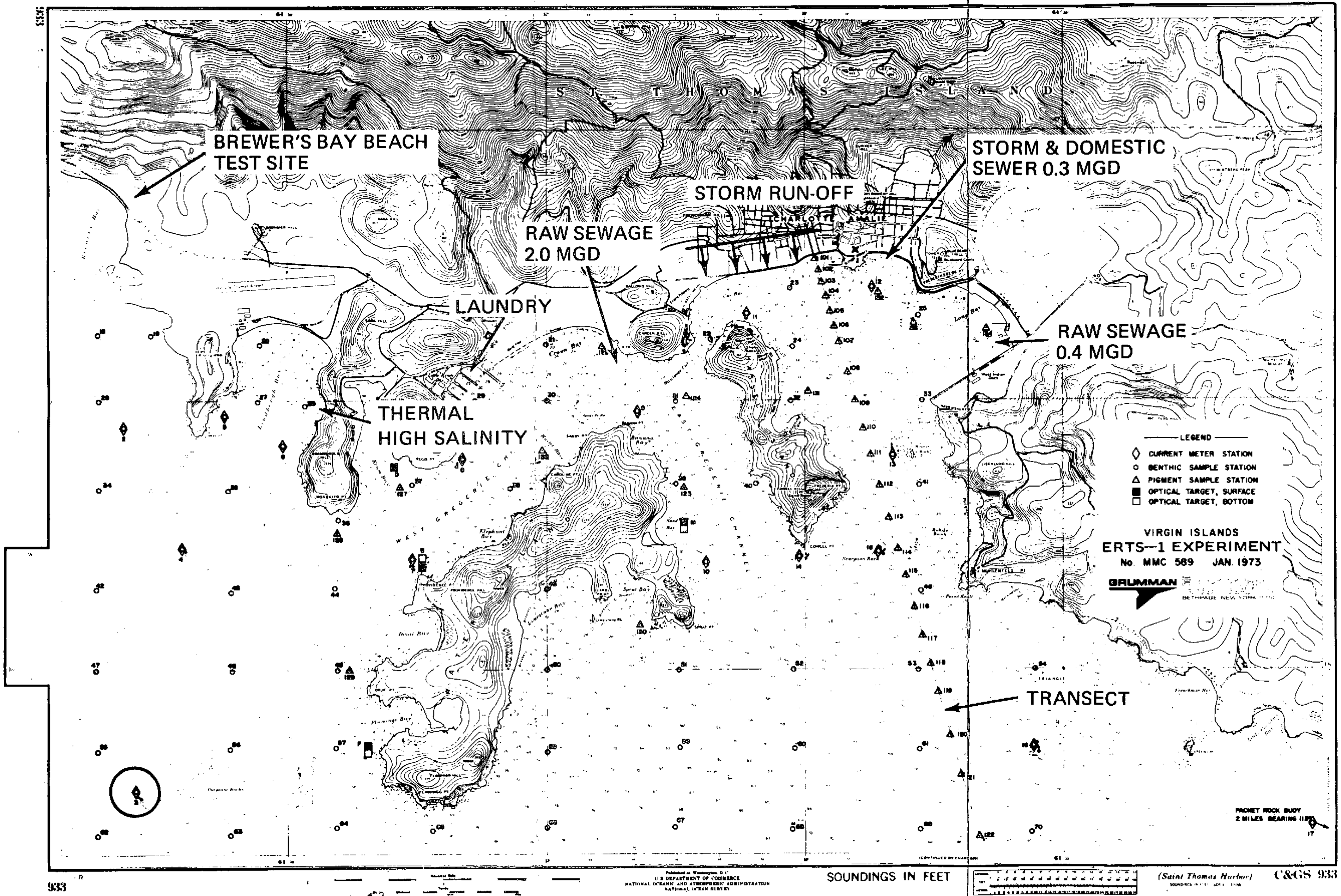

Figure 1-1. Chart of St. Thomas Harbor

FOLDOUT FRAME 1

FOLDOUT FRAME 2

- The Test Panel measurements on the ground gave the atmospheric filtration between the ground and the aircraft, when used in association with the aircraft imagery and permitted determination of true color in blue, green, and red of the St. Thomas Harbor water transect to the resolution of the aircraft imagery.

- The measurements on the ground, when used in association with ERTS-1 and aircraft imagery, permitted determination of true color of the St. Thomas water to the resolution of the ERTS-1 imagery in green and red spectral bands.

- The microdensitometry of three of the four (blue, green, and red) - I^2S images (the negatives) in association with the step wedge calibration of the film, and subtracting atmospheric effects, yields the true color as recorded by the aircraft of the St. Thomas Harbor water transects (and test panels) in blue, green, and red spectral bands.

- The use of the ERTS-1 tapes in association with Brewer's Bay beach coral sand measurements (and corrected by the sun measurements), and the MSS system response, yield the true color as recorded by ERTS-1 of the St. Thomas Harbor water transect.

- All ground color measurements are limited to blue (0.433 micrometers), green (0.533 micrometers) and red (0.633 micrometers) with filter band pass of approximately 0.02 μm. ERTS-1 MSS Band 4 (0.500 μm to 0.600 μm) and Band 5 (0.600 μm to 0.700 μm) were the most useful satellite spectral bands; hence, our major effort was concentrated in the corresponding green and red spectral bands.

For detailed discussion of the foregoing items of Figure 1-2 dealing with photometric data and analysis refer to Section II page 2-1 and subsequent pages.

- Harbor biological, chemical and physical data were acquired at a total of 95 sampling stations. These stations were located by Dr. D.A. Olsen based on a priori knowledge, in order to bracket the range of water conditions. These data were collected over a period of six weeks.

For detailed discussion of the methodology employed in selection of sampling sites and analysis of in situ water quality data refer to Section III page 3.2 and subsequent pages.

- Data handling, processing and computer analyses were accomplished under the direction of Mr. G.B. Heaslip, Grumman Data System Corp. The objective was to maximize the use of computers in both the presentation and analysis of the data.

1.3 DATA ACQUISITION

1.3.1 Spacecraft Data

ERTS-1 MSS data were acquired on October 17, 1972, scene #1086-14162 at 1016 a.m. local time. Figure 1-3 includes 9X enlargements of the 70 mm black and white imagery of the 4 MSS bands, 3X enlargement of the 9" x 9" color composite, and the original 70 mm MSS Band 5 scene. The acquisition of in situ data was tightly scheduled in order to match the time of the satellite passage as closely as possible. Figure 1-4 shows the chronology of data acquisition for October 17, 1972.

The harbor water data acquisition program extended over three satellite passes, October 10th to November 22nd, in order to improve chances of obtaining cloud free ERTS-1 data of the test site coincident with in situ data. (Historical weather data showed five days per month with cloud cover less than 0.3). ERTS-1 data of St. Thomas were not acquired on the preceding pass September 29th nor the two subsequent passes November 4th and 22nd.

1.3.2 Aircraft Data

Aircraft photography and thermal imagery were obtained in order to locate variances in color, turbidity, temperature, bottom features, etc. which should be detectable by the ERTS-1 satellite. (We understand the MSS might include a thermal band for subsequent ERTS spacecraft.) These data were acquired by a Kennedy Space Center/NASA team under the direction of Messrs. R. Withrow and J. O'Conner. Kennedy Space Center supplied the aircraft and remote sensing crew. Grumman Ecosystems supplied an I^2S camera, the Daedalus line scanner, and also designed and fabricated the bracketry required to install the Daedalus thermal line scanner into the aircraft, NASA 6. Maximum cooperation existed between KSC and Grumman personnel, which enabled acquisition of the remotely sensed aircraft data in a very efficient manner. The aircraft flew approximately 15 hours on station, collecting about 350 line miles of photography and a lesser amount of thermal IR imagery of particular sites. (This does not include flight time to and from Roosevelt Roads Naval Air Station for refueling and supplies.)

Four missions were scheduled to record conditions under four tidal phases; i.e., high tide slack water, ebb tide, low tide slack water and flood tide. The I^2S Multiband camera recorded in the following spectral bands Blue .410 - .470, Green .475 - .580, Red .590 - .690, Near IR .740 - .900 micrometers. The Daedalus Thermal IR scanner

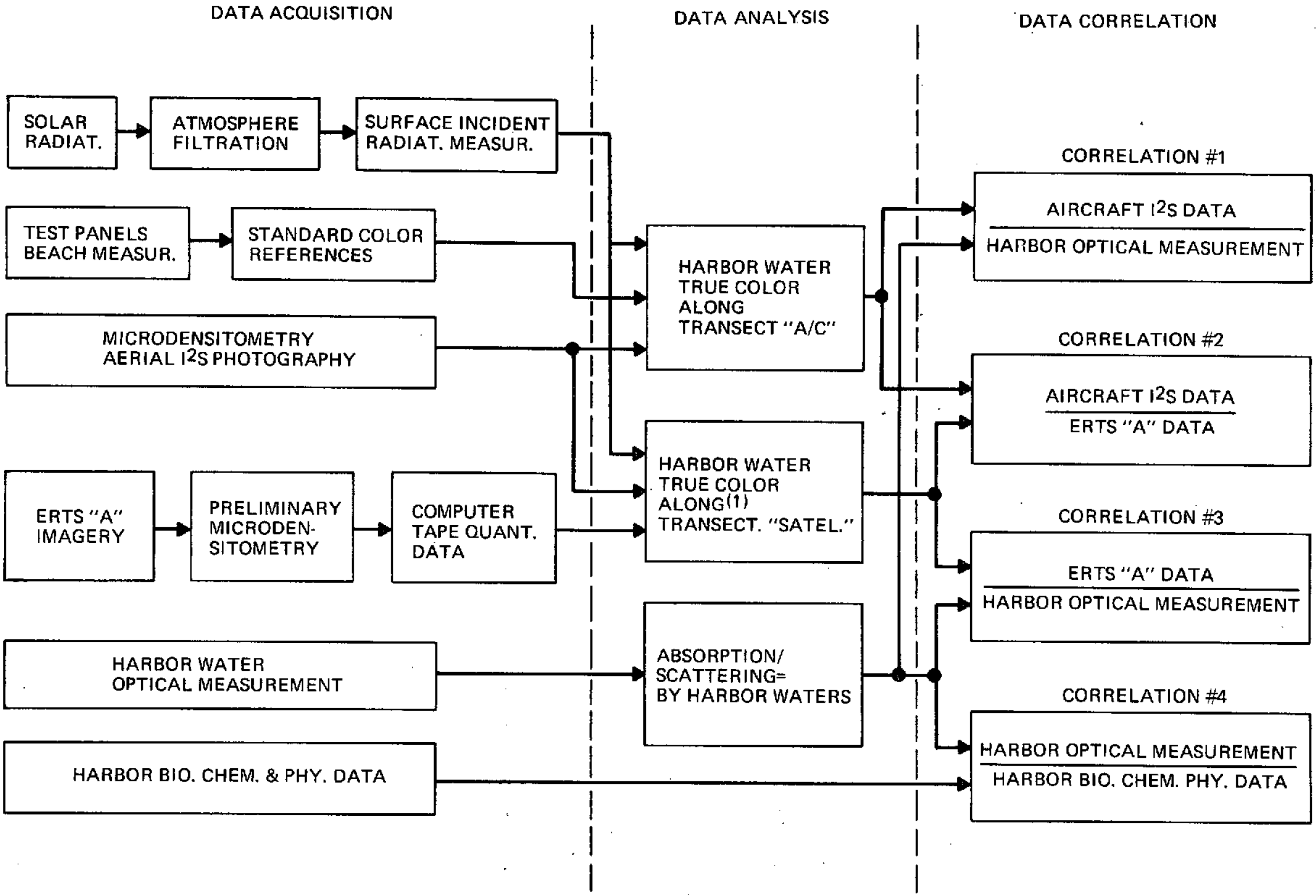

Figure 1-2. Data Acquisition, Analysis and Correlation Program Flow Diagram

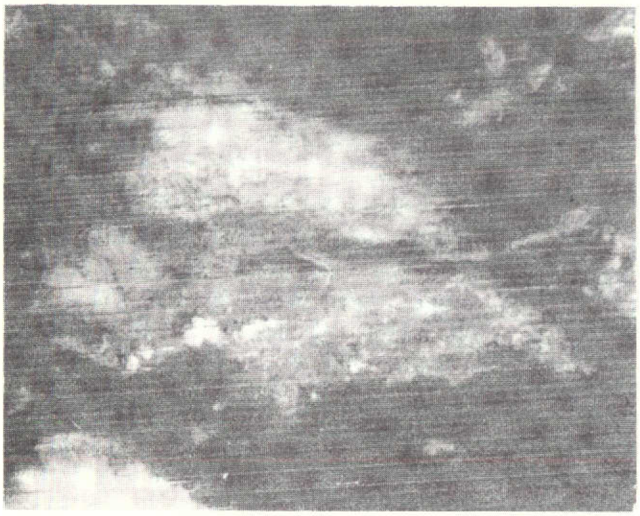

MSS-BAND 4

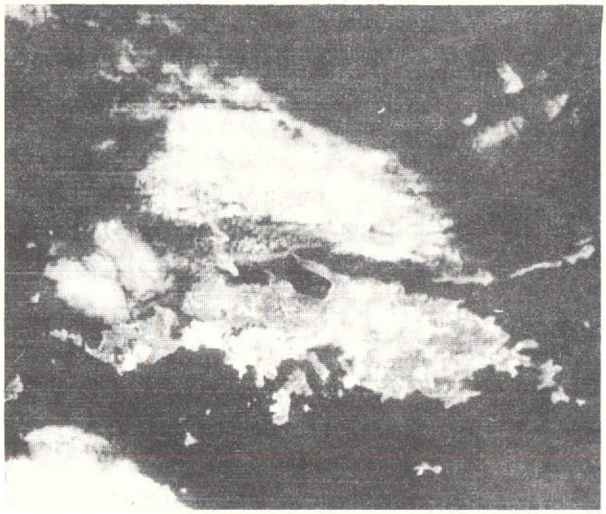

MSS-BAND 5

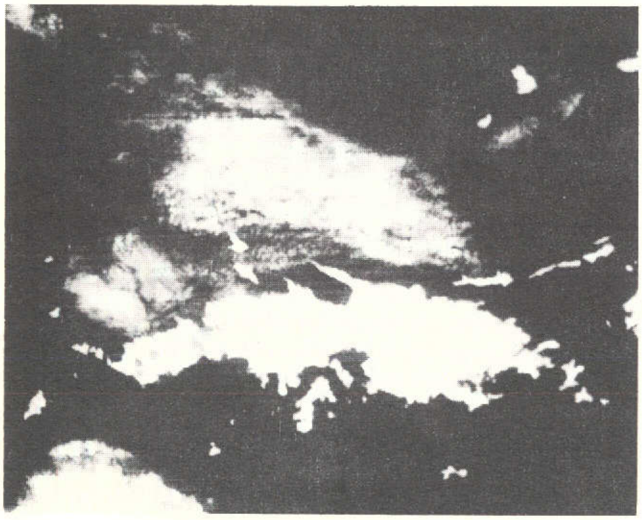

MSS-BAND 6

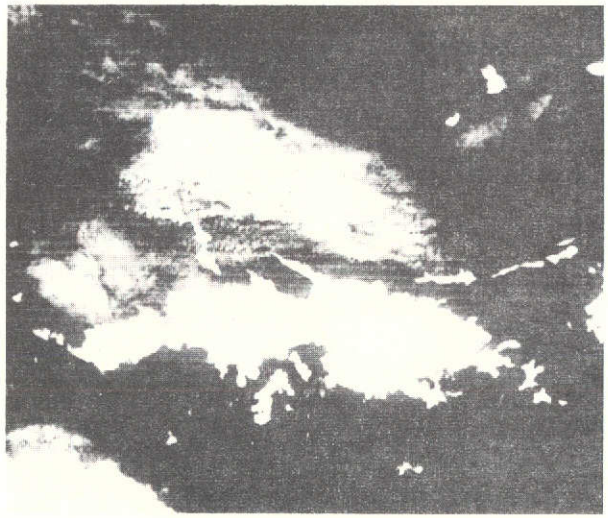

MSS-BAND 7

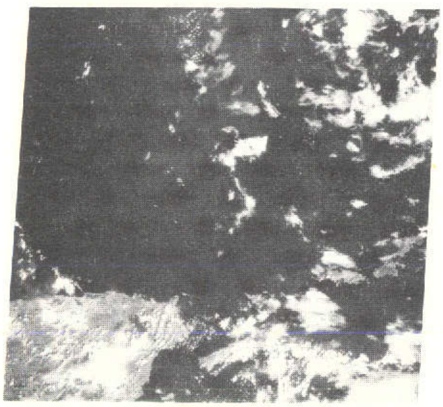

MSS-BAND 5
70MM CHIP

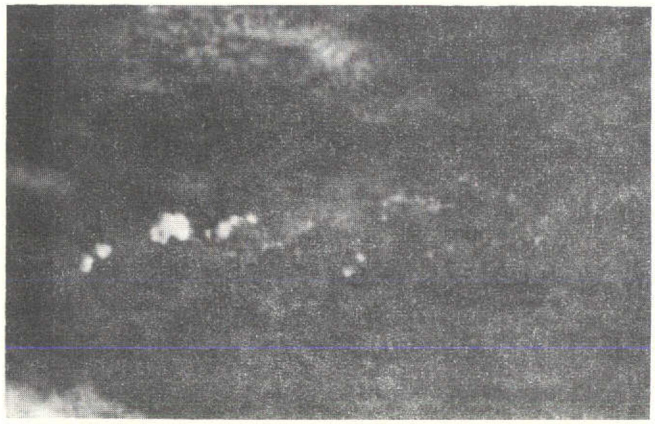

COLOR COMPOSITE

Figure 1-3. ERTS-1 Imagery of St. Thomas, Scene #1086-14162

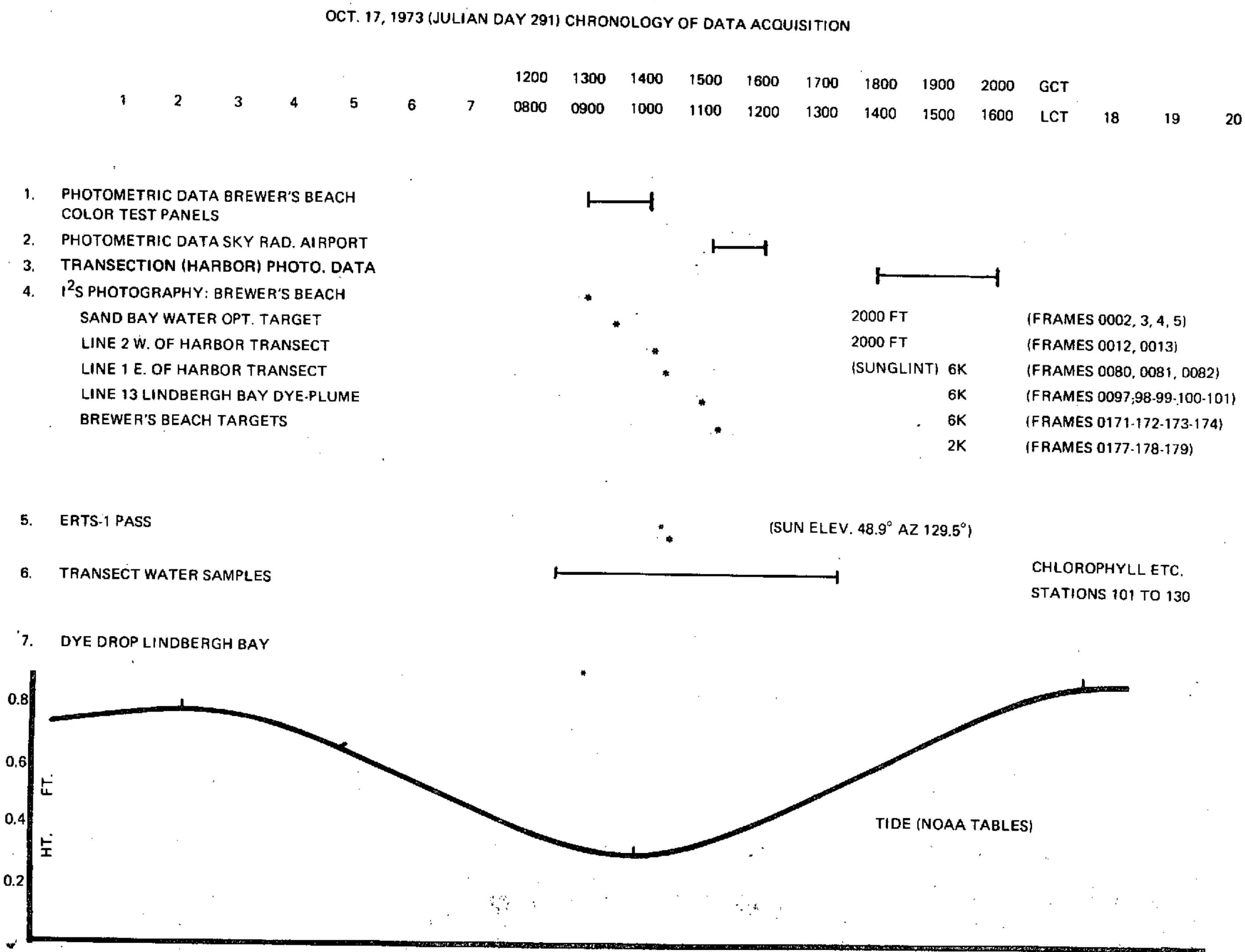

Figure 1-4. Oct. 17, 1972 (Julian Day 291) Chronology of Data Acquisition

(8.0 to 14.0 nanometers) was also used. A typical flight mission acquired data at 2000 feet altitude of the optical targets at Brewer's Bay Beach. A thermal run at 2000 feet was also made over Lindbergh Bay. The aircraft then climbed to 6000 feet altitude and flew the harbor flight lines operating both the multiband camera and the thermal line scanner. At completion of the 6000 feet altitude runs the aircraft again passed over the optical targets at 2000 feet to acquire calibration data. Kennedy Space Center in collaboration with Manned Space Center and Dr. Egan of Grumman processed the photography and supplied working positive transparencies to Grumman. Refer to Figures 1-5 and 1-6 for chart depicting flight lines.

1.3.3 Optical Photometric Data

Photometric measurements on the ground and in the harbor were acquired by Dr. W.G. Egan during ERTS-1 passage October 17, 1972 and as closely coincident thereto as was possible. These measurements involved: (1) In situ measurements of the harbor water at 7 optical stations located along the harbor transect line between biological stations 102 and 120, (2) Spectral reflectance measurements of color test panels on the ground and the coral beach sand at Brewer's Bay Beach, for use as a calibration standard for ERTS-1 and aircraft data. Refer to Figure 1-1 for location of the transect stations and Brewer's Bay Beach, north of the airport. Refer to Section II, page 2-2 and subsequent for detail discussion.

1.3.4 Biological, Chemical and Physical Water Quality Data

Biological, chemical and physical water quality data were obtained under the direction of Dr. David A. Olsen. A total of 95 stations were located about the harbor in order to bracket the water conditions. Weekly repetitive sampling was accomplished at seventeen (17) stations to obtain information on the variability of the water conditions. Current meters were also located at these 17 repetitive stations. Fort-four (44) stations were located in order to provide a geographical spread of data. These stations were sampled only once during the six-week program. Twenty-two stations were located along the transect extending from the inner harbor docks out the shipping channel a distance of approximately two miles. In situ optical data were acquired by Dr. Egan along this transect. Also, Dr. Olsen acquired pigment samples along the transect and also from 12 additional stations located to provide a geographical spread of pigment data. Diurnal variation in water quality parameters was studied at two stations (9 and 12) of the repetitive program.

Data were collected at the surface mid-depth and bottom. Benthic samples of the living matter were collected by divers. Refer to Section III, page 3.2 and subsequent for detailed discussion. Table 1-1 summarizes the harbor water quality data collected.

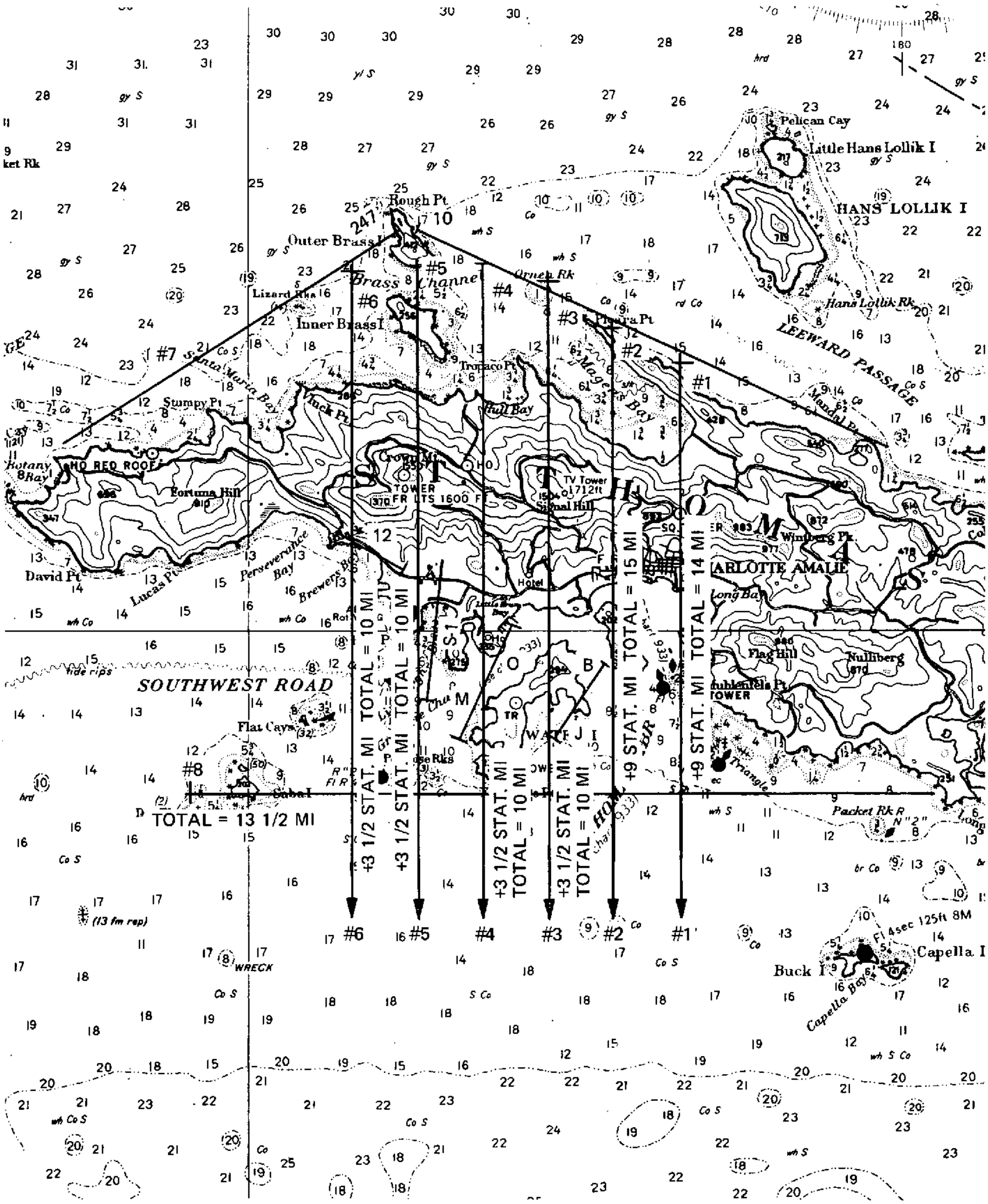

Figure 1-5. Charlotte Amalie Harbor Aircraft Flight Lines Flown by Kennedy Space Center/NASA

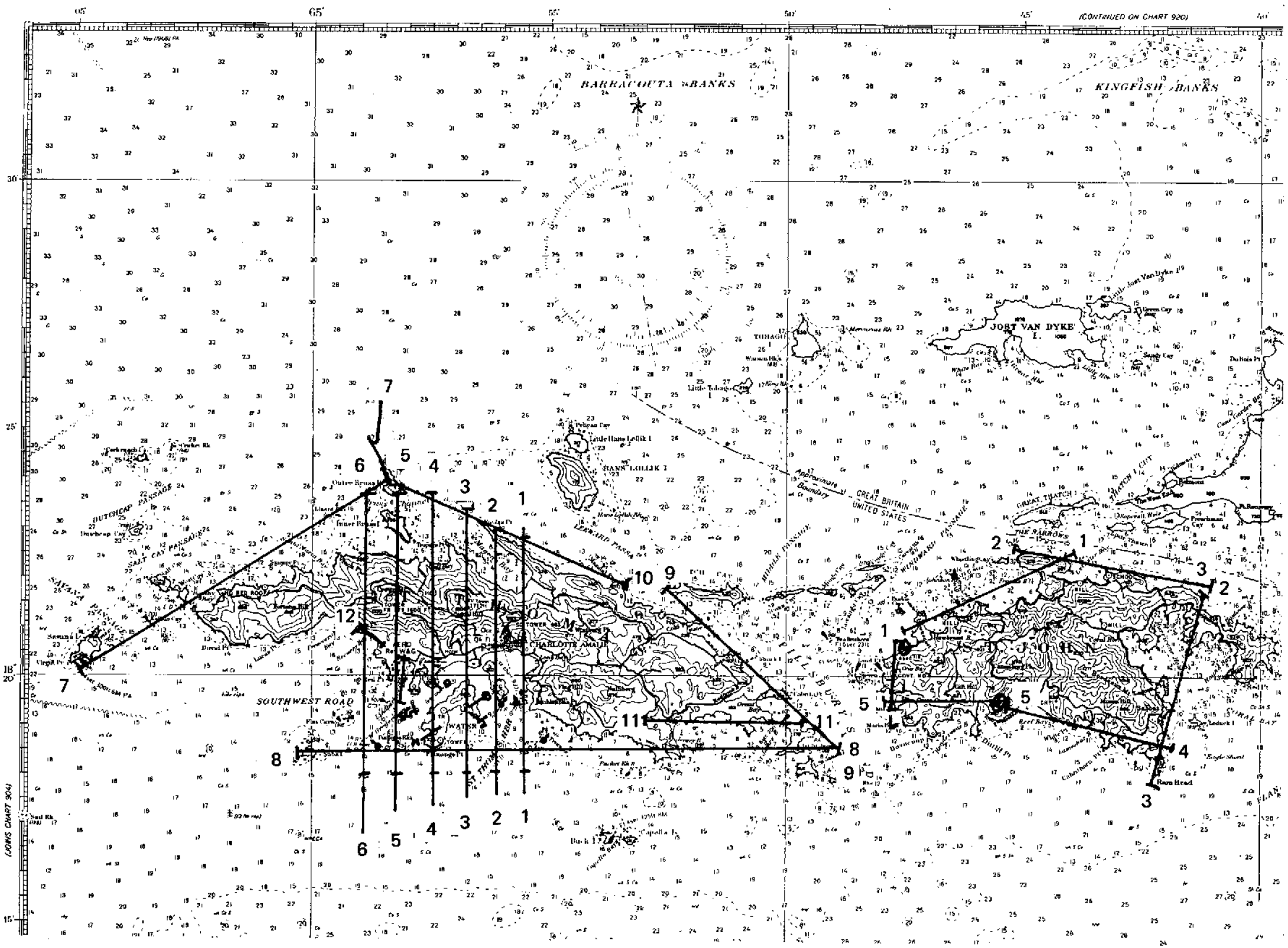

Figure 1-6. St. Thomas Flight Lines Flown by Kennedy Space Center/NASA Aircraft

Table 1-1. Summary of St. Thomas Ground Truth Data Acquisition

Parameter	Units	Depth	Max.	Min.	Average	Coef. of Variation (%)	# Samples
pH	-	5'	8.70	7.20	8.38	1.9	143
	-	mid	8.70	7.20	8.35	1.9	169
	-	bottom	8.70	7.20	8.34	1.8	163
Salinity	PPT	5'	37.00	34.30	35.12	1.0	181
	PPT	mid	37.00	34.30	35.15	1.2	209
	PPT	bottom	37.00	34.30	35.21	1.1	199
Conductivity	MHO/CM^2	5'	58.8	56.7	57.5	0.5	181
	MHO/CM^2	mid	58.8	56.7	57.5	0.5	209
	MHO/CM^2	bottom	58.8	56.7	57.5	0.5	205
Dissolved O_2	PPM	5'	7.95	5.00	6.60	8.4	182
	PPM	mid	7.95	5.00	6.56	8.2	186
	PPM	bottom	7.95	5.00	6.45	9.5	181
Depth	feet	-	78	7	35.3	46.9	205
Temperature	Deg. C	5'	29.80	29.0	28.70	1.3	181
	Deg. C	mid	29.80	27.0	28.64	1.1	209
	Deg. C	bottom	29.80	27.0	28.59	1.1	199
Turbidity	F.T.U.	5'	3.58	.12	.94	83.8	181
	F.T.U.	mid	3.58	.12	.85	90.8	209
	F.T.U.	bottom	3.58	.12	.96	89.5	199
Secchi Avg.	feet	- multiple	54.2	7.	25.	52.8	153

Table 1-1. Summary of St. Thomas Ground Truth Data Acquisition (Continued)

Parameter	Units	Depth	Max.	Min.	Average	Coef. of Variation (%)	# Samples
Extinction Coef.	1/CM	5'	12.95	1.03	3.55	78.0	153
Pigments							
Chlorophyll A	Mg/M^3	5'	11.81	0	2.28	104.4	125
Chlorophyll B		5'	9.41	0	1.71	123.5	125
Chlorophyll C		5'	26.62	0	4.94	122.8	125
Astacin Carotinoids		5'	5.96	0	1.12	121.2	125
Non Astacin Carotinoids		5'	10.94	0	2.34	100.5	125
Current Speed	Knots	5'	1.00	.10	.30	51.1	137
	Knots	mid	1.00	.10	.26	57.4	155
	Knots	bottom	1.00	.10	.26	57.4	136
Current Dir.	Deg/10	5'	39.50	1.00	21.51	42.3	148
	Deg/10	mid	39.50	1.00	22.41	38.0	164
	Deg/10	bottom	39.50	1.00	21.25	42.2	142
Plankton Dens.	CC/MTR^3	-	.353	.009	.102	70.9	
Diversity	NITS	-	2.56	.00	.96	79.5	69

1.3.5 Current Meters

Seventeen (17) current meters were emplaced, see Figure 1-7 for location. One was lost and the data from three were questionable either due to direction or speed records. Data were acquired over a period of six weeks. These data were obtained to establish the water mass movement relationship with tide and wind, and to provide a basis for comparing satellite data with in situ data acquired during a similar tidal phase but on a different date. This capability was incorporated into the program primarily for insurance against the eventuality that the ERTS-1 data of St. Thomas might not be free of clouds over the test site. ERTS-1 data were available only for October 17, 1972. Our ground and water data acquisition schedule bracketed this date satisfactorily.

Schedule and funds did not permit reducing the current meter data for the entire period, nor was this necessary inasmuch as the ERTS-1 October 17, 1972 pass was successful. However, data were analyzed for October 16, 17, and 18, Figures 1-8, 1-9 and 1-10. It is seen that the current set is from Southeast to Northwest and speeds are very low. The predicted tide tables (ref. National Ocean Surveys, NOAA) gave a maximum tidal range of about 1 foot, although during our period of data acquisition the predicted tidal range was less than 7 inches. The wind was usually from the East or Southeast with a gentle force of about 6.0 mph, see Figure 1-11. Partial reduction of the current meter and wind data substantiated our visual observations that the harbor waters are quite sluggish, and also that comparing data acquired on different dates during similar tidal phases was a reasonable procedure.

1.3.6 Rhodamine Dye Release

Rhodamine dye was released in Lindbergh Bay beginning at 0830, October 17, 1972 (1 hr. 45 min. prior to ERTS-1 pass). The dye plume was clearly defined on the I^2S photography which was acquired shortly after ERTS-1 pass at 1016. The plume covered an area about 300 feet in a north-south direction and 80 feet east-west direction. This area equates to four ERTS-1 MSS computer print out pixels along the ERTS-1 flight path and 1-1/2 pixels across the flight path. The area was too small to be identified with certainty on the ERTS-1 data print outs. Use of ERTS data, but not to the exclusion of aircraft imagery, is suggested for applications where large area studies are involved and ERTS synoptic imagery would facilitate understanding water mass movements. Of course, this application is not limited to recording dye plumes, but includes recording water masses with distinguishable differences in turbidity.

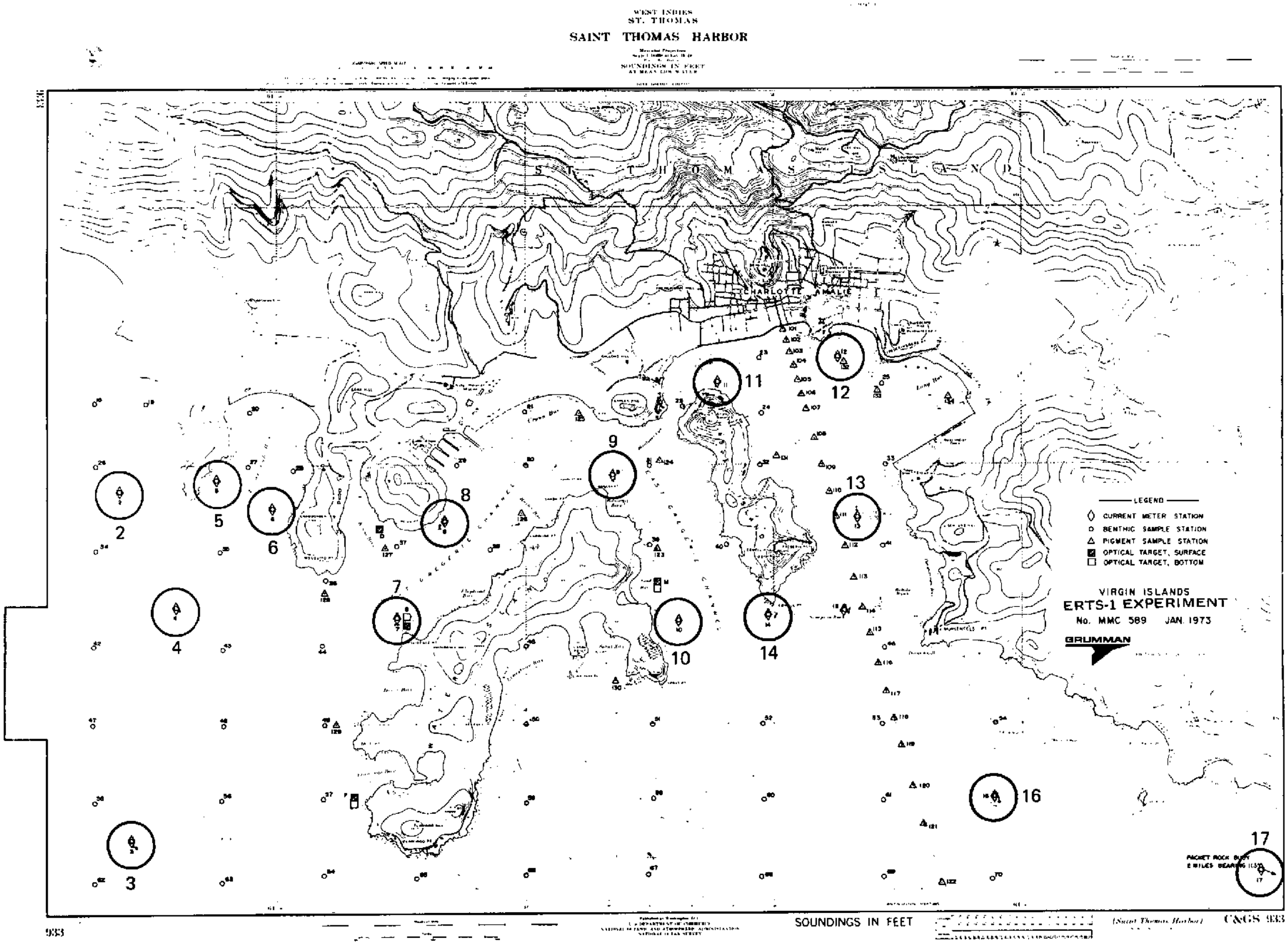

Figure 1-7. Location of Current Meter Stations

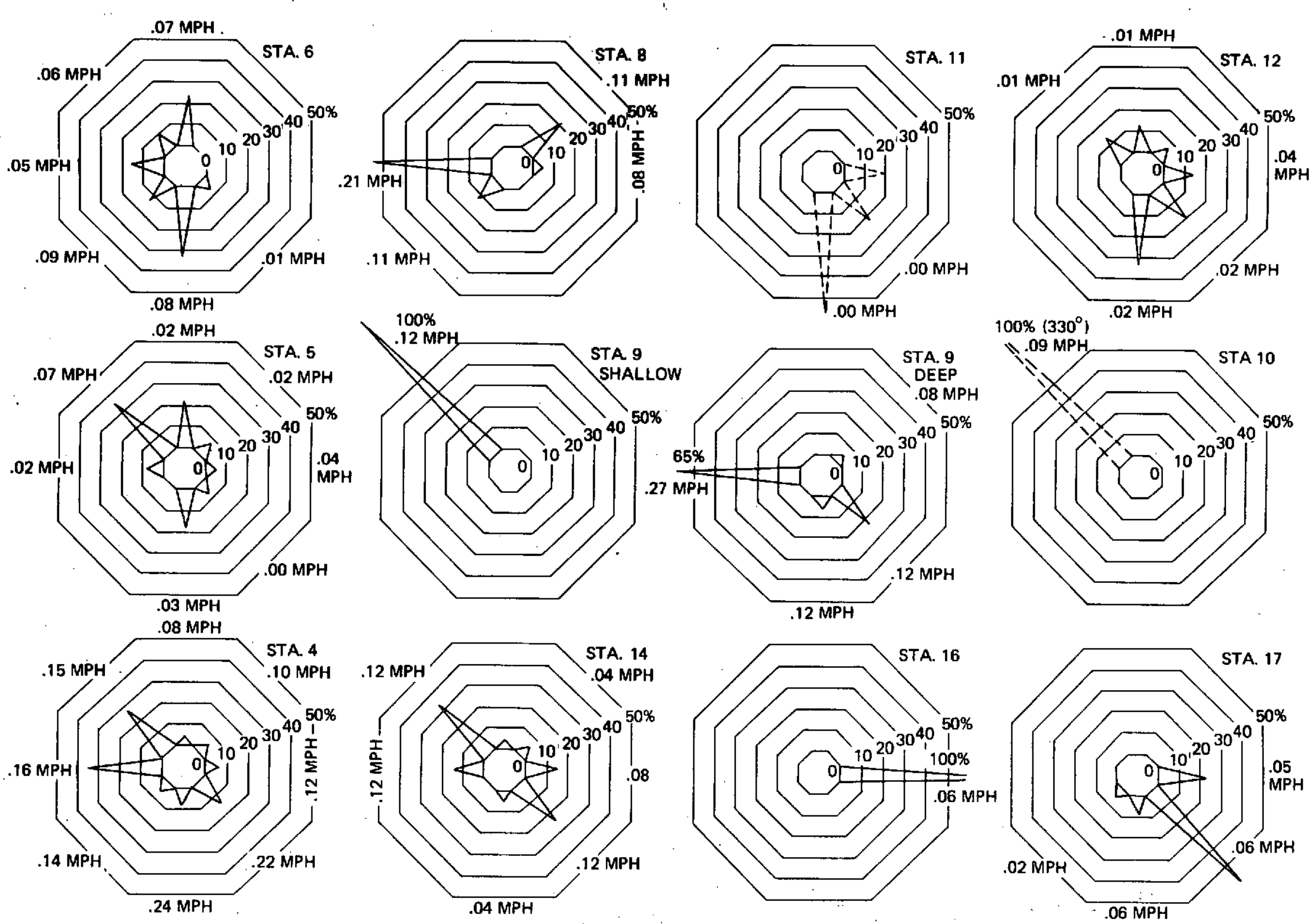

CURRENT DIRECTION – FREQUENCY OF OCCURRENCE
CURRENT VELOCITY – AVERAGED FOR EACH SECTOR
REFER TO FIGURE 1 FOR STATION LOCATION

Figure 1-8. St. Thomas Harbor Currents, Oct. 16, 1972

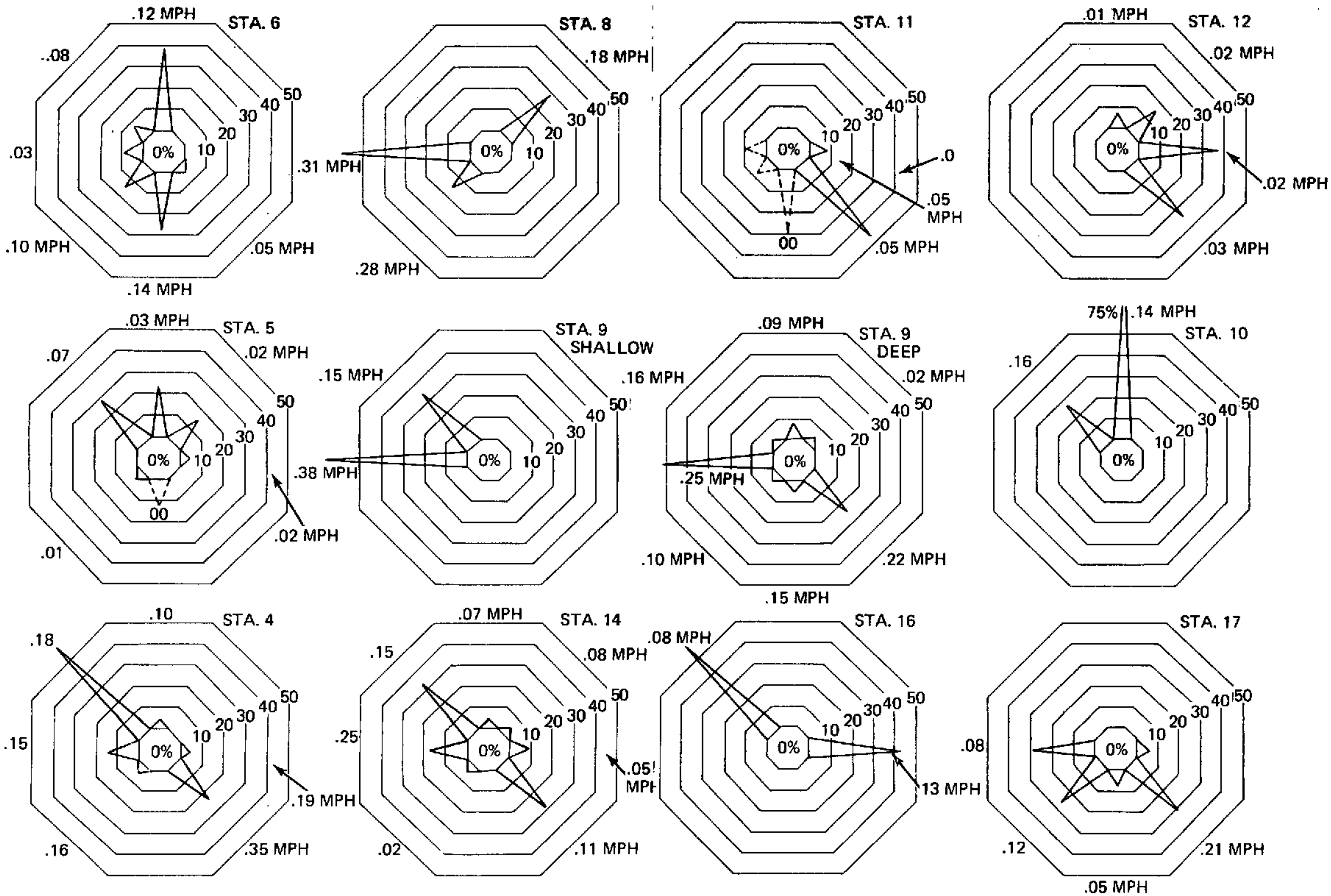

CURRENT DIRECTION – FREQUENCY OF OCCURRENCE
CURRENT VELOCITY – AVERAGED FOR EACH SECTOR
REFER TO FIGURE 1 FOR STATION LOCATION

Figure 1-9. St. Thomas Harbor Currents, October 17, 1972

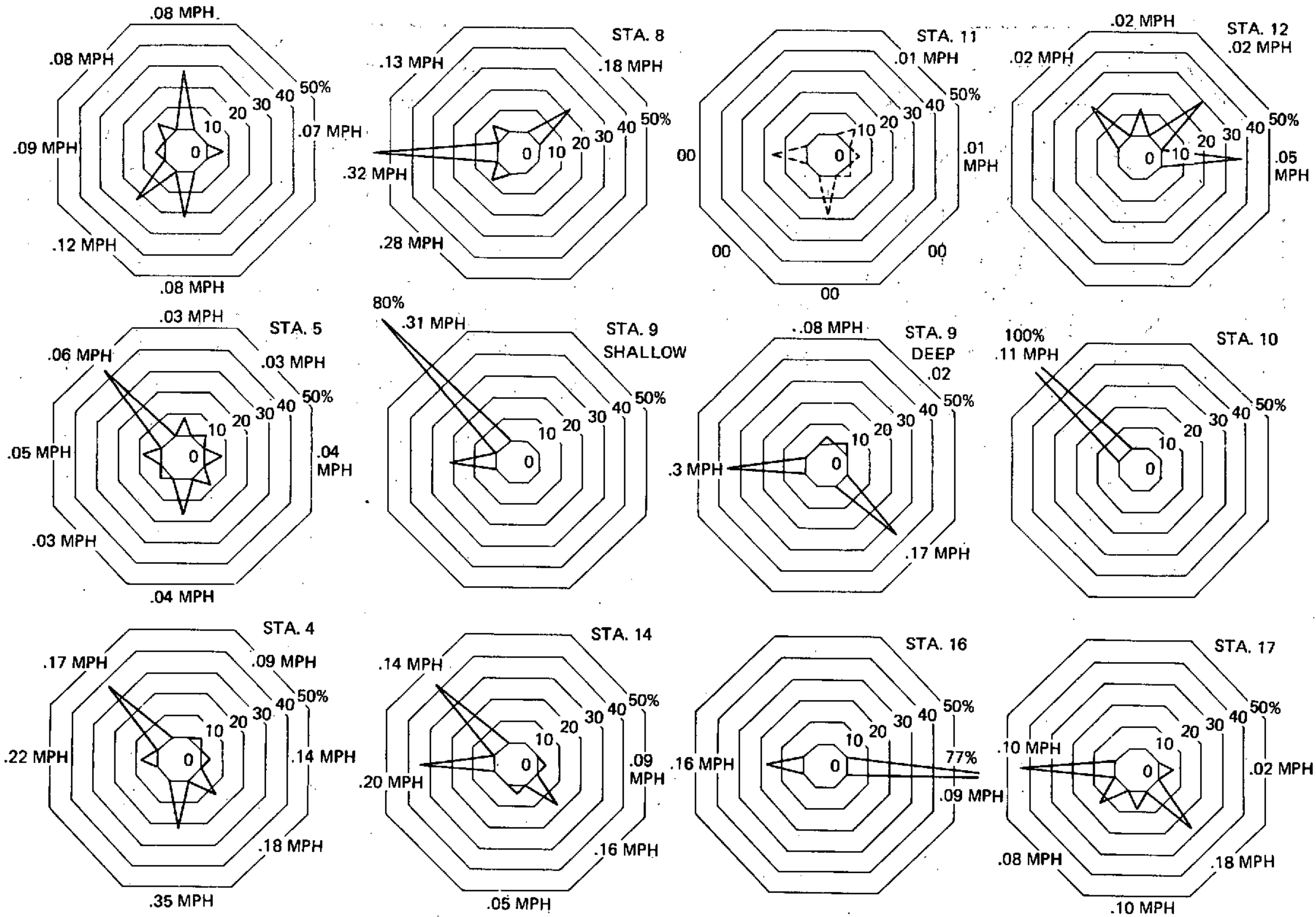

CURRENT DIRECTION – FREQUENCY OF OCCURRENCE
CURRENT VELOCITY – AVERAGED FOR EACH SECTOR
REFER TO FIGURE 1 FOR STATION LOCATION

Figure 1-10. St. Thomas Harbor Currents, Oct. 18, 1972

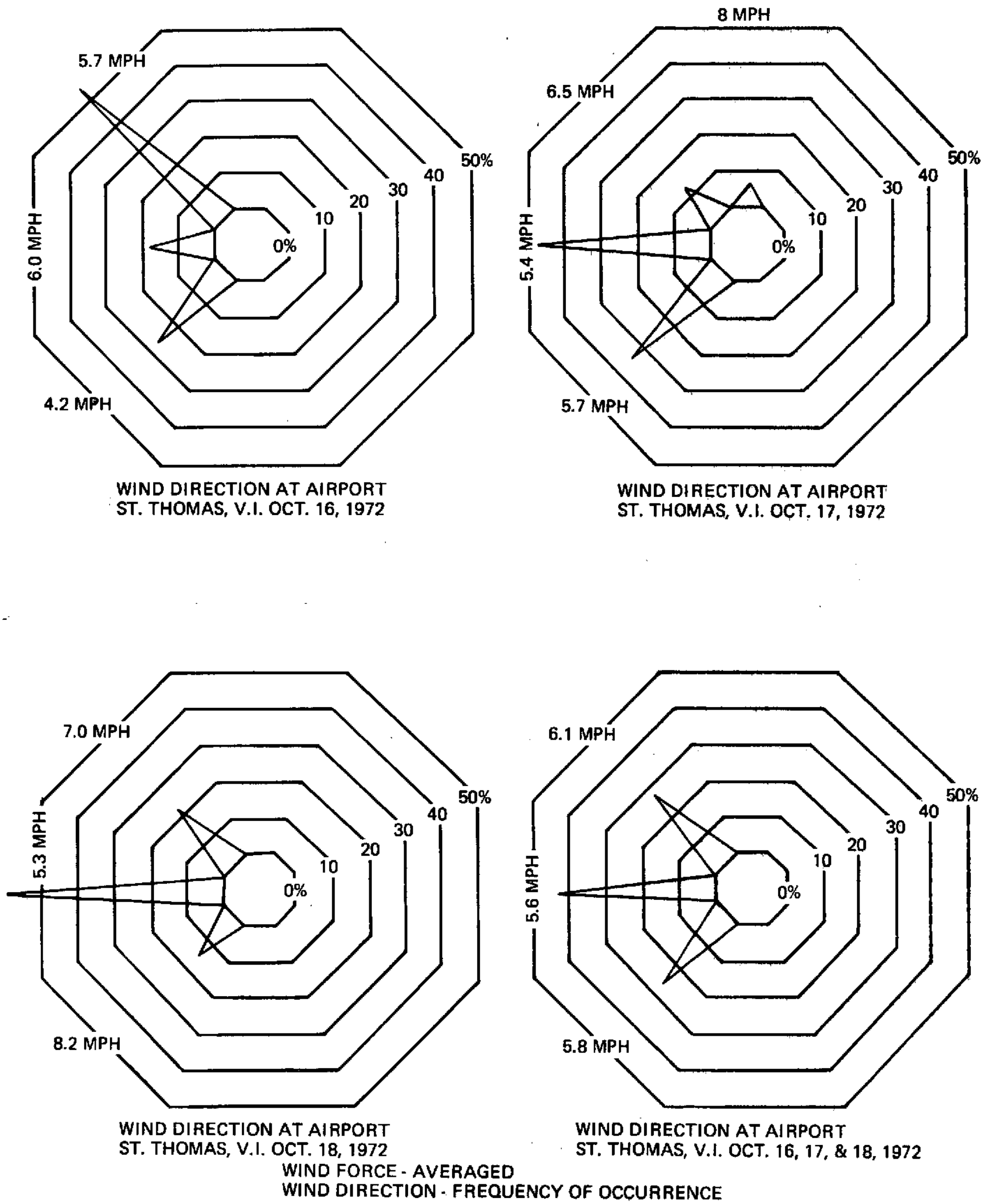

Figure 1-11. St. Thomas Airport Tower Wind Plots, Oct. 16, 17, 18, 1972

1.4 DATA PROCESSING

1.4.1 Summary of Data Products

Data processing procedures were developed under the direction of Mr. G. Heaslip, Grumman Data Systems Corporation. Computer print-out in four formats of all data by stations (refer to page 4-2) constitutes the expandable data bank which pertain to the status of the harbor waters of St. Thomas, as of the fall of 1972. This data bank should be useful as a baseline for future investigations. Computer base maps were designed where each computer line printer character represented a one-second latitude cell by one-second longitude cell, and provided a means of accurately displaying ERTS-1 precision data as well as in situ data. Computer maps were generated using scaled shaded circles, in lieu of numeric values, for use in first look analysis of data. Level slicing of aircraft thermal IR data, time-history charts, current meter plots, etc. were also provided. Refer to Section IV, page 4-3 and subsequent pages for detailed description of these data products.

1.4.2 Geographical Location of Bulk CCT Computer Print-Out Pixels

Goddard Space Flight Center/NASA supplied imagery of scene #1086-14162 all bands in 70 mm bulk black and white, 9 x 9 bulk black and white positive prints, 9 x 9 color composite (4, 5, 7), 9 x 9 precision black and white positive transparencies and both bulk and precision CCTs. The scale of the enlarged 9 x 9 imagery is approximately 1 to 1 million. The problem of locating a sampling station on such imagery (Figure 1-3), within 80 meters (one CCT print-out pixel) is very difficult. This combined with loss in photometric and radiometric fidelity, spatial resolution and non linearities resulting from conversion of digital data to imagery, dictated the necessity of working with the CCT data. We developed a program for computer print-out of the precision CCT data pixels corresponding to each of the sampling stations. Preliminary evaluation of the precision print-out values indicated the desirability of using the bulk CCT data tapes for their greater radiometric accuracy. A program was written to print out the bulk tapes and the geographical accuracy problem (location of the pixels on a harbor chart) was solved as follows: The direction of satellite track, approximately 191° true, was plotted on a chart of the St. Thomas harbor. Prominent points of land-water boundaries on the chart were selected and located on the MSS Band 7 print-out at a convenient distance apart both along track and across track. (Band 7 was best for land-water delineation.) The number of MSS scan lines between the two points for across track and a second two points for along track compared with the distance measured on the chart determined the scale of the scan lines and consequently the grid layout. The grid overlay scan lines were numbered to match the corresponding computer CCT print outs.

Each pixel of Band 7 could then be accurately located on the chart to within the original land-water interface determination (instrumentation non linearities are assumed to be negligible). We believe this positional accuracy is within 1 pixel for the St. Thomas harbor area. Refer to Figure 1-12.

1.4.3 Cloud and Cloud Shadow Boundaries

The chart overlay grid (Figure 1-12) was essential in accurately establishing boundaries of clouds and cloud shadows in the test area. With reference to (Figure 1-13), ERTS-1 MSS quantum values were contoured for highest pixel grouping (clouds) and lowest grouping (cloud shadows). For confirmation the sun's azimuth was computed and laid on the computer print out. Sample stations 112 and 115 were also laid on the print out. Station 112 was wholly within the cloud shadow and115 partially within the shadow. Accordingly, in comparing ERTS-1 data with in situ data we discarded ERTS-1 values for station 112 and 115 and utilized closely adjacent data pixels which were free of the cloud influence.

1.4.4 Effect of MSS Response Time Characteristics

In a similar manner the chart overlay grid was utilized to investigage ERTS-1 MSS quantum values for station 102. With reference to Figure 1-14, the pixels corrpsponding to the concrete waterfront street and sea wall have high values (about 60), and about 3 pixels are involved before the across track scan values fall to a level representative of the water. This delay is due to the response time characteristics of the ERTS-1 MSS scanner. Also in this particular case by using the grid overlay we could eliminate those pixels which included the town dock and Coast Guard ship, and in lieu thereof use closely adjacent pixels which appeared to be more representative of the actual water characteristics of station 102.

1.4.5 Calibration Test Site, Brewer's Bay Beach - Location and Registration Between Bands of ERTS-1 MSS Data

In order to establish more accurately the geographical location of ERTS-1 Bulk CCT print out pixels relative to the calibration test site, a grid overlay was made to match the scale of the aircraft I^2S imagery, Figure 1-15 of the test site. Figures 1-16, 1-17, 1-18 and 1-19 show the bulk CCT print out values superimposed on this grid overlay. Geographical location of the CCT print out by this method checked precisely, line to line, with the orientation for the entire St. Thomas Harbor. The highest MSS quantum value for each band occurred at the same pixel location, across track line 1584 and along track line 846. The geographical location of this pixel was the coral sand parking lot at Brewer's Bay Beach where the color test panels were laid out. We therefore concluded that registration

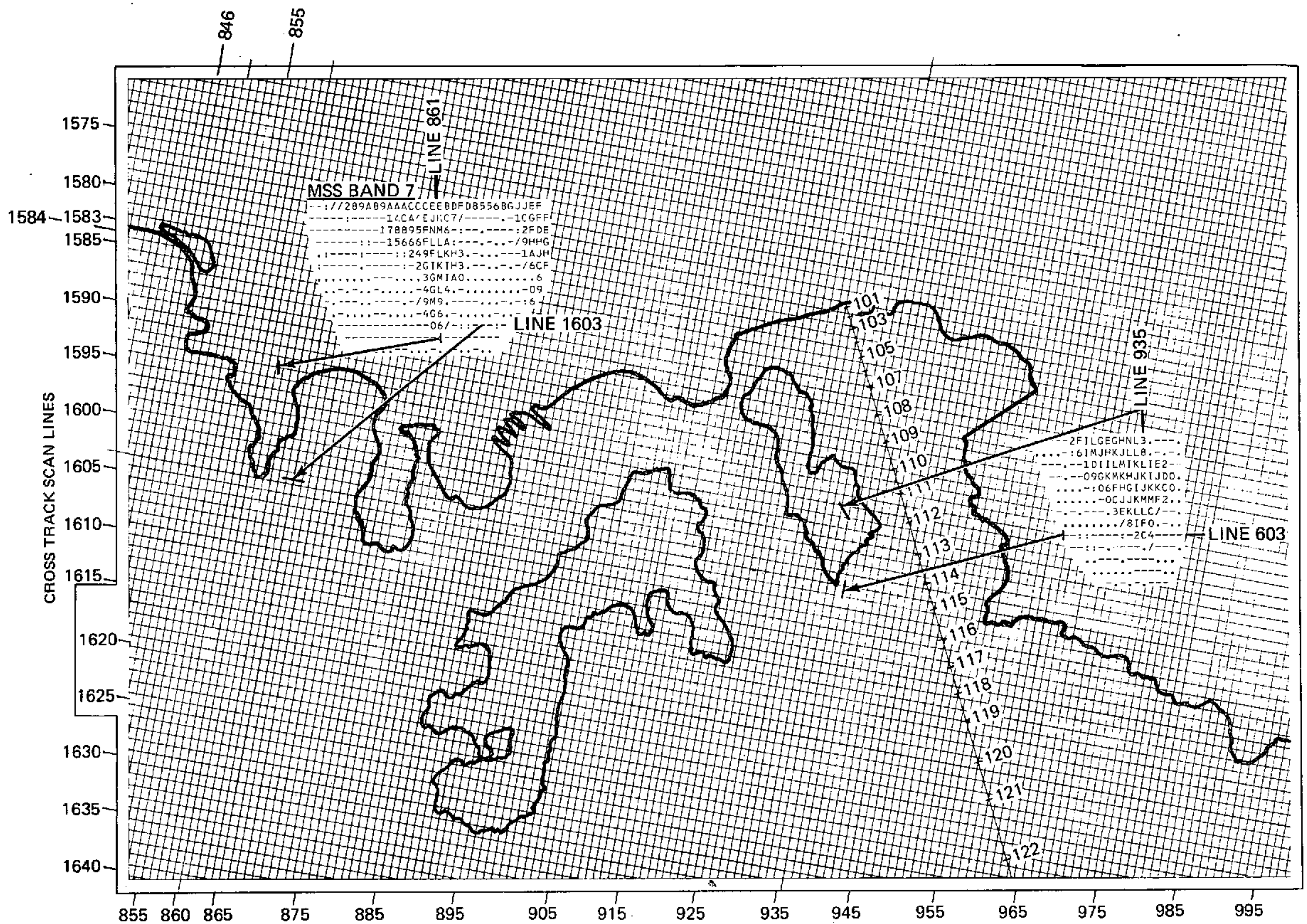

Figure 1-12. ERTS-1 MSS Bulk CCT Computer Print Out Grid of Scene 1086-14162. Scaled to Match C & GS Chart #933, St. Thomas, V.I.

ERTS MSS BAND 4 - BULK CCT VALUES'

ALONG TRACK SCAN LINES SCALE 234m. PER INCH

ACROSS TRACK SCAN LINES SCALE: 465m PER INCH

	939	940	941	942	943	944	945	946	947	948	949	950	951	952	953	954	955	956	957	958	959	960	961	962	963	964	965				
1594	24	26	26	28	26	28	29	28	28	29	28																				
1595	25	25	25	27	27	25	27	25	27	28	28	28	28	32	28	27	30	28	25	25	28	37	44	51	62	84	95				
1596	24	18	18	19	21	24	24	21	23	21	23	27	29	31	29	27	27	29	25	24	24	27	37	41	50	78	89	89			
1597	24	20	19	19	19	20	20	23	25	22	21	21	27	29	32	32	33	28	28	27	25	27	32	38	33	38	65	86	89		
1598	25	20	19	19	20	19	19	20	24	27	24	20	21	25	28	28	27	28	27	27	25	28	35	35	39	57	69	72	64		
1599	28	20	19	19	19	19	19	19	21	24	27	24	25	28	28	31	35	36	35	31	27	28	31	28	31	36	45	45	36	32	31
1600	32	31	27	22	19	18	19	21	21	21	23	28	29	35	38	35	38	45	38	38	38	31	38	43	38	31	29	31	31	29	
1601		28	23	20	20	20	20	21	27	27	21	23	28	34	41	45	41	41	41	38	48	53	45	37	38	28	28	28	28	25	24
1602		24	24	23	23	21	24	21	31	32	25	28	31	38	56	85	99	63	32	41	66	66	45	31	29	27	25	24	25	23	23
1603		25	25	25	27	25	21	21	27	28	32	38	32	33	52	82	100	100	100	89	55	52	52	38	29	32	28	25	25		
1604		24	24	24	25	24	24	25	25	25	25	27	27	36	64	96	100	100	100	92	61	57	60	51	49	49	32	25	27	28	
1605		24	24	25	25	24	25	25	25	24	24	27	25	28	41	60	79	98	100	79	58	43	36	36	36	39	43	48	31	28	28
1606		21	21	22	23	23	22	23	23	23	26	26	26	33	43	49	61	76	84	71	49	38	28	28	29	31	29	29	29	31	31
1607		21	21	25	23	23	23	23	25	25	25	25	23	27	32	48	59	45	41	34	32	30	28	25	21	27	25	25	25	27	28
1608		19	23	25	23	25	23	23	24	24	24	25	24	24	24	27	27	25	25	27	25	25	25	25	25	25	27	24	24	23	23
1609		25	21	23	25	25	25	25	25	27	33	32	27	25	25	25	25	23	27	33	33	28	25	25	27	27	28	28	28	27	23

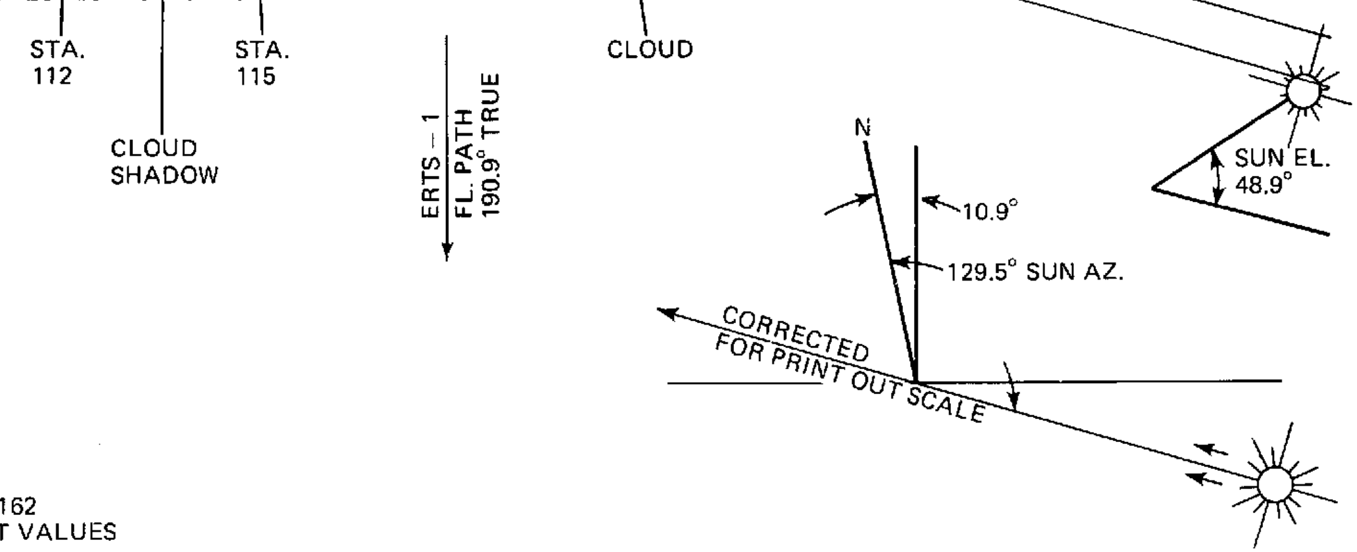

ERTS-1 SCENE #1086-14162
MSS BAND - 4, BULK CCT VALUES

Figure 1-13. Print Out of Bulk Band 4 Showing Cloud and Cloud Shadow Effects on ERTS-1 Imagery.

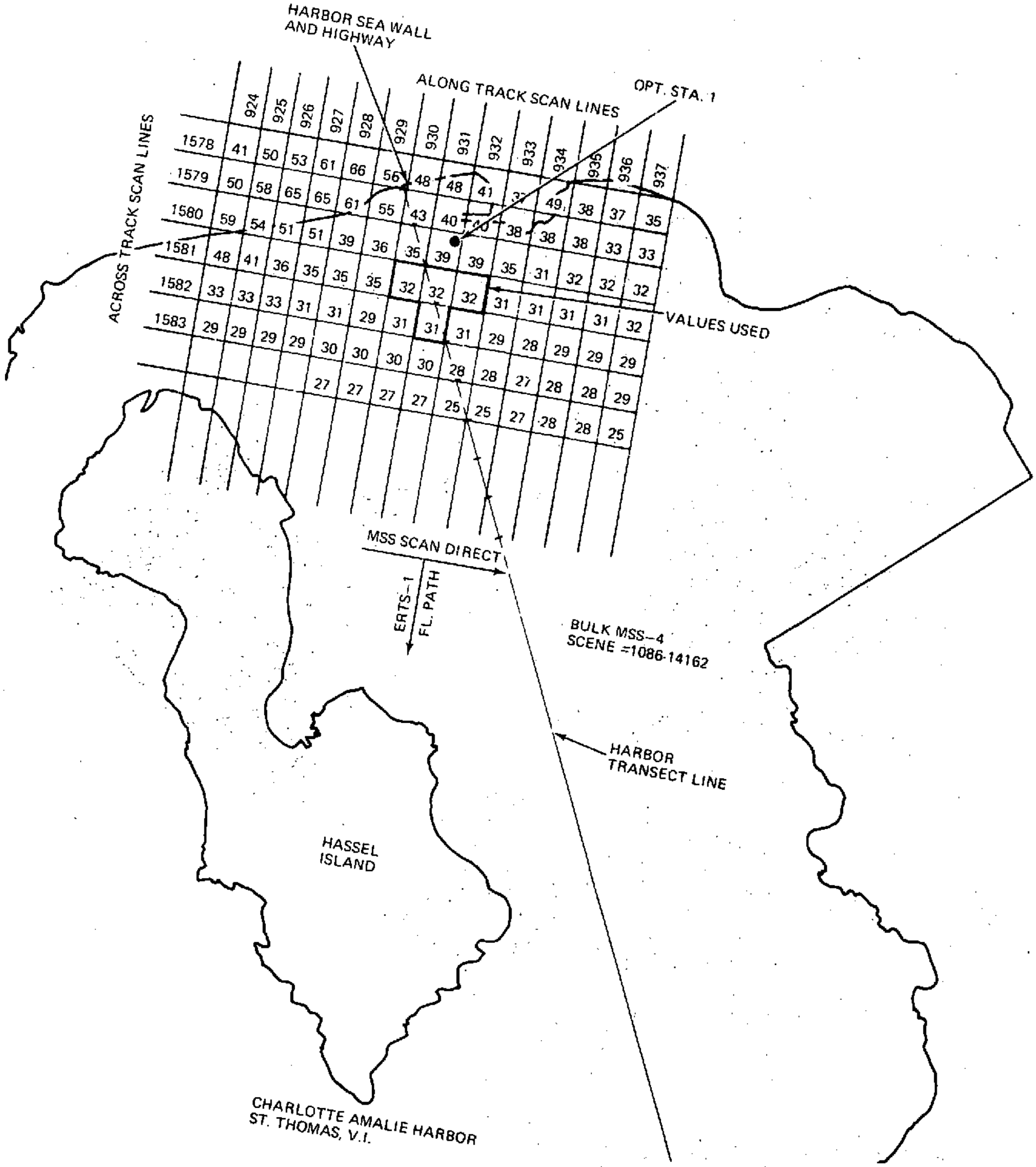

Figure 1-14. Print Out of Bulk Band 4 Showing Effect of MSS Response Time Characteristics When Scan Passes From a Bright Area (Sea Wall) to a Darker Area (Water)

Figure 1-15. Aircraft I^2S Photograph of Brewer's Bay Beach Calibration Test Site

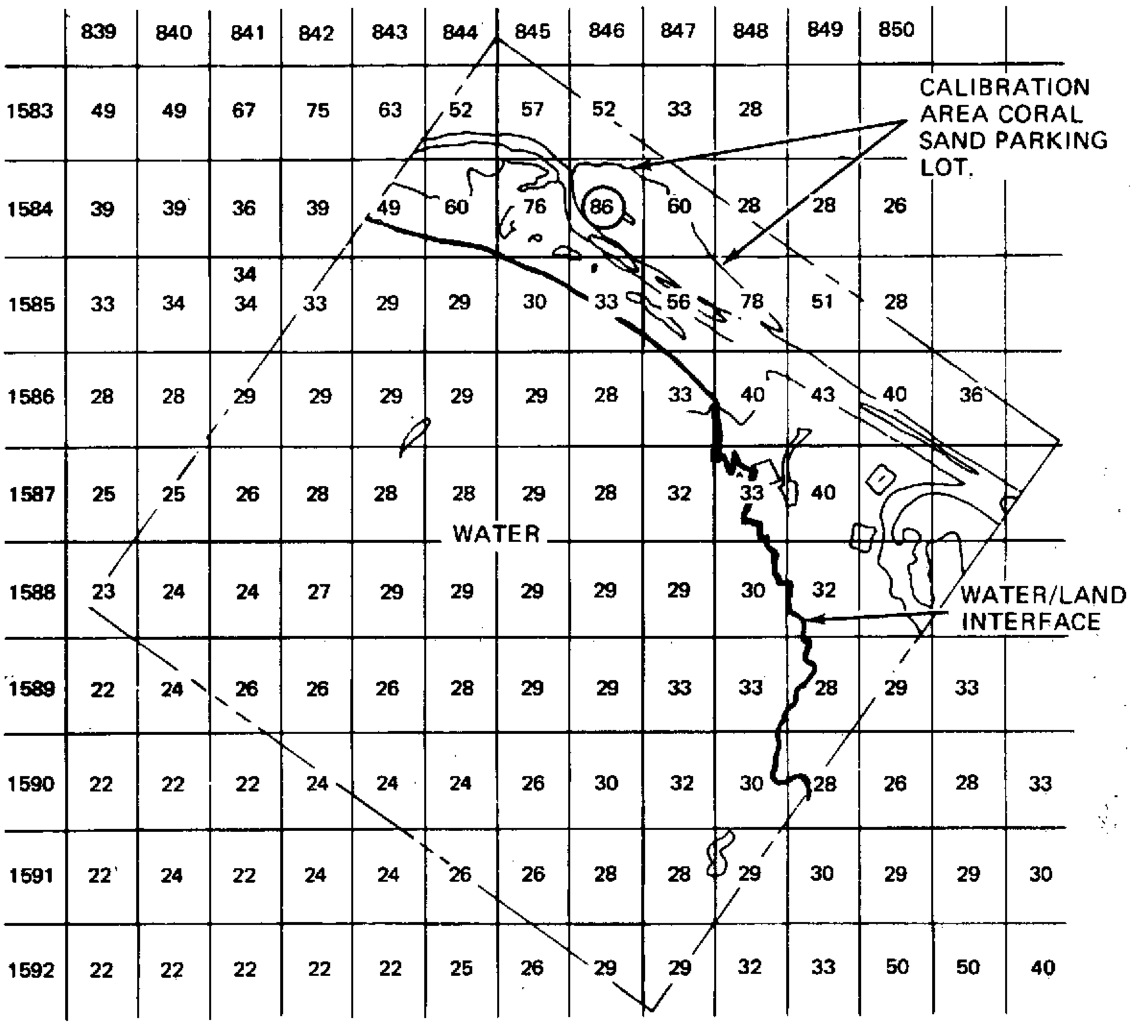

	839	840	841	842	843	844	845	846	847	848	849	850		
1583	49	49	67	75	63	52	57	52	33	28				
1584	39	39	36	39	49	60	76	86	60	28	28	26		
1585	33	34	34 34	33	29	29	30	33	56	78	51	28		
1586	28	28	29	29	29	29	29	28	33	40	43	40	36	
1587	25	25	26	28	28	28	29	28	32	33	40			
1588	23	24	24	27	29	29	29	29	29	30	32			
1589	22	24	26	26	26	28	29	29	33	33	28	29	33	
1590	22	22	22	24	24	24	26	30	32	30	28	26	28	33
1591	22	24	22	24	24	26	26	28	28	29	30	29	29	30
1592	22	22	22	22	22	25	26	29	29	32	33	50	50	40

BREWER'S BAY BEACH CALIBRATION TEST SITE

BAND #4 SCENE 1086-14162

SCALE = $\frac{1}{6,100}$
CROSS TRACK ≅ 58 M/CHARACTER
ALONG TRACK ≅ 78 M/CHARACTER

Figure 1-16. ERTS-1 MSS Bulk Band 4 Print Out, Scaled to Overlay I^2S Photograph of Brewer's Bay Beach Calibration Test Site

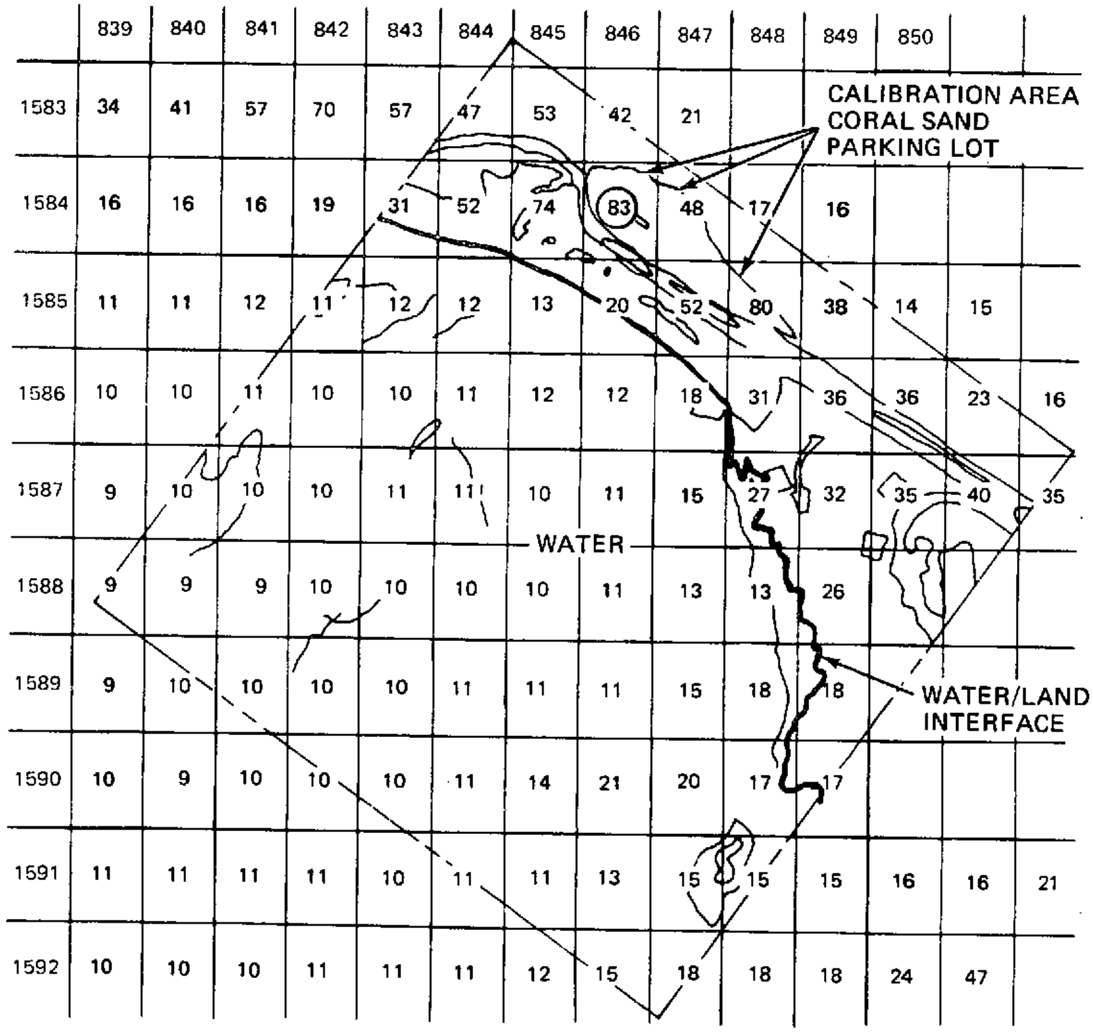

	839	840	841	842	843	844	845	846	847	848	849	850		
1583	34	41	57	70	57	47	53	42	21					
1584	16	16	16	19	31	52	74	83	48	17	16			
1585	11	11	12	11	12	12	13	20	52	80	38	14	15	
1586	10	10	11	10	10	11	12	12	18	31	36	36	23	16
1587	9	10	10	10	11	11	10	11	15	27	32	35	40	35
1588	9	9	9	10	10	10	10	11	13	13	26			
1589	9	10	10	10	10	11	11	11	15	18	18			
1590	10	9	10	10	10	11	14	21	20	17	17			
1591	11	11	11	11	10	11	11	13	15	15	15	16	16	21
1592	10	10	10	11	11	11	12	15	18	18	18	24	47	

BREWER'S BAY BEACH CALIBRATION TEST SITE

BAND #5, SCENE 1086-14162

SCALE = $\frac{1}{6,100}$

CROSS TRACK = 58 M/CHARACTER

ALONG TRACK = 78 M/CHARACTER

Brewer's Bay Beach Calibration Test Site
ERTS-1 Scene 1086-14162 MSS Band #5

Figure 1-17. ERTS-1 MSS Bulk Band 5 Print Out, Scaled to Overlay I^2S Photograph of Brewer's Bay Beach Calibration Test Site

	839	840	841	842	843	844	845	846	847	848	849	850			
1583	8	7	7	69	66	64	66	61	52						
1584	7	6	6	9	19	43	70	80	62	50					
1585	6	6	7	5	6	7	7	12	4	69	59	47			
1586	6	6	6	5	6	5	5	7	12	38	52	48	46		
1587	5	5	5	6	5'	6	5	5	10	29	46	48	50	50	
1588	4	5	5	5	4	4	4	4	6	19	40	54	62	54	
1589	4	4	4	4	5	5	4	4	8	46	41	36			
1590	5	4	4	5	5	5	6	9	16	21	28	35	48	48	
1591	6	6	6	6	6	7	7	7	10	10	8	9	15	36	49
1592	6	5	6	6	6	6	8	11	11	22	46	42	32	32	

BREWER'S BAY BEACH CALIBRATION TEST SITE

MSS BAND #6 BULK QUANTUM VALUES

SCALE $\cong \frac{1}{6,100}$

CROSS TRK ≅ 58 M/CHARACTER

ALONG TRK ≅ 78 M/CHARACTER

Figure 1-18. ERTS-1 MSS Bulk Band 6 Print Out, Scaled to Overlay I^2S Photograph of Brewer's Bay Beach Calibration Test Site

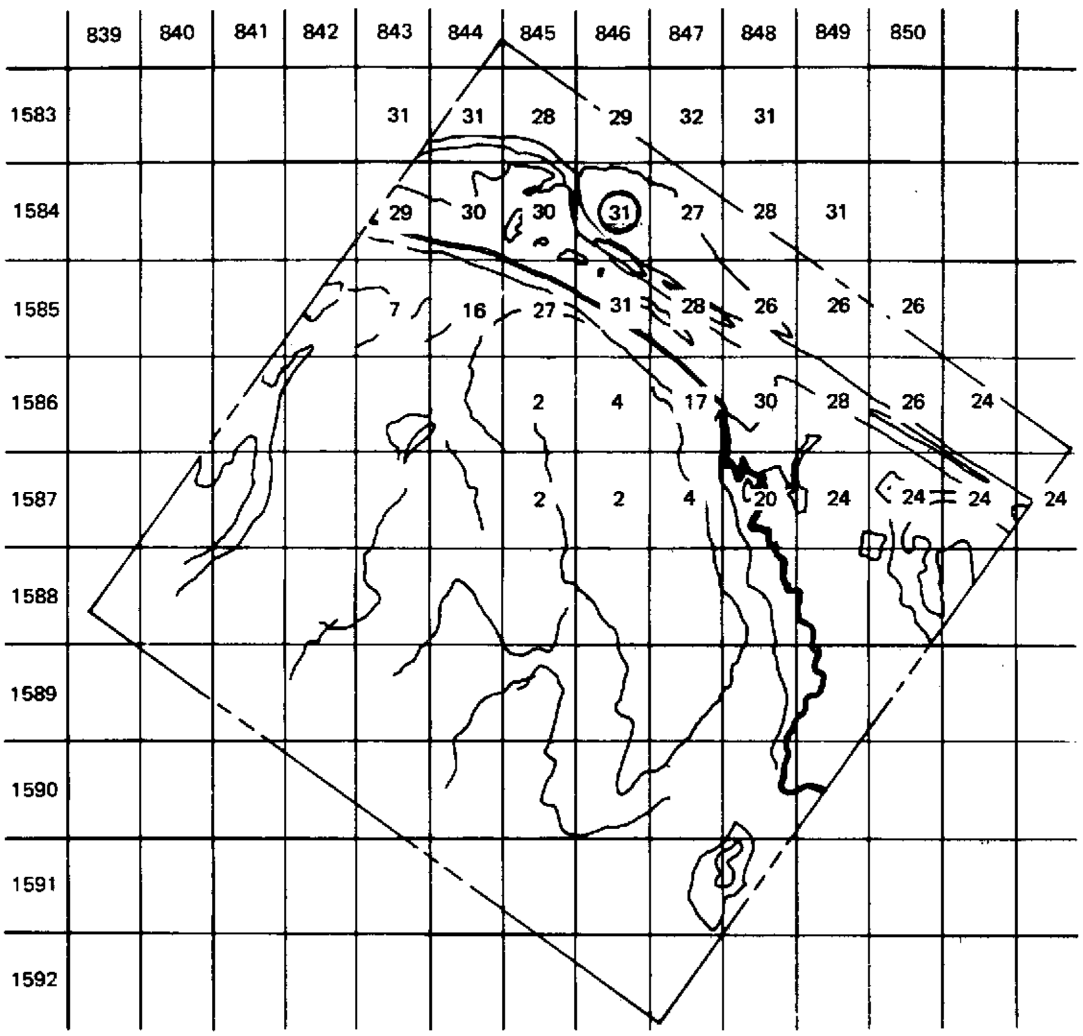

BREWER'S BAY BEACH CALIBRATION TEST SITE

MSS BAND # 7 BULK QUANTUM VALUES

SCALE $\cong \frac{1}{6,100}$

CROSS TRK ≅ 58 M/CHARACTER

ALONG TRK ≅ 78 M/CHARACTER

Figure 1-19. ERTS-1 MSS Bulk Band 7 Print Out, Scaled to Overlay I^2S Photograph of Brewer's Bay Beach Calibration Test Site

between MSS bands was within one pixel and further that the portion of the bulk CCT print out relating to St. Thomas was geographically located to within one pixel.

Photometric use of MSS Bands 4 and 5 calibration test site data is described by Dr. Egan in Section II.

1.5 DATA ANALYSIS AND CORRELATION

1.5.1 Optical Measurements and Correlation

As discussed by Dr. Egan in Section II of this report, emphasis was placed on analysis of the in situ data collected along the harbor transect line on October 17th (ERTS-1 pass). With reference to the chart, Figure 1-1, the transect ran from the town dock, station 101, out the shipping channel to station 122, a distance of 2.2 miles. The water varied from a polluted highly turbid condition at station 101, to quite clear at station 108 where the bottom is usually visible, to the very clear Caribbean waters offshore where the bottom is visible to depths of 60 feet or more.

In situ water optical measurements made with a M-H Photometer were peaked at 0.433, 0.533 and 0.633 nanometers. Data were taken at seven optical stations along the transect, Table 2-1, page 2-5.

Spectral reflectance characteristics of Brewer's Bay Beach coral sand were measured in the Grumman Optics Laboratory on samples returned from the test site. The color test panels were also calibrated in the Laboratory. These calibration data are plotted as Figures 2-2, 2-3, 2-4, 2-5 and 2-6, pages 2-7 through 2-11. Radiance measurements were recorded closely coincident with ERTS-1 and aircraft I^2S passes on October 17, 1972 on the white test panel in blue, green and red spectral bands, Table 2-2, page 2-12. Photometric measurements of the clear blue sky in a direction away from the sun were also made. The calibration test panels laid out at Brewer's Bay Beach were measurable on the I^2S photography and the Brewer's Bay Beach coral sand was clearly detected on the ERTS MSS CCT print out; hence, the photometric measurements enabled calculation of radiance at the surface for the aircraft I^2S and ERTS-1 MSS data. Refer to Tables 2-4 and 2-5, page 2-28, 2-29.

The resultant radiance calculations for the seven optical stations on the harbor transect are summarized in Table 1-2 and graphically presented in Figure 1-20 which can be compared with Figure 1-21, Graphical Correlation of Turbidity, Chlorophyll, and Carotenoids along the Harbor Transect. As discussed by Dr. Egan on page 2-50 and Dr. Olsen on page 3-19 use of computer generated correlation matrices is a useful technique to indicate the degree of correlation of the several variables. For example, Table 1-3

Table 1-2. Comparison Optical, I^2S Photographic and ERTS Data for Optical Stations on Harbor Transect(4)

Station	Green Band			Red Band		
	(1)Optical .533/cm	(2) I^2S Photo. mw/cm^2-sr	(3)ERTS-4 mw/cm^2-sr	Optical .633/cm	I^2S Photo. mw/cm^2-sr	ERTS-5 mw/cm^2-sr
1	.014	.165	.201**	.019	.160	.048**
2	.014	.188	.164	.019	.136*	.039
3	.014	.108	.117	.019	.188*	.023
4	.0044	.098	.117	.0066	.094*	.023
5	.0030	.101	.119	.0052	.123*	.022
6	.0019	.083	.101	.0047	.092*	.020
7	.0019	.061	.047	.0041	.092*	.014

NOTES:

(1) Absorption coefficients. Refer to page 2-5 for definition
(2) Refer to Table 2-10 for calculation procedure.
(3) Refer to Table 2-12 for calculation procedure.
(4) These data are plotted as Figure 1-20 and 2-25.

* Less accurate values because film latitude was exceeded; see text of Section 2 for discussion.
** Limited accuracy due to spatial resolution of ERTS-1 MSS.

(correlation matrix for inner harbor optical stations) shows high direct correlation of aircraft and spacecraft data with turbidity and similarly high inverse correlation with total chlorophyll and carotenoids. (This latter correlation reverses to positive direct correlation at the seaward end of the transect. Refer to Section II, detailed discussion.)

1.5.2 Harbor Biological, Chemical and Physical Data Analysis and Correlation

As described by Dr. D.A. Olsen in Section III of this report the harbor water quality investigation program was primarily centered around the acquisition of the plankton pigment data for the times of ERTS overflight. The three diurnal studies assessed the hourly variation of plankton pigment and the relation between it and basic water quality parameters. These studies showed a homogeneity between different times at the same locale, but short term temporal variability was too great to permit valid statistical analysis between locales.

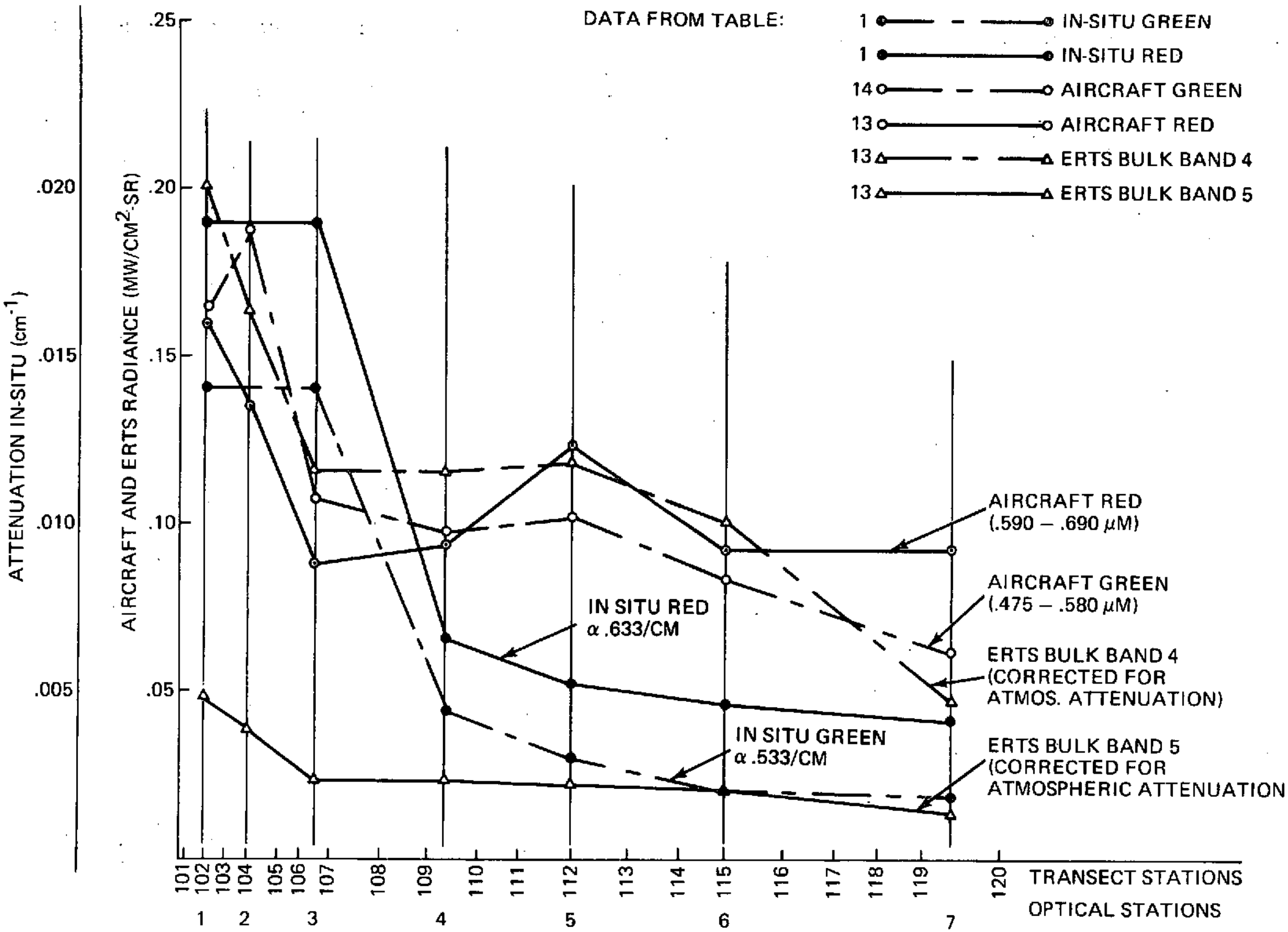

Figure 1-20. Comparison of ERTS-1, Bands 4 and 5, Aircraft Green and Red and In Situ Harbor Transect Optical Data

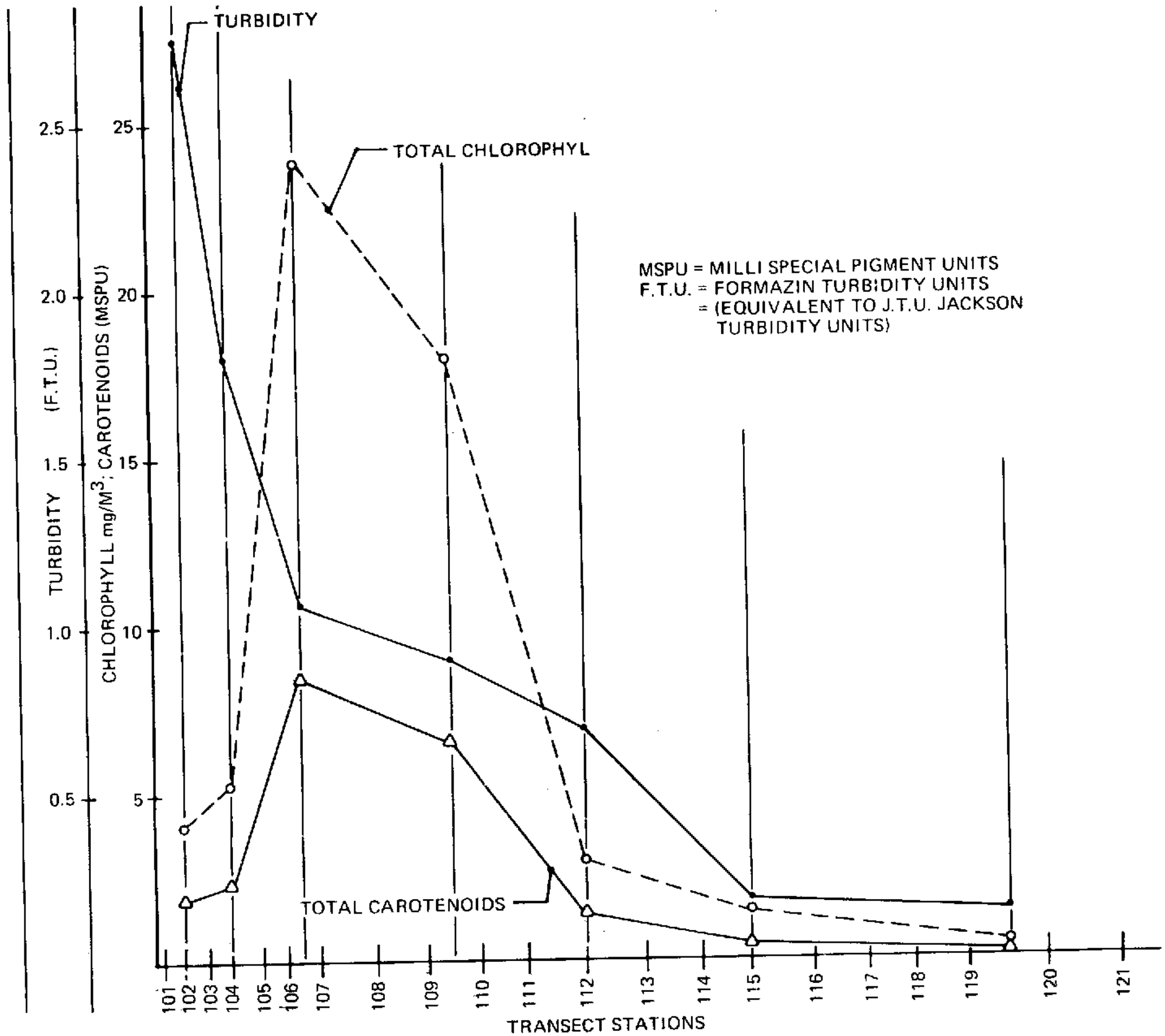

Figure 1-21. Graphical Correlation of Turbidity, Chlorophyll and Carotenoids Along the Harbor Transect

Table 1-3. Transect Correlations (Optical Stations 2, 3 and 4)

	In Situ Red	Aircraft Green	Aircraft Red	Prec. MSS 4	Bulk MSS 4	Bulk MSS 5	Turbidity	Chlorophyll a	Total Chlorophyll	Pigment Diversity	Total Carotenoids	Bulk MSS 4 UC*	Bulk MSS 5 UC*	Bulk 4 MUC*	Bulk 5 MUC*	Chlorophyll C	Bulk MSS 6
In Situ Green	**100**	59	52	80	63	50	63	17	-21	**99**	-25	-29	50	0	87	-31	**97.5**
In Situ Red		59	52	80	63	50	63	17	-21	**99**	-25	-29	50	0	87	-31	**97.5**
Aircraft Green			**99.7**	**95**	**99.9**	**99.5**	**99.0**	-69	**-92**	70	**-93**	**-94**	**99.4**	81	**91**	**-95**	40
Aircraft Red				**93**	**99**	**100**	**99**	-75	**-94**	64	**-95**	**-97**	**100**	85	88	**-97**	33
Precision MSS 4					**97**	**92**	**97**	-44	-75	88	-77	-80	**92**	59	**99**	-81	65
Bulk MSS 4						**99**	**100**	-66	-89	74	**-91**	**-93**	**99**	78	**93**	**-93**	45
Bulk MSS 5							**99**	-76	**-95**	62	**-96**	**-97**	**100**	86	87	**-98**	30
Turbidity								-66	-89	73	**-91**	**-93**	**99**	78	**93**	**-93**	44
Chlorophyll A									**93**	3	**91**	89	-76	**-99**	-34	88	39
Total Chlorophyll										35	**99.9**	**99.7**	**-95**	**-98**	-67	**99.5**	1
Pigment Diversity											-38	-42	62	14	**93**	-44	**93**
Total Carotenoids												**99.9**	**-96**	**-97**	-69	**99.8**	-3
Bulk MSS 4 UC*													**-97**	**-96**	-73	**100**	-7
Bulk MSS 5 UC*														87	87	**-98**	30
Bulk MSS 4 MUC**															50	**-95**	-22
Bulk MSS 5 MUC**																-74	74
Chlorophyll C																	-9

*MSS quantum value (0-127) uncorrected for atmospheric attenuation

**Midpoint pixel MSS quantum value (0-127) uncorrected for atmospheric attenuation

ERTS data providing synoptic information would eliminate the temporal variable between stations and enable studies of wide geographical areas within the spatial resolution of ERTS-1. The sampling at the three depths measured the homogeneity of the water column. The repetitive sampling program enabled assessment of variations associated with depth as well as time-related variances extending over 1.5 lunar cycles. Data obtained at geographical sampling stations enabled assessment of the geographical extent or generality of the trends observed at the repetitive stations. The benthic samples described communities that have developed over a period of years in response to water conditions and are therefore "bio-indicators" of long term trends. There is a growing body of evidence (Hutchinson, 1969) indicating that community structure can be an indicator of environmental stress. In this manner of sampling, time variables were assessed so that the periodic 18 day overflights of ERTS could be related to long term trends over broad geographical areas, and perhaps used to monitor such trends.

The results point up the complexity of the interrelations of the oceanographic-biological system in the Virgin Islands. Benthic diversity is used to delineate the long term responses by the biotic community to water quality degradation from pollutants. Turbidity correlates with benthic diversity and ERTS-1 data; hence, offers promise of providing a key for monitoring some aspects of water quality. Refer to Section III, page 3-42 and subsequent for discussion of data correlation.

1.6 DISCUSSION OF APPENDICES

Appendix 1, Water Quality Survey of the Virgin Islands by the EPA, Region II lists results of analysis for heavy metals of sediment and water samples collected by Grumman. This appendix is included in this report not only to acknowledge the interest of EPA but also to acquaint the reader with another source of water quality data pertinent to St. Thomas.

Water Quality Survey of Virgin Islands
By
Environmental Protection Agency, Region II

Appendix 1

The Environmental Protection Agency, Region II, conducted a water quality survey of the Virgin Islands in November and December 1972. As an assist to EPA, and while collecting in situ data for the ERTS experiment, eight water samples and four sediment samples were collected, preserved and shipped by air to EPA, Region II Labs, Edison, New Jersey for analysis for heavy metals. Results of analyses by the EPA Labs are attached.

In addition EPA obtained the following water quality data and sediment data at selected stations on the coasts of St. Thomas, St. John, St. Croix, and Buck Island: TOC, TKN, NO_3-N, T-P, Cu, Cd, Zh, Al, Hg, Cr, Pb, MF Total Coliform, MF Fecal Coliform. Further information concerning this EPA program may be obtained from:

Environmental Protection Agency
Region II Office
Woodbridge Avenue
Edison, New Jersey 08817

Attention: Dr. R. Dewling

This appendix is included in this report not only to acknowledge the interest of EPA but also to acquaint the reader with another source of water quality data. For temporal reasons, the data were not used in the experiment analysis program of correlation of in situ data with ERTS data.

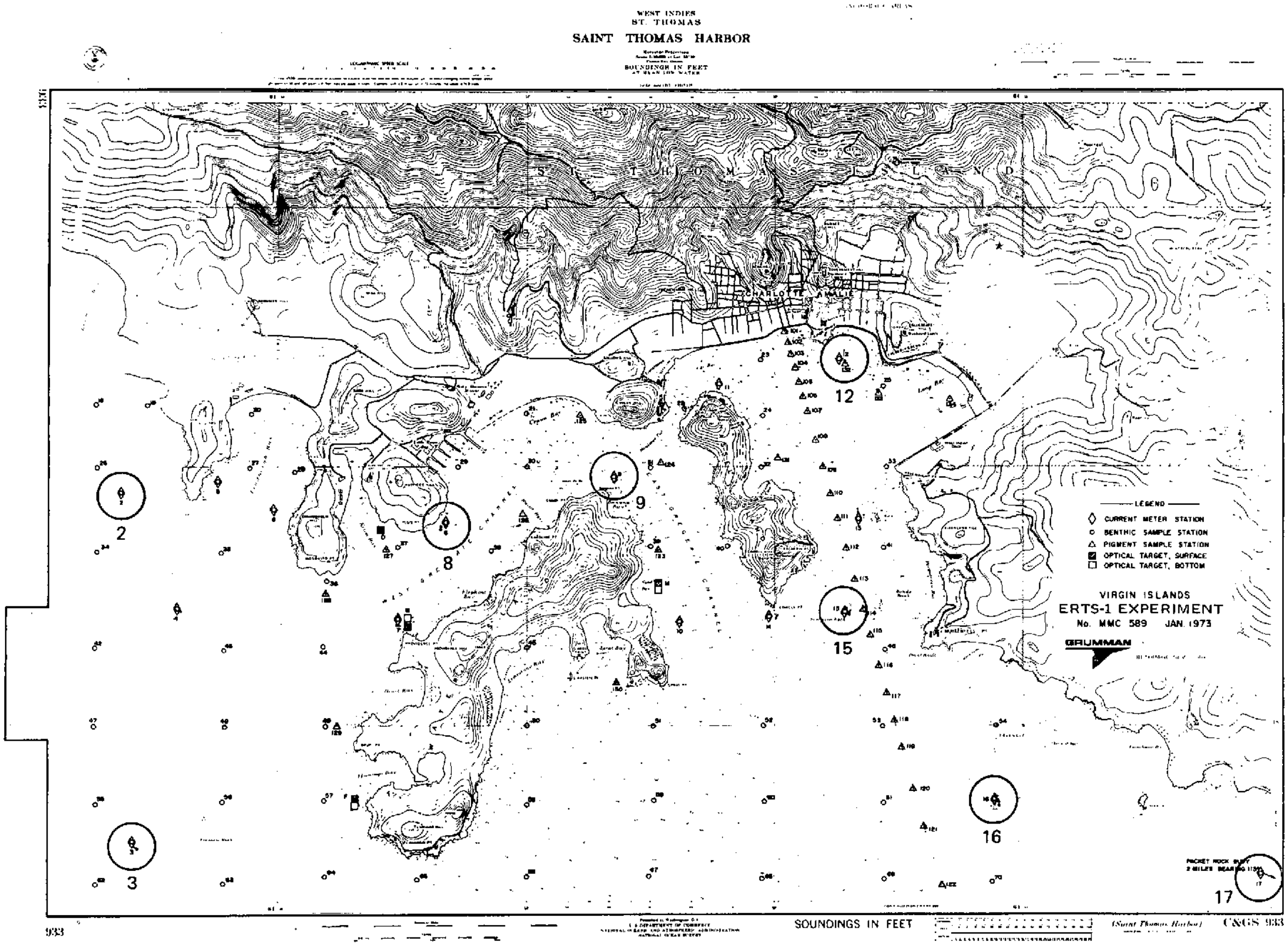

Figure 1-22. Location of Water Sample Stations

U.S. VIRGIN ISLANDS STUDY

GRUMMAN ECOSYSTEM SAMPLES

Water Samples - 11/3/72

EPA Lab #	Station No.	Cd mg/l	Cr mg/l	Pb mg/l	Zn mg/l	Al mg/l	Cu mg/l	Hg mg/l
25826	2	0.059	< 0.01	< 0.1	0.22	0.24	0.026	< 0.00025
25827	3	0.053	< 0.01	< 0.1	0.21	0.24	0.026	< 0.00025
25828	8	0.053	< 0.01	< 0.1	0.24	0.30	0.030	< 0.00025
25829	9	0.047	< 0.01	< 0.1	0.41	0.20	0.030	< 0.00025
25830	12	0.053	< 0.01	< 0.1	0.48	0.28	0.034	< 0.00025
25831	15	0.035	0.012	< 0.1	0.22	0.24	0.034	< 0.00025
25832	16	0.053	0.011	< 0.1	0.41	0.24	0.028	< 0.00025
25833	17	0.035	0.011	< 0.1	0.21	0.26	0.023	< 0.00025

Metal values were obtained by Atomic Absorption Spectroscopy.

U.S. VIRGIN ISLANDS STUDY

GRUMMAN ECOSYSTEM SAMPLES

Sediment Samples - 11/3/72

EPA Lab #	Station No.	% Solids	Cd mg/kg	Cr mg/kg	Pb mg/kg	Zn mg/kg	Al mg/kg	Cu mg/kg	Hg mg/kg
25834	12S	63.3	8.0	12	114	127	7,600	53	1.5
25835	15S	71.7	6.6	6.3	51	10	980	10	0.23
25836	16S	72.8	3.7	1.2	14	0.97	6.1	2.4	0.056
25837	17S	69.6	39	6.4	44	42	4,400	21	0.032

EPA Lab #	Station No.	% Solids	Fe mg/kg	Mn mg/kg	Sr mg/kg	Ti mg/kg	Si mg/kg	Mg mg/kg
25834	12S	63.3	10,700	504	1,450	378	50,500	8,200
25835	15S	71.7	1,460	<90	3,050	<90	8,330	10,400
25836	16S	72.8	560	<90	2,900	<90	2,400	12,000
25837	17S	69.6	99	<90	2,000	<90	1,460	9,300

All values are based on wet weight.

Values for Cd, Cr, Pb, Zn, Al, Cu, and Hg were obtained by Atomic Absorption Spectroscopy.

Values for Fe, Mn, Sr, Ti, Si, and Mg were obtained by Emission Spectroscopy.

ACKNOWLEDGMENTS

Execution of the program, data acquisition, analysis, and report writing required skills in several disciplines. The result, this report, demonstrates a willingness to share ideas between participants. Mr. D. Cutler, project field engineer for Grumman, deserves much credit for schedule execution at St. Thomas; Dr. W. Egan for planning, executing and reporting on the photometric aspects of the experiment, Section II; Dr. D. Olsen for directing and executing the harbor water in situ biological, chemical and physical data acquisition program and reporting on same, Section III; Mr. G. Heaslip for devising the Data Handling Plan, directing digital processing of the data, and authoring Section IV; and Mr. R. Skirkanich for his consulting assistance in all phases of digital processing and analysis of the data.

On very short notice, Kennedy Space Center agreed to acquire the aircraft data. Equipping the NASA 5 aircraft with the Daedalus Line Scanner and putting the plane on station at St. Thomas in about five weeks from "Go-Ahead" was an outstanding performance. Our thanks go to Messrs. R. Withrow, P. Claybourne, and J. O'Conner for planning and successfully executing this phase of the experiment.

The active interest of Mr. W. Beller, Chief Insular Affairs, Environmental Protection Agency is gratefully acknowledged.

N74-15003

SECTION II

CORRELATION OF ERTS-1 AND AIRCRAFT OPTICAL DATA WITH WATER QUALITY PARAMETERS OF CHARLOTTE AMALIE HARBOR, ST. THOMAS, V.I.

acknowledgement

This section as been prepared by:

DR. W.G. EGAN
Research Department
GRUMMAN AEROSPACE CORPORATION

in association with

GRUMMAN ECOSYSTEMS CORPORATION
Bethpage, N.Y. 11714

ABSTRACT

We report on our work, at Charlotte Amalie Harbor, St. Thomas, Virgin Islands, attempting to correlate optical aircraft remote sensing of water quality with the optical data from the ERTS-1 satellite using calibrated imagery. The harbor at Charlotte Amalie has a concentration of a number of factors affecting water quality: untreated sewage, land runoff and sediment from navigation and dredging operations. Grumman has originated calibration procedures and applied them to ERTS-1 and I^2S camera imagery. The results indicate that the ERTS and I^2S imagery are correlated with optical in situ measurements of the harbor water. The aircraft green photographic and ERTS-1 MSS-4 bands have been found most suitable for monitoring the scattered light levels under the conditions of this investigation. The application of satellite or aircraft for optical remote sensing depends upon the physical scale and frequency of sensing since both sensor systems generally have sufficient photometric sensitivity. The chemical parameters of the harbor water were found to be correlated to the optical properties for two stations investigated in detail. The biological properties of the harbor water (chlorophyll and carotenoids), correlate inversely with the optical data near the pollution sources compared to further away.

Calibration procedures developed by Grumman incorporated in this investigation were essential to the interpretation of the photographic and ERTS-1 photometric responses.

2.0 INTRODUCTION

The Virgin Islands ERTS-1 experiment has the object to determine the feasibility of using both airborne and spacecraft sensors quantitatively in coastal zone water quality management by establishing the boundaries of applicability of each technique separately. In order to sense water quality remotely, two requirements must be fulfilled: (1) the optical properties of the water must be affected by the pollutants in a predictable way; and (2) the remote sensor must be capable of distinguishing these variations. There are thus two aspects associated with the program, the first requiring measurements of the optical properties of the polluted water itself with the ultimate aim of correlating these with the biological, chemical and other physical properties of the water. It would be expected that generally there would be an average level of pollution with temporal variations caused by tides, winds, and miscellaneous local effects, and these variations would cause corresponding related changes in the optical, biological, chemical and other physical properties of the water. The second aspect deals with two types of remote sensors, the first being aircraft and the other being those in the ERTS-1. The ERTS-1 system has been thoroughly described in the user's manual (Ref. 1), and the present operating sensor is the MSS (multispectral scanner). The remotely sensed light reflected and scattered by polluted water is significantly affected by absorption and scattering in the atmosphere and solar illumination geometry. In order to account quantitatively for this atmospheric absorption and scattering and solar illumination geometry, precision remote sensing measurements of color were made using Grumman developed optical calibration standards. These standards took the form of calibrated optical test panels placed on the ground for aircraft measurements, and a sufficiently large calibrated optical target for the ERTS-1. Thus, knowing the true color of these targets from laboratory measurements and the response of the aircraft photographic or satellite sensing system, the absorption and scattering of the atmosphere was deduced.

The study of water quality in the Virgin Islands, and in particular in the Harbor at Charlotte Amalie, St. Thomas, was carried out by Grumman Ecosystems Corp. under NASA sponsorship on Experiment No. 589, in association with:

- Grumman Aerospace Corp. - Research Dept.

- Grumman Data Systems Corp. - Environmental data services section
- Marine Resources Development Foundation - Puerto Rico

2.1 STUDY AREA

The optical study area lies along the ground truthing marine biological transect between stations 102 through 120 (Figure 2-1). The optical stations, 1 through 7, were fewer than those used for the marine biology, mainly because of the length of time required for each in situ set of optical observations (location and measurement ≈ 1/2 hour). There was also a limited time for the entire optical transect, because it was made in the afternoon following the 1016 HRS. ERTS-1 passage over St. Thomas Harbor on October 17, 1972, ERTS-1 SCENE #1086 - 14162.

A supplementary optical calibration area was situated at Brewers Bay Beach, located about 3 miles west of the optical study area.

The St. Thomas Harbor optical transect begins in a region of high pollution from sewage effluent (near the Coast Guard Dock) and terminates in a region of low pollution past Muhlenfels point (see Figure 2-1). Raw sewage was discharged into the harbor at a peak rate of about 3 million gallons per day (Ref. 2). Since there is no aquifer on the Island of St. Thomas, drinking water is obtained from catch basins and a desalination plant. Sanitary sewage (toilet waste) is flushed using bay water pumped inland through a separate water system. The raw sewage is presently discharged into the bay along the sea wall at the northerly rim (Figure 2-1).

There are additional sources of sediment in the harbor water. One source is the daily docking of cruise ships, generally at the West Indian Dock (east of the initial portion of the harbor optical transect, Figure 2-1). Another cause of sediment is a dredge operating along the harbor entrance channel, acquiring coral sand for building construction.

Also, the ships docked at the West Indian pier discharge raw sewage, as well as do small craft docked nearby at the Yacht Haven Marina.

2.2 OPTICAL CALIBRATION PROGRAM

Why do we need an optical calibration program? Why can't we simply use contrasts in color to determine pollution?

These two rhetorical questions serve to introduce a section in this report which is unique in the present thinking on interpretation of ERTS-1 and aircraft imagery. There are techniques in use of contrast enhancement in imagery using false colors so that we may

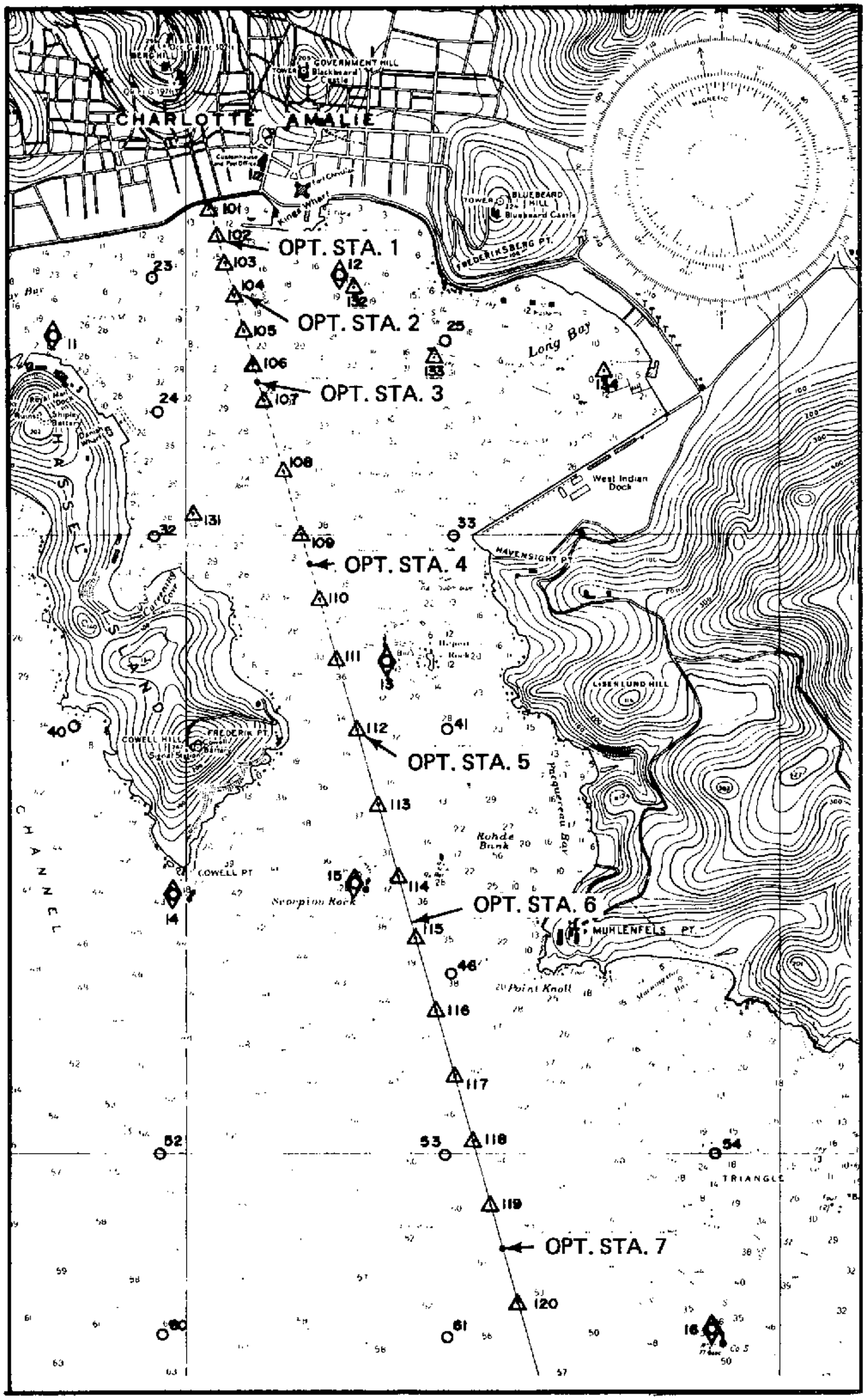

Figure 2-1. Optical Study Area in the St. Thomas Harbor; the optical stations lie along biological transect between stations 102 and 120

"see" pollution in brilliant color hues, but there is no quantitative assessment. It has been pointed out that sun illumination geometry, atmospheric filtration, imaging system response, and data reduction techniques all affect contrast (see Refs. 3 and 4 for instance). Court cases may be based on visual evidences of pollution, but the final decision always rests with the exact degree, with well defined specification; an image of water with discoloration does not quantitatively yield information on degree of pollution or even the nature. There must be optical calibration, and this calibration must include spectral (color) effects.

Reference 3 pointed up the need for color calibration and control in true false color photography; this is more difficult with color film than with panchromatic black and white film because of interlayer effects in color film. Therefore the preferred approach for aircraft imagery is the use of a 4 lens camera with selective color filtration (such as the I^2S), with automated film processing (as with the Kidak Versimat).

Satellite imagery (ERTS-1) suffers from the absolute calibration problem, with complicating factors resulting from atmospheric scattering and absorption combined with effects of reduced spatial resolution. Absolute calibration becomes necessary for ERTS-1 imagery to quantify color levels absolutely and to determine the effects of atmospheric scattering and absorption.

The implementation of the optical calibration program involves four aspects: (1) In situ harbor water transect measurements, (2) Brewers Bay Beach and Color Panel Calibration, (3) Calibration of the I^2S photographic imagery, and (4) Calibration of the ERTS-1 data. These four aspects will now be described.

2.2.1 In Situ Harbor Water Measurements

The optical property of the harbor water that will be sensed will be its brightness. The brightness is the result of many factors which include scattering of particulates in the water, sun elevation, and waves which may reflect as sun glint along with the sky reflection. Where the water surface waves are small, and the sun glint does not significantly affect the water surface brightness, the brightness of the water will depend upon the light that is backscattered by macroscopic, microscopic, and submicroscopic particulates in the water. If the water is relatively uncolored by dissolved constituents, the transmission of light in the water is a good indicator of the concentration of scattering particles. The more scattering particles there are in the water, the lower will be the transmission. However, this is only an approximation. Further, the transmission will generally depend upon the wavelength of the light used in the transmission measurement.

The water optical transmission measurements for this program were made using a portable battery operated Minneapolis-Honeywell photometer (with interchangeable narrow-band interference filters) mounted on a submarine viewing tube. The submarine tube had a water-tight plexiglass window that permitted photometric measurements under water without interference from surface waves. The optical filters used in the measurements were peaked at 0.433, 0.533 and 0.633 μm; they were Optics Technology narrow band interference filters with a bandpass of 0.02 μm. These measurements for the 7 optical stations are presented in Table 2-1; the location of the optical stations relative to the biological transect station is indicated in the second column. Where two biological stations are indicated, the optical station is located about midway between them. The quantities listed in Table 2-1 are in units of cm^{-1}, as defined by the relation

$$I = I_o^{-\alpha d},$$

where:

I_o = Intensity of incident (sun) light

I = Intensity of transmitted (sun) light

α = the absorption coefficient

d = path distance in centimeters.

It is to be noted that at optical stations 1, 2 and 3, the concentration of particulates was so great that a short path length had to be used, and the measurements have a lower accuracy (±30%) than the other stations which have a photometric accuracy of ±3 to 5%.

The absorption coefficients are listed in Table 2-1 for the ground truth transect which is used subsequently in this report.

Table 2-1. Optical Data on St. Thomas Harbor Transect on 10/17/72

OPTICAL STATION	TRANSECT STATION	* α.433/cm	* α.533/cm	* α.633/cm
1	102	.019	.014	.019
2	104	.019	.014	.019
3	106-107	.019	.014	.019
4	109-110	.0033	.0044	.0066
5	112	.0018	.0030	.0052
6	115	.0014	.0019	.0047
7	119-120	.0008	.0019	.0041

* Half Bandwidth of Filters = 20 nanometers.

2.2.2 Brewers Bay Beach and Color Panel Calibration

The spectral reflectance of the coral beach sand used as a calibration standard for the ERTS-1 and the aircraft imagery at 6000 feet altitude is presented in Figure 2-2 under illumination conditions closely analogous to those existing during the ERTS-1 overpass. The sand in the central area is brighter because it is finer, more firmly packed and free of larger shells that exist in the sand near the water. However the reflectance from the sand also depends upon the viewing angle and wavelength of the incident light; this is shown in Figure 2-3 (the phase angle on the abscissa is the sum of the incident angle of 40° and a variable viewing angle). The reason that the spectral reflectance (Figure 2-2) must be known is so that one can use any apparent spectral variation observed from the ERTS-1 or from high altitude photography to determine the amount of atmospheric filtration and scattering. The angular dependence (Figure 2-3) is used to determine the vignetting of the photographic lens and filter system on a selected photographic image where the Brewers Bay Beach area extends completely across the frame.

The spectral reflectance of the test panels on Brewers Bay Beach (Figure 2-4) used for low altitude (2000 ft) aircraft imagery is presented in Figure 2-5. The white (W) and gray panels (G1, G2, and G3) have reasonably uniform reflectance between 0.4 and 1.0 μm, but drop rapidly below 0.4 μm. The red (R) is almost saturated, but the blue (B) and green (G) are weaker in saturation; the important consideration is that the paints be "flat" (i.e. have uniform reflectance at all viewing angles in order not to introduce additional corrections). The actual "flatness" of the reflectance is shown in Figure 2-6, which reveals small changes in reflectance between phase angles of 20 and 110°. At phase angles below 20°, the pronounced increase in reflectance is characteristic of nearly all materials, and is generally much stronger.

The reason for using 7 test panels is that they serve as an additional check on the film response in low altitude aircraft imagery, and as a cross calibration check on the sand photometry. As a bare minimum, a single panel (such as white) could be used, but this checks the response at only one reflectance level.

2.2.3 Calibration of the I^2S Photographic Imagery

Photographic calibration of the imagery obtained from the I^2S Cameras involves quantification of the light absorption properties from the ground to the film emulsion. The elements involved are the radiance from the ground calibration areas (test panels

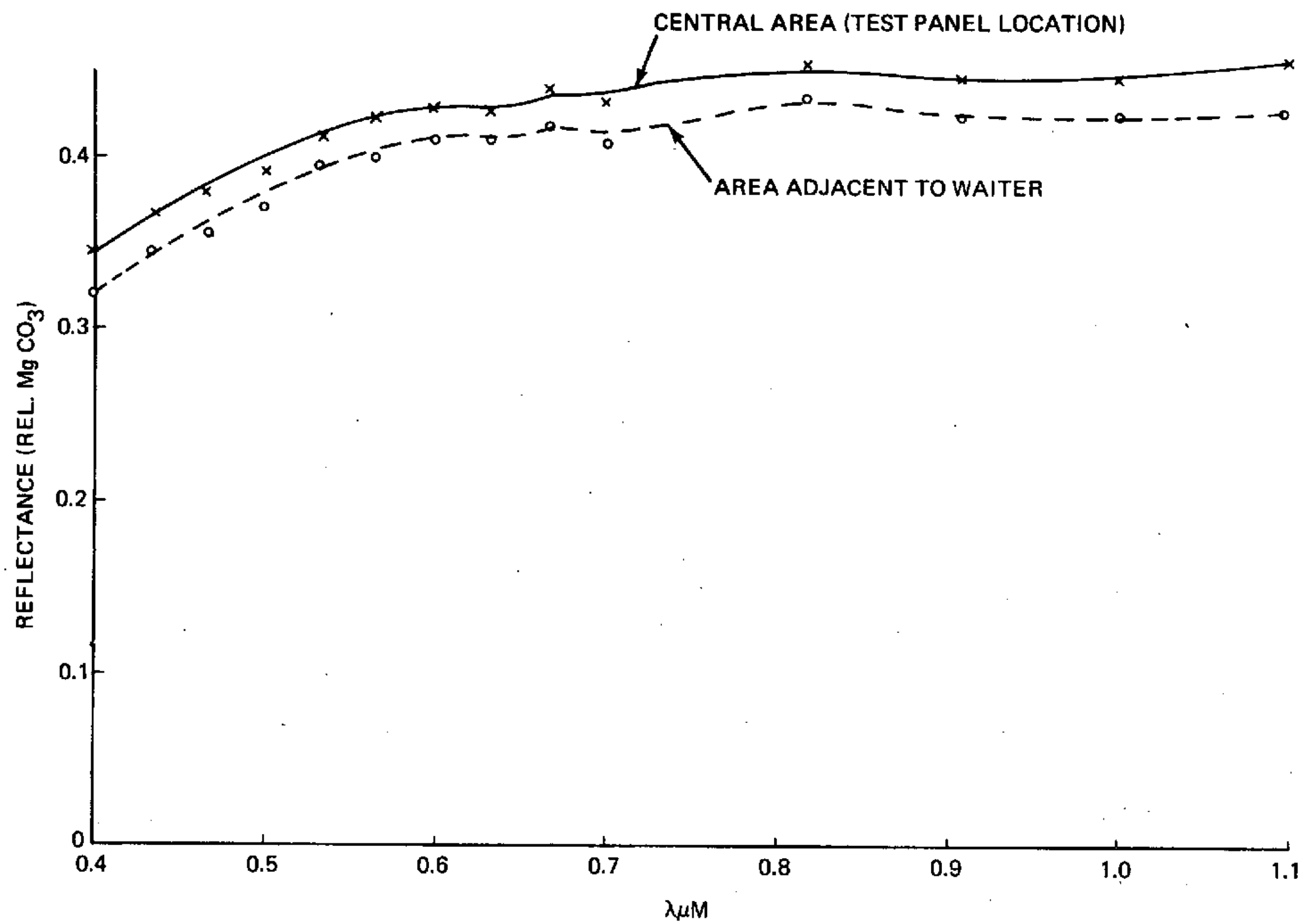

Figure 2-2. Laboratory Spectral Reflectance (Relative to M_gCO_3) of Brewers Bay Beach Sands at an Incident Angle of 40°, and a Phase Angle of 3°

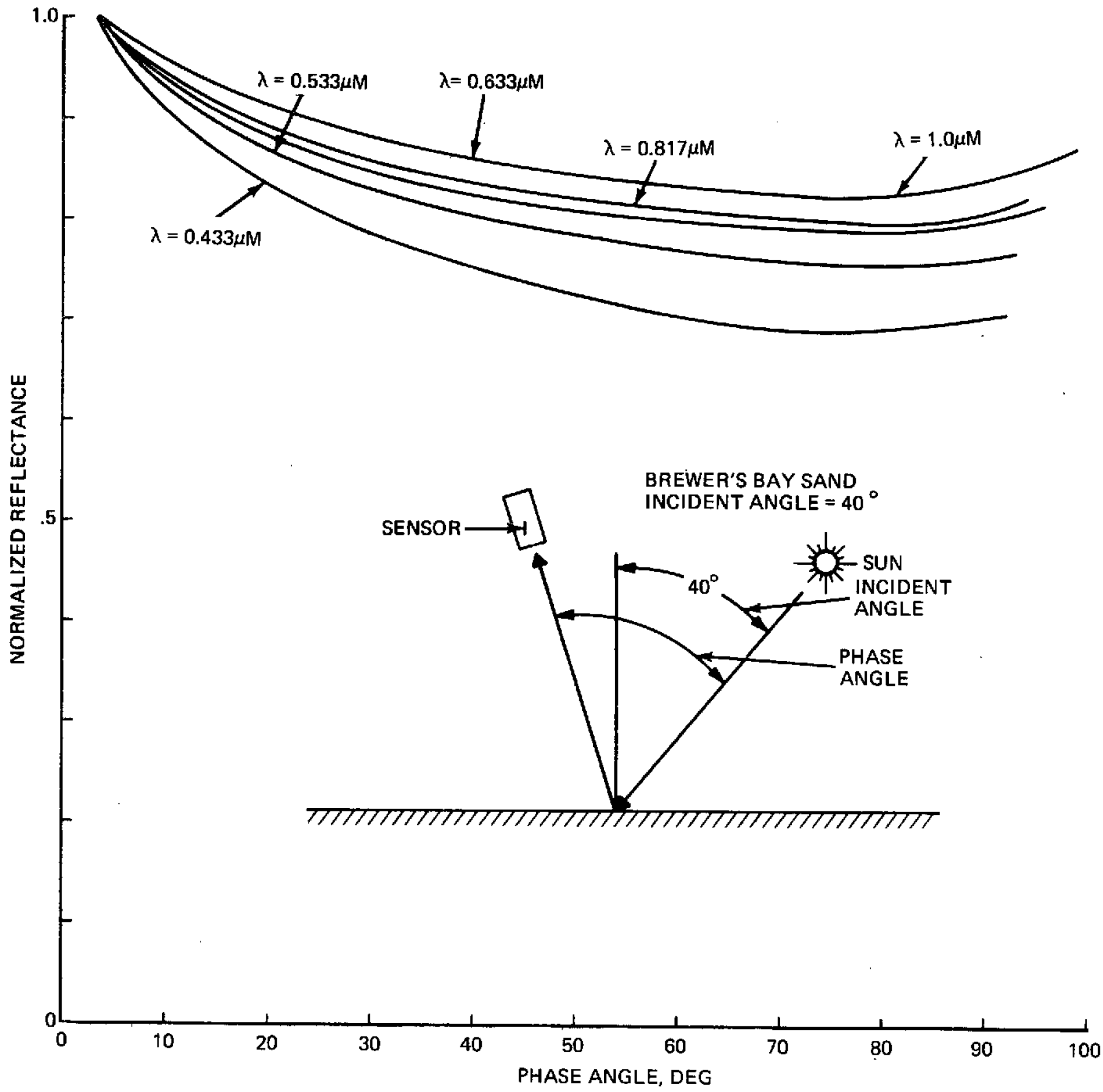

Figure 2-3. Laboratory Spectrophotometric Properties of Brewers Bay Beach Sand from Test Panel Location at an Incident Angle of 40°

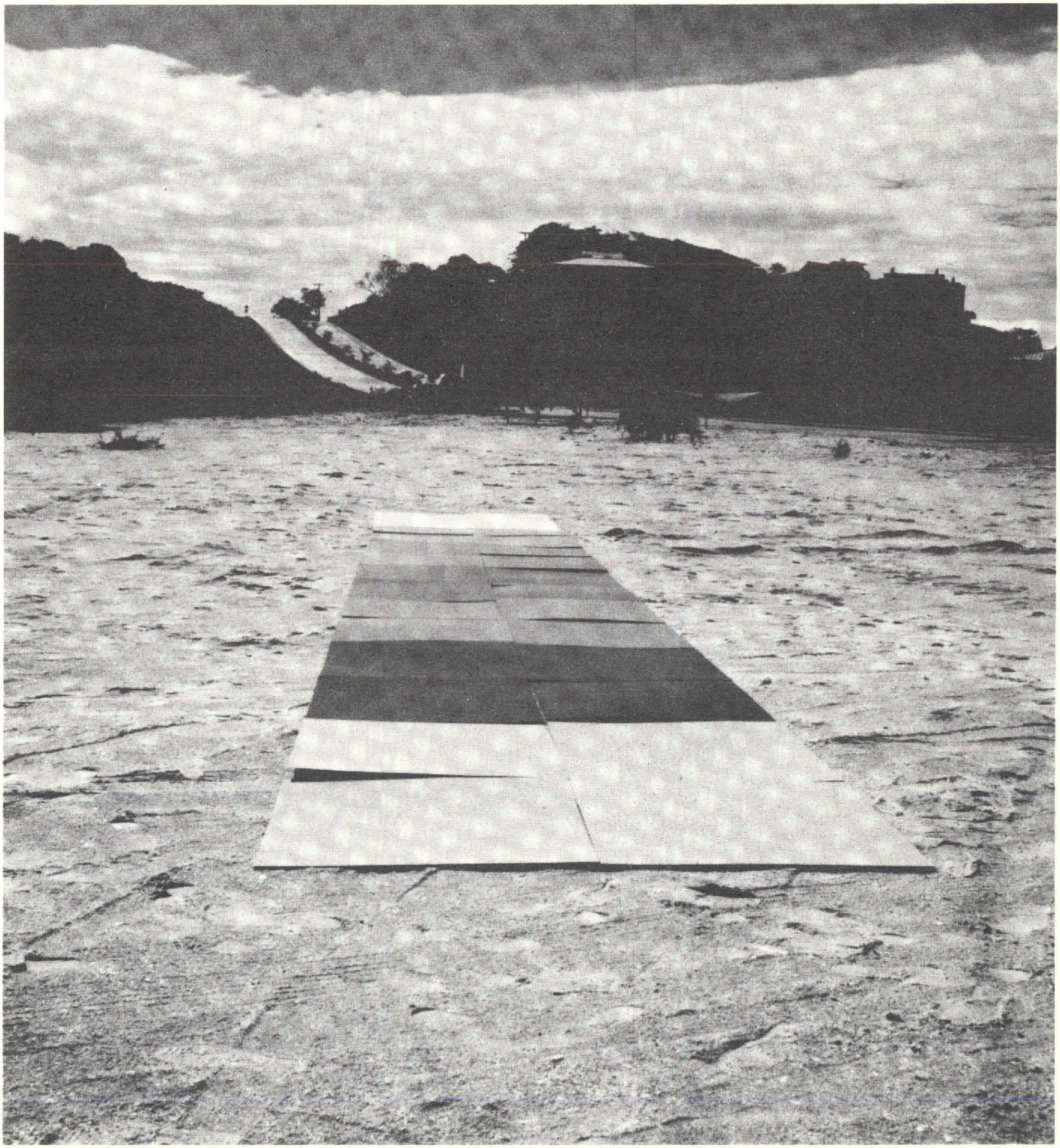

Figure 2-4. Ground View of Color Test Panels on Brewers Bay Beach

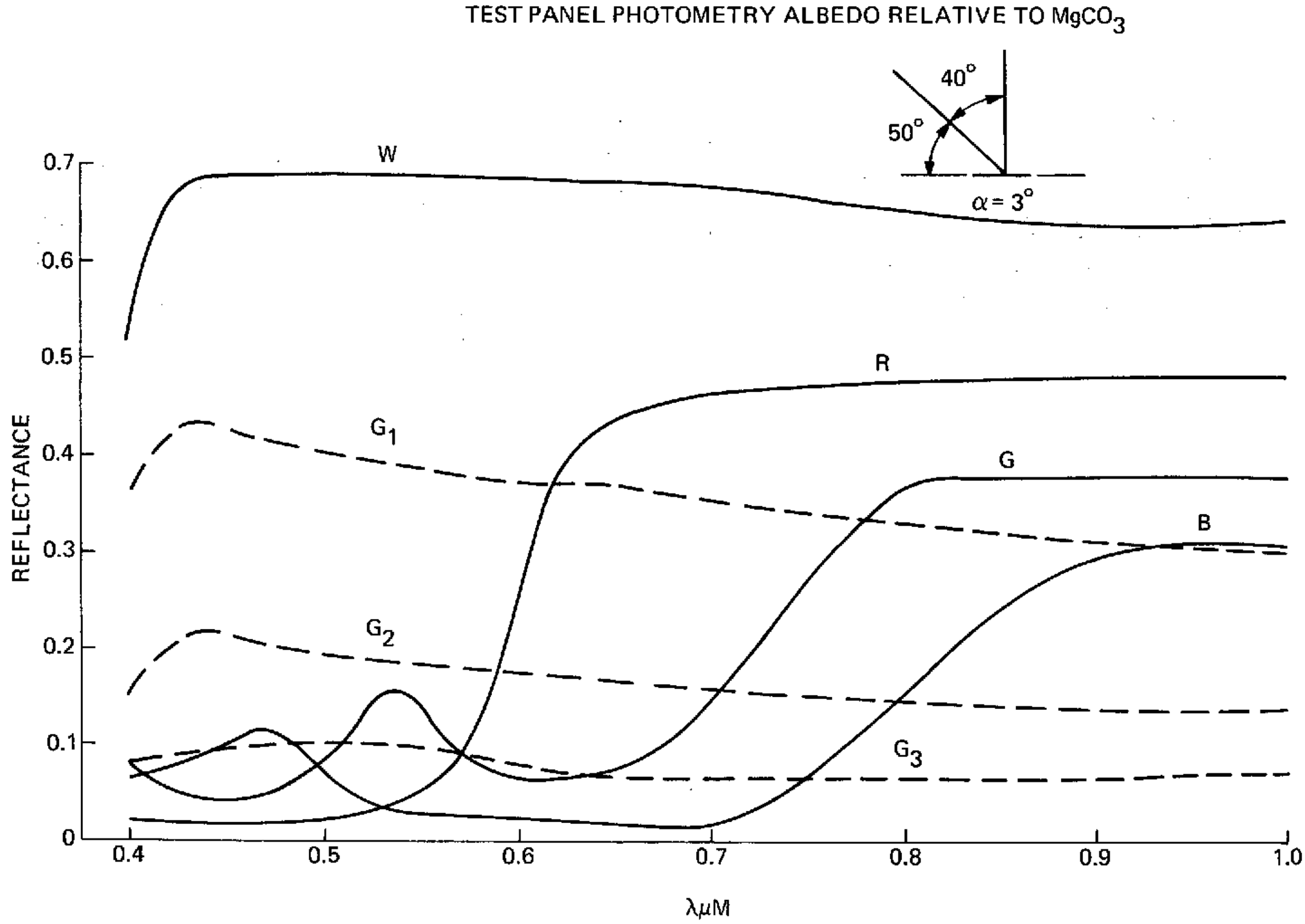

Figure 2-5. Laboratory Spectral Reflectance (Relative to $MgCO_3$) of Test Panels at an Incident Angle of 40°, and a Phase Angle of 3° (W-White; G1, G2, G3 - Gray Shades; R-Red; G-Green; B-Blue (From Ref. 5)

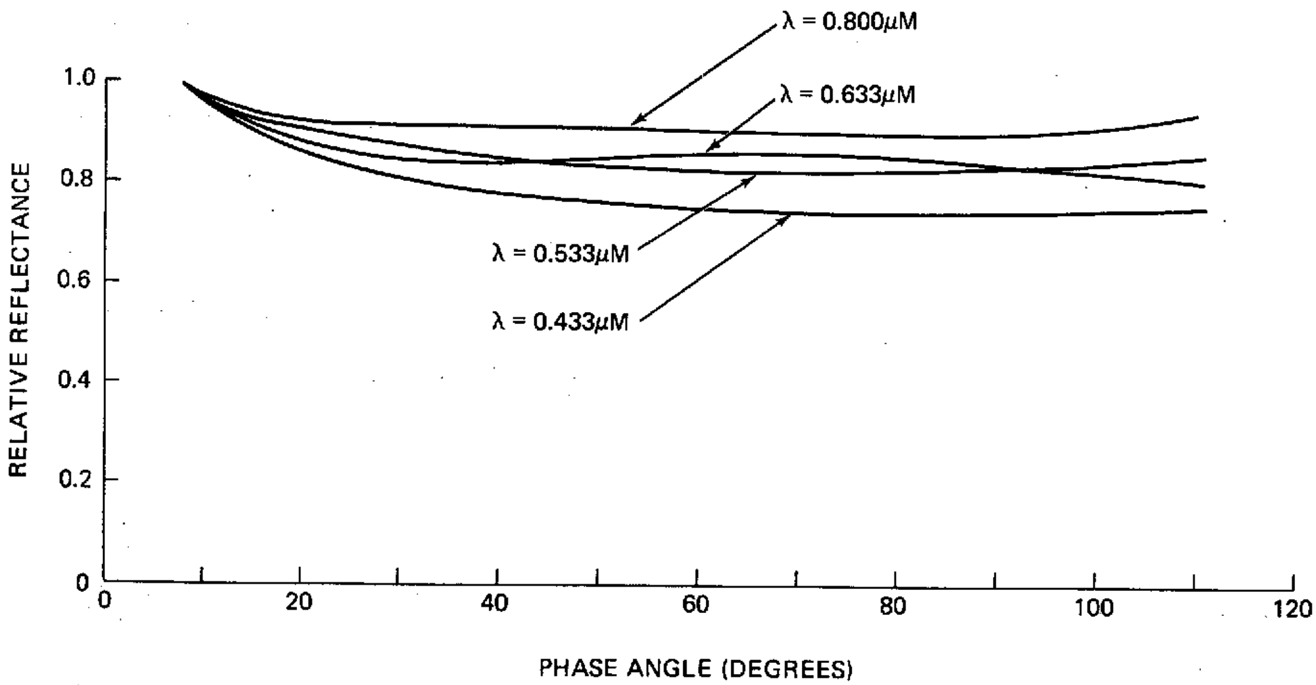

Figure 2-6. Laboratory Spectrophotometric Properties of 3-M Nextel White 110-A-10 Paint as a Function of Phase Angle and Wavelength for an Incident Illumination Angle of 40° (from Ref. 5)

and Brewers Bay Beach sand), the atmospheric absorption, the camera lens and filter absorption, the distribution of brightness in the film plane, and the spectral sensitivity of the film. These elements now will be discussed in that sequence.

Radiance calibration: The ground truth radiance measurements were made with the same portable battery operated 3 degree acceptance angle Minneapolis-Honeywell photometer (with interchangeable narrow-band interference filters) as was used for the in situ harbor water measurements. Measurements were made at Brewers Bay Beach adjacent to the test panel location (see Figure 2-7). The photometer was calibrated with an Eppley thermopile in the laboratory. Measurements were made at center wavelengths of 0.433, 0.533 and 0.633 μm, with the aforementioned filters, having bandpasses of 0.02 μm. The radiance values on the white test panel, when corrected for the wider acceptance bands of the I^2S cameras, are listed in Table 2-2. The light level was subject to some variation because of clouds occasionally obscuring the sun. The observation time, of 0944 hrs, is earlier than the satellite over pass time of 1016 hrs, and later than the aircraft 2000 foot altitude overflight at 0920. These time variations will introduce a small correction to the observations.

Table 2-2. Radiance Measurements on White Test Panel at Brewers Bay Beach on 10/17/72

TIME	BLUE BAND	GREEN BAND	RED BAND
0944	.69 mw/cm^2/sr	1.25 mw/cm^2/sr	2.00 mw/cm^2/sr

Atmospheric absorption: The atmospheric absorption for a 2000 foot altitude flight line would be expected to contain some atmospheric haze contribution, but those at a 6000 foot altitude would contain more. The actual quantitative evaluation of the atmospheric absorption and scattering will be discussed in the subsection on Data Analysis, and tabulated in Table 2-4.

Camera Filters and lenses; brightness in the film plane: The I^2S camera consists of four Schneider Xenotar f/2.8, 100 mm focal length lenses. The four lenses produce four images 9.25 cm square on nine inch wide aerial film. The field of view of the lens in 55.2° (half angle of 27.6°). The relative spectral transmission of the lenses is shown in Figure 2-8a. The transmission varies with wavelength, and this must be taken into account in calculating the attenuation by the lens. The filter attenuation curves are shown in Figure 2-9. The Wratten filter transmission curves are shown for the red, green, and blue sensing cameras; since the infrared band will not be used in the present photometric

Figure 2-7. Radiance Measurements Being Made at Brewers Bay Beach Adjacent to Test Panel Location

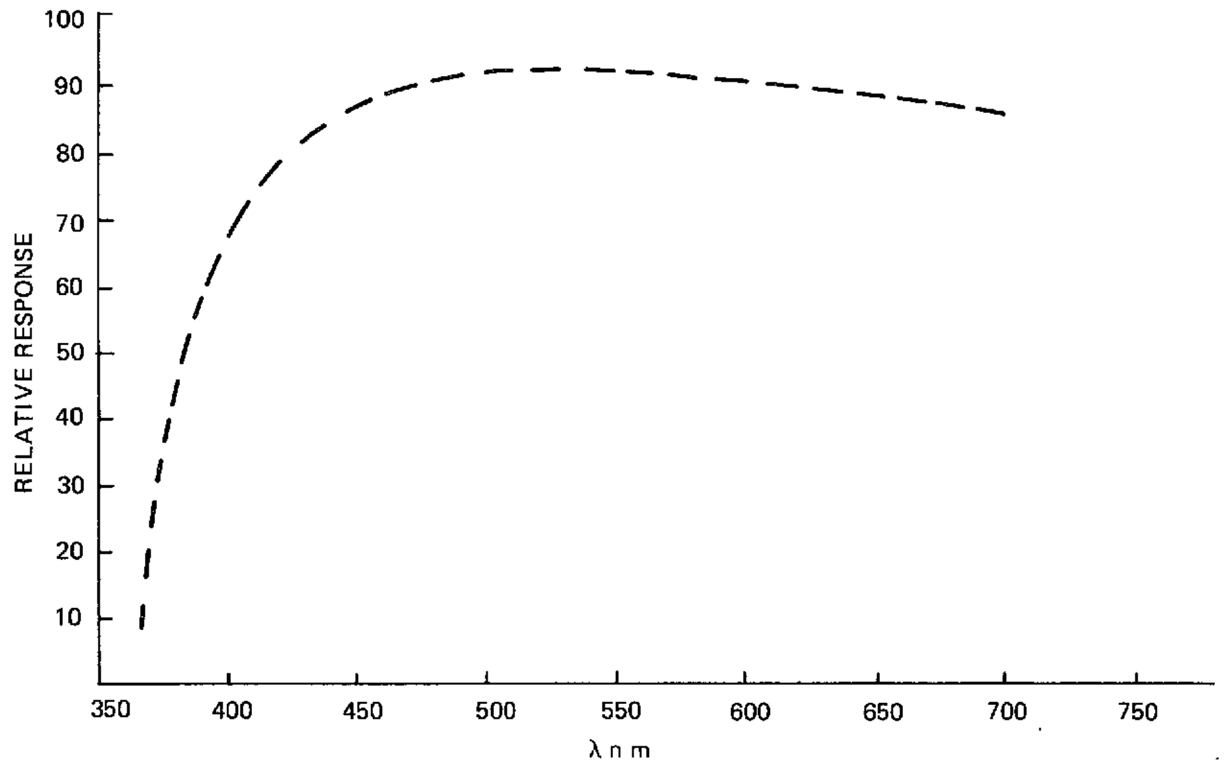

Figure 2-8a. Relative Spectral Transmission of Schneider Xenotar f/2.8/100 mm Lenses at f/2.8 Aperture

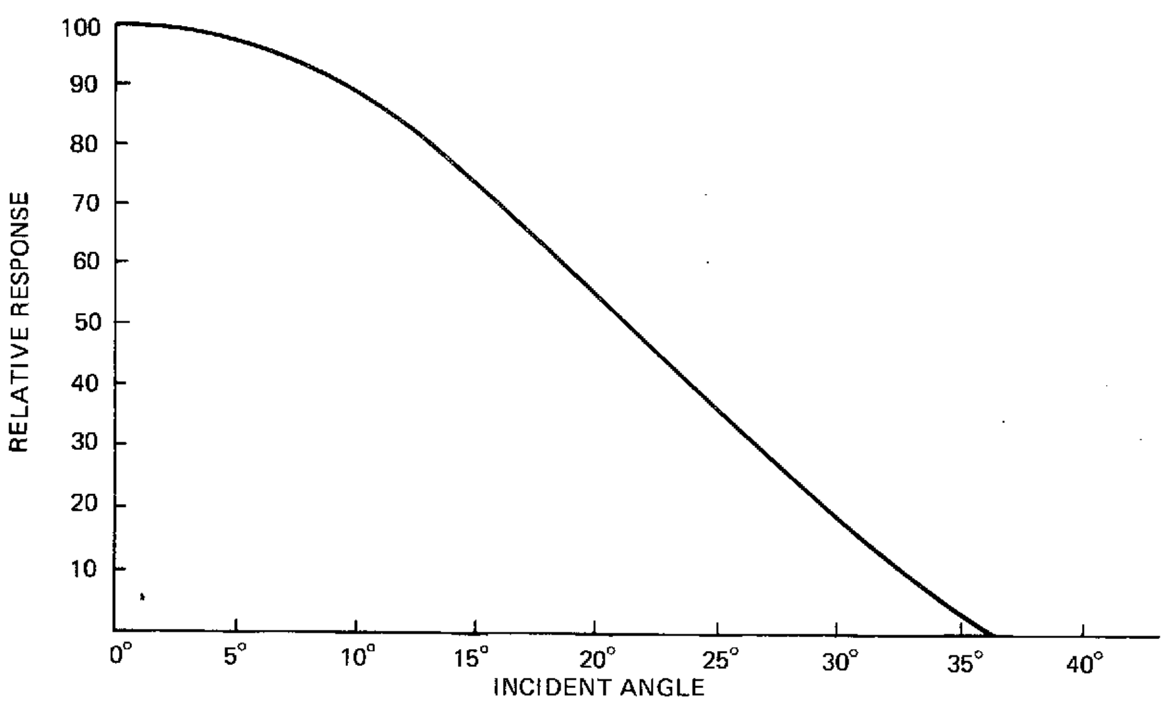

Figure 2-8b. Relative Brightness in the Image Plane of Schneider Xenotar f/2.8/100 mm Lenses at f/2.8 Aperture

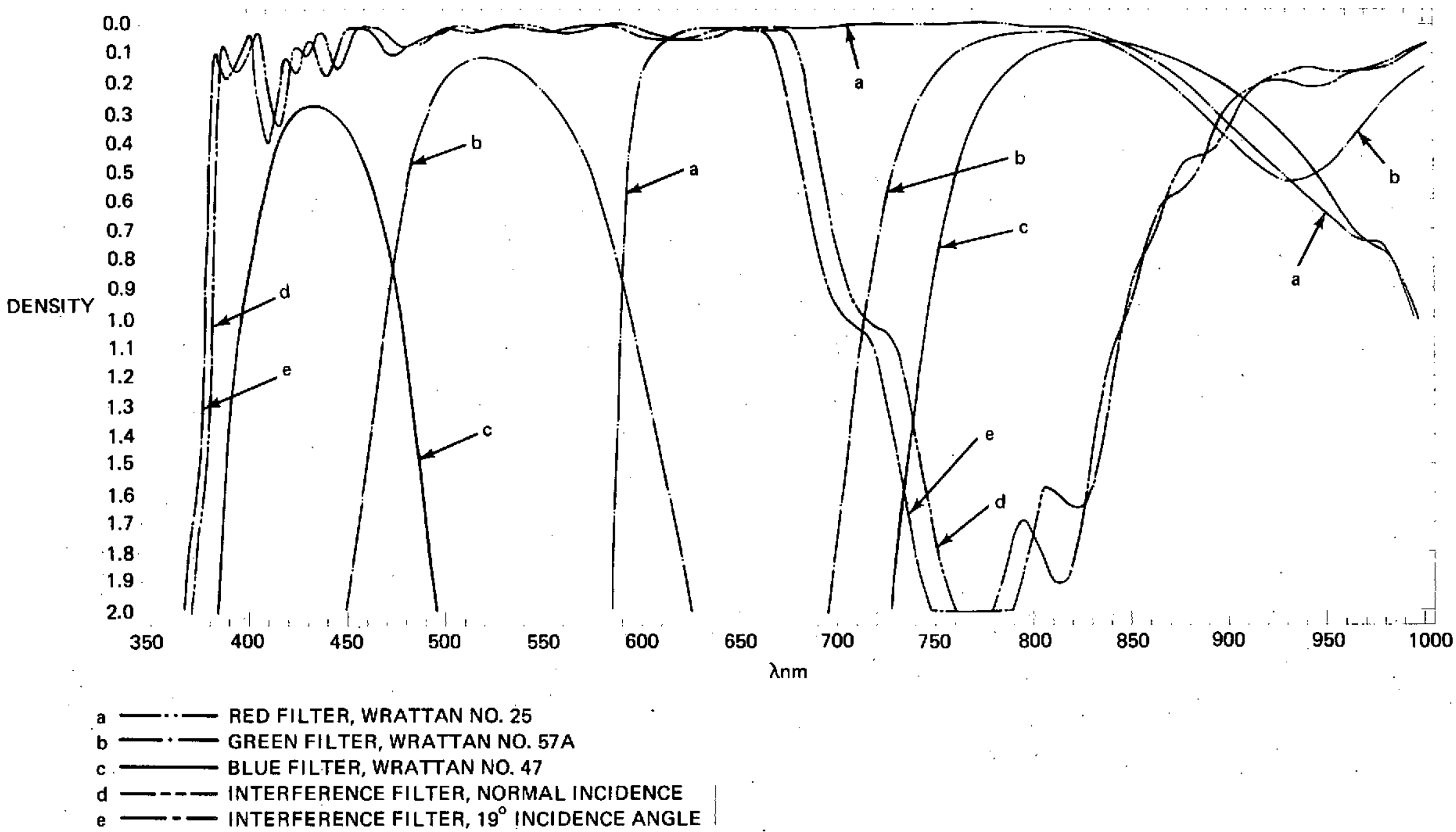

Figure 2-9. Laboratory Spectral Transmission Curves for Red, Green and Blue Camera Band Pass Filters and Infrared Interference Filter; Obtained on Cary 14 Spectrophotometer

analysis (because of the low information content due to water opacity, and the lack of a photometer for ground truth calibrations in the infrared), the filter for this band was not included in the measurements. It is to be noted that the red, green and blue Wratten filters all have pass bands in the infrared; hence an infrared blocking filter is necessary in addition because the Type 2424 film, which was used in this investigation, has a response in the infrared portion of the spectrum (Figure 2-10). These infrared filters must pass the red, green or blue bands and yet block the infrared; the best type of filter for this application is an interference filter. However, interference filters have different characteristics for different angles of incidence.

In Figure 2-9 are presented transmission curves for the green band interference filter. This curve is representative of the other interference filters. It is seen that the transmission at normal incidence is shifted toward shorter wavelengths at 19° incidence angle. This is important because the extreme rays incident through the camera lens enter the filter (which is placed in front of the lens) at an angle of 27.6° to normal, increasing this effect. This can then affect the bandpass of the combination of Wratten filter and interference filter so as to narrow or expand the bandpass, and thus the response of the photographic system will be angularly dependent.

However, inherent in the imaging process of a lens is a $\cos^3$ dependence on incident angle. This is in addition to the angular dependence on the filter transmission properties just mentioned. This $\cos^3$ dependence is quite pronounced and produces a vignetting of the image. Anti-vignetting filters are sometimes employed to minimize this vignetting effect, but they slow down the effective speed of the imaging system. It is also to be noted that the vignetting effect shown in Figure 2-8b is aperture dependent; smaller f stops result in less vignetting. Ultimately the brightness distribution in the film plane must be checked experimentally against imagery having a known brightness distribution. This can be accomplished in the laboratory or in the field; one approach is to photograph a beach area (such as Brewers Bay Beach, St. Thomas) so as to cover an entire frame. Then the brightness variation in the photographic image can be used to calibrate the vignetting effect of the lens. Also, there may be differences between the lenses, and the use of a curve such as Figure 2-8b on one lens would not take these differences into account.

Film sensitivity: The spectral response of the type 2424 film is shown in Figure 2-10. However, this does not reveal the density as a function of exposure. This requires a particular calibration program. Such a calibration program was carried out through the cooperation of Kennedy Space Center/NASA and Manned Space Center/NASA for the present investigation.

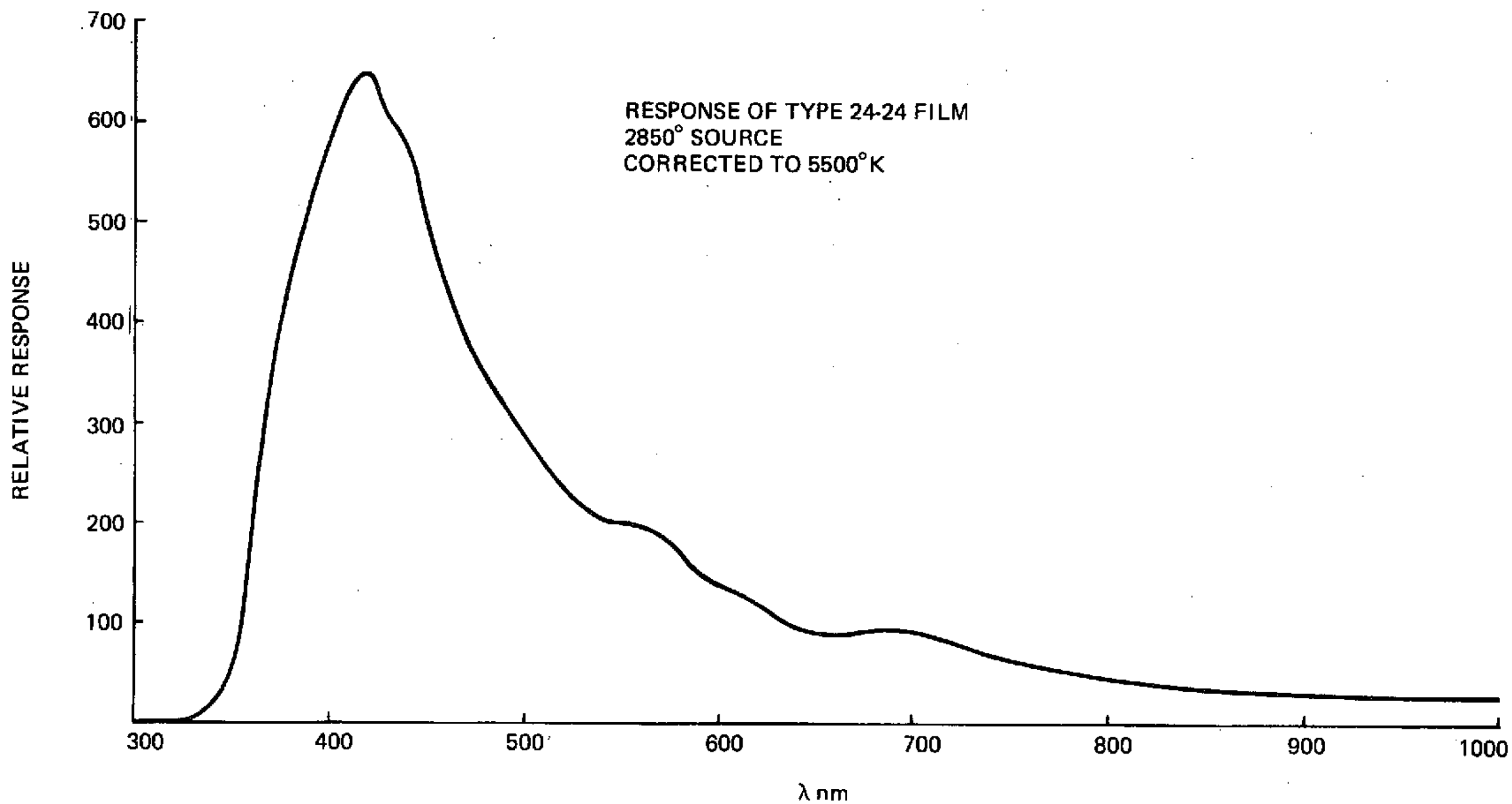

Figure 2-10. Spectral Response of Type 2424 film.

Essentially, the original undeveloped, exposed negative type 2424 film was sent to the Phototechnology Division, Houston. There the film was exposed to a 2850°K lamp using Corning C5900 and C2043 filters. The exposures are tabulated in Table 2-3. Using the exposure information given in Table 2-3, the camera system response may be computed; these data are presented in the last column of Table 2-3. The exposures listed in Table 2-3 have produced densities in the type 2424 negative film from a calibrated step tablet; this calibrated step tablet was exposed on the type 2424 negative film through the three filters. By plotting the measured densities on the negative against the original step tablet calibrated density, an H-D curve is obtained for 3 colors for the 2424 negative film.

Table 2-3. Exposures by Phototechnology Division/Manned Space Center/NASA and System Response on Type 2424 Film in I^2S Camera Used in Thomas Imagery

FILTER	EXPOSURE	ENERGY	CAMERA SYSTEM RESPONSE
47B (Blue) + IR	0.1002 sec	7.9496-10 erg	40 $mw/cm^2/sr$
58 (Green) + IR	0.0399 sec	8.0743-10 erg	67 $mw/cm^2/sr$
25 (Red) + IR	0.0399 sec	7.9155-10 erg	46 $mw/cm^2/sr$

However, as mentioned in Ref. 3, the response of different densitometers depend upon their optical system, and the amount of optical scattering in the film being measured. The measurements made in our program were made on a Joyce-Loebl recording microdensitometer, because it permitted measurements to be made on microscopic areas such as the images of the test panels. The comparative response of the Macbeth and Joyce-Loebl densitometer is presented in Figure 2-11. It is seen that the Macbeth reads lower densities than the Joyce-Loebl, and that the relation is non-linear. The differences are the result of differences in the optical systems of the two units; if a non-scattering absorber were compared in the two densitometers, the readings would be the same. Because of scattering, some of the light is not sensed by the Joyce-Loebl optical system and this leads to the higher density readings on it. This does not lead to any problems as long as one densitometer is used consistently for a set of readings.

The H-D curves for red, green, and blue on the type 2424 negative film are presented in Figures 2-12, 2-13 and 2-14. The exposure is the reading on the Macbeth densitometer, and the density is read on the Joyce-Loebl microdensitometer with an effective aperture of

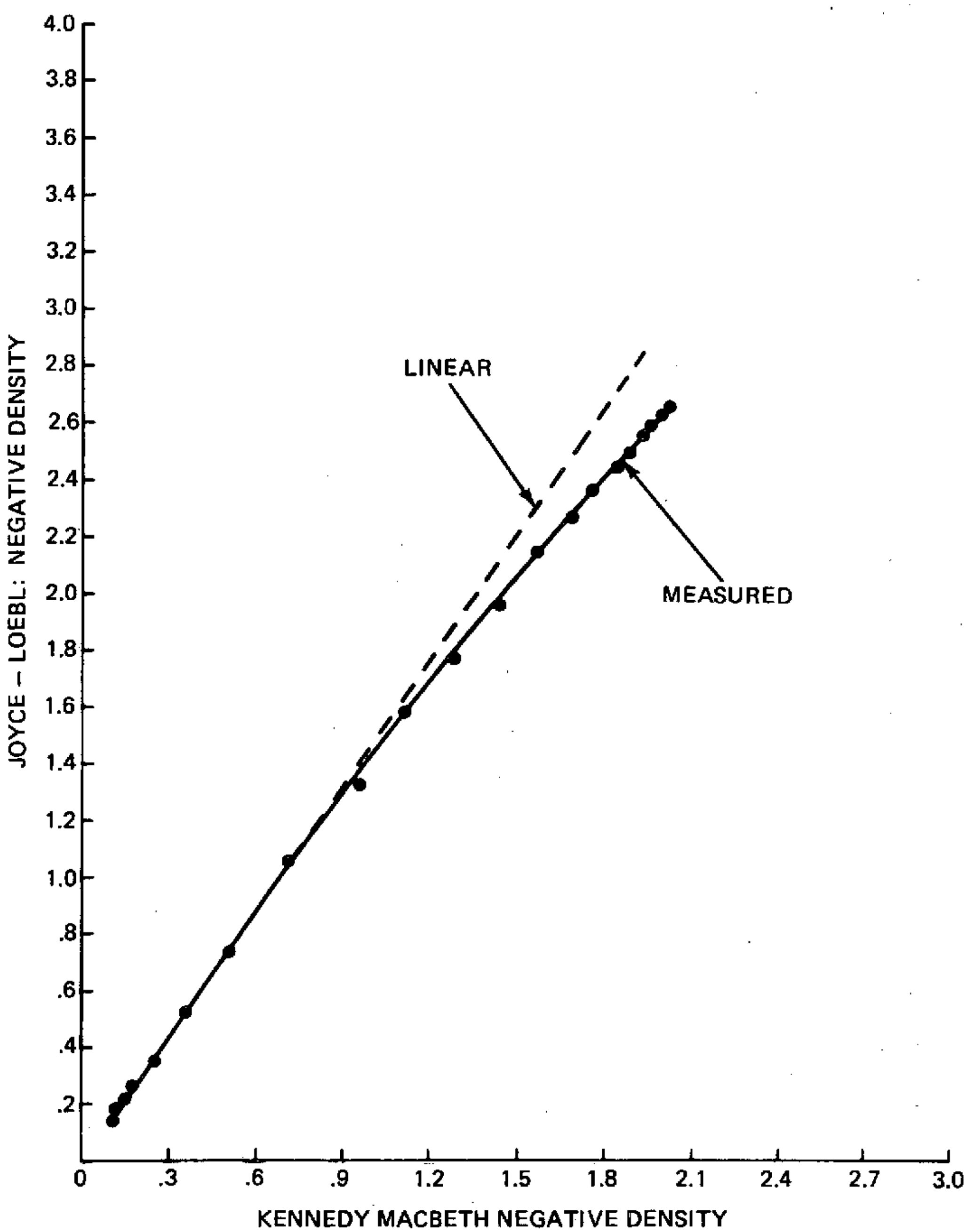

Figure 2-11. Macbeth to Joyce - Loebl Densitometer Conversion

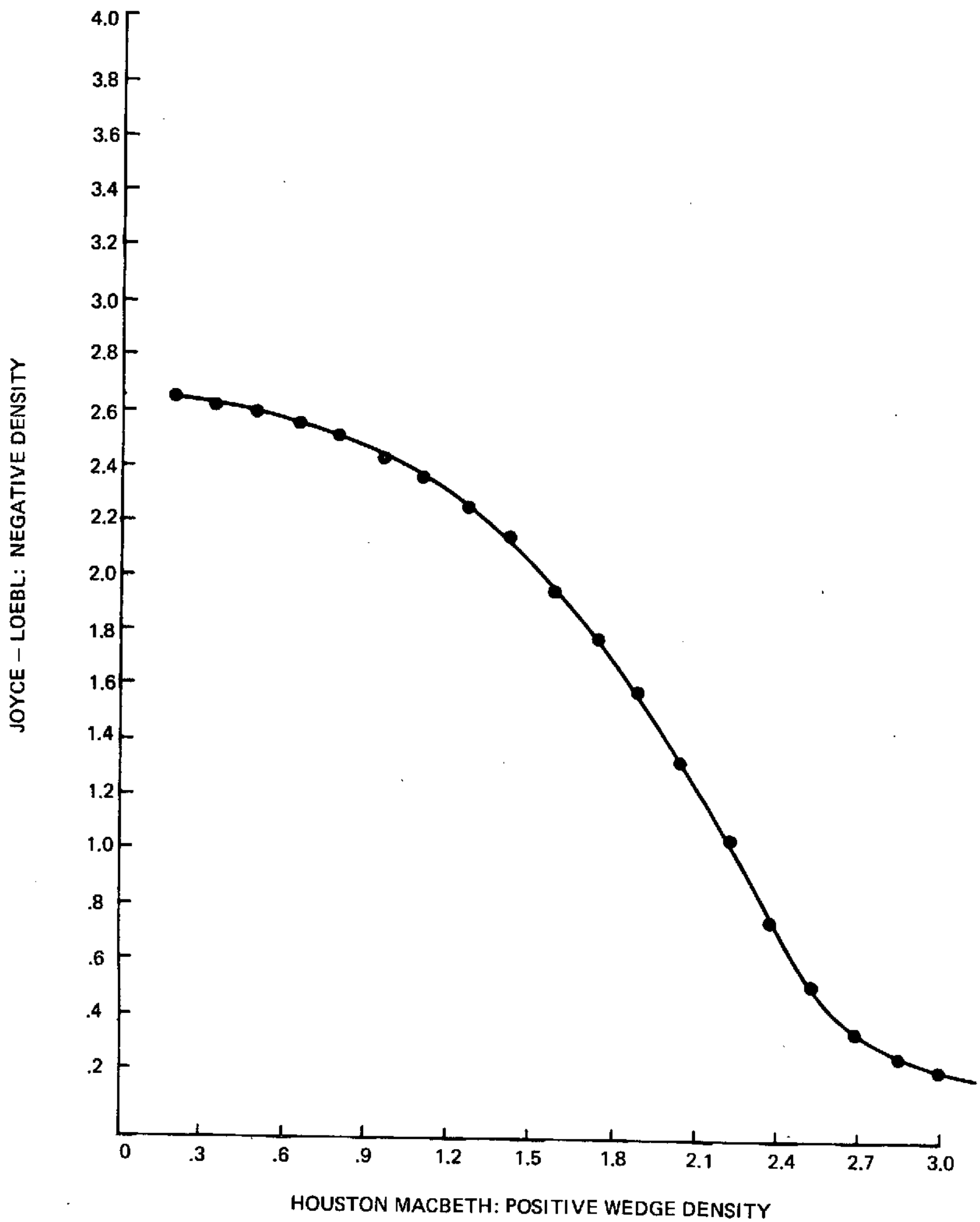

Figure 2-12. Red Response of Type 2424 film; Macbeth vs Joyce-Loebl (with No. 25 and IR Filters)

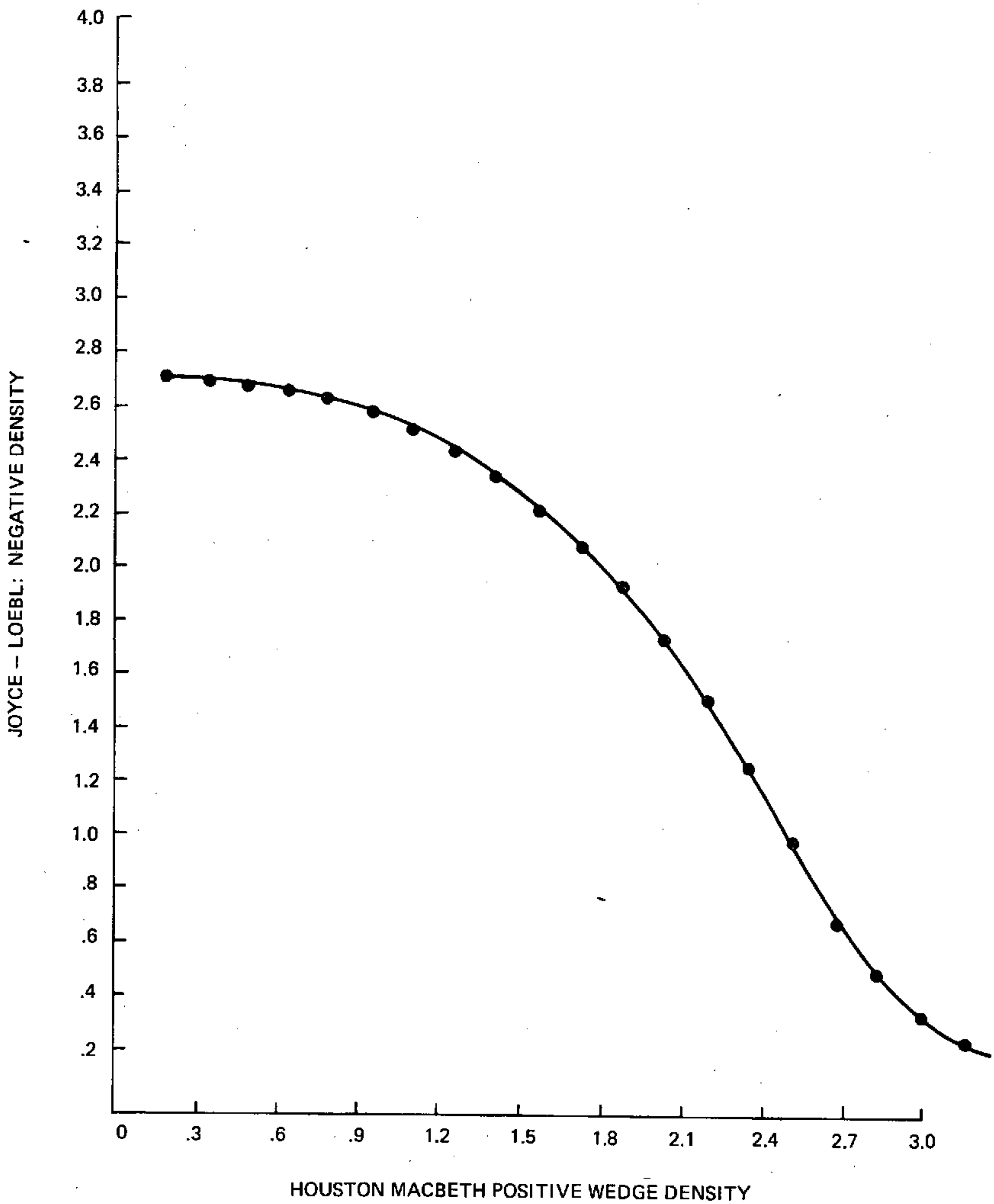

Figure 2-13. Green Response of Type 2424 film; Macbeth vs Joyce - Loebl (with No. 57A and IR filters)

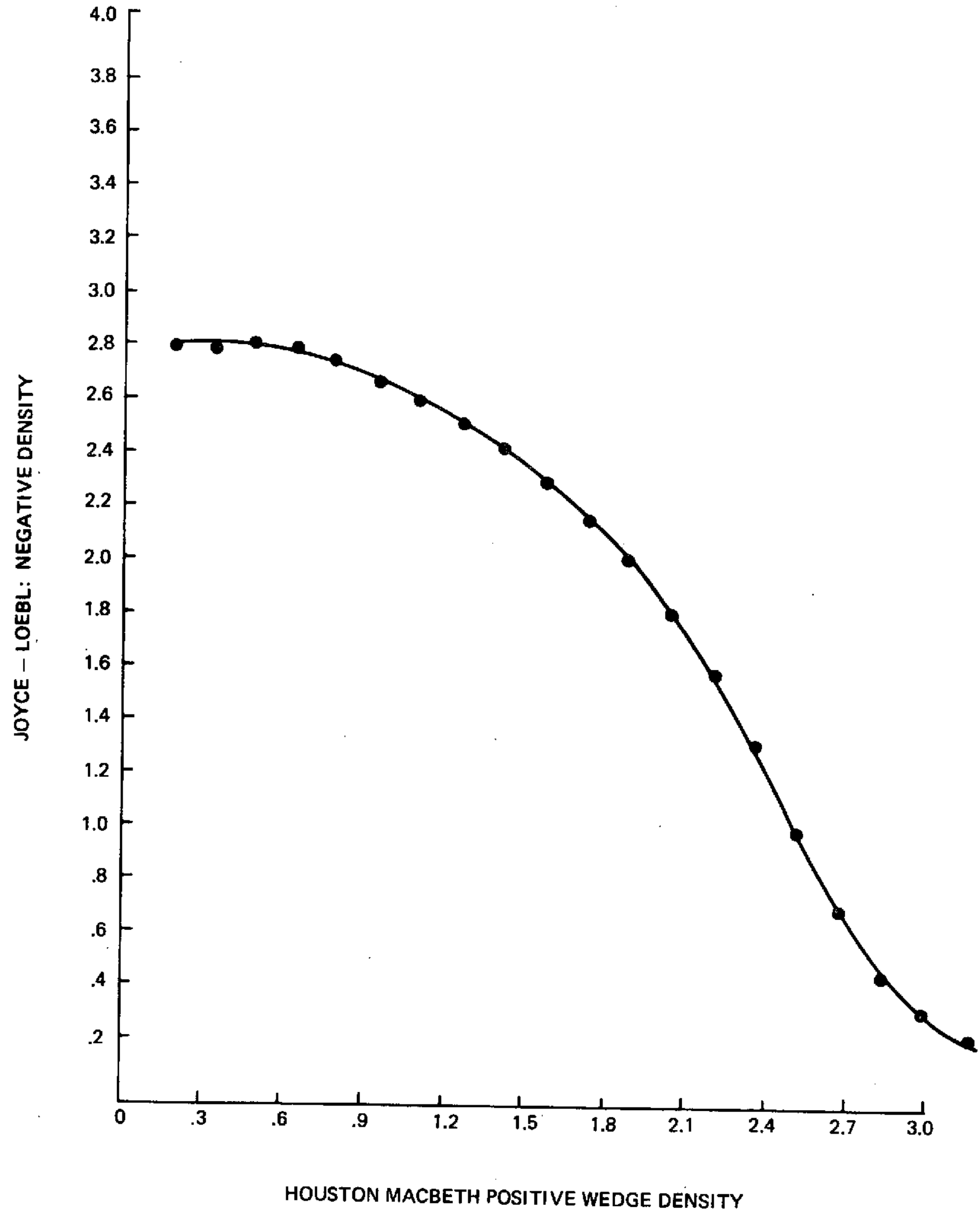

Figure 2-14. Blue Response of Type 2424 film; Macbeth vs Joyce-Loebl (with No. 47B and IR Filters)

150μ. This aperture was large enough to average over the photographic emulsion grains. It is to be noted that the images of the original step wedge were not constant in density variation, but increased slightly in density (due to scattering) toward the less dense end of the wedge.

The type 2424 negative was then used by NASA, Kennedy to make a duplicate positive print. By printing one of the step wedge images from the type 2424 film (No. 25 filter one) on the duplicate positive, the H-D curve for the duplicate positive is obtained (Figure 2-15). There are two curves shown in Figure 2-15, one for the head and tail of a duplicate positive roll prepared in June 1973, and those of another duplicate positive prepared in July 1973 of Frame 0004 containing the test panels. The second duplicate positive was necessitated by inferior resolution in the duplicate positive Frame 0004 of the red and green I^2S bands. Because of processing variations, the positive densities may vary by as much as 0.2D (Joyce-Loebl) for the same exposure. This is one of the limitations of photograhic photometry.

The method of use of the sensitometry curves (Figures 2-12 through 2-15) is as follows: first a density is measured with the Joyce-Loebl microdensitometer on the duplicate positive of an area of interest. This density of the positive on the ordinate of Figure 2-15 yields the type 2424 negative density, as read on the Joyce-Loebl for the black and white image of the red, green or blue bands. Then using either Figure 2-12, 2-13, or 2-14 depending upon whether the red, green, or blue original image was the one of interest that was measured, we determine what was the required Macbeth exposure. Then using this Macbeth exposure (density), and the values listed in Table 3 (Last column), the radiance may be calculated. This procedure will be followed in the section on Data Analysis.

2.2.4 Calibration of the ERTS-1 Data

The IN ORBIT calibration of the ERTS-1 MSS scanner is inoperable because the calibration pulse has dropped considerably and appears to have shifted. Therefore we must depend on ground truth measurements for calibration. However the relative radiance levels from the ERTS-1 are still valid.

Since ground truth was obtained only in the green and red bands, the discussion will be limited to the corresponding ERTS-1 bands 4 and 5.

The calibration area of Brewers Bay Beach is shown in the I^2S Blue Band Photograph (Figure 2-16). The corresponding Grumman Data Systems computer printout from the bulk tape is shown in Figures 2-17a and 2-17b for Bands 4 and 5 respectively. The digital value used for computation is the highest value for the Coral Beach Sand, which occurred along

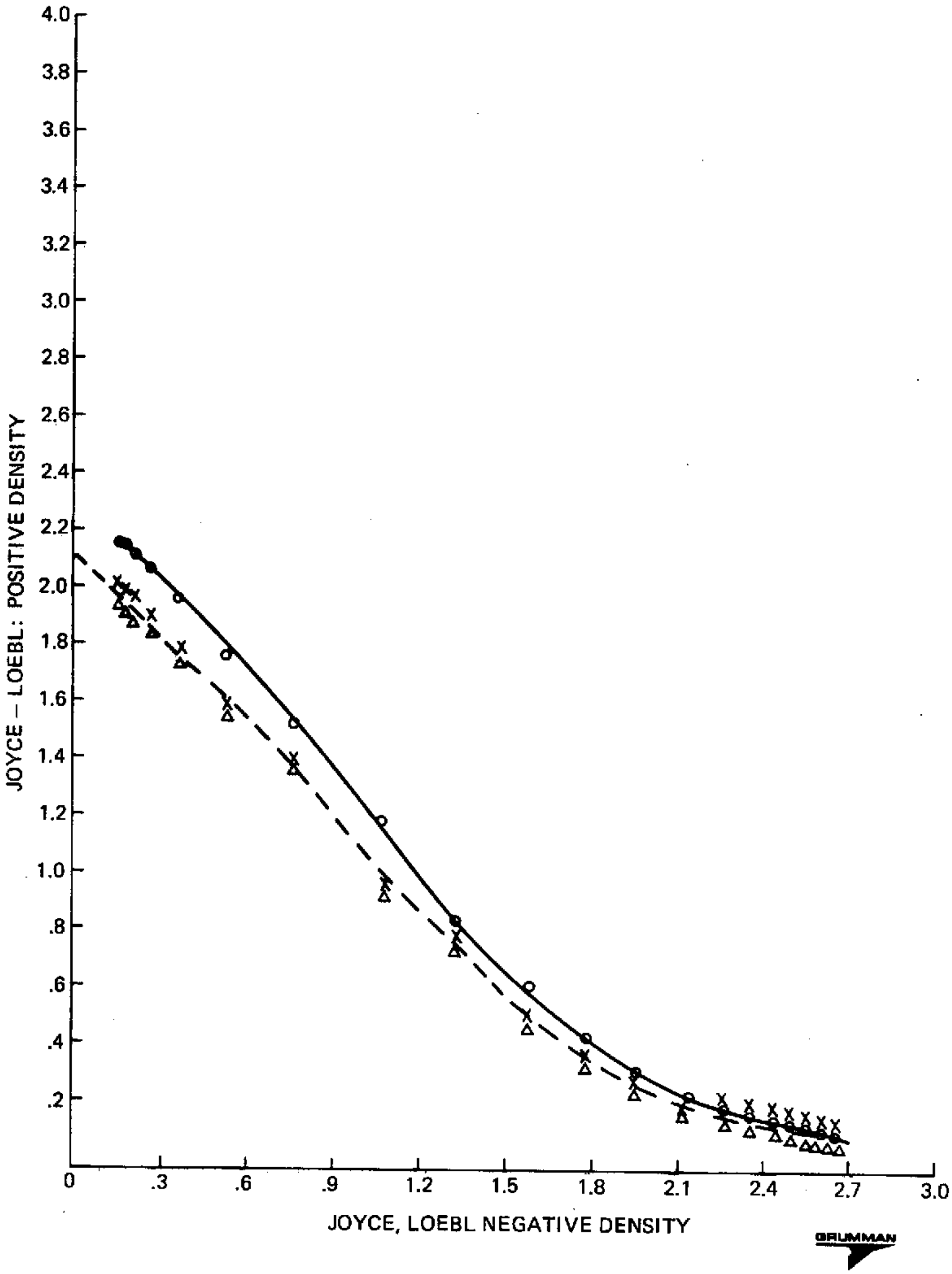

Figure 2-15. Response of Duplicate Positive Print on June 1973 Print, and July 1973 Print (X-Head, June 1973, △ Tail, June 1973; ⊙ July 1973 print)

SPECTRAL BAND .410 TO .470μ

Figure 2-16. I^2S Aircraft Photograph of Brewer's Bay Beach Calibration Test Site

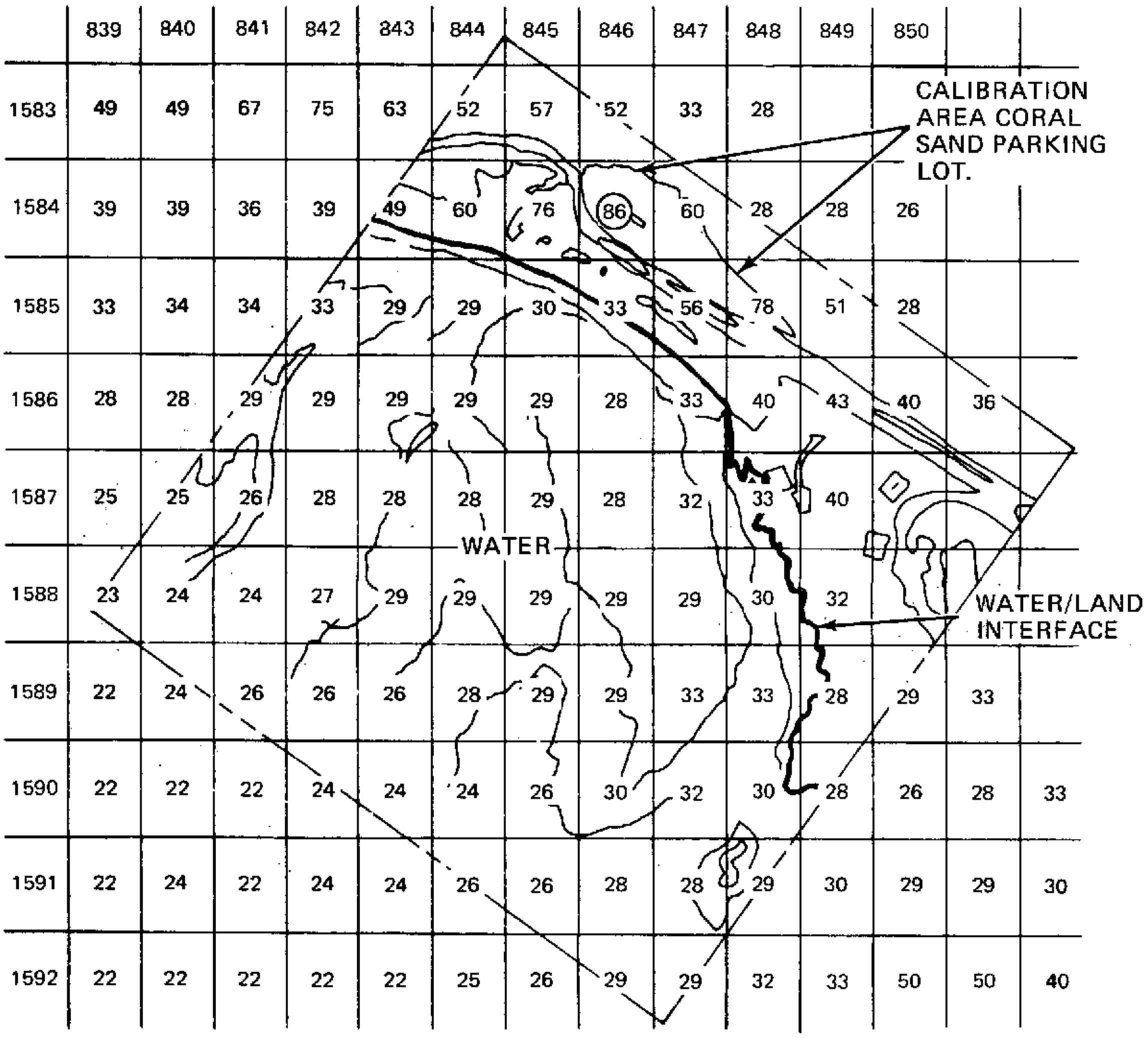

	839	840	841	842	843	844	845	846	847	848	849	850		
1583	49	49	67	75	63	52	57	52	33	28				
1584	39	39	36	39	49	60	76	86	60	28	28	26		
1585	33	34	34	33	29	29	30	33	56	78	51	28		
1586	28	28	29	29	29	29	29	28	33	40	43	40	36	
1587	25	25	26	28	28	28	29	28	32	33	40			
1588	23	24	24	27	29	29	29	29	29	30	32			
1589	22	24	26	26	26	28	29	29	33	33	28	29	33	
1590	22	22	22	24	24	24	26	30	32	30	28	26	28	33
1591	22	24	22	24	24	26	26	28	28	29	30	29	29	30
1592	22	22	22	22	22	25	26	29	29	32	33	50	50	40

BREWER'S BAY BEACH CALIBRATION TEST SITE

BAND #4 SCENE 1086-14162

SCALE = $\frac{1}{6,100}$

CROSS TRACK ≅ 58 M/CHARACTER

ALONG TRACK ≅ 78 M/CHARACTER

Figure 2-17a. ERTS-1 MSS Bulk Band #4 Print Out, Scaled to Overlay I^2S Photograph of Brewer's Bay Beach Calibration Test Site. (Figure 2-16.)

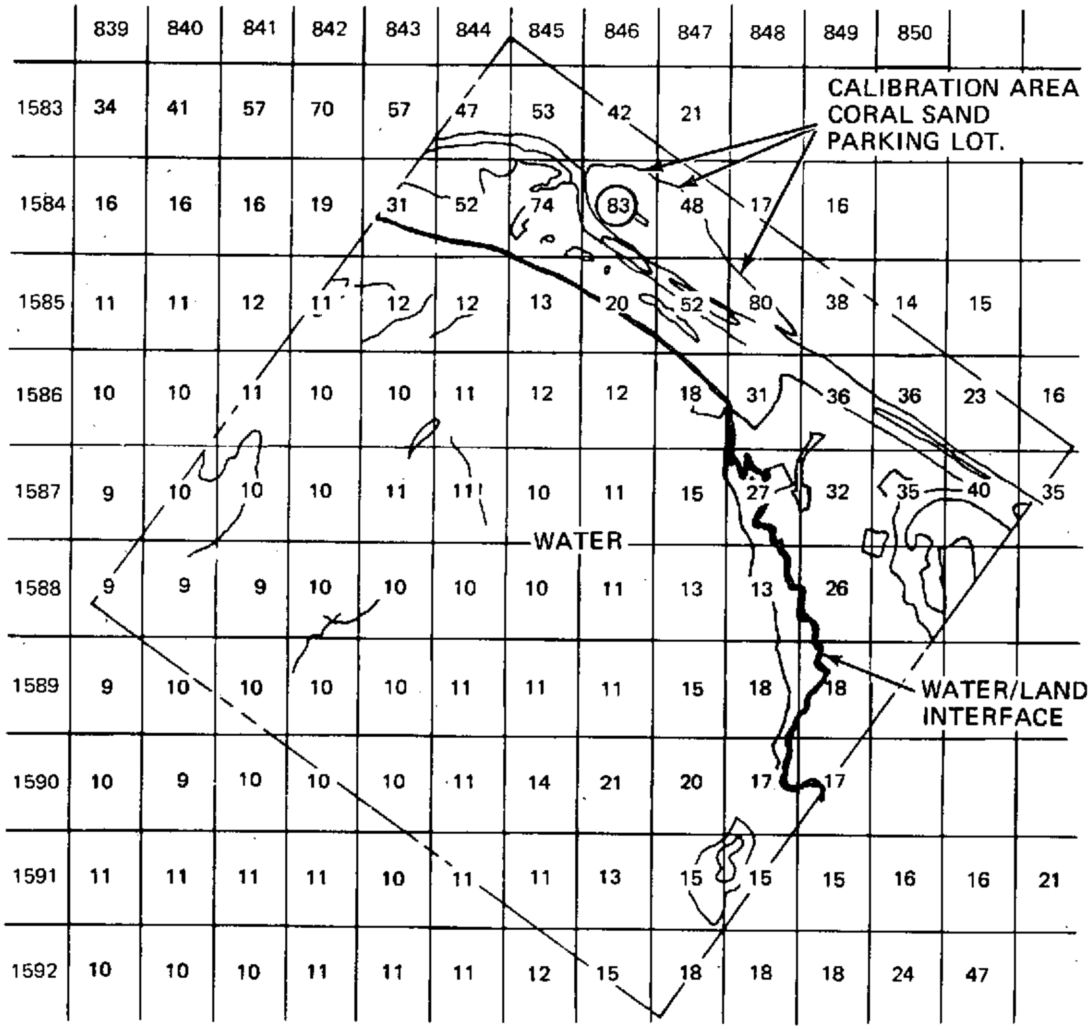

	839	840	841	842	843	844	845	846	847	848	849	850		
1583	34	41	57	70	57	47	53	42	21					
1584	16	16	16	19	31	52	74	83	48	17	16			
1585	11	11	12	11	12	12	13	20	52	80	38	14	15	
1586	10	10	11	10	10	11	12	12	18	31	36	36	23	16
1587	9	10	10	10	11	11	10	11	15	27	32	35	40	35
1588	9	9	9	10	10	10	10	11	13	13	26			
1589	9	10	10	10	10	11	11	11	15	18	18			
1590	10	9	10	10	10	11	14	21	20	17	17			
1591	11	11	11	11	10	11	11	13	15	15	15	16	16	21
1592	10	10	10	11	11	11	12	15	18	18	18	24	47	

BREWER'S BAY BEACH CALIBRATION TEST SITE

BAND #5, SCENE 1086-14162

SCALE = $\frac{1}{6,100}$

CROSS TRACK = 58 M/CHARACTER

ALONG TRACK = 78 M/CHARACTER

Brewer's Bay Beach Calibration Test Site
ERTS-1 Scene 1086-14162 MSS Band #5

Figure 2-17b. ERTS-1 MSS Bulk Band #5 Print Out, Scaled to Overlay I^{2}S Photograph of Brewer's Bay Beach Calibration Test Site. (Figure 2-16.)

track line 1584 and across track line 846. This value is least likely to have been apprecia-bly affected by the adjacent lower reflectance water or tree area in either the green (Band 4) or red (Band 5). This highest value is circled on Figures 2-17a and 2-17b. There is the possibility of some error being introduced by this procedure.

In order to convert the digital levels on Figures 2-17a and 2-17b to the true radiance of the Brewers Bay Beach sand, the atmospheric scattering and attenuation must be taken into account. These atmospheric corrections are listed in Table 2-4 for ERTS-1 Bands 4 and 5. The clear atmospheric attenuation (from Ref. 6) is listed in the second column, and the atmospheric scattered radiance in the third column. The atmospheric scattered radiance was derived from sky photometric measurements at Brewers Bay Beach (Figure 7), of clear blue sky in a direction away from the sun.

Table 2-4. Atmospheric Corrections

BAND	CLEAR (1) ATMOSPHERIC ATTENUATION (%)	ATMOSPHERIC SCATTERED RADIANCE ($mw/cm^2/sr$)
4	17	.13
5	10	.04

(1) Reference 6

By using the corrections in Table 2-4, and the digital levels in Figures 2-16 and 2-17, the radiance levels at the surface, based on ERTS-1 bulk digital data, may be computed. The results of these computations are presented in the last column of Table 2-5, with the intermediate computational steps shown. The comparisons of these levels with the ground measurements and photographic imagery will be made in the Data Analysis section following.

The ERTS-1 imagery was found to be unusable for microdensitometry for various reasons. The Band 5 imagery was unusable because of horizontal striations caused by non-uniform gain in the ERTS-1 sensor channels. There were also displacements of some lines horizontally. Band 4 posed problems as to the location of the shore lines, as fiducial points, to initiate microdensitometric scans. The I^2S viewer was used to superimpose the imagery, and some photographs were made; however for quantitative work, the processed bulk tapes proved to be the most suitable.

Table 2-5. Brewer's Bay Beach Radiances from ERTS-1 Data for Bands 4 and 5

	1 COUNT 127 BASE	2 COUNT 63 BASE (1/2 COL. 1)	3 GSFC CALIBR TABLE (VOLT. SIG.)	4 % RADIANCE FULL SCALE (COL. 3x25)	5 EQUIVALENT RADIANCE AT ERTS-1 (COL. 4xR) (mw/cm^2/sr)	6 ATMOSPHERIC SCATTERING CORRECTION (COL. 5-S) (mw/cm^2/sr)	7 RADIANCE AT SURFACE (ATMOS. ATTEN.) (CORRECTION) (COL. 6xA) (mw/cm^2/sr)
				%	(R = 2.48)	(S = .13)	(A = 1.17)
BAND 4	86	43	1.916	48	1.19	1.06	1.24
BAND 5	83	41 1/2	1.877	47.0	.94	(S = .04) .90	(A = 1.10) .99

2.3 DATA ANALYSIS

This section is concerned with an analysis of the calibration procedures, and the determination of the validity and the consistency of Brewers Bay Beach and test panel ground measurements, I^2S imagery densitometry of these objects, and the ERTS-1 computer processed bulk CCT data of Brewers Bay Beach. Also considered will be the validity of the atmospheric corrections.

2.3.1 Aircraft I^2S Camera Vignetting Correction

The first point to be checked is whether the I^2S vignetting is actually described by Figure 2-8b in view of the fact that the optical bandwidth of the interference filters used with the I^2S cameras is a function of incident angle. This dependence of optical bandwidth on incident angle of the rays into the camera lens will affect vignetting depending upon the properties of the red, green and blue filters and the corresponding interference filter.

Frame 0178, taken at 2000 foot altitude, images Brewers Bay Beach across the entire frame, and thus is suitable for checking vignetting providing the viewing angle dependence of the sand reflectance (Figure 2-3) and the calibrated sensitometry of Figures 2-12 through 2-15 are utilized. The results of such an analysis are presented in Figures 2-18, 2-19 and 2-20 for the red, green and blue imagery respectively. The blue correction is the least, the green is the greatest, and the red intermediate. There is still some residual viewing angle dependence of the Brewers Bay Beach sand in the curves, causing a displacement of the maxima to the northwest direction. This is the result of a variation between the experimental conditions for Figure 2-3 and those actually existing at the time of the Frame 0178 imagery (i.e. sun angle different, and the data for Figure 2-3 was taken in the plane of the sun and the normal to the sand surface). The blue variation (Figure 2-20) is least because the shift in the interference filter bandpass compensates for the vignetting effect of the lens shown in Figure 2-8b. The red vignetting (Figure 2-18) is about that to be expected with no effect from the interference filter, whereas the green vignetting (Figure 2-19) is augmented. These vignetting curves must be used to correct for vignetting when the imagery does not lie in the center of the image field.

2.3.2 Microdensitometry Of I^2S Imagery Of Calibration Test Site (Panels and Beach)

The microdensitometry for the test panels on Frame 0004 ran into some problems. In the initial duplicate positive imagery furnished in June 1973 from a Kodak versamat the blue (1) and infrared (4) bands produced sharp imagery of the test panels. But the test panel imagery of the green (2) and red (3) bands was blurred. This obviated any densitometry

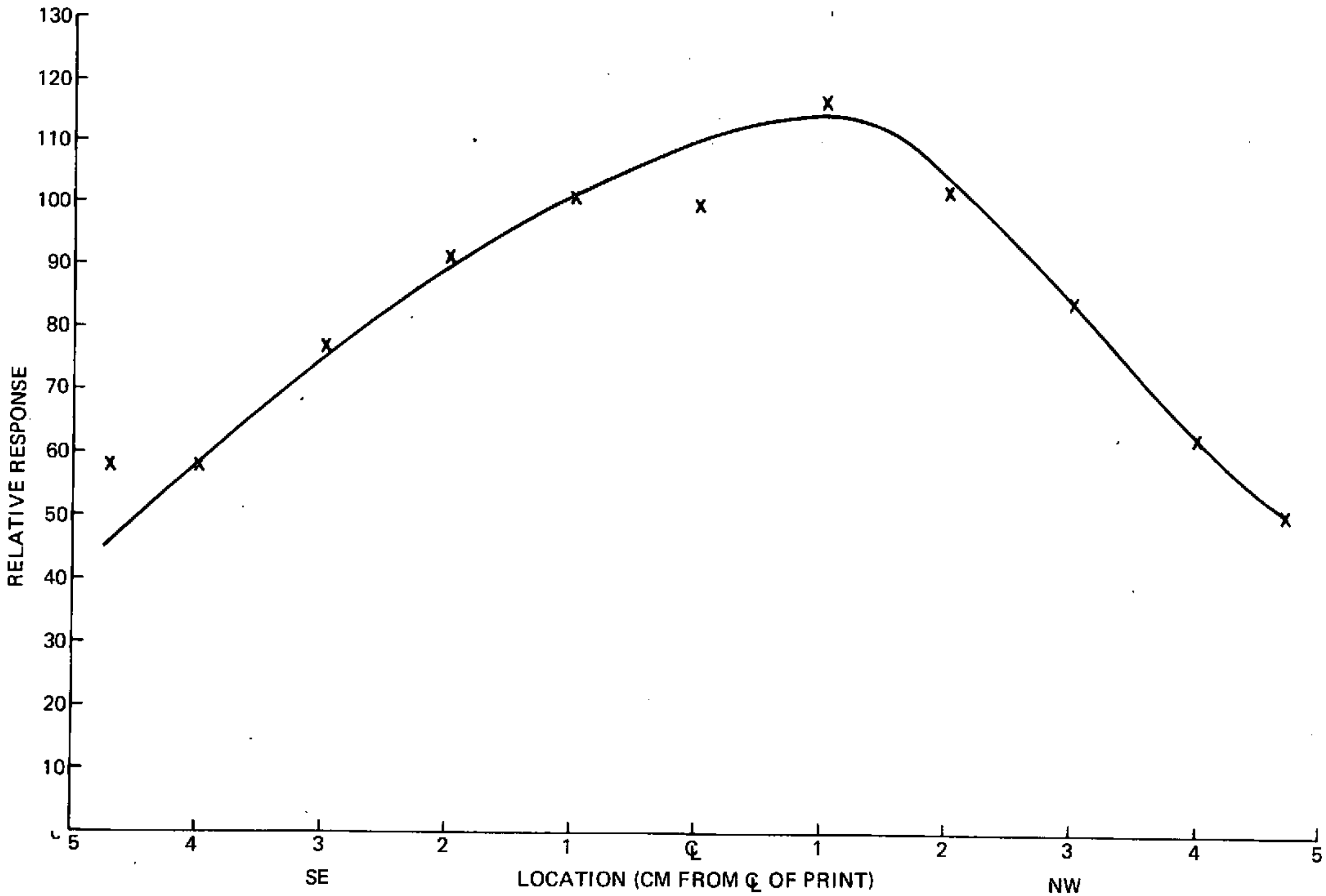

Figure 2-18. Red Vignetting Correction

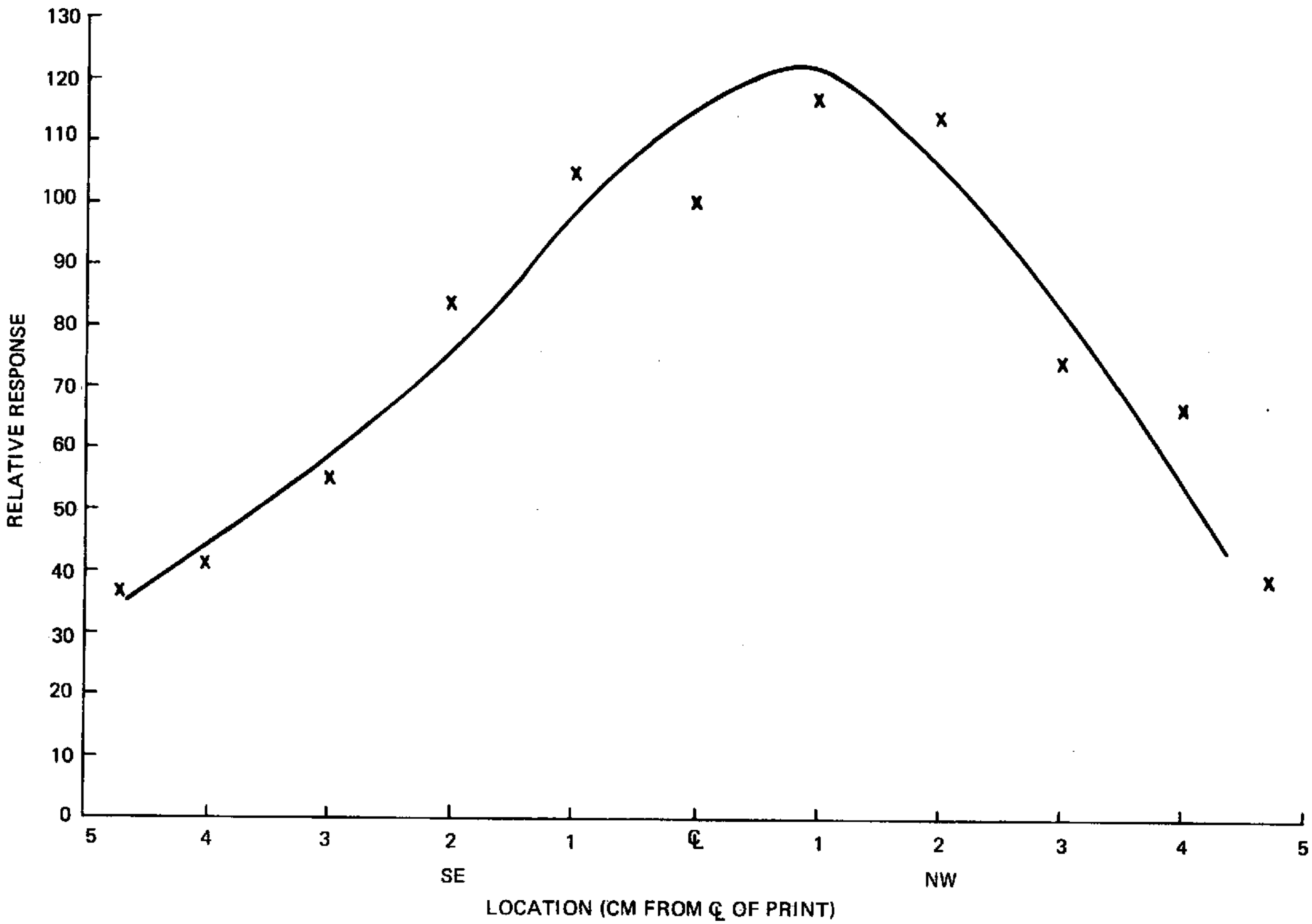

Figure 2-19. Green Vignetting Correction

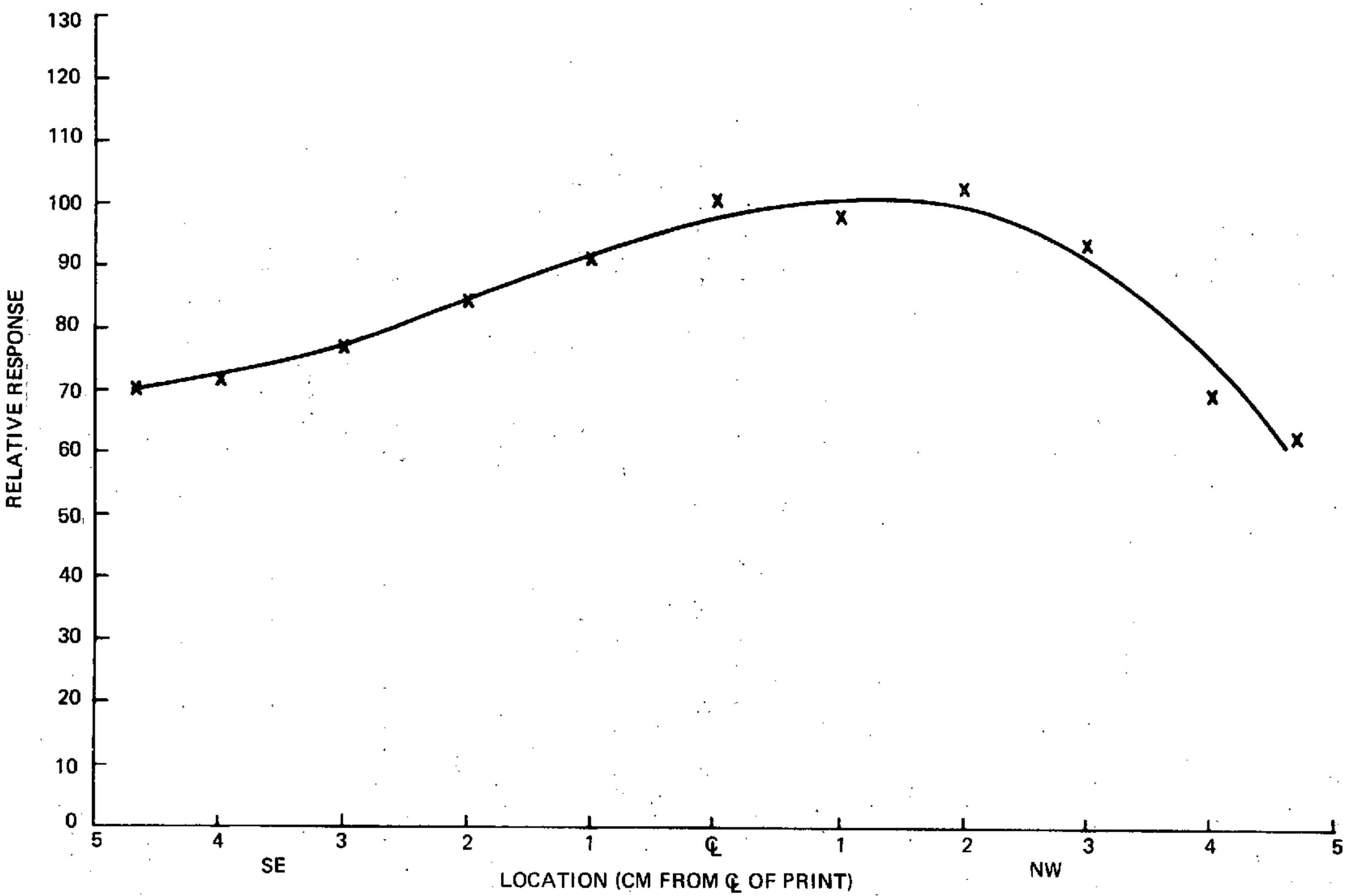

Figure 2-20. Blue Vignetting Correction

measurements. Inspection of the original negative of Frame 0004 revealed sharp imagery in all four bands. An improved remake of that frame was accomplished in July 1973 on the Kodak Versamat #11 CM, (Developer VER 641). The red and green bands of the remake lacked resolution for the test panels; this can be seen by referring to Figures 2-21 and 2-22, which are microdensitometric traces of the test panels on Brewers Bay Beach in the blue and red bands. The effective microdensitometer aperture is 91 μ. (This aperture size was determined experimentally to be sufficiently large to average out over enough grains in the print to yield useful densitometry values.) Figure 2-21 clearly reveals the test panel densitometry in the sharp blue print; even the center junction in the 6 foot panel array is revealed. However in the red band (Figure 2-22) it was difficult to resolve the panels, much less the density values.

The more dense direction in Figures 2-21 and 2-22 is toward the right, and each major division is equivalent to 0.082D.

Using the density levels indicated in Frame 0004 taken at a 2000 ft altitude and the procedure outlined in Table 2-6, we obtain the radiances for the test panels and Brewers Bay Beach sand (Table 2-7). Also listed in Table 2-7 are the photographically determined radiances at a 6000 foot altitude of the Brewers Bay Beach sand at the panel location on the beach parking lot, and also along the beach area both at 0945 hrs. (Frame 0036), and at 1430 hrs. (Frame 178). It is seen that both the red and green radiances decrease with altitude change from 2000 to 6000 feet, but the blue only increases slightly indicating the dominant effect of atmospheric scattering in the blue. The sand near the water is slightly darker than the parking lot at 0945 hrs, but the illumination level increases at 1430 hours for a 6000 foot altitude.

2.3.3 Comparison Of Radiance Measurements, Ground, Aircraft I^2S and ERTS-1

A comparison of the radiance measurements, by the various techniques, of the Brewers Bay Beach sand in the parking lot is presented in Table 2-8. Agreement is excellent except for the ERTS-1 green band. The most probably source of error is that the green atmospheric scattering correction for the ERTS-1 should be greater than that used in Table 2-4. This is evident from the fact that at 2000 foot altitude the photographic green photometric level is greater than at ground level (Table 2-8).

2.3.4 Observed Color Temperature Effects

Another item of atmospheric information may be obtained from the white test panel calibrations: the color temperature of the sun. During aerial photography, the apparent color temperature of the sun will change as a result of atmospheric filtration. This color

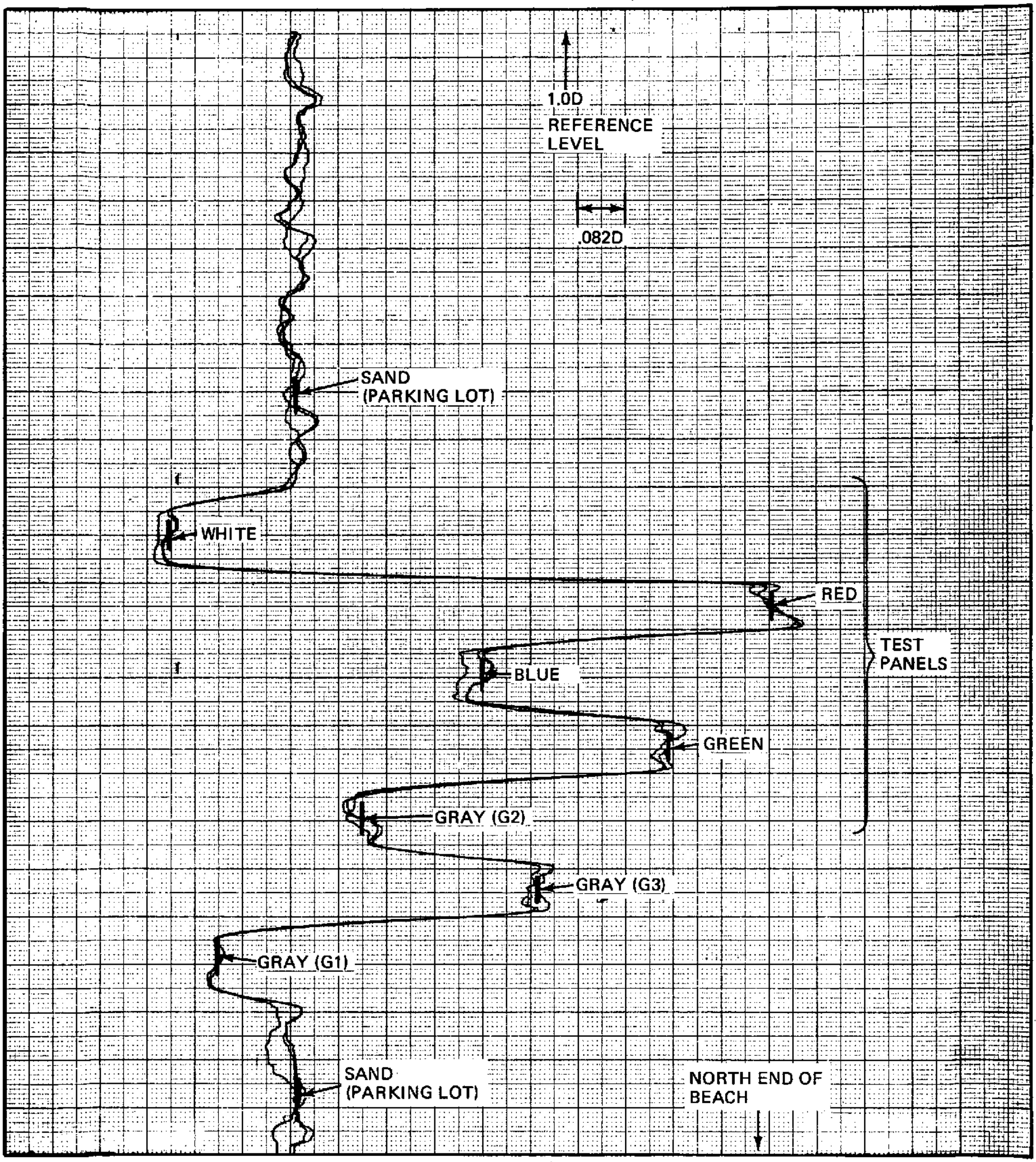

Figure 2-21. Test Panel Microdensitometry Trace in the Blue Band

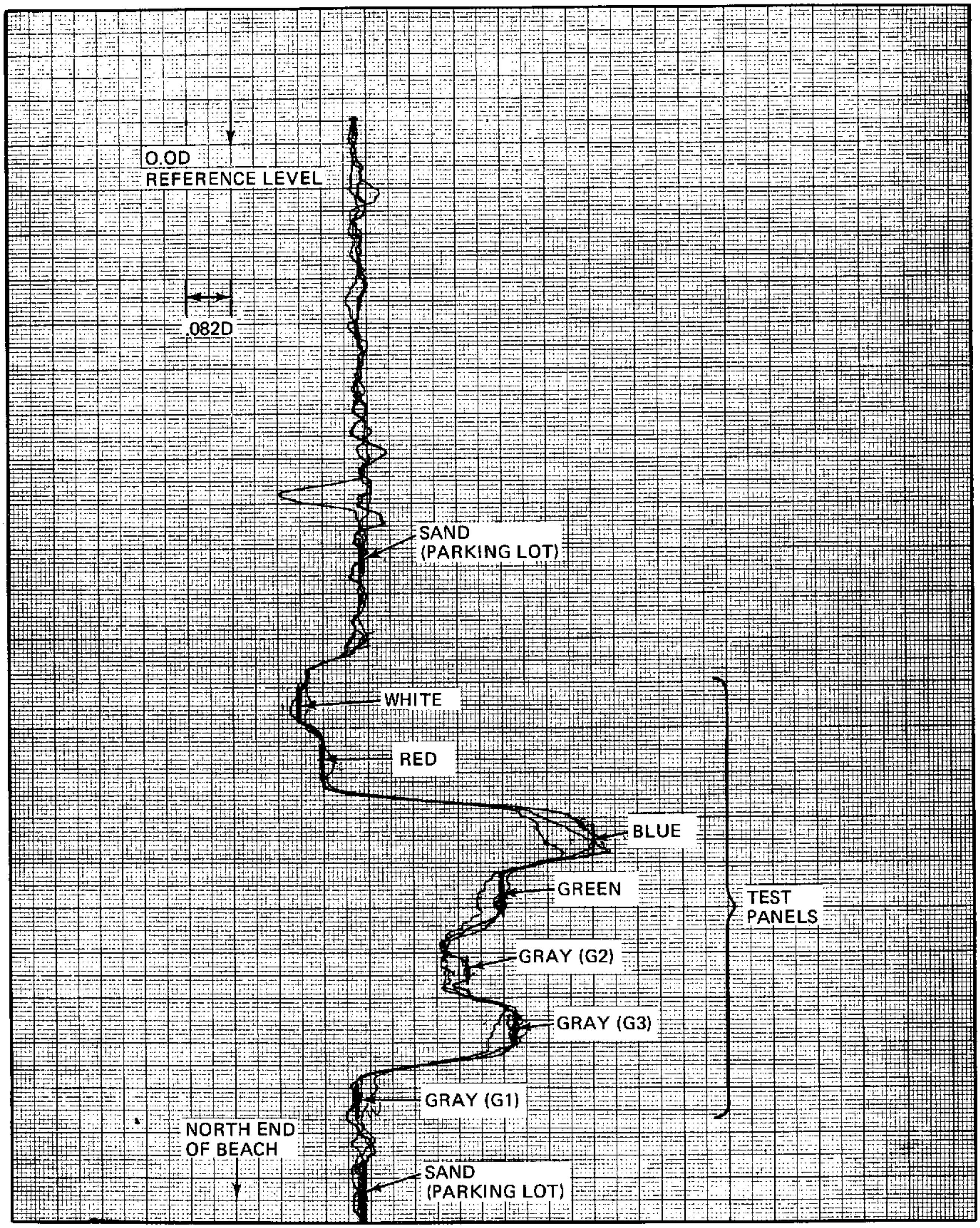

Figure 2-22. Test Panel Microdensitometry Trace in the Red Band

Table 2-6. Calculation Procedure For Test Panel And Brewers Bay Beach Data Reduction

Green (= 0.52 μm), Frame 0004, positive print, White Panel

J-L POSITIVE PRINT DENSITY	J-L NEGATIVE DENSITY	MACBETH POSITIVE DENSITY	FILTER AND LENS CORRECTION	CORRECTED MACBETH DENSITY	MACBETH TRANSMISSION %	RADIANCE CONVERSION FACTOR AT 0 DENSITY ($mw/cm^2/sr$)	RADIANCE ($mw/cm^2/sr$)
.279	.202	1.80	-.204	1.596	2.54	66.5	1.69

Table 2-7. Test Panel and Brewers Bay Beach Sand Photometry

TARGET	BLUE (= 0.4 μm)		GREEN (= 0.52 μm)		(RED (= 0.65 μm)	
	J-L DENSITY	RADIANCE (mw/cm²/sr)	J-L DENSITY	RADIANCE (mw/cm²/sr)	J-L DENSITY	RADIANCE (mw/cm²/sr)
Test Panels, 2000 ft. alt. (Frame 004)						
White	.203	.585	.279	1.69	.201	1.96
Red	1.237	.091	1.203	.345	.244	1.22
Blue	.739	.151	1.135	.379	.742	.418
Green	1.928	.371	1.070	.400	.570	.555
Gray(G1)	.287	.379	.463	.99	.303	1.08
Gray(G2)	.537	.209	.800	.55	.508	.62
Gray(G3)	.835	.138	1.050	.415	.595	.53
Brewers Bay Beach Sand (Parking Lot) 2000 ft. alt. (Frame 004)	.422	.262	.553	.82	.316	1.10
Brewers Bay Beach Sand (Parking Lot) 6000 ft. alt. (Frame 0036)	.412	.267	.696	.61*	.376	.85*
Brewers Bay Beach Sand (near water) 6000 ft. alt. (Frame 0036)	.463	.239	.562	.82	.322	1.00
Brewers Bay Beach Sand (near water) 6000 ft. alt. (Frame 178)	.209	.454	.400	1.05	.264	1.20

* Light cloud haze suspect.

Table 2-8. Comparison of Brewers Bay Beach Sand Radiance Data

BAND	GROUND MEASUREMENT ($mw/cm^2/sr$)	PHOTOGRAPHIC DETERMINATION ($mw/cm^2/sr$)	ERTS-1 DETERMINATION ($mw/cm^2/sr$)
4	0.72	.82	1.24
5	1.16	1.10	0.99

temperature is defined in terms of black body radiation curves (Figure 2-23). The usually assumed color temperature of the sun is 5500° K, but this color temperature is decreased at dawn and sunset by the longer sunlight path through the atmosphere; the color temperature may also be decreased by atmospheric aerosols and haze.

Table 2-9 indicates the observed color temperature effects; briefly, various targets (i.e. the test panel and Brewers Bay Beach sands) are compared to the black body power density ratios for various color temperatures. The effective color temperature of the sun may then be evaluated. The white panel laboratory reflectances are listed in order to indicate that the white panel is a useful constant reference as a function of wavelength for the spectral region under consideration.

The apparent color temperature of the sand at a 2000 foot altitude is about 5000° K, whereas at a 6000 foot altitude, the apparent color temperature of the sand is about 7000° K. There is a measurable reddening of the incident sunlight at 0920 Hrs as a result of atmospheric scattering.

2.3.5 Uniformity Of Photographic Printing Process

One last point to be covered in the data analysis is the uniformity of the photographic printing process. On the duplicate positive received in June 1973 the cross frame Macbeth density variability was 0.03D, and the head to tail 0.05D. This was an improvement from 0.04D cross frame variability in the Nov. 72 print, but a deterioration of the head to tail variability above 0.04D. Some of this variability is in the original negative, being 0.01D cross frame and 0.03D head to tail. All the previous measurements were made with a Macbeth TD102 densitometer which has a published variability of ± 0.02D; by careful checking of the zero of the instrument, this has been reduced.

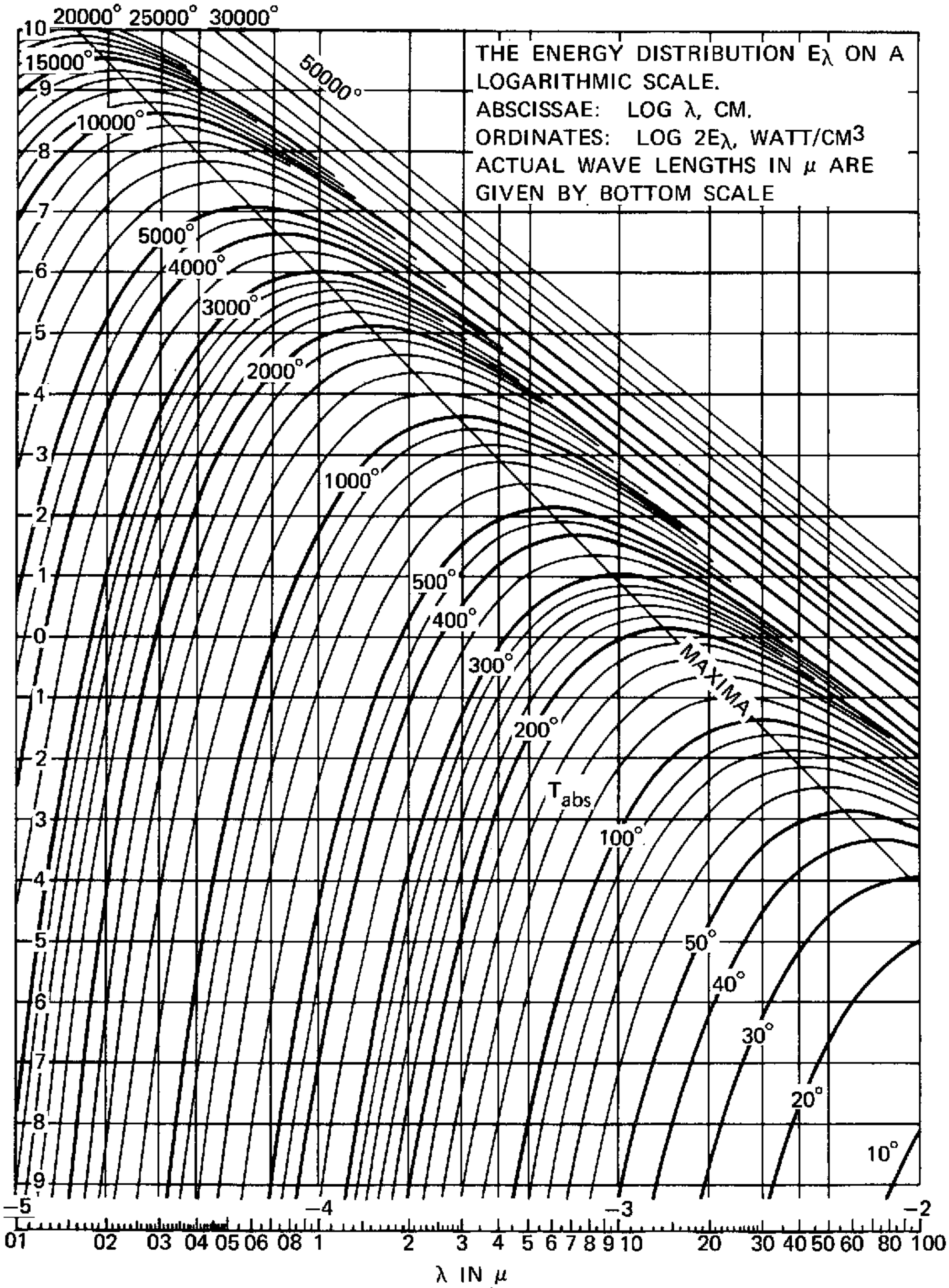

Figure 2-23. Black Body Radiation Curves

Table 2-9. Color Temperature Effects on I^2S Imagery

ITEM	BLUE BAND ($mw/cm^2/sr$)	GREEN BAND ($mw/cm^2/sr$)	RED BAND ($mw/cm^2/sr$)
White Panel at 2000 ft. alt. at 0920 hrs	.585	1.69	1.96
White Panel in Laboratory (equal energy illumination)	.68	.68	.66
Brewers Bay Beach Parking Lot Sand at 2000 ft. alt. at 0920 hrs.	.262	.805	1.095
Brewers Bay Beach Parking Lot Sand at 6000 ft. alt. at 0945 hrs	.267	.61	.845
Brewers Bay Beach Front Sand at 6000 ft. alt. at 0945 hrs.	.239	.82	1.00
Brewers Bay Beach Front Sand at 6000 ft. alt. at 1430 hrs.	.454	1.05	1.20
Ground Radiance of White Panel at 0944 hrs	.69	1.25	2.00
Black Body at 5500 K°	.91	.99	.93
at 7000 °K	.98	.87	.70
at 5000 °K	.80	.97	.985

Our observations generally concur, with the Macbeth measurements indicating a cross frame variation of 0.05D read on the Joyce-Loebl and a head to tail variation of 0.06D.

These process limitations form a limit on the accuracy of photographic photometry since a 0.05D error produces an error of 19% in the density measurement. Since these are the maximum variations, and the effect of a variation in density is dependent on the overall photographic system response, the average error would be expected to be of the order of 5% in the present photometric procedures, for brighter images.

2.4 RESULTS AND DISCUSSION

Having set forth the groundwork for the calibrations of the aircraft and ERTS-1 imagery, we may now apply them to a specific problem, the St. Thomas Harbor optical transect shown in Figure 2-1. The radiance of the water in blue, green and red bands has been determined photographically, and compared to previously determined in situ optical absorption, and ERTS-1 data corrected for atmospheric absorption.

2.4.1 Comparison of Harbor Transect Radiance Based on I^2S, ERTS-1 and in situ Optical Data

The photographic densitometry was performed on the I^2S aircraft red, green and blue bands along the harbor transect. A sample densitometric green band trace is presented in Figure 2-24, with stations 1 through 4 indicated. Using the data reduction procedure outlined in Table 2-10, we obtain the radiances indicated in Table 11 along the 7 stations of the harbor transect in the red, green and blue photographic bands.

The ERTS-1, Bands 4 and 5 data reduction is presented in Table 2-12, along with the calculations to arrive at the radiances at the 7 optical stations.

A comparison of the photographic and ERTS-1 radiances along the harbor transect is made in Table 2-13. The ERTS-1, Band 4 radiances follow the photographic radiances in trend and magnitude, but the photographic radiances are higher than the ERTS-1, Band 5 radiances, because the Type 2424 and duplicate positive film latitudes were exceeded. This is not a fault of the initial negative exposure or positive duplicate printing. It is the result of the fact that the red reflectance of the water is too low to produce an accurately readable density change; the density level of the red reflectance of the larger numbered optical stations is of the order of 0.01D, which is less than the noise (the processing variations may amount to as much as 0.06D). Because of the processing variations, the density observations for the St. Thomas Harbor transect were referred to the maximum density rather than the clear transmission.

A graphical comparison of the bulk ERTS-1 Bands 4 and 5 data with photographic and in situ water observations is made in Figure 2-25, and the tabular data is presented in Table 2-13.

2.4.2 Effect of Clouds and Cloud Shadows

The ERTS-1 data in Table 2-13 and Figure 2-25 have been corrected for the effect of a cloud shadow falling along the transect at Stations 112 and 115. This can be seen by referring to Figure 2-26 which is a Grumman Data Systems digital printout of Bulk Band 4; the sun elevation and aximuth are located to scale in the lower right hand corner of the figure, and the projected cloud shadow is seen to envelop the biological station 112 (Optical Station 5). For the digital value of Optical Station 5, the pixels closely adjacent outside of the cloud shadow were used.

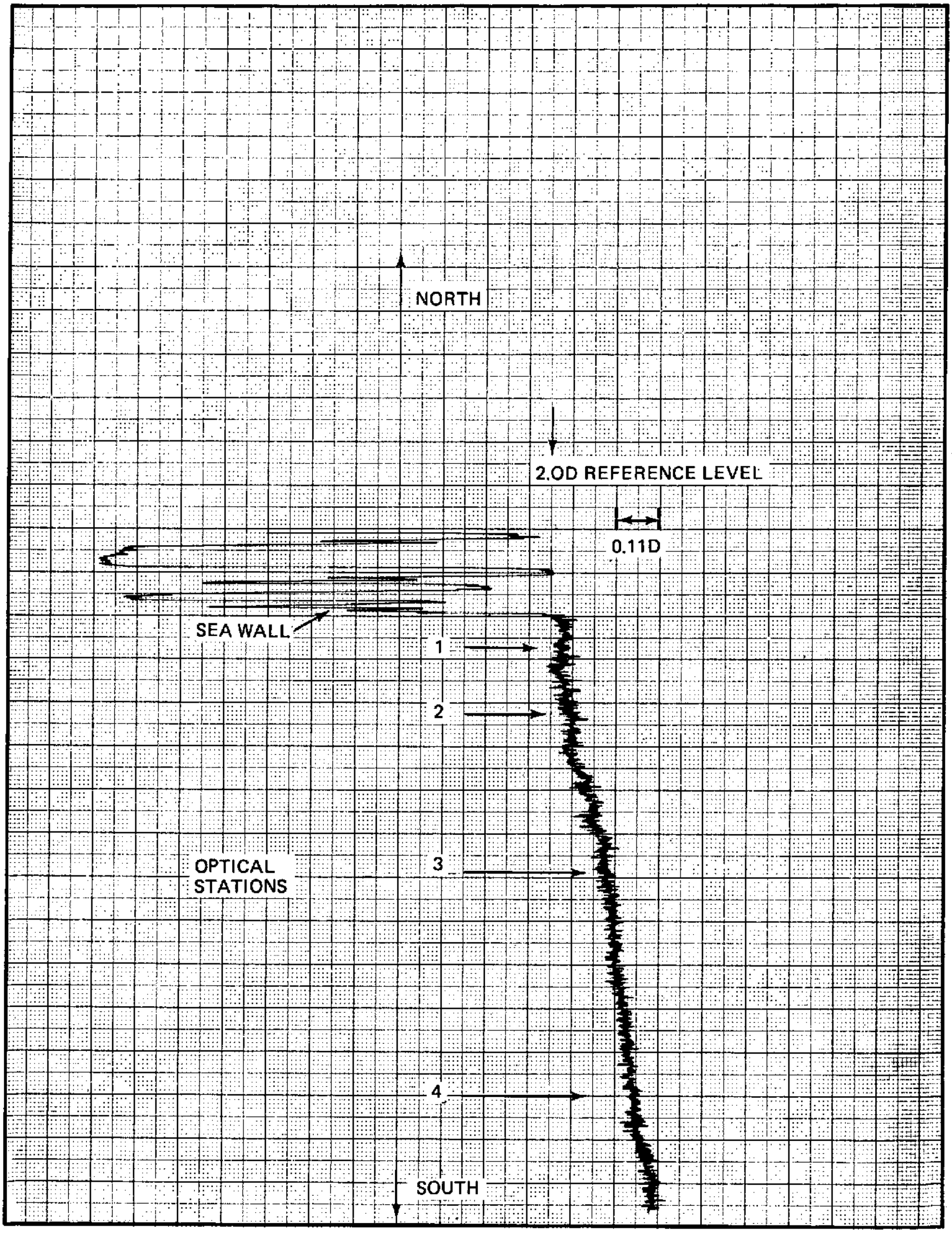

Figure 2-24. Microdensitometry of St. Thomas Harbor Optical Stations 1 through 4 in Green Band

Table 2-10. Calculation Procedure for Harbor Transect Data Reduction
Green (= 0.52 μm). Frame 0097, positive print, Station 1

J-L POSITIVE PRINT DENSITY	J-L NEGATIVE DENSITY	MACBETH POSITIVE DENSITY	MACBETH TRANS MISSION (%)	PRINT LOCATION CORRECTION	SHUTTER SPEED CORREC-TION	FILTER AND LENS CORREC-TION	RADIANCE CONVERSION FACTOR AT 0 DENSITY ($mw/cm^2/sr$)	RADIANCE ($mw/cm^2/sr$)
1.1741	0.37	2.93	0.117	2.63 (= 1/.38)	1.29	1.64	66.5	1.65

Table 2-11. St. Thomas Harbor Transect Photometry

PHOTOMETRIC STATION	LOCATION (FIG. 1)	FRAME NO.	BLUE (λ=0.43μm) J-L DENSITY	BLUE (λ=0.43μm) RADIANCE (mw/cm^2/sr)	GREEN (λ=0.52μm) J-L DENSITY	GREEN (λ=0.52μm) RADIANCE (mw/cm^2/sr	Red (λ = 0.65μm) J-L DENSITY	Red (λ = 0.65μm) RADIANCE (mw/cm^2/sr)
1	102	0097	1.427	.281	1.741	.165	1.889	.160
2	104	0097	1.452	.274	1.757	.188	1.905	.136
3	106 107	0097	1.573	.227	1.842	.108	1.942	.088
4	109 110	0097	1.741	.173	1.917	.098	1.955	.094
5	112	0098	1.509	.245	1.796	.101	1.895	.123
6	115	0100	1.295	.278	1.746	.083	1.900	.092
7	119 120	0101	1.405	.248	1.845	.061	1.895	.092

Table 2-12. Bulk CCT Data Reduction for Bands 4 and 5 from ERTS-1 for St. Thomas Harbor Transect

OPTICAL STATION	BIO STA	1 COUNT 127 BASE	2 COUNT 63 BASE (1/2 COL. 1)	3 GSFC CALIBR TABLE (VOLT. SIG.)	4 % RADIANCE FULLSCALE (COL. 3 X 25)	5 EQUIVALENT RADIANCE AT ERTS-1 (COL. 4 X R (mw/cm²/sr)	6 ATMOS-PHERIC SCATTERING CORRECTION (COL. 5-S) (mw/cm²/sr)	7 RADIANCE AT SURFACE (ATMOS. ATTEN.) CORRECTION (COL 6 X A) (mw/cm²/sr)
BAND 4					%	(R = 2.48)	(S = .13)	(A = 1.17)
1	102	32.4	16.2	.487	12.17	.302	.172	.201
2	104	29.8	14.7	.439	10.98	.272	.14	.164
3	106-7	26.8	13.4	.385	9.64	.238	.10	.117
4	109-110	26.2	13.1	.375	9.38	.232	.10	.117
5	112	26.25	13.12	.375	9.37	.232	.102	.119
6	115	24.67	12.33	.348	8.70	.216	.086	.101
7	119-120	20.3	10.1	.274	6.85	.170	.040	.047
BAND 5					%	(R = 2.00)	(S = .04)	(A = 1.10)
1	102	12.8	6.4	.161	4.03	.081	.041	.045
2	104	12.4	6.2	.155	3.88	.076	.036	.039
3	106-7	10.3	5.1	.123	3.08	.061	.021	.023
4	109-110	10.3	5.1	.123	3.08	.061	.021	.023
5	112	9.9	4.9	.118	2.95	.059	.019	.021
6	115	9.7	4.8	.115	2.87	.057	.017	.019
7	119-120	8.9	4.4	.104	2.60	.052	.012	.013

Table 2-13. Comparison of St. Thomas Harbor Transect Photographic and ERTS-1 Radiance

OPTICAL STATION	GREEN BAND RADIANCE		RED BAND RADIANCE	
	PHOTOGRAPHIC	ERTS-1 (BAND 4)	PHOTOGRAPHIC	ERTS-1 (BAND 5)
1	.165	.201**	.160	.045**
2	.188	.164	.136*	.039
3	.108	.117	.088*	.023
4	.098	.117	.094*	.023
5	.101	.119	.123*	.021
6	.083	.101	.092*	.019
7	.061	.047	.092*	.013

*Less accurate values because film latitude was exceeded; see text for discussion.
**Accuracy limited by spatial resolution of ERTS-1 MSS.

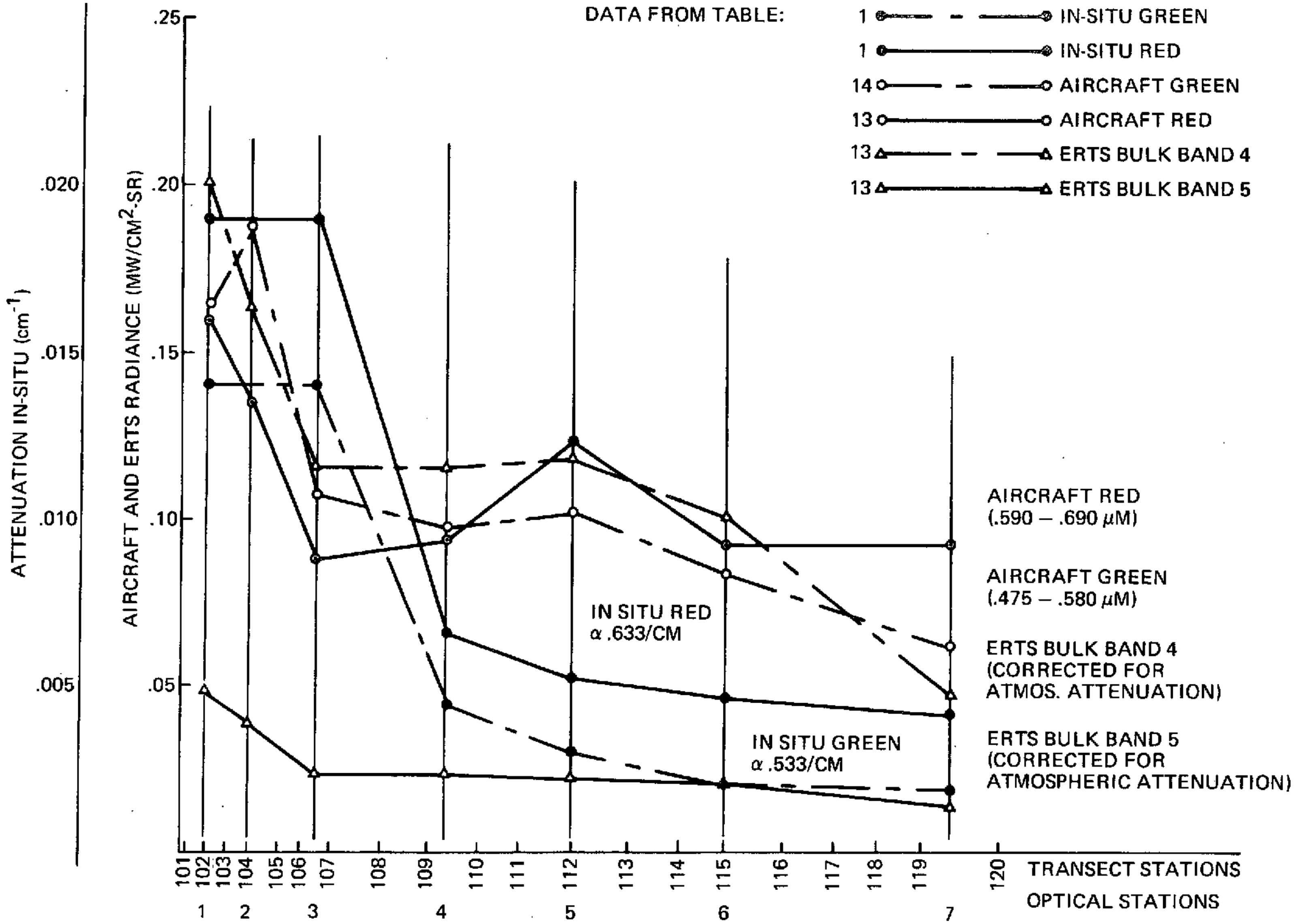

Figure 2-25. Comparison of ERTS-1, Bands 4 and 5, Aircraft Green and Red and In Situ Harbor Transect Optical Data

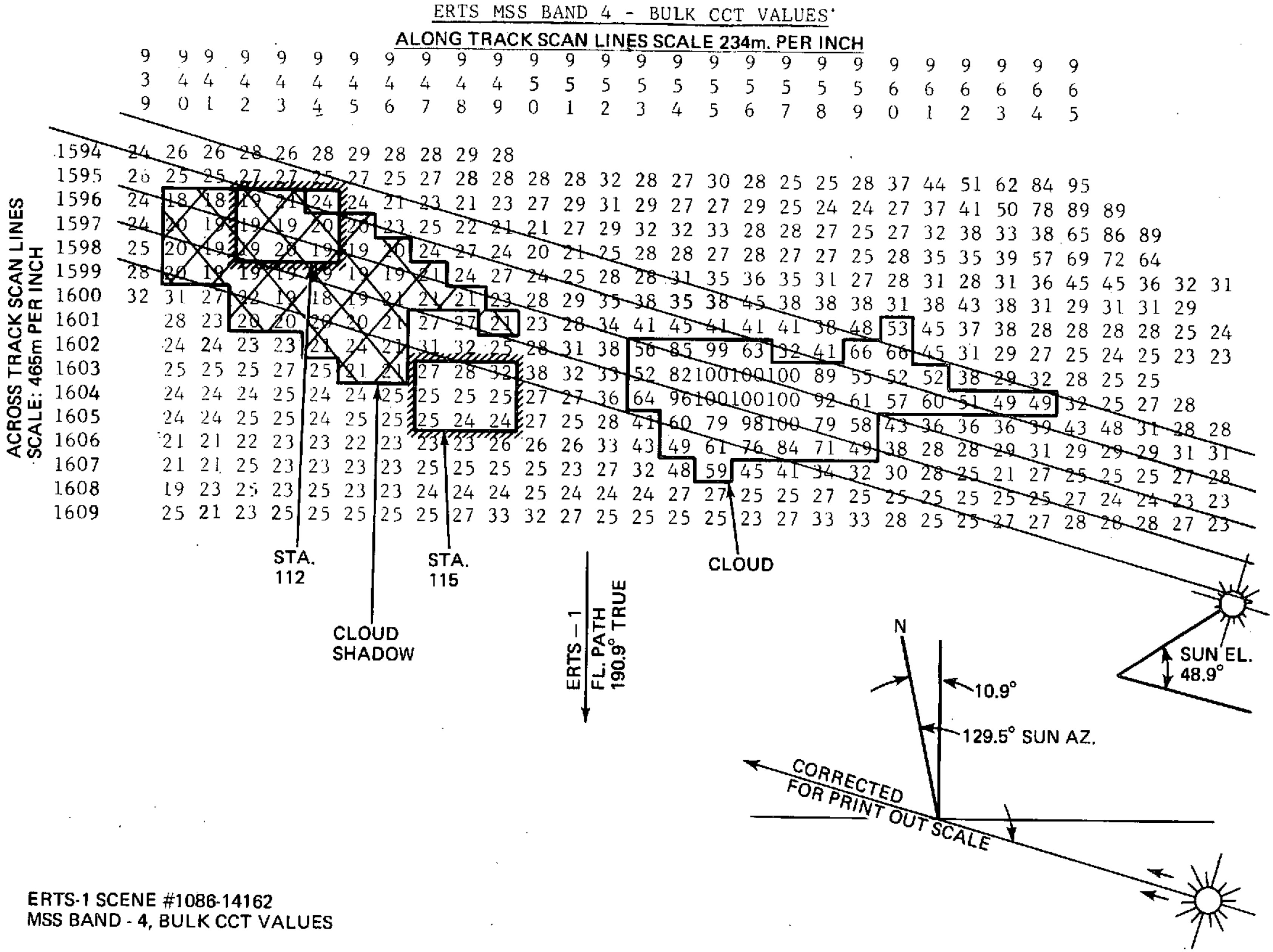

Figure 2-26. Printout of Bulk Band 4 showing Cloud Shadow Effects on ERTS-1 Imagery

2.4.3 Effect of ERTS-1 MSS Response Time Characteristics

Another effect on the digital pixels is shown by Figure 2-27. The MSS detectors have a finite response time to a step function. The step function is introduced when the scanner passes from a bright area to a dark area or vice versa. In Figure 2-27, the bright area is the cement sea wall at the St. Thomas Harbor edge; when the scanner passes from the sea wall to the much darker water, there is a finite time required to drop to the lower photometric level (response time). Thus the sea wall reads 61 (Line 1579 Band 4) and the water 40, and 3 pixels are involved in this transition; this effect is not the result of overlap in resolution elements of the scanner. In addition the town dock and Coast Guard ship appeared to contribute to the high values of line 1580; hence, we used the values of line 1581-930 through 932 inclusive as being most representative of the water at optical station #1.

2.4.4 Computer Correlation of ERTS-1, I^2S (Aircraft) and In Situ Optical, Biological and Chemical Water Data

The most feasible technique for comparison is the use of the computer generated matrices of Tables 2-14 through 2-18. These matrices indicate the degree of correlation from -100 through 0 to +100. A value of +100 indicates a direct correlation and -100 an inverse correlation. A value of 0 indicates no correlation.

Table 2-14 is a representation of the correlation features, over the entire transect, of the optical in situ data, the aircraft photographic data, the ERTS-1 data, and the biological transect data of chlorophylls a and c, total chlorophyll, turbidity, pigment diversity, and total carotenoids.

It can be seen in Table 2-14 that the in situ green and red as well as the aircraft red and green photography correlate well with the Bulk ERTS-1 Bands 4 and 5 and turbidity. The pigment diversity shows some evidence of weak correlation with the in situ, aircraft photographic and ERTS-1 data: chlorophylls a and c, total chlorophyll and total carotenoids reveal a yet weaker correlation.

In order to investigate these variations more fully, we devised the 3 station matrices presented in Tables 2-15 through 2-18. The combinations are, sequentially: optical stations 1, 2 and 3; 2, 3 and 4; 4, 5 and 6; and 5, 6 and 7. All correlations will not be discussed, because there is evident good correlation between the in situ aircraft photographic and ERTS-1 red and green band data. However, the establishment of a correlation with the water biology and chemistry is less clear.

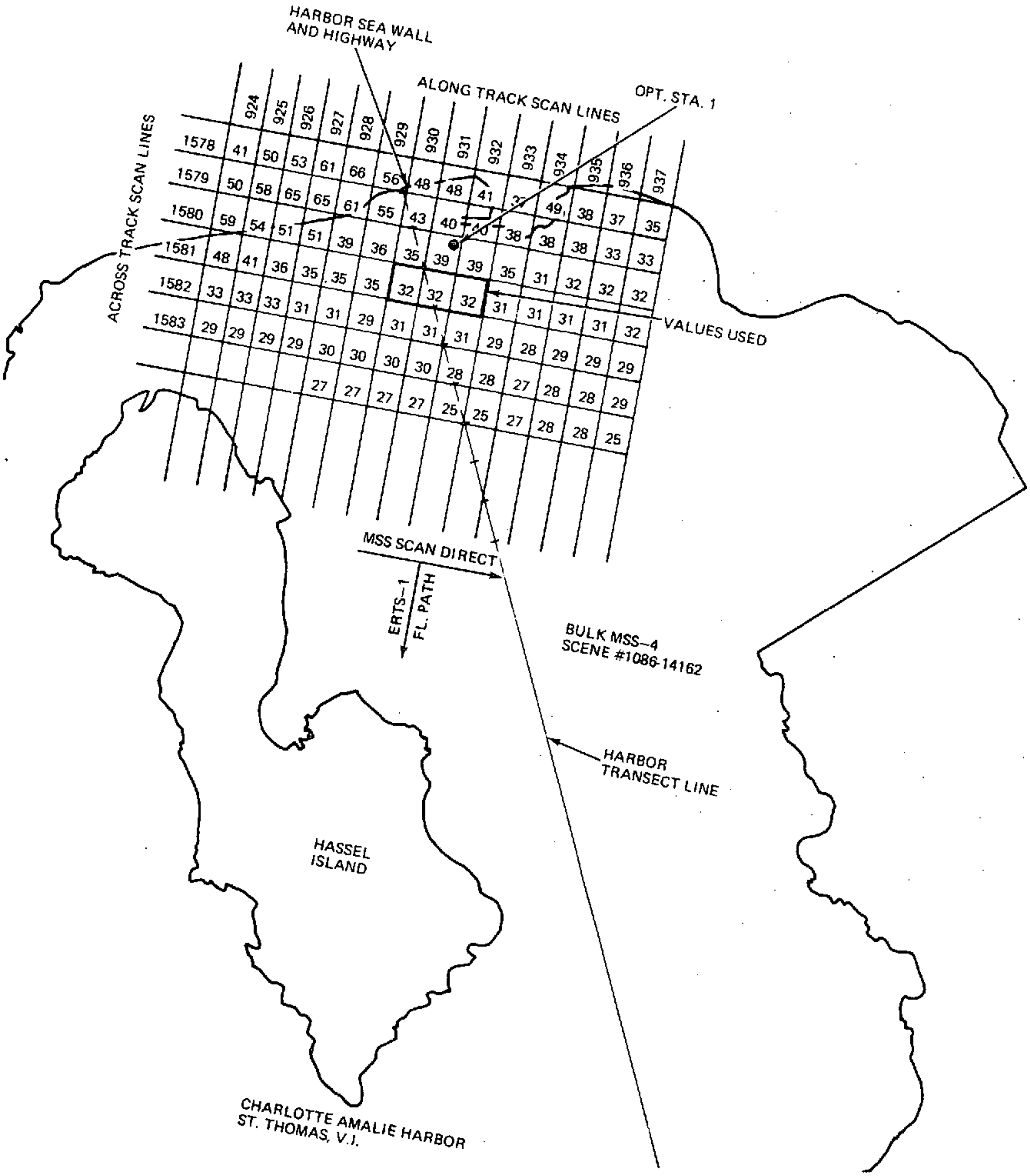

Figure 2-27. Printout of Bulk Band 4 Showing Effect of MSS Response Time Characteristics When Scan Passes From a Bright Area (Sea Wall) to a Darker Area (Water)

Table 2-14. Overall Variable Correlations (Optical and Biological)

	In Situ Red	Aircraft Green	Aircraft Red	Prec. MSS 4	Bulk MSS 4	Bulk MSS 5	Turbidity	Chlorophyll a	Total Chlorophyll	Pigment Diversity	Total Carotenoids	Bulk MSS 4 UC*	Bulk MSS 5 UC*	Bulk 4 MUC*	Bulk 5 MUC*	Chlorophyll C	Bulk MSS 6
In Situ Green	(99.9)	83	85	86	78	64	79	62	40	48	43	57	65	76	62	31	47
In Situ Red		82	83	86	78	64	79	60	38	49	41	56	65	75	62	29	51
Aircraft Green			(97)	69	(98)	83	(94)	47	23	68	28	82	84	(96)	79	14	46
Aircraft Red				78	(90)	71	88	61	35	54	41	70	72	(90)	66	27	28
Precision MSS 4					63	14	64	47	15	25	19	20	45	57	38	5	21
Bulk MSS 4						83	(91)	42	17	80	22	86	83	(97)	79	8	60
Bulk MSS 5							(96)	3	-11	49	-6	81	(100)	82	(99.4)	-16	53
Turbidity								26	5	53	10	80	(96)	(90)	(9)	-2	47
Chlorophyll A									(93)	38	(94)	34	4	49	1	88	11
Total Chlorophyll										23	(99.8)	26	-11	29	-11	(99.4)	5
Pigment Diversity											25	78	50	78	48	17	81
Total Carotenoids												30	-6	34	-7	(99)	46
Bulk MSS 4 UC*													81	86	82	22	60
Bulk MSS 5 UC*														83	(99.3)	-15	53
Bulk MSS 4 MUC**															78	23	60
Bulk MSS 5 MUC**																-15	55
Chlorophyll C																	0

Circled values are shown in parentheses.

*MSS quantum value (0-127) uncorrected for atmospheric attenuation
**Midpoint pixel MSS quantum value (0-127) uncorrected for atmospheric attenuation

Table 2-15. Transect Correlations (Optical Stations 1, 2 and 3)

	In Situ Red	Aircraft Green	Aircraft Red	Prec. MSS 4	Bulk MSS 4	Bulk MSS 5	Turbidity	Chlorophyll a	Total Chlorophyll	Pigment Diversity	Total Carotenoids	Bulk MSS 4 UC*	Bulk MSS 5 UC*	Bulk 4 MUC*	Bulk 5 MUC*	Chlorophyll C	Bulk MSS 6
In Situ Green																	
In Situ Red																	
Aircraft Green			**93.7**	6	**100**	**94**	**98**	**-99.6**	**-90**	**90**	-89	65	**94**	**99**	89	-88	68
Aircraft Red				40	**94**	76	85	**-97**	**-99.6**	69	**-99.5**	34	77	88	68	**-99**	38
Precision MSS 4					7	-28	-14	-15	-48	39	-49	-72	-28	-8	-40	-53	-69
Bulk MSS 4						**94**	**98**	**-99.7**	**-90**	**90**	-90	64	**94**	**99**	89	-88	67
Bulk MSS 5							**99**	**-91**	-70	**99**	-69	87	**100**	**98**	**99**	-66	89
Turbidity								**-96**	-80	**97**	-80	78	**99**	**99.8**	**96**	-76	81
Chlorophyll A									**94**	-86	**94**	-58	**-91**	**-97**	-85	**92**	-61
Total Chlorophyll										-62	**100**	-25	-71	-83	-61	**99.8**	-30
Pigment Diversity											-62	**92**	**99.3**	**95**	**100**	-57	**93**
Total Carotenoids												-25	-70	-83	-61	**99.9**	-29
Bulk MSS 4 UC*													86	75	**92**	-20	**99.9**
Bulk MSS 5 UC*														**98**	**99**	-66	89
Bulk MSS 4 MUC**															**95**	-80	78
Bulk MSS 5 MUC**																-56	**94**
Chlorophyll C																	-24

*MSS quantum value (0-127) uncorrected for atmospheric attenuation
**Midpoint pixel MSS quantum value (0-127) uncorrected for atmospheric attenuation

Table 2-16. Transect Correlations (Optical Stations 2, 3 and 4)

	In Situ Red	Aircraft Green	Aircraft Red	Prec. MSS 4	Bulk MSS 4	Bulk MSS 5	Turbidity	Chlorophyll a	Total Chlorophyll	Pigment Diversity	Total Carotenoids	Bulk MSS 4 UC*	Bulk MSS 5 UC*	Bulk 4 MUC*	Bulk 5 MUC*	Chlorophyll C	Bulk MSS 6
In Situ Green	100	59	52	80	63	50	63	17	-21	99	-25	-29	50	0	87	-31	97.5
In Situ Red		59	52	80	63	50	63	17	-21	99	-25	-29	50	0	87	-31	97.5
Aircraft Green			99.7	95	99.9	99.5	99.0	-69	-92	70	-93	-94	99.4	81	91	-95	40
Aircraft Red				93	99	100	99	-75	-94	64	-95	-97	100	85	88	-97	33
Precision MSS 4					97	92	97	-44	-75	88	-77	-80	92	59	99	-81	65
Bulk MSS 4						99	100	-66	-89	74	-91	-93	99	78	93	-93	45
Bulk MSS 5							99	-76	-95	62	-96	-97	100	86	87	-98	30
Turbidity								-66	-89	73	-91	-93	99	78	93	-93	44
Chlorophyll A									93	3	91	89	-76	-99	-34	88	39
Total Chlorophyll										35	99.9	99.7	-95	-98	-67	99.5	1
Pigment Diversity											-38	-42	62	14	93	-44	93
Total Carotenoids												99.9	-96	-97	-69	99.8	-3
Bulk MSS 4 UC*													-97	-96	-73	100	-7
Bulk MSS 5 UC*														87	87	-98	30
Bulk MSS 4 MUC**															50	-95	-22
Bulk MSS 5 MUC**																-74	74
Chlorophyll C																	-9

*MSS quantum value (0-127) uncorrected for atmospheric attenuation

**Midpoint pixel MSS quantum value (0-127) uncorrected for atmospheric attenuation

Table 2-17. Transect Correlations (optical stations 4, 5 and 6)

	In Situ Red	Aircraft Green	Aircraft Red	Prec. MSS 4	Bulk MSS 4	Bulk MSS 5	Turbidity	Chlorophyll a	Total Chlorophyll	Pigment Diversity	Total Carotenoids	Bulk MSS 4 UC*	Bulk MSS 5 UC*	Bulk 4 MUC*	Bulk 5 MUC*	Chlorophyll C	Bulk MSS 6
In Situ Green	98	91	95	91	82	99	95	99	93	92	95	82	99	90	0	92	-79
In Situ Red		80	88	81	69.4	99.9	87	99.8	99	82	99	69	99.8	97	0	98	-65
Aircraft Green			99	100	99	83	99	84	69	99.9	72	99	84	63	0	66	-98
Aircraft Red				99	96	89	100	90	78	99.5	81	95	90	73	0	75	-94
Precision MSS 4					99	83	99	84	69	100	73	99	84	63	0	66	-98
Bulk MSS 4						72	96	73	56	-98	60	100	74	49	0	52	-100
Bulk MSS 5							88	100	98	-84	99	72	100	96	0	97	-68
Turbidity								90	77.2	99.6	80	96	90	72	0	74	-94
Chlorophyll A									98	-85	98	73	100	95	0	96	-70
Total Chlorophyll										-71	99.9	56	99.5	99.6	0	99.9	-52
Pigment Diversity											-74	-98	-85	-65	0	-68	97
Total Carotenoids												59	98	.99	0	99.6	-55
Bulk MSS 4 UC*													73	49	0	52	-100
Bulk MSS 5 UC*														95	0	96	-70
Bulk MSS 4 MUC**															0	99.9	-44
Bulk MSS 5 MUC**																-	-
Chlorophyll C																	-47

*MSS quantum value (0-127) uncorrected for atmospheric attenuation
**Midpoint pixel MSS quantum value (0-127) uncorrected for atmospheric attenuation

Table 2-18. Transect Correlations (optical Stations 5, 6 and 7)

	In Situ Red	Aircraft Green	Aircraft Red	Prec. MSS 4	Bulk MSS 4	Bulk MSS 5	Turbidity	Chlorophyll a	Total Chlorophyll	Pigment Diversity	Total Carotenoids	Bulk MSS 4 UC*	Bulk MSS 5 UC*	Bulk 4 MUC*	Bulk 5 MUC*	Chlorophyll C	Bulk MSS 6
In Situ Green	84	92.6	99.8	26	72	65	99.8	96	90	34	96	71	66	50	50	86	-30
In Situ Red		98	80	-30	98	96	87	96	99.4	79	96	98	96	89	89	99.9	27
Aircraft Green			90	-13	93	89	95	99.4	98	67	99	92	90	79	79	99	85
Aircraft Red				32	67	60	99	94	86	27	94	66	61	44	44	82	-36
Precision MSS 4					-49	-56	20	-1	-20	-82	-1	-50	-55	-71	-71	-27	-99.9
Bulk MSS 4						99.7	76	88	95	90	88	100	99.8	96	96	97	46
Bulk MSS 5							70	84	92	93	84	99.8	100	98	98	95	53
Turbidity								98	92	40	98	74	75	71	55	89	-24
Chlorophyll A									98	58	100	87	84	72	72	97	-3
Total Chlorophyll										72	98	95	93	83	83	99.7	16
Pigment Diversity											58	90	93	98	98	77	80
Total Carotenoids												87	84	72	72	97	-3
Bulk MSS 4 UC*														99.8	97	97	46
Bulk MSS 5 UC*														98	98	95	52
Bulk MSS 4 MUC**															100	87	68
Bulk MSS 5 MUC**																87	68
Chlorophyll C																	22

*MSS quantum value (0-127) uncorrected for atmospheric attenuation
**Midpoint pixel MSS quantum value (0-127) uncorrected for atmospheric attenuation

The turbidity correlates well with the in situ, aircraft photographic and ERTS-1 data; this is to be expected because the turbidity is the same as the weighted average of the in situ optical attenuation in red, green, and blue.

The more obscure relationship deals with the chlorophylls a and c, the total carotenoids, and total chlorophyll. The correlation of all of these parameters is generally negative in Tables 2-15 and 2-16 (near the sewage effluent area), and positive in Tables 2-17 and 2-18, far from the sewage effluent area. This means that there is low biological level, in terms of plant life, near the sewage effluent area, where the light scattering properties of the harbor water is highest, (Ref 2), as generally would be expected. However, the reversed trend is apparently the result of pigmentation and physical size of the biota in the St. Thomas Harbor entrance increasing the optical reflectance.

The strong correlation of pigment diversity with turbidity is an indication that there are strong variations in the factors making up the pigment diversity at the location where the turbidity is highest. The five factors considered in pigment diversity are chlorophylls a, b and c, the astacin and non-astacin carotenoids. This would be inferred to mean that the level of biological activity is highest in the turbid areas even though the level of pigments is not high.

As a further check on the optical properties of the St. Thomas Harbor transect, water spectral transmission measurements were made on samples taken near optical stations 1 and 6. These results are presented in Figures 29a and b. It is observed that the water near the Coast Guard Dock (Optical Station 1) is highly absorbing throughout the visible spectrum, with the strongest absorption in the blue region due to Gelbstoff. Further out at biological station 46 (near optical station 6) the level of Gelbstoff drops as expected. It is possible that humic acids, dissolved nitrates and phosphates also could be associated with the reduction in water quality near the Coast Guard Dock. Analysis of water samples was made for these factors by C. Bassett at the Adelphi Institute of Marine Sciences. The results are presented in Table 2-19. It is noted that the humic acids and the disolved nitrates and phosphates are highest in the region near the Coast Guard Dock (Optical Station 1) as would be expected.

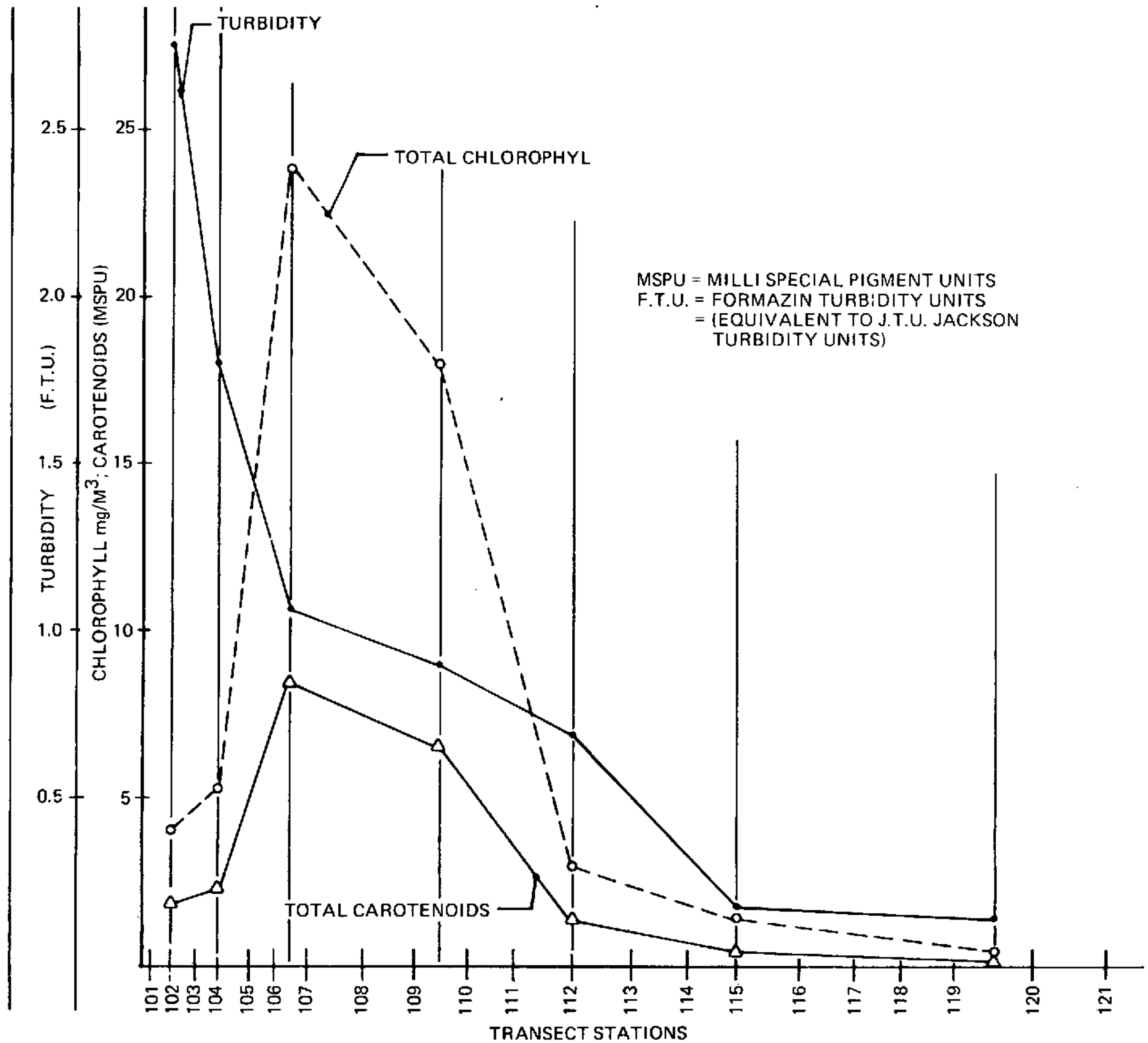

Figure 2-28. Graphical Correlation of Turbidity, Chlorophyll and Carotenoids Along the Harbor Transect

Table 2-19. Chemical Data at Optical Stations 1 and 6

	OPTICAL STA. 1	OPTICAL STA. 6
Dissolved Phosphates	0.0118 ppm	0.0046 ppm
Dissolved Nitrates	0.03 ppm	undetected
Humic Acids		
Dissolved	< 0.1 ppm	< 0.1 ppm
Particulate	1.5 ppm	0.3 ppm

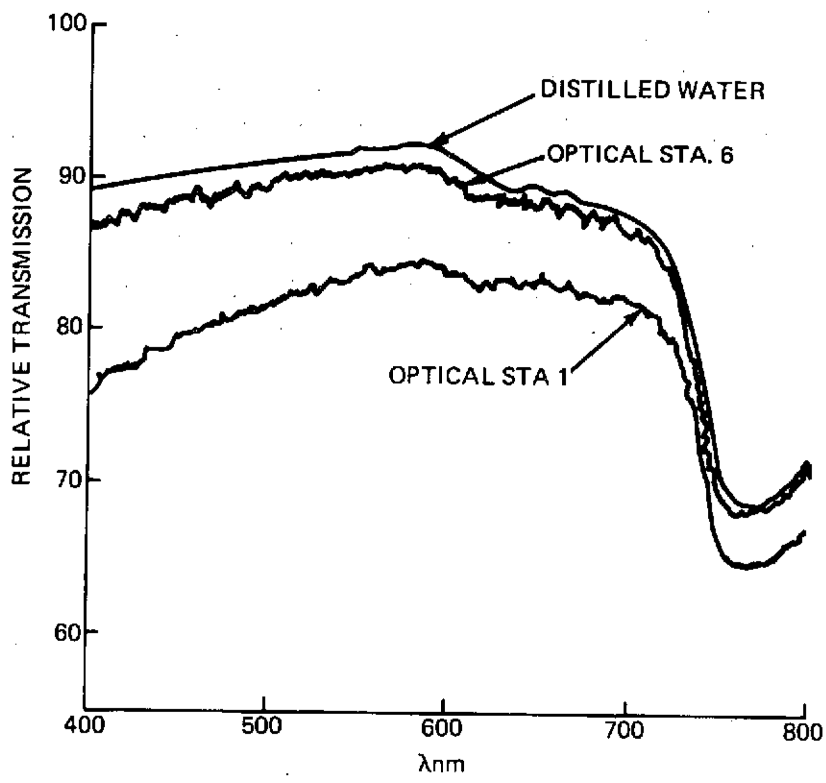

Figure 2-29. Laboratory Optical Transmission Measurements of St. Thomas Harbor Transect Water a) at Coast Guard Dock; b) at Optical Station 6

2.5 CONCLUSIONS

The in situ optical scattering properties of St. Thomas Harbor water correlate with calibrated aircraft I^2S and ERTS-1 imagery. The ground spatial resolution for the aircraft imagery is of the order of one foot and that of the ERTS-1 is about 250 feet. The ERTS-1 green band (Band 4) is better than the red (Band 5) for pollution sensing in the St. Thomas Harbor. The aircraft I^2S camera green band was the only usable band for pollution sensing under the conditions of operation in St. Thomas; for the red I^2S band to be useful, the exposure in this band would have to be increased.

The relation of the imagery (I^2S and ERTS-1) to biology via turbidity is strong; the correlation to chlorophyll (total, a and c) and carotenoids is opposite in the region of high pollution to that in the lower pollution areas. Also the correlation to chemistry via turbidity is promising in terms of humic acids, nitrates and phosphates.

The optical remote sensing technique applied to a particular area depends upon the desired spatial resolution and time of the survey. Both ERTS-1 and I^2S camera have sufficient photometric resolution to distinguish optical reflectance changes due to particulate matter in the water. The exact correlation to the type of pollution must be made with a suitable ground truth program, periodically updated.

However the success of the entire program, particularly the photographic portion, depended upon an adequate photometric calibration program as here used. In particular, atmospheric filtration effects were revealed in so far as they affected color photography.

ACKNOWLEDGEMENTS

The author wishes to thank W. Coulbourn, Program Manager, and his staff in Grumman Ecosystems for their help and support during the data acquisition and analysis; Grumman Data Systems for special data analysis; Kennedy Space Center/NASA, and Manned Space Center/NASA, in particular W. Covington and N. Lamar for their cooperation in the absolute calibration of the aircraft imagery.

REFERENCES

1. ERTS Data Users Handbook Prepared by ERTS Program, Goddard Space Flight Center, 1972.

2. Report 2-SA-TEC; Laboratory Results - U.S. Virgin Islands, to Chief Surveillance Branch E.P.A. from F.T. Brezenski, Chief Technical Support Branch.

3. Egan, W.G., Practical Calibration and Control Technique for Type 8443 and Ektachrome Films. Symp. Aerial Color Photography in Plant Sci. Proc.; University of Florida, 1969, pp. 104-116.

4. Egan, W.G. Water Quality Determinations in the Virgin Islands from ERTS-1 Data. Proceedings of the 8th International Symposium on Remote Sensing of the Environment, Ann Arbor Michigan, October 1972, pp. 685-708.

5. Egan, W.G. and Hair, M.E., Automated Delineation of Wetlands in Photographic Remote Sensing, Proceedings of Seventh International Symposium on Remote Sensing of Environment, Institute of Science and Technology, The University of Michigan, Ann Arbor, May 1971, pp. 2231-2252.

6. Allen, C.W., Astrophysical Quantities, University of London, the Athlone Press, 2nd Edition, 1963; p. 122.

GLOSSARY OF TERMS

H-D Curve	Hurter-Druffeld curve plotting density in a photographic film versus the exposure to light
I^2S	Abbreviation for International Imaging Systems, Mountain View, California
I^2S Camera	A four lens camera responding to four photographic bands in blue (.410μ-.470μ), green (.475μ-.580μ), red (.590μ-.690μ), and near infrared (.740μ-.900μ).
D	Density = $\log_{10} \frac{T_2}{T_1}$ the logarithim to base 10 of the transmission ratio, T_1 usually taken as unattenuated transmission
Chlorophyll <u>a</u>, <u>b</u>, <u>c</u>	Living plant pigments of three types
Carotenoids	Dead plant and animal pigments
ERTS-1	Earth Resources Technology Satellite No. 1, Launched July 1972
MSS	Multispectral Scanner
Band 4	MSS sensor band between 0.5 and 0.6 micrometers
Band 5	MSS sensor band between 0.6 and 0.7 micrometers
Band 6	MSS sensor band between 0.7 and 0.8 micrometers
Band 7	MSS sensor band between 0.8 and 1.1 micrometers
Head	Beginning end of a roll of film
Tail	End of a roll of film
Transect	A path of a particular direction (across an area) where scientific (biological, optical, chemical) observations are made
in situ measurements	Measurements made in place; i.e. in the water
Pixels	Picture elements (digital levels)
Sensitometry	Exposure-Density properties in a film emulsion

Gelbstoff	Yellow pigments in water due to melanoidines
Turbidity	As used herein, it is Engineering Index measured by the Hach Model 2100A Turbidimeter. The data provide a relative indication of volume scattering in the water. Operation of the Hach Turbidimeter is as follows: Light passing through the water sample is scattered by suspended perticulate matter. An amount of light (proportional to scattering particles present) is sensed at a 90° angle to the illuminating light beam. The unit of measure is FORMAZIN TURBIDITY UNITS (F.T.U.), which units are equivalent to Jackson Turbidity Units (J.T.U.). The instrument is calibrated by reference to a standard Formazin stock suspension.

N74-15004

SECTION III

WATER QUALITY PARAMETERS OF HARBORS OF CHARLOTTE AMALIE, ST. THOMAS, V.I.

ACQUISITION OF IN SITU WATER DATA, INTERCORRELATION OF SELECTED WATER PARAMETERS, AND INITIAL CORRELATION OF THESE IN SITU BIOLOGICAL, CHEMICAL AND PHYSICAL DATA WITH ERTS-1 BULK CCT MSS BAND 5 DATA.

acknowledgement

This section has been prepared by:

DR. DAVID A. OLSEN
MARINE RESOURCES DEVELOPMENT FOUNDATION
P.O. BOX 387
San German, Puerto Rico 00753

in association with

GRUMMAN ĒCOSYSTEMS CORPORATION
Bethpage, N.Y. 11714

ABSTRACT

Remote sensing by the ERTS-1 satellite was compared with selected water quality parameters including pH, salinity, conductivity, dissolved oxygen, water depth, water temperature, turbidity, plankton concentration, current variables, Chlorophyll a, total carotenoids, and species diversity of the benthic community. Strong correlation[1] between turbidity and MSS-sensed radiance was recorded and less strong correlations between the two plankton pigments and radiance. Turbidity and benthic species diversity were highly correlated furnishing and inferential tie between an easily sensed water quality variable and a sensitive indicator of average "water quality" conditions.

[1] Correlation of in situ data with aircraft and ERTS-1 data is treated in Sections II and IV also.

3.0 INTRODUCTION

The Earth Resource and Technology Satellite program offers one of the most exciting technological advances in the field of environmental quality to date. With this technology, investigators are developing methods for monitoring environmental quality which will greatly reduce the fiscal and scientific expenditure involved in monitoring man's endangered surroundings. Recent results (Colwell, 1973; Finch, 1973) indicate ever increasing areas of applicability. The program study assesses the feasibility of using ERTS satellite imagery (particularly spectral radiance) as an indicator of water quality in Charlotte Amalie Harbor, St. Thomas, U.S. Virgin Islands.

The purpose of the study was two-fold. The primary mission was to assess the feasibility of, and develop methodology for, the use of satellite data to measure water quality. The secondary mission was to apply that methodology concurrently in order to present a baseline measure of the water quality in the region at the time of the study. The study was conducted over six weeks in October and November in 1972. No attempt was made to measure long-term changes in either water quality or biotic response to water quality, but the sampling program was structured so that some time-related statements are possible. These will be discussed later.

St. Thomas is located approximately 65° west and 18° north. It is situated on a common shelf with the islands of Puerto Rico and all of the Virgin Islands except St. Croix, which is separated from this small "continental mass" by the Anegada Trough. This shelf is an underwater plateau with its top lying 100 to 300 feet below the surface and falling off abruptly around the edge into very deep water. It covers about 2000 square miles. A summary of the shelf geology is to be found in Garrison et al (1971) and Nagle (1971).

According to Donnelly and Whetten (1968) the shelf and the islands are late Cretaceous - early Tertiary in origin but are still in the process of formation. They are also "oceanic islands" and hence have probably never been connected with the continental mass. This isolation has profoundly effected changes in the biotic configuration.

Small oceanic islands such as St. Thomas have little effect on the oceanic weather and currents. The predominant currents affecting St. Thomas originate from the North Equatorial and Carribbean currents which sweep in across the Atlantic and encounter the lesser Antilles Island arc. The current in the region of St. Thomas comes from the ESE at about 0.5 kt. (U.S. Navy Oceanographic Office, 1972) during the months of October and November. This same source shows that the wind in the region is either from the east or ENE between 60 and 80% of the time. Tabb and Michel (1968) summarized the wind direction data for Truman field and showed that the wind is either east or ENE 57% of the time, further indicating the lack of land mass effects upon the weather.

The general oceanographic parameter trends have been summarized in Dammann (1969) and will be discussed alter with results from the present study.

It is particularly fortuitous that the present study should occur, since a primary sewage treatment plant will be put in operation by late fall 1973. This plant will eliminate most of sewage effluent into St. Thomas Harbor, and should do much to relieve St. Thomas' overtaxed facilities. This strain has resulted from the fact that the population has more than doubled in the last ten years to the 1970 census level of 30,000 people in approximately 32 square miles of available land. Added to this is the island's yearly influx of tourists, which increases the population level greatly. The present study should serve as a valuable baseline with which to compare later changes, subsequent to the initiation of the treatment plant.

Besides raw sewage (3 million gallons per day peak) there are three other sources of pollution within the study area. A black strap molasses plant pumps 154,000 gallons of industrial effluent into Charlotte Amalie Harbor daily. A combined desalinization and hydroelectric plant, located on the peninsula between Krum Bay and Lindbergh Bay, pumps 121,000 gallons per minute of coolant water into Lindbergh Bay at 38° C. It also discharges 2,000 gpm of brine (70 ppm). All of the brine and most of the coolant water is discharged into Lindbergh Bay. At the western extremity of the test site, adjacent to Truman airport, is a solid waste dump and fill operation.

3.1 METHODOLOGY

Sampling sites throughout the ground truth study are shown in Figure 3-1. Sampling The six types of sampling programs undertaken throughout the six week period-given as Julian dates- are listed below. The parameters sampled and the devices used are listed in Table 3-1.

1. Repetitive sampling stations were selected based on a priori knowledge by the field team to bracket the range of water conditions. They were also selected to supply information on the variability within the entire study period. They

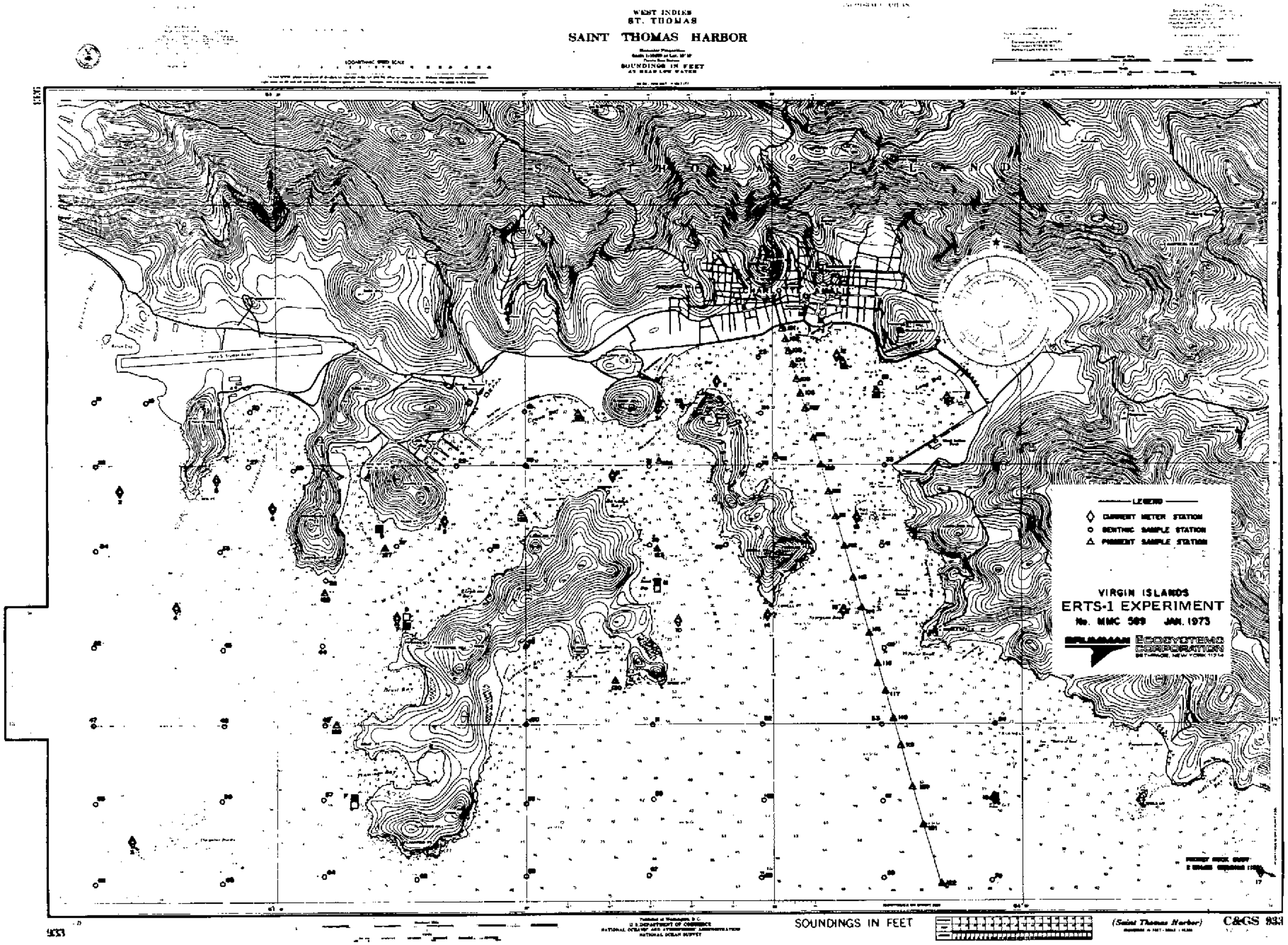

Figure 3-1. Chart of Charlotte Amalie and Adjacent Region Showing Sampling Stations for the Virgin Islands Experiment

Table 3-1. Summary of Parameters Measured With Primary And Backup Measurement Devices.

PARAMETER	1° MEAS. DEVICE	2° MEAS. DEVICE	3° MEAS. DEVICE	CALIBRATION	SAMPLING USE
Ph	I	B		Buffers	All
Salinity	I	ES		ES	All
Conductivity	I	C		Conductivity Simulator	
D. O.	I	W	Y	W	All
Depth	F	I	E	Lead Line	All
Temp.	I	M	E	Thermometer	All
Turbidity	H			Standard Solutions	All
Clarity	S				All
Visual Band Extinction Coefficient	L*			Calibrated Photocells	All
Bottom Type	D				1
Pigments	SP			Strickland & Parsons (1968)	3, 4
Diversity	D				1, 2
Plankton	P				All
Current Speed	E	E_2		Internal Calibration	All
Current Direction	E			Compass	All

INSTRUMENTATION CODE

I	Interocean C, S, T, D, DO, Ph Probe	W	Wingler Titration
M	Martek Temperature Probe	P	Plankton Net (80)
E	Endeco 110 Current Meter	F	Fathometer
E_2	Endeco Type 105 Recording Current Meter	C	Conductivity Meter
		H	Hach Model 2100A Turbidometer
D	Diver	S	Secchi Disk
B	Beckman Expandometer pH Meter	L	G. M. Mfg. & Inst. Corp. Model 15M02 Photometer
ES	Endeco Salinometer		
Y	YSI Model 5Y 0_2 Probe	SP	Spectrophotometer Lab Equip't

SAMPLE TYPE

1 Geographical Stations

2 17 Repetitive Stations with recording current meters

3 Overflight

4 Diurnal Studies

*The (visual band) extinction coefficient (EC) was calculated from the equation:

$$EC = \frac{1}{N-1} \sum_{i=1}^{N-1} \frac{\ln (SC_1/SC_{i+1})}{DP_{i+1} - DP_1}$$

Where: SC_i is the Sea Cell photometer reading and depth; in (microamps)

DP_i is the sample depth (in cm.)

ln is the logarithm to the base $\underline{e}$

were sampled weekly and Endeco recording current meters were emplaced for continuous data acquisition. At each of these stations and at the geographic stations (discussed next) samples were collected at six feet above the bottom, 50% of the depth and five feet below the surface waters. This vertical sampling was augmented by diver collection of all of the living matter within a randomly placed 0.25M^2 quadrat. This benthic sample was collected once at each of the Repetitive and Geographic stations. A vertical plankton tow was also taken with an 80 μ mesh net. The volume of plankton was measured with a graduated cylinder and later converted to cc/M^3 of sea water.

2. Geographic stations were sampled once in the course of the study to give an idea of geographic distribution of water parameters and location of various bottom types and community associations. The sampling program was exactly as described for the repetitive stations.

3. Diurnal variation in water quality parameters was studied at two stations (9 and 12) from the repetitive program. Station 12 was an area of low circulation inside Charlotte Amalie Harbor, while at station 9 current was highly variable. Both stations were sampled on similar tidal series to assess variability between locales. Station 9 was sampled again on a high tidal variation period to assess the within locales variability. The sampling program was the same as in (1) and (2) with the exception that plankton pigments were also sampled at this time.

4. ERTS overflights were documented through the collection of plankton pigments in the surface waters along a transect line running from inner Charlotte Amalie Harbor out into clear oceanic waters (Figure 1.1). These collections were commenced at about 0700 and ended at 1100 on three different overflight days, although ERTS-1 data was available for Oct. 17, 1972 only. This reduced influence of diurnal variability on the data and maximized the correlative potential of the ground truth-data with the satellite.

5. Thermal ground truth was collected in Lindbergh Bay on day 291 with Martek temperature probe for correlation to aircraft infrared sensing.

6. Spectral attenuation data from the surface waters were collected by Grumman personnel from a series of sites along the transect lines used in (4). These data were collected during the first overflight period only.

In summary the "ground truth" data acquisition was primarily centered around the acquisition of the plankton pigment data during the times of ERTS overflight. Three diurnal studies were accomplished to assess the hourly variation in this parameter and the relation between it and basic water quality parameters. The sampling at the three depths measured the homogeneity of the water column. The repetitive sampling program continued to assess variation associated with depth as well as continuing and extending the time-related variance assessment over 1.5 lunar cycles. The geographical sampling stations were chosen so as to measure and assess the generality of the trends observed at the repetitive stations. The benthic samples described communities that have developed over a period of years in response to water conditions and are therefore "bio-indicators" of long term trends.

There is a growing body of evidence (Hutchinson, 1969) indicating that community structure can be an indicator of environmental stress. In this manner of sampling, time variables have been assessed in such a way that the instantaneously acquired data from ERTS can be related to long term trends over broad geographical areas.

3.2 RESULTS

3.2.1 Benthic Sampling

Four main community types were noted and their distribution displayed in Figure 3-2. Offshore there is a rich and diverse area of algal plain. The predominant algal genera were the Phaeophytes Pocockiella, and Dictyota, and the Chlorophytes Anadyonome, Valonia, and Avranvillea. The sponges were abundant in this area, primarily several species of Haliclona. Exploratory dives throughout much of the "continental shelf" of the Virgin Islands and Puerto Rico lead us to believe that this community is a general feature of the offshore.

The inshore and inner harbor were covered by the remaining three community types. Immediately abutting the land mass and extending variously offshore was a typical reef community dominated by the hard corals Millipora, Porites, Acropora Montastrea. The soft corals were most frequently represented by Pseudopterogorgia and Eunicea. The urchins Diadema and Tripneustes were common and an abundant flora of various rhodophycean and chlorophycean algae was encountered.

Immediately adjoining the reef areas is the region of barren sand noted by Randall (1965) which is in turn bordered by an early successional state of low diversity dominated by the Spermatophyte Halophila. Inshore the Halophila band grades into a community

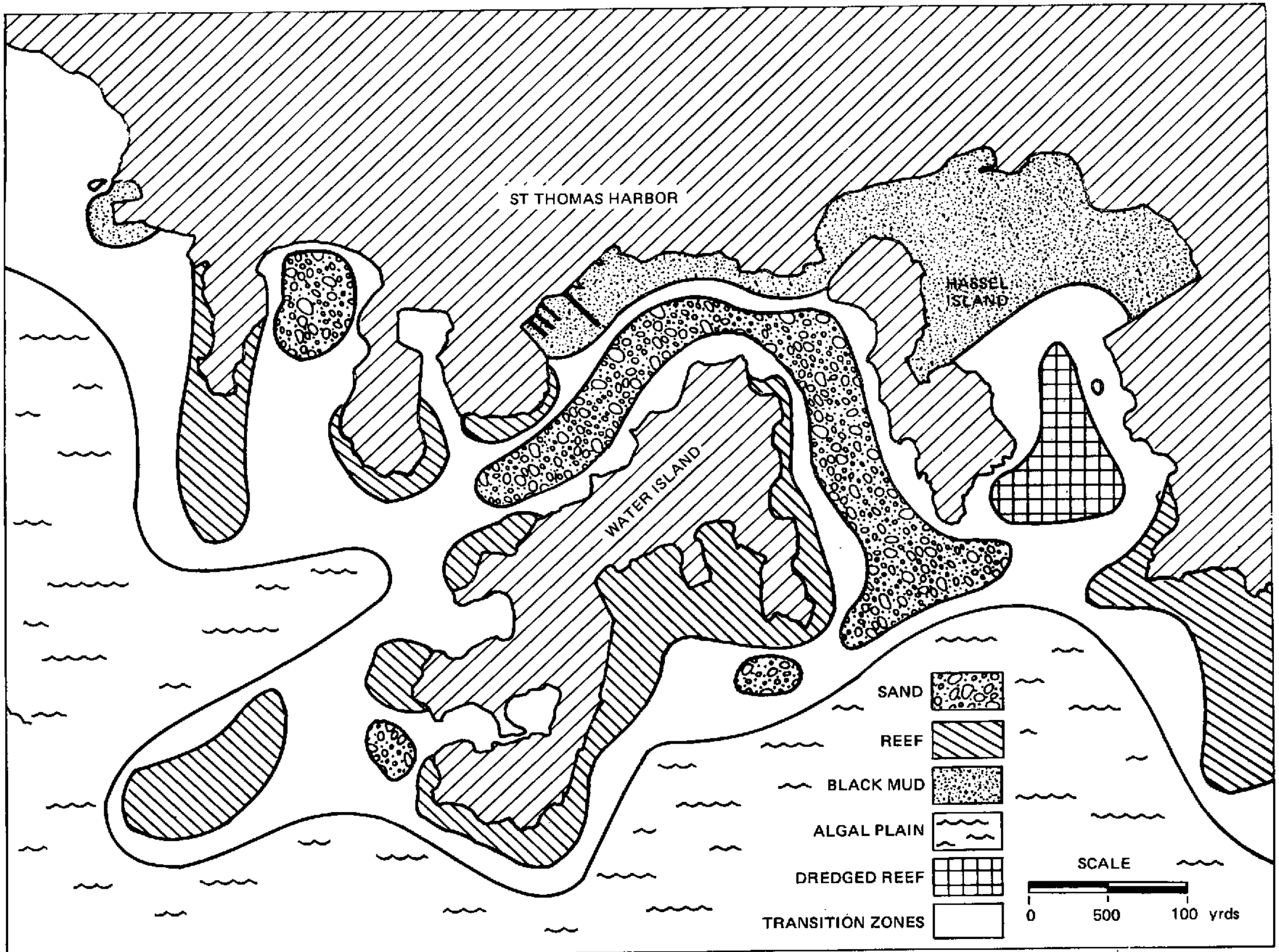

Figure 3-2. Benthic community types based on quantitative sampling by divers.

characterized by the spermatophyte Thallassia and a number of Chlorophytes, most notably, Caulerpa, Avranvillea, Penicillus and Halimeda (which is responsible for much of the sand production in the Caribbean).

The inner bay of Charlotte Amalie and the area fronting Crown Bay is almost devoid of life, as a fine black reducing mud covers most of the bottom. The only animals found in this region were two small clams Trachycardium sp. and Chione cancellata.

Table 3-2. Average Sample Diversity ($\bar{H}$) of Benthic Communities of St. Thomas

COMMUNITY	ALGAL PLAIN	REEF	SAND-GRASS	BLACK MUD
# Samples	14	27	13	15
$\bar{H}$	1.6304	1.1247	1.1613	0.2333
Standard Deviation	..5767	.9119	.7316	.1206

The sample diversity of the various community types was calculated using the standard Shannon-Weaver Information theory equation:

$$\bar{H} = \sum_{i=1}^{n} p_i \quad \ln (p_i) \quad ; \qquad (1)$$

where: H is the coefficient of diversity for a sample

P_i is the abundance of species i divided by the total for all species within the sample.

n is the number of species

Table 3-2 shows the average Diversity ($\bar{H}$) for all of the samples taken during the study. From this table it can be seen that the inner harbor and Crown Bay regions contained a low diversity community within the black mud bottom. These regions were areas of high pollution from sewage release and light industry within the region. Since the sampling centered around the Charlotte Amalie region, the samples collected from the reef communities were taken from areas where there was at least some effect of the dumping within the harbor. The sand and turtle grass community was also sampled from regions where there was secondary influence of pollution (as in the case of the channel between St. Thomas, Water and Hassel Islands) or perturbations induced by the dredging and thermal effluent with Lindbergh Bay. The algal plain community was found offshore in cleaner oceanic waters and was higher in diversity. Table 3-3 shows the ranges between the mean community values. A student-Neuman-Keuls test for the least significant ranges indicated that the algal plain was significantly higher in diversity (at the 0.05% level) than the next highest community, the sand and grass community. The sand-grass community did not differ significantly from the reef community which did differ from the black mud community at the 0.05% probability level.

Diversity values for different communities with the same biome are generally similar unless outside perturbations have induced changes. The present data indicate that the inner bay is highly reduced in diversity while the adjoining reef and sand-grass communities are existing in regions that are less disturbed. The offshore algal plain is fairly high in diversity when compared to the inshore communities but slightly lower than several samples taken from a similar community in Puerto Rico (Olsen, Wells and Sheen, 1972).

Table 3-3. Student-Neumann-Keuls Test of Diversity ($\bar{H}$) Ranges Between Community Types Indicate Significant Differences.

Community	Range**			
	1	2	3	4
Algal Plain	_____			
Sand-grass	.4692*	_____		
Reef	.5057	.0366 n.s	_____	
Black mud	1.3971	.9280*	.8912*	_____

* Significant at the 0.05% level
**Derived from Table 3-2 n.s.
non significant
Unmarked values were not tested because a smaller range was found to be significant.

3.2.2 Water Chemistry

Table 3-4 summarizes the findings from the ground truth data acquisition. Water chemistry measurements are plotted in figures 3-3 through 3-8. They indicate a relatively homogeneous water mass which is substantiated by the finding that the coefficient of variation for pH, slainity, conductivity and water temperature were all less than 2%. Dissolved oxygen (Figure 3-6) was more variable (Coefficient of variation between 8 and 10%)

Table 3-4. Summary of St. Thomas Ground Truth Data Acquisition

PARAMETER	UNITS	DEPTH	MAX.	MIN.	AVERAGE	COEF. OF VARIATION (%)	# SAMPLES
pH	-	5'	8.70	7.20	8.38	1.9	143
	-	mid	8.70	7.20	8.35	1.9	169
	-	bottom	8.70	7.20	8.34	1.8	163
Salinity	PPT	5'	37.00	34.30	35.12	1.0	181
	PPT	mid	37.00	34.30	35.15	1.2	209
	PPT	bottom	37.00	34.30	35.21	1.1	199
Conductivity	MHO/CM^2	5'	58.8	56.7	57.5	0.5	181
	MHO/CM^2	mid	58.8	56.7	57.5	0.5	209
	MHO/CM^2	bottom	58.8	56.7	57.5	0.5	205
Dissolved O_2	PPM	5'	7.95	5.00	6.60	8.4	182
	PPM	mid	7.95	5.00	6.56	8.2	186
	PPM	bottom	7.95	5.00	6.45	9.5	181
Depth	feet	-	78	7	35.3	46.9	205
Temperature	Deg. C	5'	29.80	29.0	28.70	1.3	181
	Deg. C	mid	29.80	27.0	28.64	1.1	209
	Deg. C	bottom	29.80	27.0	28.59	1.1	199
Turbidity	F.T.U.	5'	3.58	.12	.94	83.8	181
	F.T.U.	mid	3.58	.12	.85	90.8	209
	F.T.U.	bottom	3.58	.12	.96	89.5	199
Secchi Avg.	feet	-	54.2	7.	25.	52.8	153
Extinction Coef.	1/CM	multiple 5'	12.95	1.03	3.55	78.0	153
Pigments							
Chlorophyll A	Mg/M^3	5'	11.81	0	2.28	104.4	125
Chlorophyll B		5'	9.41	0	1.71	123.5	125
Chlorophyll C		5'	26.62	0	4.94	122.8	125
Astacin Carotenoids		5'	5.96	0	1.12	121.2	125
Non Astacin Carotenoids		5'	10.94	0	2.34	100.5	125

Table 3-4. Summary of St. Thomas Ground Truth Data Acquisition (Continued)

PARAMETER	UNITS	DEPTH	MAX.	MIN.	AVERAGE	COEF. OF VARIATION (%)	# SAMPLES
Current Speed	Knots	5'	1.00	.10	.30	51.1	137
	Knots	mid	1.00	.10	.26	57.4	155
	Knots	bottom	1.00	.10	.26	57.4	136
Current Dir.	Deg/10	5'	39.50	1.00	21.51	42.3	148
	Deg/10	mid	39.50	1.00	22.41	38.0	164
	Deg/10	bottom	39.50	1.00	21.25	42.2	142
Plankton Dens.	CC/MTR^3	-	.353	.009	.102	70.9	
Diversity	NITS	-	2.56	.00	.96	79.5	69

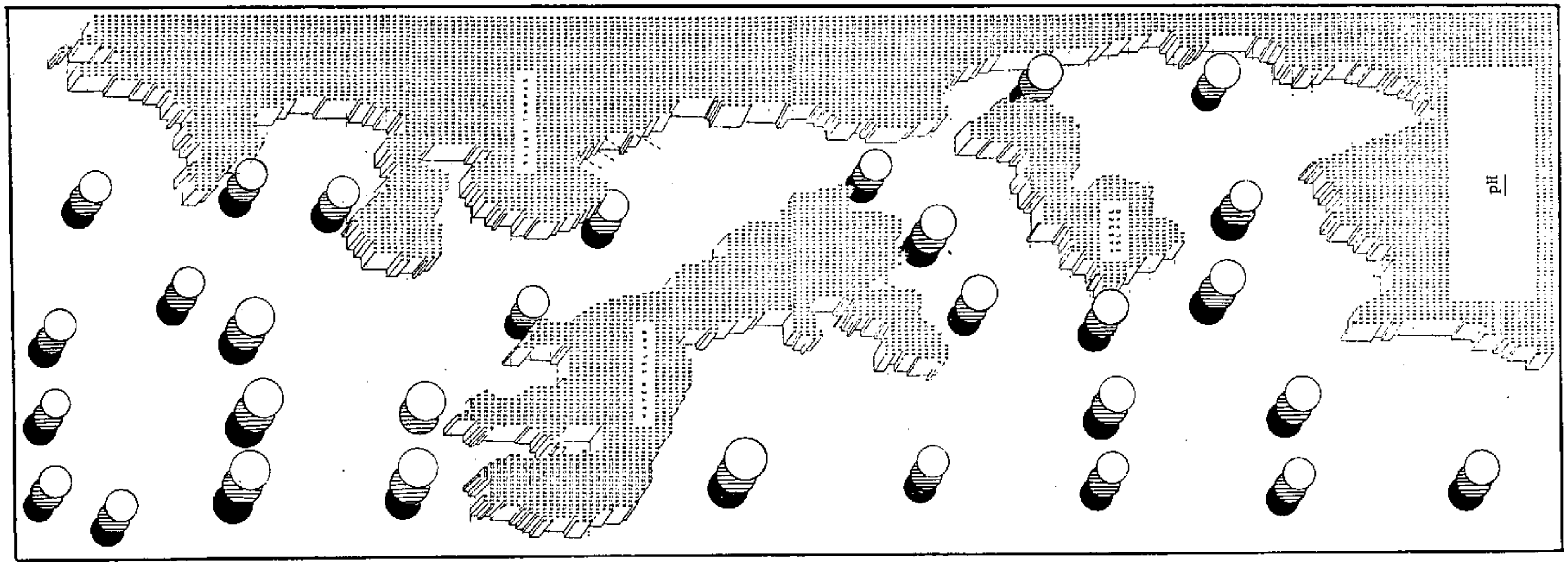

pH
DEPTHS: 5' (±1'), MIDPOINT (±15%) & BOTTOM (to +7')
RECORDED MIN./MAX. = 7.20/8.70; AVERAGE = 8.34
TEST PERIOD: Day 283 to Day 326, 1972
SCALED: ● MIN. ● MAX

Figure 3-3. Sampling of pH in the St. Thomas Region Indicates Slight Increase in the Inshore Region. Open Circles Represent Surface Waters, Shaded Circles Represent Mid Water (50%) of Bottom Depth) While Closed Circles Show the Value at 6 Feet Above Bottom Depth for this and Subsequent Figures

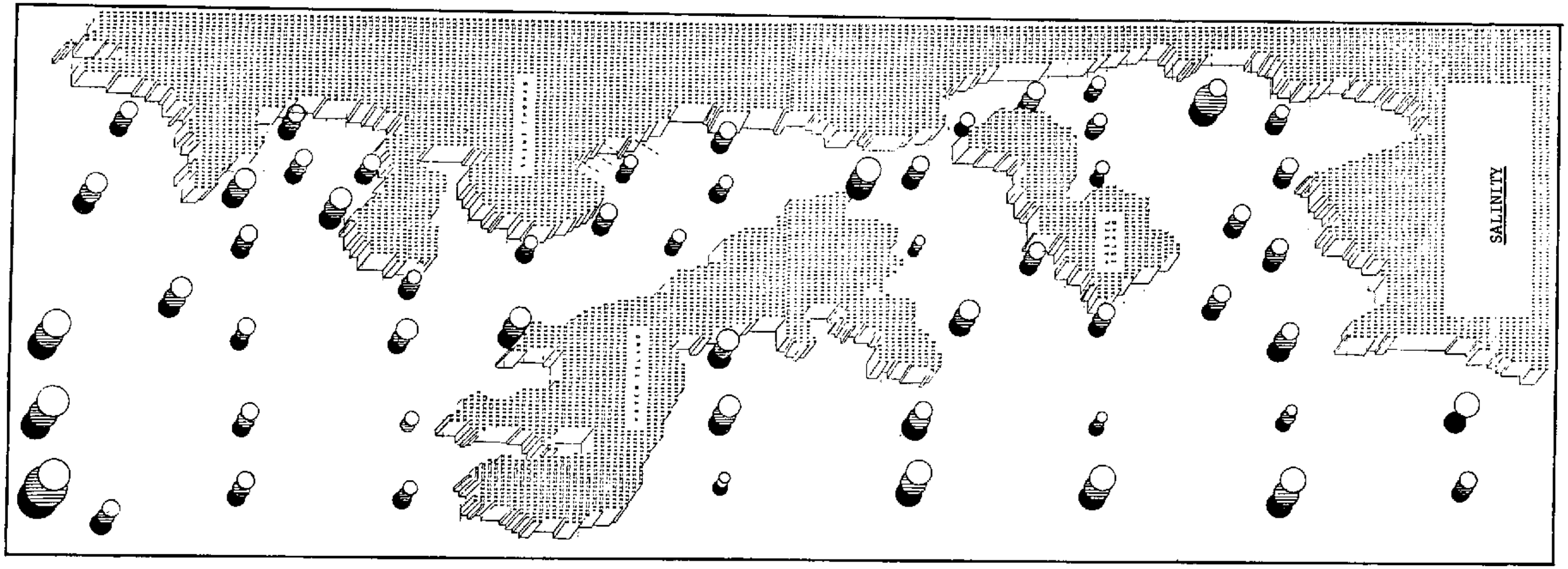

SALINITY (Parts/Thousand)
DEPTHS: 5' (+1'), MIDPOINT (+15%) & BOTTOM (to + 6')
RECORDED MIN./MAX. = 34.30/37.00; AVERAGE = 35.12
TEST PERIOD: Day 283 to Day 326, 1972
SCALED: ● MIN ● MAX.

Figure 3-4. Salinity Sampling From the St. Thomas Region Shows Significant Variability Between Depths and Sampling Sites. For Legend Explanation Consult Figure 3-3

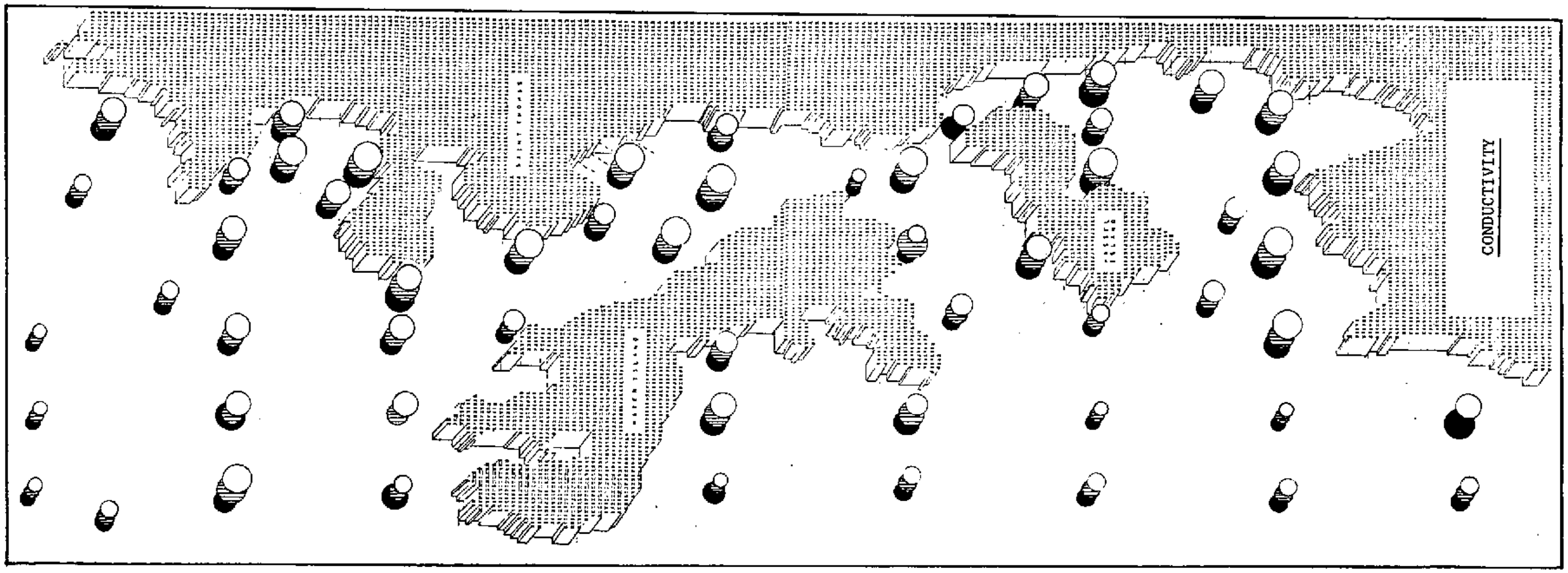

CONDUCTIVITY (MHO/CM^2)
DEPTHS: 5' (±1'), MIDPOINT (±15%) & BOTTOM (to +7')
RECORDED MIN./MAX. = 56.70/58.80 AVERAGE = 57.52
TEST PERIOD: Day 283 to Day 326, 1972
SCALED: ● MIN ● MAX.

Figure 3-5. Conductivity From the St. Thomas Region. For Legend Explanation Consult Figure 3-3

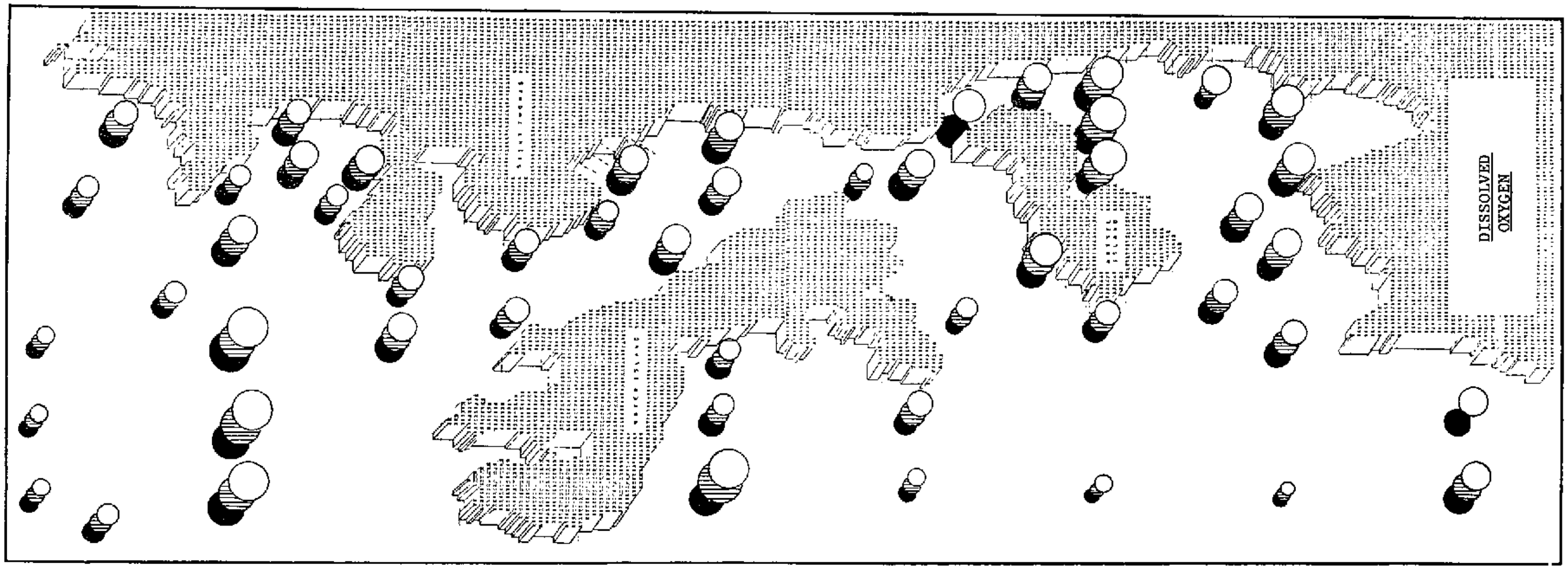

DISSOLVED OXYGEN (Parts/Million)
DEPTHS: 5' (±1'), MIDPOINT (±15%) & BOTTOM (to +6')
RECORDED MIN./MAX. = 5.00/7.95; AVERAGE = 6.60
TEST PERIOD: Day 283 to Day 326, 1972
SCALE: ● MIN. ● MAX.

Figure 3-6. Dissolved Oxygen From the St. Thomas Region. For Legend Explanation Consult Figure 3-3

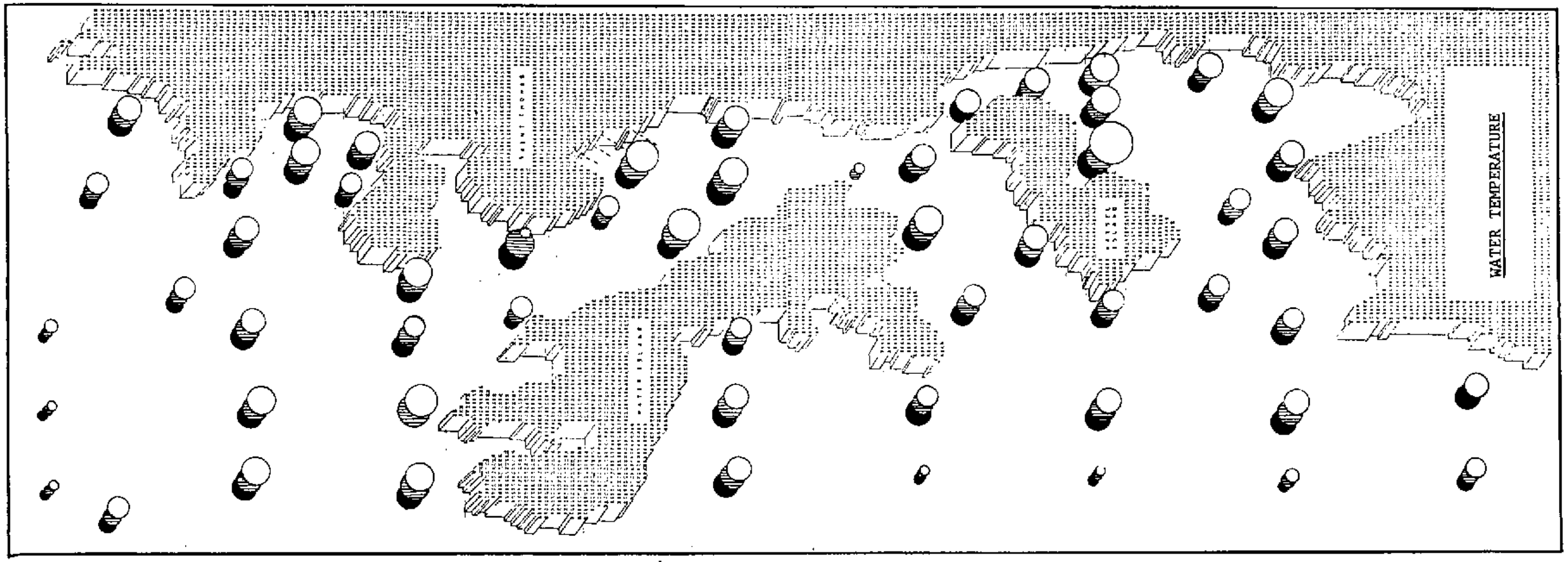

WATER TEMPERATURE (Degrees Centigrade)
DEPTHS: 5'(±1'), MIDPOINT (±15%) & BOTTOM (to +6')
RECORDED MIN./MAX. = 27.82/29.80; AVERAGE = 28.70
TEST PERIOD: Day 283 to Day 326, 1972
SCALED: ● MIN ● MAX.

Figure 3-7. Water Temperature From the St. Thomas Region Indicates Cooler Offshore Waters and Vertical Stratification. For Legend Explanation Consult Figure 3-3

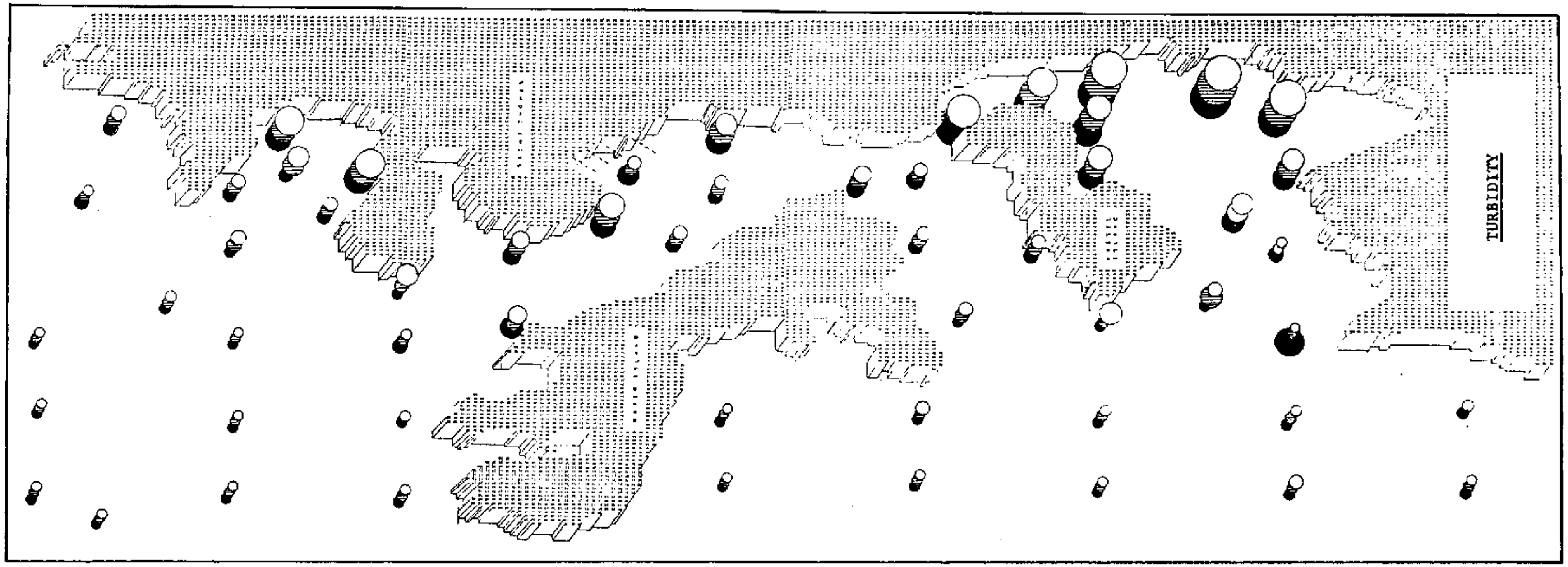

TURBIDITY (F.T.U.)
DEPTHS: 5' (+1'), MIDPOINT (+15%) & BOTTOM (to + 6')
RECORDED MIN./MAX. = 0.12/3.58; AVERAGE = 0.96
TEST PERIOD: Day 283 to Day 326, 1972

Figure 3-8. Turbidity Sampling From the St. Thomas Region Indicates That the Offshore Waters Are Low in Turbidity and Relatively Homogeneous Throughout the Water Column; While the Inshore Waters, Particularly Inner Charlotte Amalie Are High in Turbidity and With Much Heterogeneity Throughout the Water Column but this is in part due to difficulties in measurement and instrumentation problems. Water temperature (Figure 3-7) was a strong indicator of the differences between the cooler offshore waters and the warmer inshore areas where the shallow depth has allowed increase in temperature to occur. This homogeneity was primarily lateral. It appears that the deeper waters are slightly more saline while being cooler and with lower disolved oxygen and pH.

Pronounced stratification was not uncommon, particularly in Lindbergh Bay where the effluent from the desalinization plant moved variously in and out of the bay with the prevailing currents and tides. This movement (in Lindbergh Bay) is suggested quite clearly by the aircraft imagery in figure 3-9 which shows the position of the thermal plume. Figure 3-9 also indicates that the effluent from the desalinization plant is generally confined to the south eastern portion of the bay.

Temporal variability between sampling dates prevented detailed trend analysis.

The data thus far indicate the complexity of the oceanographic-biological system. Many of the parameters measured are either directly correlated or have some common causal root. In an attempt to analyze for the interrelations between the oceanographic variables, factor analysis was employed.

3.2.3 Factor Analysis.

Factor analysis is a multivariate technique that analyzes a correlation matrix for patterns of inter-correlation. It was first developed for the behavioral sciences by Spearman (1904) but has become a frequently used tool in systems-oriented ecological investigations. It is used here as a device for describing the interrelationships between the parameters measures. A glance at the correlation matrices from the surface (Table 3-5) and midwater sampling (Table 3-6) shows a high degree of correlation between the various parameters measured in this study. The factor analytical approach searches the correlation matrix for interrelated parameters and presents them as "factors" which are given in order of "importance" in explaining the variability of the statistical system. The "importance" of each factor is quantified as the % of the systems' variance accounted for by that factor. Rotated factor values greater than 0.3 (underlined here) are generally considered significant (Wenner et al, 1967).

In Table 3-7 the rotated factor matrix for 14 of the water quality parameters from the midwater depth (N = 155 observations) is shown. The first column (Factor A) describes the expected relation between increased wind speed and swell height. Most of the higher winds during the study were encountered offshore, accounting for the occurence of water

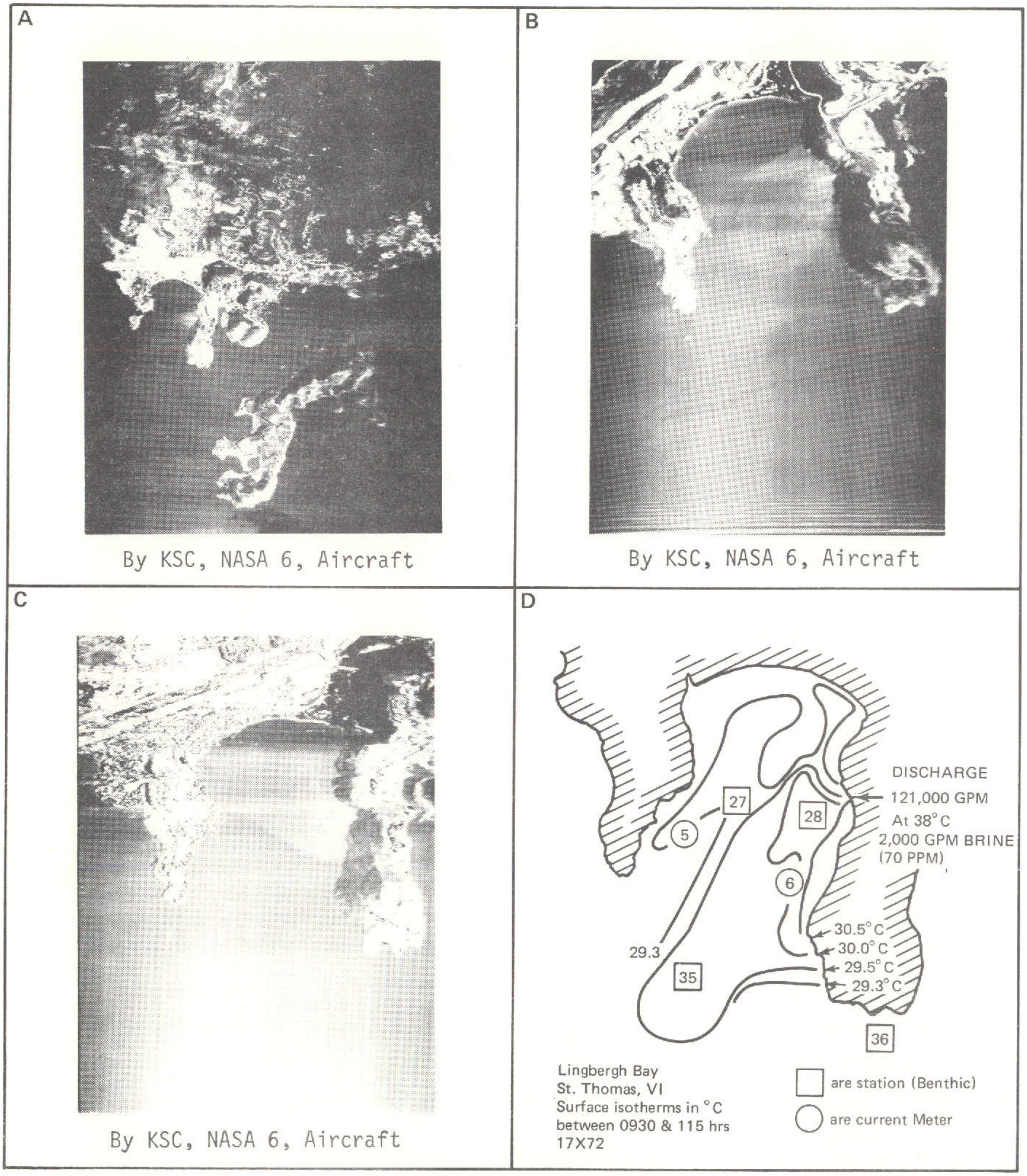

POWER/DESALINIZATION PLANT
DISCHARGE INTO LINDBERG BAY
ST. THOMAS, VIRGIN ISLANDS

Figure 3-9. Thermal Imagery Taken From an Aircraft Mounted I^2S Sensor Shows Varying Distributional Patterns of Thermal Effluent Into Lindbergh Bay. Figure A Was Taken on 10-16-72 at an Altitude of 6000 ft., Figure B on 10-17-72 at 2000 ft., and Figure C on 10-19-72 at 2000 ft. Figure D is From Thermal "Ground Truth" Gathered 10-18-72

Table 3-5. Correlation Matrix for Selected Atmospheric and Oceanographic Parameters Shows a High Degree of Inter-Correlation for Samples Taken From the Surface Waters

	WIND SPEED	WIND DIRECTION	CLOUD COVER	AMBIENT TEMP.	SWELL HEIGHT	SWELL DIRECTION	WATER DEPTH	SAMPLE DEPTH	DISSOLVED O_2	pH	CONDUCTIVITY	SALINITY	WATER TEMP.	TURBIDITY	SECCHI AVG.	PLANKTON VOL.
Wind Speed	1.000															
Wind Dir.	-.217	1.000														
Cloud Cover	-.031	-.096	1.000													
Ambient Temp.	-.130	.077	.164	1.000												
Swell Height	.389**	.025	.182	-.166	1.000											
Swell Dir.	-.164	.120	-.173	.070	-.210	1.000										
Water Depth	.200	.063	.150	-.052	.605**	-.307**	1.000									
Sample Depth	.067	.112	-.117	-.048	.252*	-.333**	.410**	1.000								
Dissolved O_2	-.262	.258	-.065	-.116	-.008	.092	.053	.411**	1.000							
pH	-.331**	.150	.170	.029	.076	-.332**	.190	.416**	.375**	1.000						
Conductivity	-.336**	.172	.277*	.391**	.299**	.198	-.426**	-.372**	.010	.073	1.000					
Salinity	.398**	-.242	-.236*	-.257*	-.023	.234*	-.283*	-.547**	-.312**	-.658**	-.065	1.000				
Water Temp.	-.446	.107	.389**	.447**	-.135	-.013	-.072	.028	.098	.382**	.624**	-.584**	1.000			
Turbidity	-.206	-.151	.086	-.268*	-.473**	.316**	-.535**	-.623**	-.069	-.302**	.341**	.307**	.010	1.000		
Secchi Avg.	.138	.160	.069	.058	.634**	-.302**	.844**	.430**	.043	.261*	-.428**	-.347**	-.016	-.699**	1.000	
Plankton Vol.	.374**	-.144	-.183	-.431**	.279*	-.028	.161	.139	.046	-.295*	-.518**	.393**	-.627**	-.120	.057	1.000

*Significant at .05% level
**Significant at .01% level

Table 3-6. A Correlation Matrix for Selected Atmospheric and Oceanographic Parameters Shows a High Degree of Inter-Correlation for Samples Taken From Midwater (50% of Bottom Depth) During the Sampling Program

	WIND SPEED	WIND DIRECTION	CLOUD COVER	AMBIENT TEMP.	SWELL HEIGHT	SWELL DIRECTION	WATER DEPTH	SAMPLE DEPTH	DISSOLVED O_2	pH	CONDUCTIVITY	SALINITY	WATER TEMP.	TURBIDITY
Wind Speed	1.000													
Wind Direction	-0.148	1.000												
Cloud Cover	.136	.054	1.000											
Ambient Temp.	.224	.256	.421**	1.000										
Swell Height	.369	.107	.290**	.088	1.000									
Swell Dir.	-0.184	.096	-0.232*	-0.048	-0.273*	1.000								
Water Depth	.218	.137	.310**	.125	.670**	-0.376	1.000							
Sample Depth	.110	.092	.162	.065	.370**	-0.205	.538**	1.000						
Dissolved O_2	-0.257	.217	-0.100	-0.140	-0.024	.087	-0.028	-0.053	1.000					
pH	-0.259	.175	.114	-0.016	.116	-0.338**	.185	.104	.270*	1.000				
.	-0.171	.238*	.328**	.376**	-0.079	.158	-0.170	-0.111	-0.017	.007	1.000			
Salinity	.202	-0.219	-0.268*	-0.250*	-0.078	.242	-0.261*	-0.120	-0.110	-0.542**	.006	1.000		
Water Temp.	-0.349**	.233	.396**	.366**	.002	-0.007	.011	-0.056	.084	.295*	.608**	-0.497**	1.000	
Turbidity	-0.200	-0.123	-0.047	-0.089	-0.461**	.364**	-0.547**	-0.296*	-0.039	-0.254	.282*	.280*	.041	1.000

*Significant at .05% level
**Significant at .01% level

FOLDOUT FRAME
)

FOLDOUT FRAME
2

depth (and consequently sample depth since they are redundant variables in this case) in this factor which accounts for 25% of the total systems variance. Factor B is related to the weather pattern that persists when rain squalls hit the island. There is a drop in air temperature following the increased cloud cover, which is subsequently followed by a precipitation-related drop in conductivity. This factor accounts for 16% of the systems variance. When there are high winds (usually from the south east) slight changes in the pH level are observed. Fifteen percent of the total systems variance is described by this factor.

Table 3-7. Varimax Rotated Factor Matrix for Samples Taken from Midwater (50% of Bottom Depth) Shows the Interrelationships Between 14 Selected Water Quality Parameters.*

FACTOR	A	B	C	D
1. Wing Speed	.46	.05	-.43	.46
*2. Wind Dir.	.23	.30	.01	-.71
3. Cloud Cover	.25	.67	.18	.25
4. Ambient Temp.	.17	.75	-.05	.05
5. Swell Height	.80	.11	-.02	.02
*6. Swell Dir.	-.38	.03	-.50	-.47
7. Water Depth	.85	.07	.16	.02
8. Sample Depth	.64	.01	.02	-.06
9. Disolved O_2	-.01	-.20	.24	-.64
10. pH	.12	-.01	.81	-.15
11. Conductivity	-.27	.77	-.05	-.19
12. Salinity	-.15	-.25	-.76	.07
13. Water Temp.	-.16	.70	.46	-.19
14. Turbidity	-.70	.13	-.27	.00
% OF VARIANCE	25	16	15	10

*Additional analyses using tidal window data and omitting wind and swell direction as variables are discussed in Section 4-5.2.

Table 3-8 shows the factor analysis of the data collected from the near surface waters. Complex patterns of variable interaction arise from the introduction of the biological variable of total plankton volume. A detailed analysis of the water chemistry variables shown as interrelated in this factor would be required to explain the effects on plankton volume. This volume is the crude measure and is definitely related to sample depth over which the vertical tow was made, although this is not apparent from Table 3-8. The parameter interactions in this factor A, are basically the same as in Factor A from the

Table 3-8. Varimax Rotated Factor Analysis for 16 Parameters Sampled From 5 Feet Below the Surface Shows the Interrelationships Between Parameters and Their Importance to the Analytical System

FACTOR	A	B	C	D	E
1. Wind Speed	.36	-.27	-.52	-.30	-.10
2. Wind Dir.	.18	.13	.23	.71	-.08
3. Cloud Cover	.14	.18	.06	-.18	.82
4. Ambient Temp	.10	.86	-.10	.03	-.13
5. Swell Height	.79	-.25	-.09	.02	.26
6. Swell Dir.	-.30	.02	-.28	.68	-.04
7. Water Depth	.85	-.11	.12	-.04	.10
8. Sample Depth	.46	-.09	.61	-.16	-.39
9. Dissolved 0_2	-.02	-.25	.67	.39	-.06
10. pH	.15	.14	.80	-.13	.11
11. Conductivity	-.42	.57	.02	.25	.41
12. Salinity	-.24	-.38	-.77	.04	-.06
13. Water Temp.	-.08	.69	.40	.04	.38
14. Turbidity	-.77	-.18	-.17	.10	.40
15. Secchi Avg.	.90	.02	.15	.00	-.02
16. Plankton Vol.	.18	-.72	-.22	-.04	-.19
% OF VARIANCE	42	16	12	8	6

midwater data. Factor A accounts for 42% of the systems variance. Factor B accounts for 16% of the variance. Factor B is a salinity factor which ties together the temperature and conductivity variables. In factor C (accounting for 12% of the variance) water chemistry variables combine with wind speed to describe the parameters interactions in the offshore waters.

Briefly summarized, the factor analysis points out the complexity of the oceanographic system in the Virgin Islands. The small land mass has little effect in dampening perturbations induced by the weather-related variables. Further work should be done to quantitatively define the nature of the parameter interactions, but at least the interaction between weather, water, and biotic variables has been documented.

3.2.4 Currents

Sampling the currents with the over-the-side current meter revealed several interesting patterns. Interpretation of the results is of course qualified by the fact that the observations were taken only once at the benthic stations and six times for the 16 repetitive stations; boat swinging introduced another source of possible error. The Pilot Chart for the St. Thomas region shows that the general current is from the southeast at about .5 knots. The offshore patterns observed in our sampling of the surface waters (Figure 3-10) and the midwater samples (50% of bottom depth) shown in Figure 3-11 show that this general trend is preserved until the waters reach within two miles of the island. At this time the water mass is split into three recognizable entities. The first enters the harbor at Charlotte Amalie through the passage between Hassell Island and the main island of St. Thomas. We interpret the low current velocities within the harbor itself to indicate that the current eddies at this point. Tidal fluctuations through the main entrance and Frenchman's Cut result in some movement in the peripheral parts of the harbor, but for the most part, the inner harbor is subject to little flushing.

The second water mass splits off at the point of Hassel Island and generally flows northward through East Gregerie Channel (Figure 3-12) between Hassel and Water Islands. It is reflected by both the land mass of St. Thomas and the water flow out of Charlotte Amalie harbor through West Gregerie Channel where it rejoins the northeasterly flowing oceanic water mass that represents the third water mass. This pattern generally holds for both the surface and sub-surface water masses, although it was not uncommon to record differing directions for surface and subsurface currents.

At both flood tides during the course of the study we recorded currents flowing towards the southeast, directly opposite to the general flow patterns. The cause of this

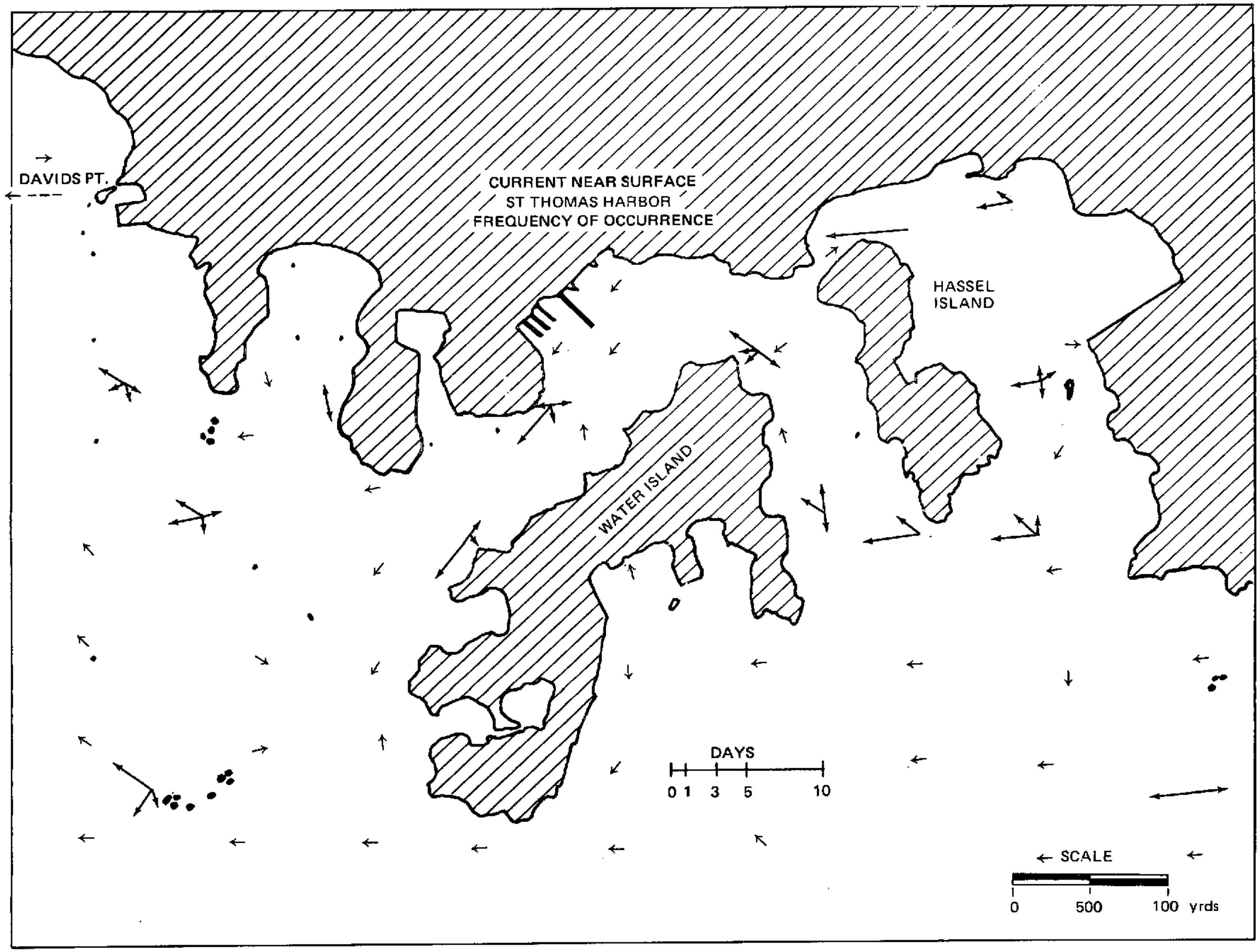

Figure 3-10. Surface currents from day 285-321, approximately 1 day a week. Length of arrows show number of days per direction. Dotted arrows indicate single measurement.

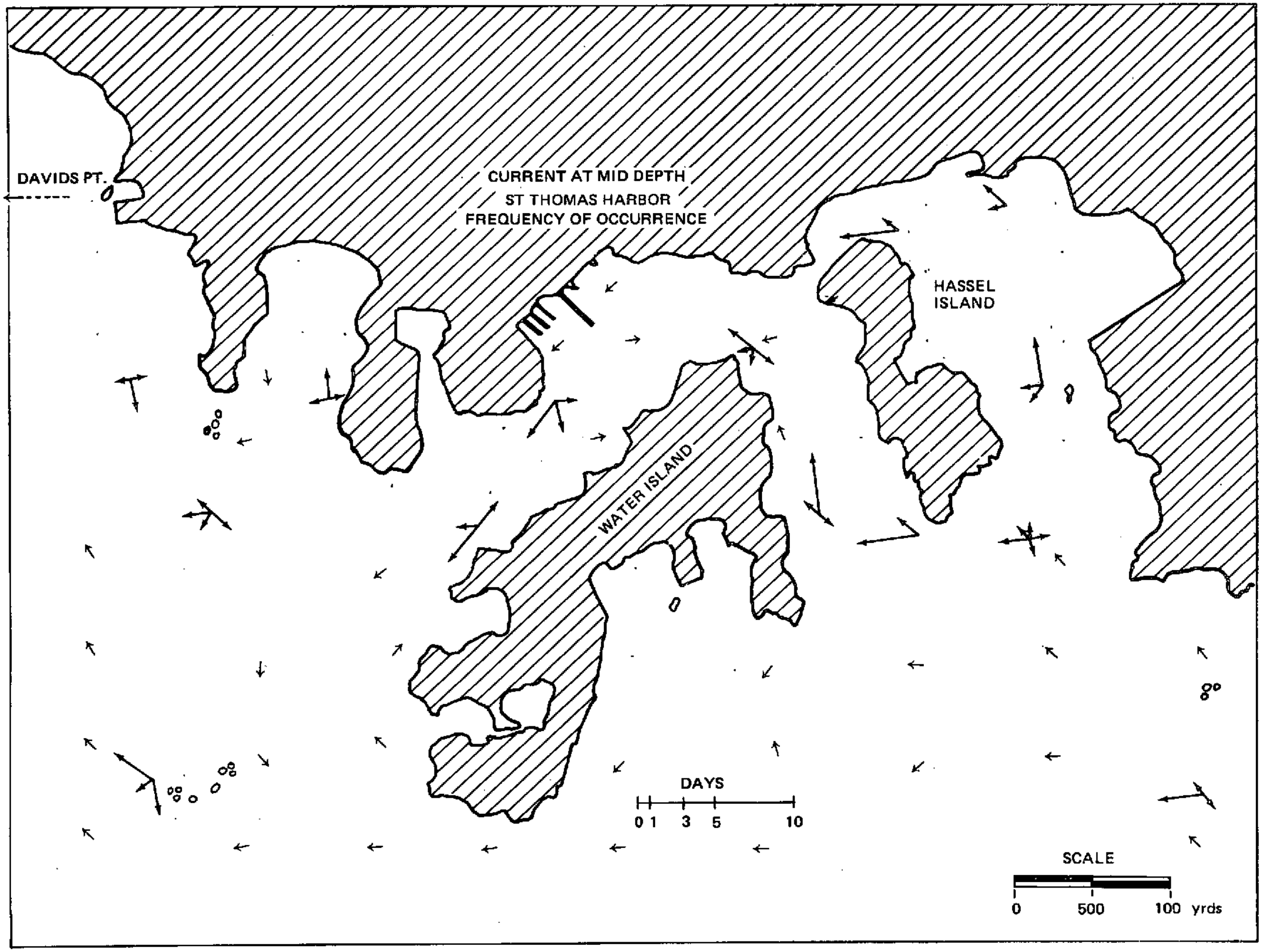

Figure 3-11. Mid water current direction from days 285-321, taken approximately 1 day per week. Length of arrows shows number of days per direction. Dotted arrows indicate single measurement.

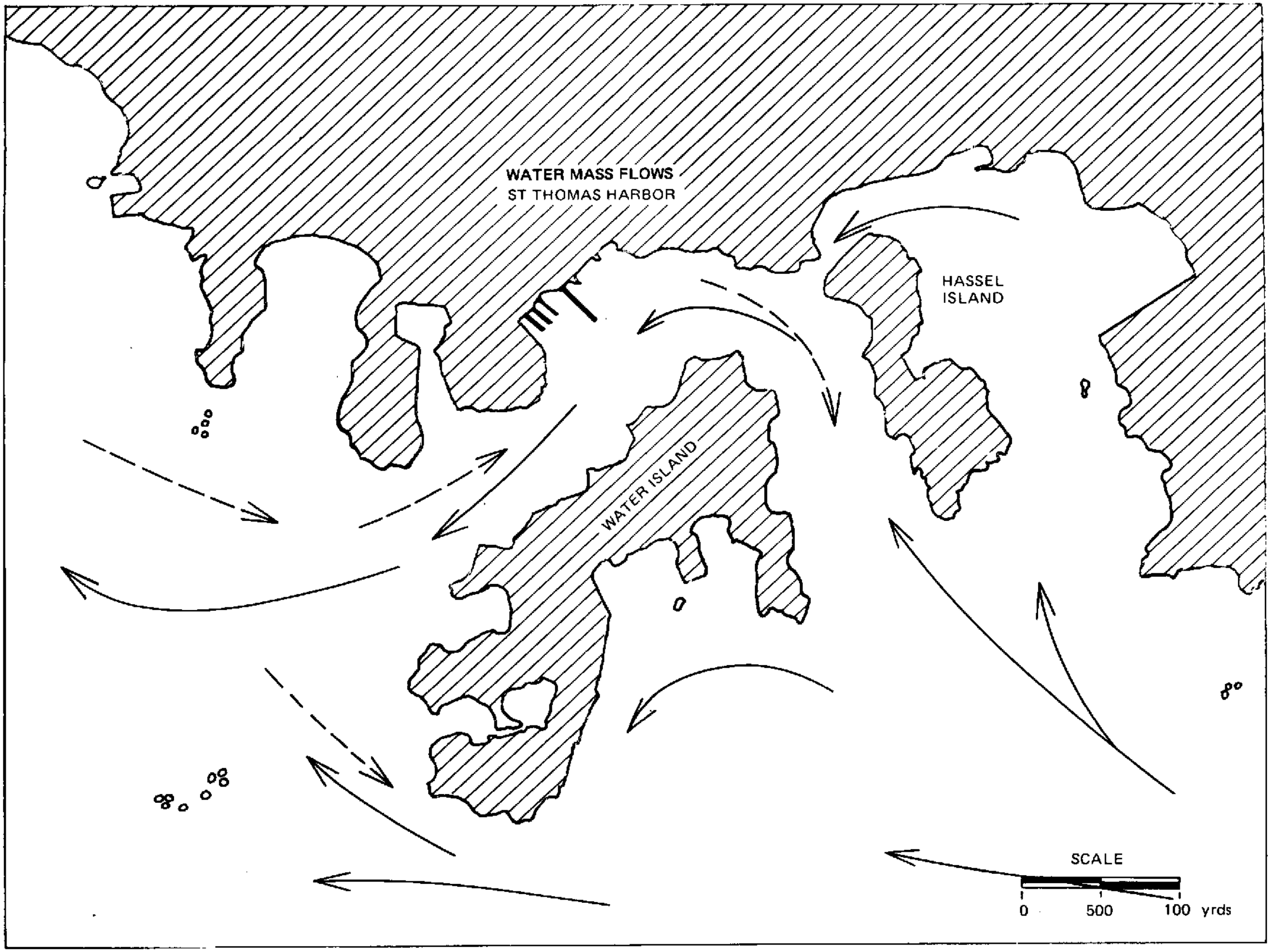

Figure 3-12. Inshore current patterns from Charlotte Amalie, St. Thomas. Solid lines represent prevailing conditions while dotted lines indicate conditions during a Flood-tide related reversal.

reversal is uncertain at present, although it may represent Atlantic waters coming around the northwest corner of the island. A similar reversal has been reported from Puerto Rico (Frank Torres, personal communication). At these times the flow was reversed through the Gregerie channels and some minor effect was observed in the inner harbor although it was confined to the northwest end.

The current patterns during the three diurnal studies are shown in Figures 3-13 through 3-15. At station 12, inner Charlotte Harbor, for days 311 and 312, the current never exceeded .2 knots and flowed towards the northwest on the incoming tide and southeast on the outgoing tide. There were no apparent differences between surface, midwater and bottom currents and the low current velocities confused the directional picture somewhat. It seems clear that this area was an unfortunate choice for the existing outfalls since there is little circulation and the effluent tends to remain in the area.

Station 9 exhibited strong current patterns over the course of the two diurnal studies conducted there. The narrow passage between Water and St. Thomas islands restricts the directional variation markedly. Maximum currents occurred during the incoming tide during the 325-326 (Figure 3-15), and on the outgoing tide on the 318-319 (Figure 3-14) observations. Since the normal current pattern is for the southeast oceanic current to the branch off through the Gregerie channels, it would follow that during normal tidal conditions the oceanic current would enhance the tidal current out the West Gregerie Channel. The period of 318-319 marked a period when the previously mentioned current reversal was occuring. In this case the oceanic current was flowing in opposition to the tidal current and damping the current velocity. Directional uniformity at this station was to be expected since the narrow channel did not offer much potential for directional variability.

3.2.5 Salinity/Temperature and Water Mass

Plots of salinity against temperature are frequently used to give indications of the existence of water mass differences (Percious et al, 1972). In Figures 3-16 through 3-19 Salinity-Temperature (ST) plots give further evidence of the pollutive effects from Charlotte Amalie harbor. In the one-time areal sampling, there is an inherent temporal variability, but Figures 3-16 (bottom depth) and 3-17 (5 feet below surface) indicate the offshore cool water mass (cluster A in both figures) as being distinct from the inshore mass which is both warmer and lower in salinity (cluster B in both figures). Temporal variation is also evidenced in these figures by cluster C in both figures which were subjected to increased salinity (when compared to the inshore cluster of points). The surface waters

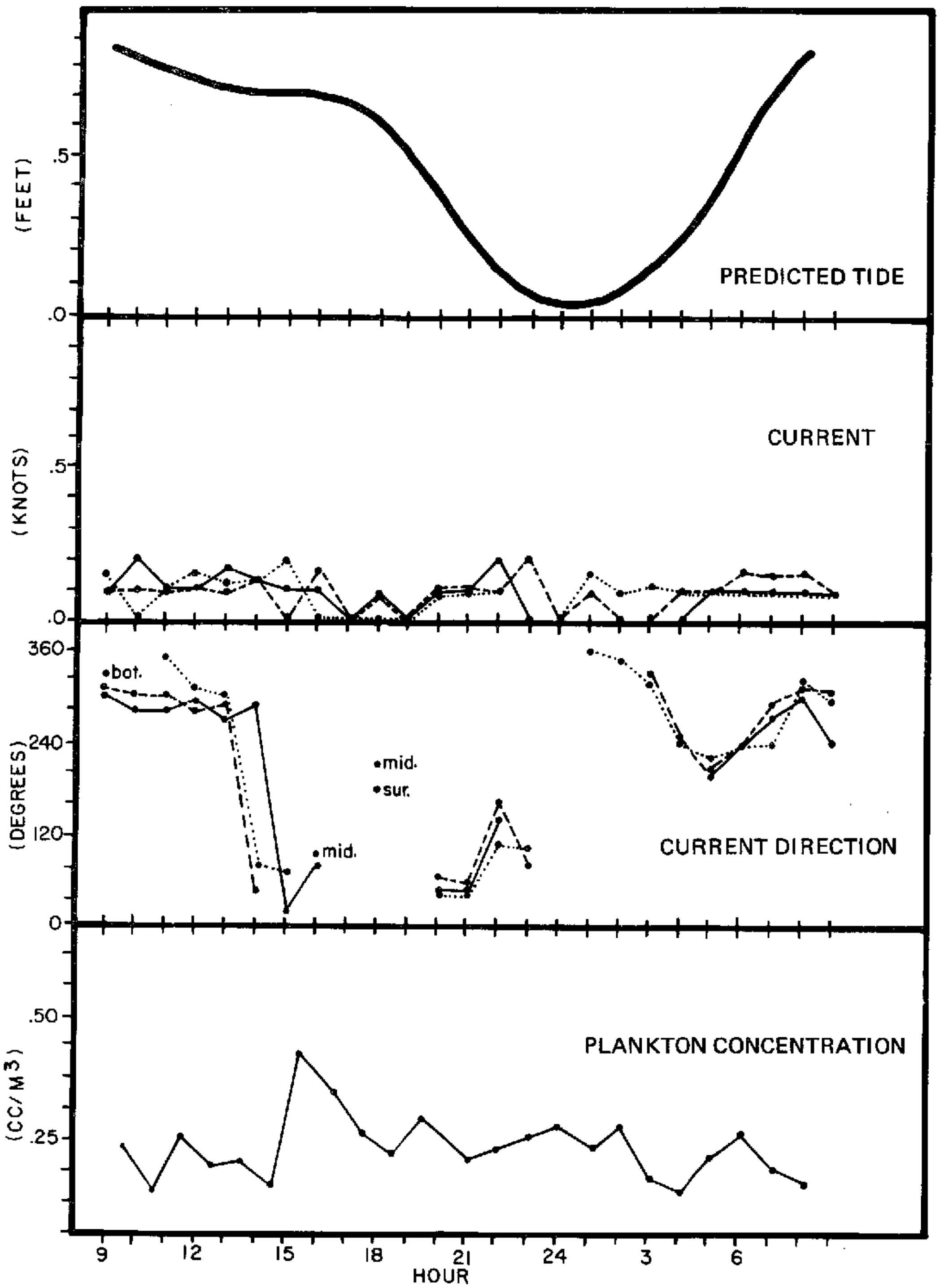

Figure 3-13. Tide (Predicted from N.O.S. tide tables), current velocity, current direction and plankton density from a diurnal study at station 12 (see Figure 1) on day 311-312. Solid line is for samples taken from the surface waters while mid water samples are shown by a dashed line and the dotted line represents samples taken 5 ft. above the bottom. Discontinuity in direction occur at times of no measurable current.

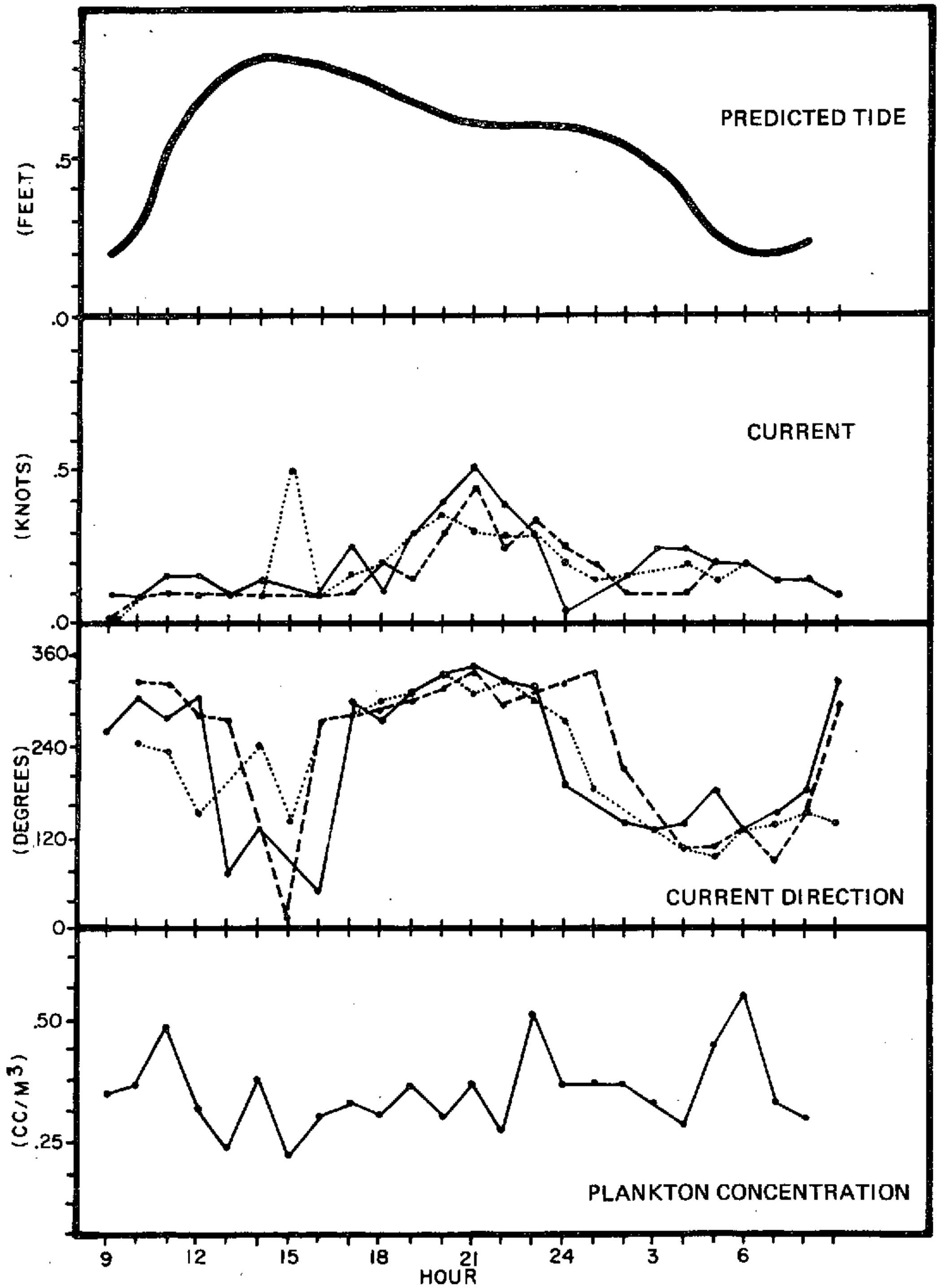

Figure 3-14. Tidal state, current velocity, current direction and plankton density from a diurnal study at station 9 (see Figure 1) on day 318-319. Solid line is for samples taken from the surface waters while mid water samples are shown by a dashed line and the dotted line represents samples taken 5 ft. above the bottom. Discontinuity in direction occurs at times of no measurable current.

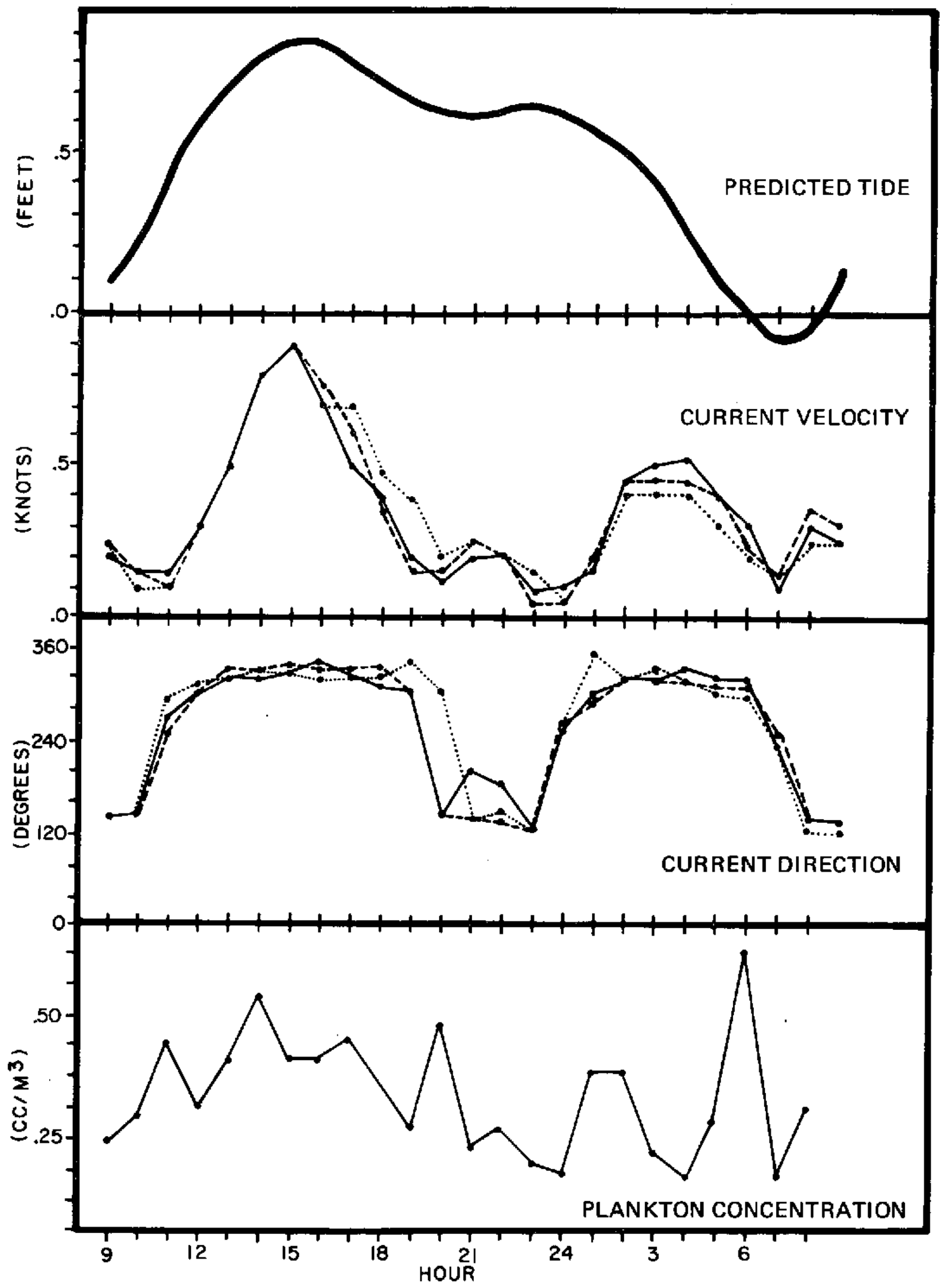

Figure 3-15. Tidal state, current velocity, current direction and plankton density from a diurnal study at station 9 (see Figure 1) on day 325-326. Solid line is for samples taken from the surface waters while mid water samples are shown by dashed line and the dotted line represents samples taken 5 ft. above the bottom. Discontinuity in direction occur at times of no measurable currents.

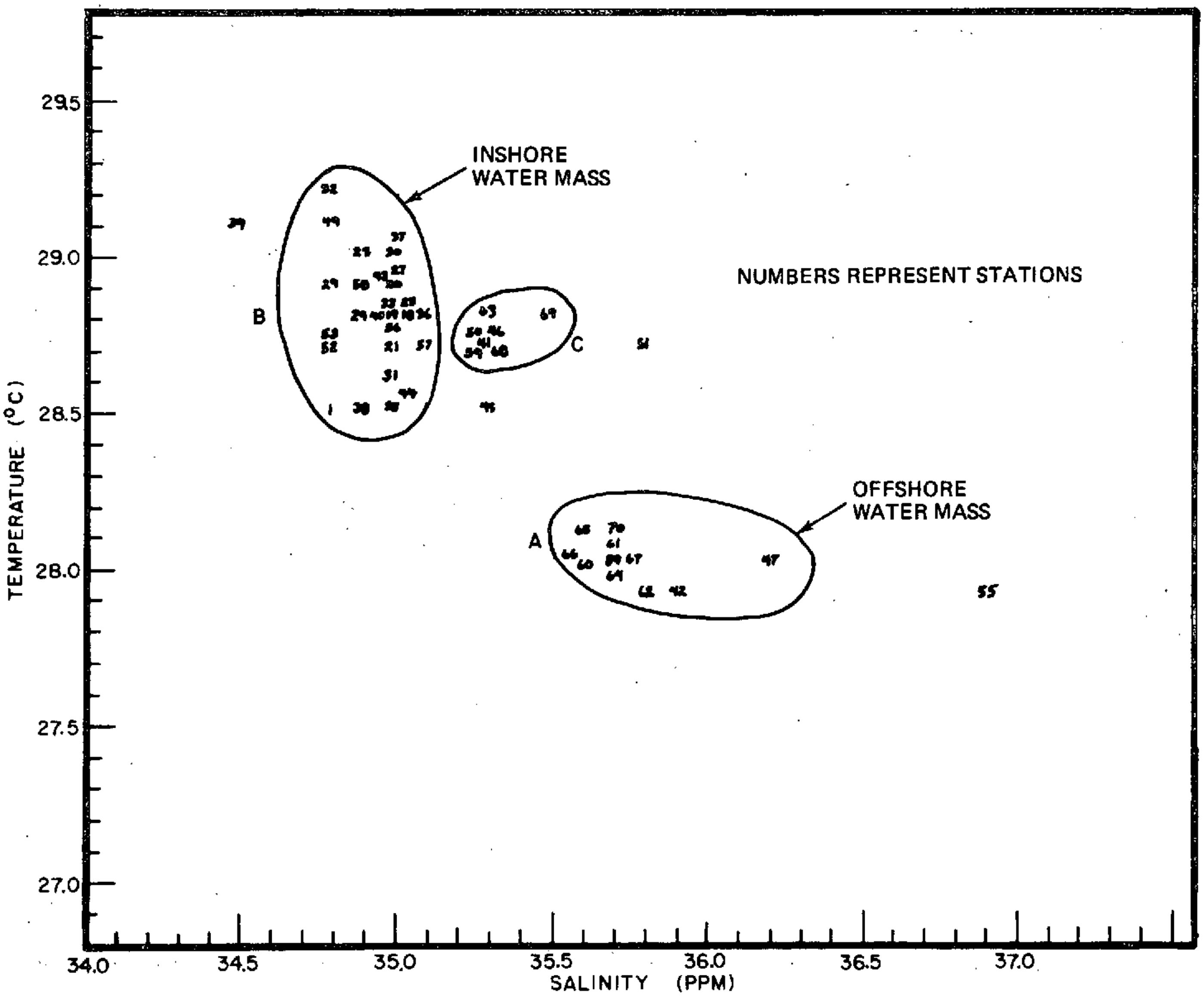

Figure 3-16. Salinity/Temperature plots for samples taken 6 feet above bottom depth during areal sampling show the existence of discrete water masses. See text for explanation of point clusters.

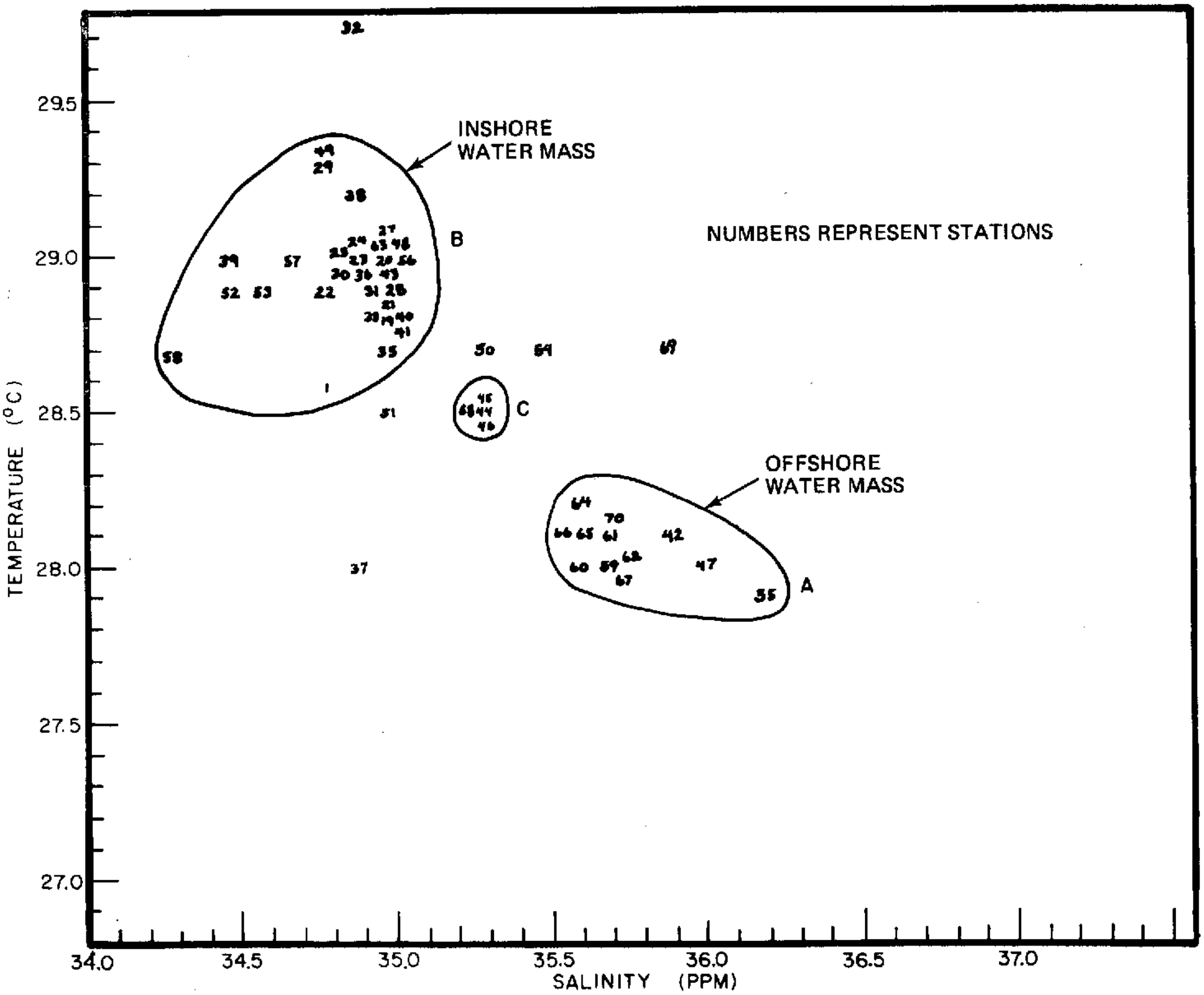

Figure 3-17. Salinity/Temperature plots for samples taken 5 feet below the surface during areal sampling show the existence of discrete water masses.

evidenced this phenomenon in the region south of Lindbergh Bay (Figure 3-17) while the bottom waters (Figure 3-16) showed it throughout the offshore samples.

In Figure 3-18 (bottom waters for the repetitive stations) temporal variation in Salinity/Temperature effects are again sorted out. The normal state is evidenced by cluster A while three distinct additional clusters are observed both south of Lindbergh Bay (Cluster C), within Lindbergh Bay (Cluster D), and in the inner harbor and West Gregerie channel (Cluster B).

Salinity/Temperature plots of the three diurnal studies indicate that Station 9 (at the junction of West and East Gregerie channels) is relatively uniform, (Figure 3-19 Clusters A and B). At Station 12 (in front of the sewage outfall at King's Wharf) there is an observable difference resulting in a cluster of daytime points (Cluster C) which are distinct from the night time points (Cluster D). This is probably related to diurnal sewage patterns.

3.2.6 Plankton Concentration

The plankton concentration was derived from the total volume of plankton captured in a vertical tow, divided by the depth of the tow. In Figure 3-20 the values for plankton concentration (cc/M^3) are plotted. The average values from the 17 repetitive stations indicate much the same water quality statements as the benthic sampling. Clean oceanic water has a concentration of between less than .01 and .15 cc/M^3. Detailed contour lines could not be drawn since the variability between days was too great. The variability from hour to hour (Figures 3-13 thru 3-15) was also very great so that samples taken from different times of the day could not be validly compared. No diurnal trends in plankton abundance were observed during the 24 hour studies.

3.2.7 Plankton Pigments

Diurnal variation in pigment and water parameters was investigated in the series of three 24 hour studies. The boat was anchored at the selected study area and the normal sampling program, described previously, was carried out over the diurnal cycle. Locations and times were selected so as to assess the variability both between sites and within sites between days. The sites were selected on the basis of prior information from the repetitive sampling program. Station 12 was selected as being typical of the inner harbor with its low circulation and high eutrophication levels from nearby outfalls. Station 9 was located in the channel between Water Island, Hassell Island and St. Thomas. It was chosen because of the great variability exhibited, presumably due to the funnelling effect of the surrounding land masses. The choice of days furnished us with comparisons between two locales at tidal cycles

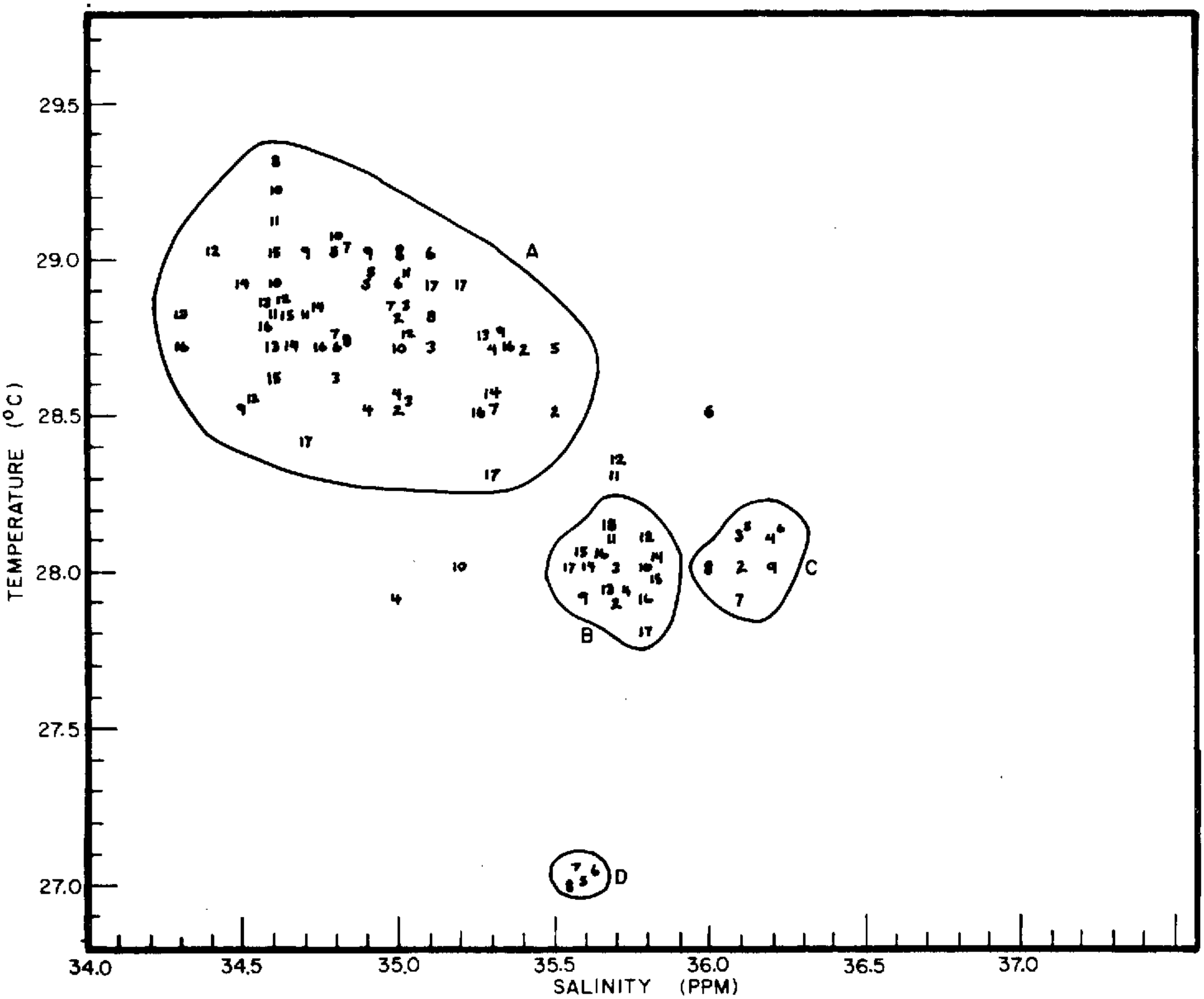

Figure 3-18. Salinity/Temperature plots for samples taken 6 feet above bottom depth for the 17 repetitive stations show the existence of discrete water masses.

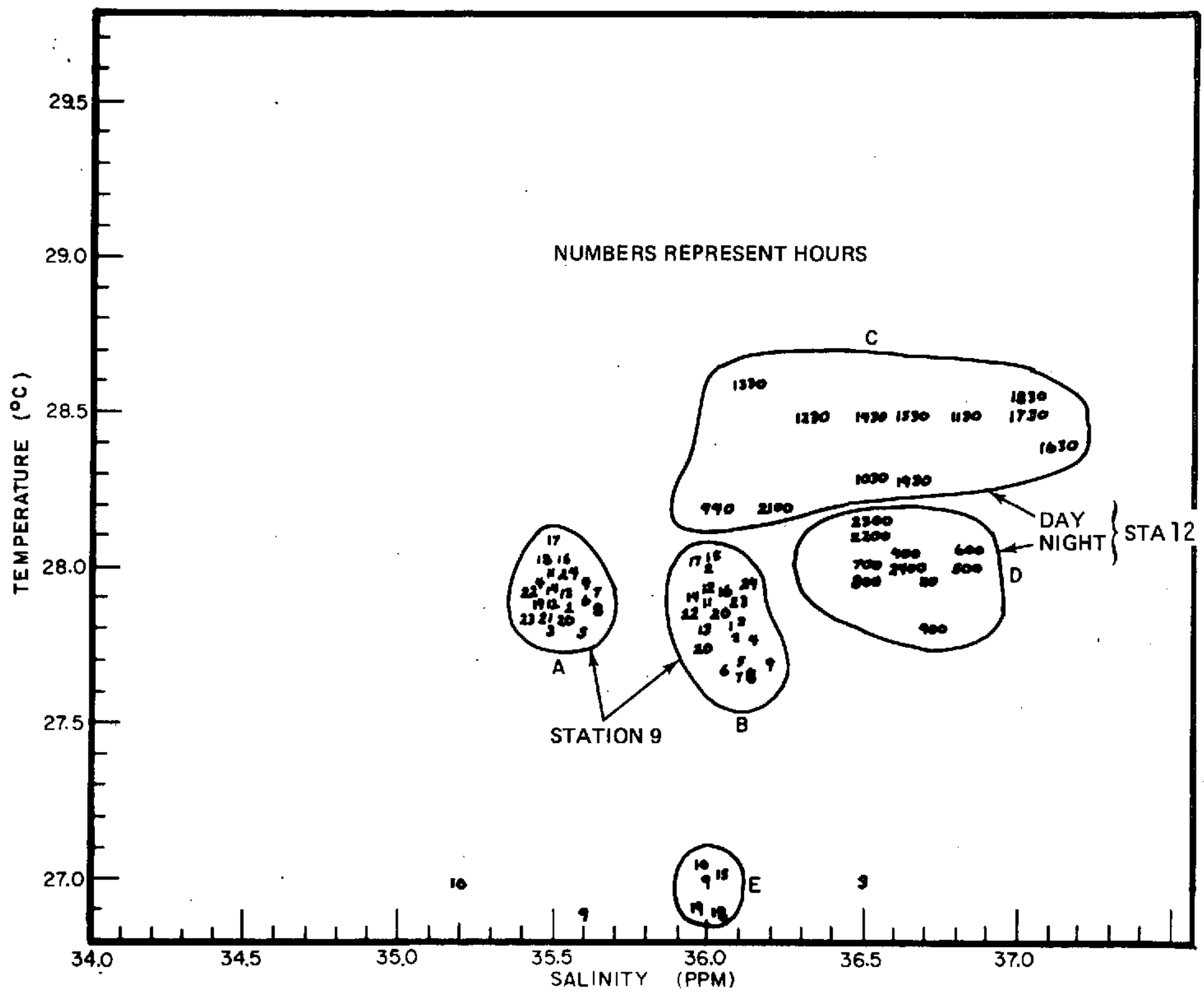

Figure 3-19. Salinity/Temperature plots for mid waters (50% of bottom depth) from the 3 diurnal studies at stations 9 & 12, show the existence of discrete water masses.

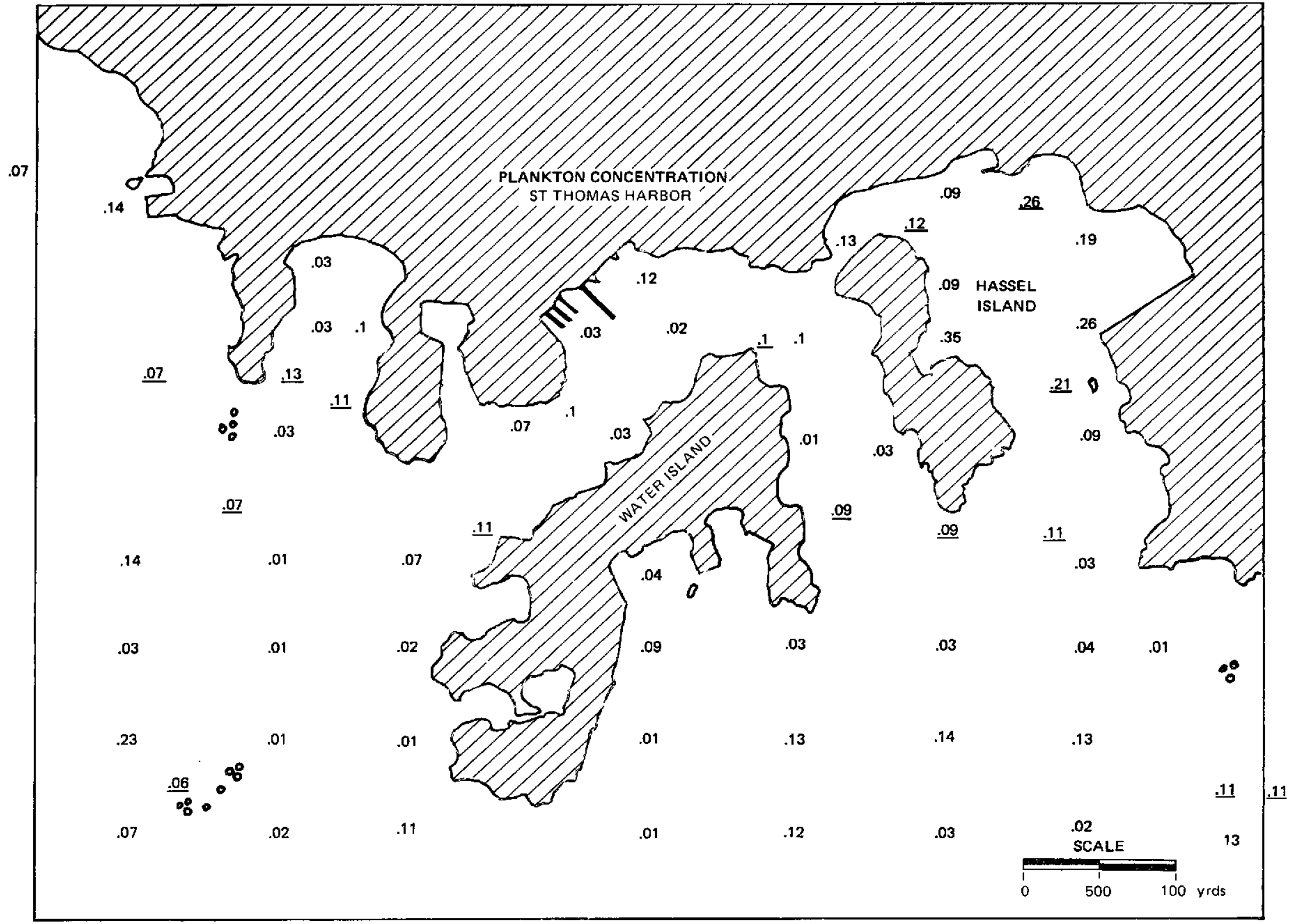

Figure 3-20. Plankton concentration (cc/M^3) from the St. Thomas region. Average values from repetitive sampling are underlined, while remainder are from one time sampling.

approximately equal (days 311 and 312 at station 12 and days 318 and 319 for station 9) and between the two days at station 9 where an "average" tidal cycle was compared to a maximal cycle (days 325-326).

The purpose of this periodic sampling was to assess the time range over which "ground truth" could be collected and still permit comparison with ERTS data. This is important because the satellite data was to be utilized to detect changes in surface radiance for comparison to long term temporal changes established by repetitive satellite coverage. The primary pigments were sampled after the method of Strickland and Parsons (1968) and the data analyzed by analysis of variance to indicate the source of variation.

All five pigment analyses gave similar results and so only the chlorophyll a tabulation is presented. From these results (Table 3-9) one can see that the variability between hourly data is indeed too great to permit ground truth to be noncoincident with the satellite passes. The variability between hours within dates was significant at the .001 level of probability. A later comparison of the data from the separate dates at station 9 indicates that the between date variation was non-significant ($F = 0.75$; $df = 1, 48$; p. was non-significant). This would seem to indicate that conditions within any site are relatively constant and once the diurnal variation is held constant or understood, then valid geographical interpretation is feasible.

Table 3-9. Analysis Of Variance (ANOVA) Of Chlorophyll A Concentrations (Mg/M^3) From 3 Diurnal Studies at 2 Locations

	LEVEL	SS	DF	MS	F
Between sites	2	215.4	1	215.4	1.9 n.s.
Within dates	1	215.7	2	107.9	33.8*
Within hours	0	226.3	71	3.2	

*Significant at .001% level n.s. non significant

In an attempt to analyze the Chlorophyll a data for the minimum interval between ERTS observation and ground truth collection that would permit valid comparisons, the pigment concentration at time t was correlated to the concentration at time $t+i$ where i was an interval between 1 hour and 12 hours. The square of the product-moment correlation coefficient is considered as an indication of the proportion of the total sum of squares explained by regression (Steel and Torrie, 1960). This statistic was plotted against i (Figure 3-21) for i equal to 1 to 12 hours for each of the three diurnal studies. The predicted decrease in the statistic r^2 with increasing values of i did not occur but a complex relation seemed to emerge. There appears to be an increase in predictability (r^2) at the intervals approximating 6 hours. We were unable to obtain significant correlation between pigment concentration and tide or light. Further work on this question (of allowance lag between ground truth and satellite observation) must certainly be undertaken before correlative data can be assigned causative interpretation.

3.2.8 Initial Correlation With Uncorrected ERTS-1 Bulk CCT Data

Statistical analysis of the relationship between ERTS imagery and ground-truth water quality variables was somewhat hampered by cloud cover on all but the October 17 overflight. Partial cloud cover on that day caused us to eliminate several data points and therefore the following treatment is based on 31 points where plankton pigment density and turbidity could be related to cloud-free ERTS bulk CCT quantum data. The Chlorophyll a pigment absorbs in the wave lengths measured by Band 5 while the carotenoids absorb in the lower end of Band 6 and Upper end of Band 5. A preliminary comparison of turbidity with MSS Band 5 was made.

In Table 3-10 the results of the statistical analysis are given for fitting the data to the linear regression equation:

$$Y = aX + c$$

Where: X is the independent variable

Y is the dependent variable

a is the slope of the regression line

c is the intercept

Table 3-10. Regression Analysis of Selected Water Quality Parameters and ERTS Bulk CCT Values Indicates Significant Relation

PARAMETER	BAND[1]	SLOPE	INTERCEPT	F[2]	P[3]
Chlorophyll A	5	.24	9.65	1.95	.25
Total carotenoids	5	.119	9.79	1.46	.25
Turbidity	5	1.63	8.51	93.31	.001

1. ERTS Bulk CCT MSS quantum values supplied by Grumman
2. F = Explained MS/Unexpalined MS
3. For 1 and 29 degrees of freedom

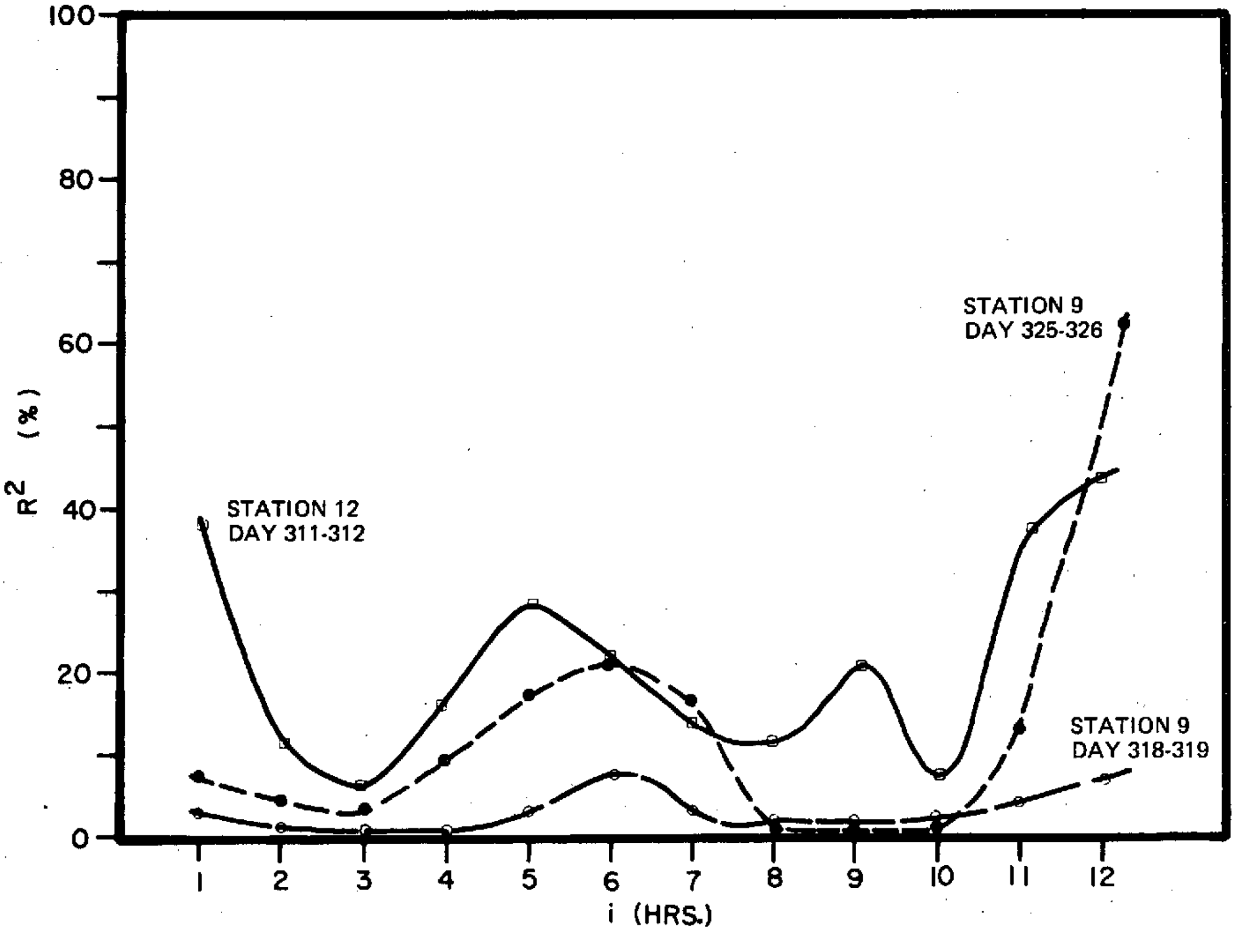

Figure 3-21. Percent of Total Sum of Squares From Correlation of Chlorophyll a Content of Surface Water at Time t and Again at Time t+i Hrs. The Data Came From 3 Diurnal Studies at Station 12 on Day 311-312 (Open Boxes), and at Station 9 on Day 318-319 (Open Circles) and Day 325-326 (Closed Circles) Sample Size is 24 AT Hr. 1, and 24-i for Each Successive Interval.

Linear regression was used because it is statistically more rigorous than logarithmically transformed data. Figures 3-22 through 3-24 suggest that there may be some non-linear relation between the ground truth and ERTS data.

Turbidity was significantly related to their MSS band 5 values (F=93.2, df - 1,29, p .001). Chlorophyll a and total Carotenoids were not significant at the .05% level) but the results indicate that further work may establish a relationship. Turbidity was highly significant in its relation to the Band 5 data. This is particularly encouraging for remote sensing since turbidity is easily measured and appears to be one of the strongest indicators of environmental disruption in the present study. This last statement is supported by the fact that benthic diversity correlated with turbidity (r = .655, p .01, df - 67). Benthic diversity has been used in the present study to delineate long-term responses by the biotic community to water quality degradation from pollutants. This tie between satellite spectral data, turbidity, and benthic diversity offers encouragement for the ERTS program for use not only as a monitoring device but also as a device for indicating changes in key variables pertinent to water quality.

3.3 DISCUSSION

The ground truth data acquisition documented the areas of long term influence from the continued disposal of raw sewage and minor industrial waste into the region of Charlotte Amalie harbor. Although the inshore areas, particularly the inner harbor which was almost devoid of benthic life, show reduced species diversity in the benthic community and increased turbidity, and higher phytoplankton pigment concentration (presumably in response to the eutrophicative effects of the dumping); this effect extends out less than two miles into the offshore sublittoral.

Analysis of the chemical and oceanographic parameters associated with "water quality" demonstrated the dynamic nature of these parameters. Water movement, light, human activity, and weather parameters all effect changes in these parameters. The resulting matrix patterns are further complicated by a high degree of intercorrelation between parameters which prevents valid univariate statements. Multiple regression analysis of the data offers some hope for establishing functional relationships within the matrix.

The studies of diurnal variability indicated a homogeneity between different times at the same locale although short time temporal variability is too great to permit valid statistical analysis between locales. This finding offers encouragement for remote sensing

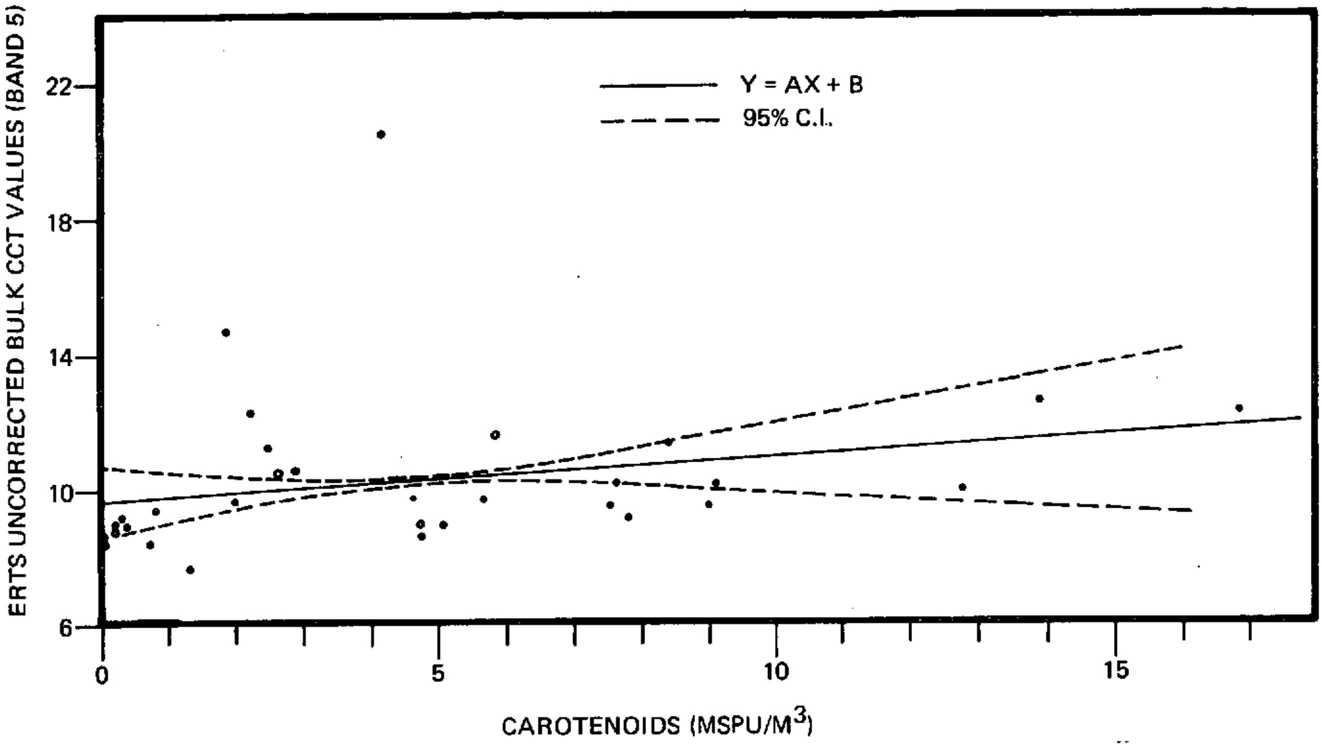

Figure 3-22. Regression of Total Carotenoids MILLI Special Pigment Unit/M^3 (MSPU/M^3) Pigment Concentration on Spectral Radiance Measured by Remote Sensing (ERTS-1 MSS Sensor, Band 5, Bulk CCT Data) Suggests the Feasibility of Satellite Monitoring of Water Chemistry Parameters. Open Circles Represent Points Where the ERTS Data Was Affected By Cloud Cover.

Solid Line Represents Line of Best Fit While Dashed Line Represents 95% Confidence Interval, A F-Test of the Significance of the Slope Was Not Significant.

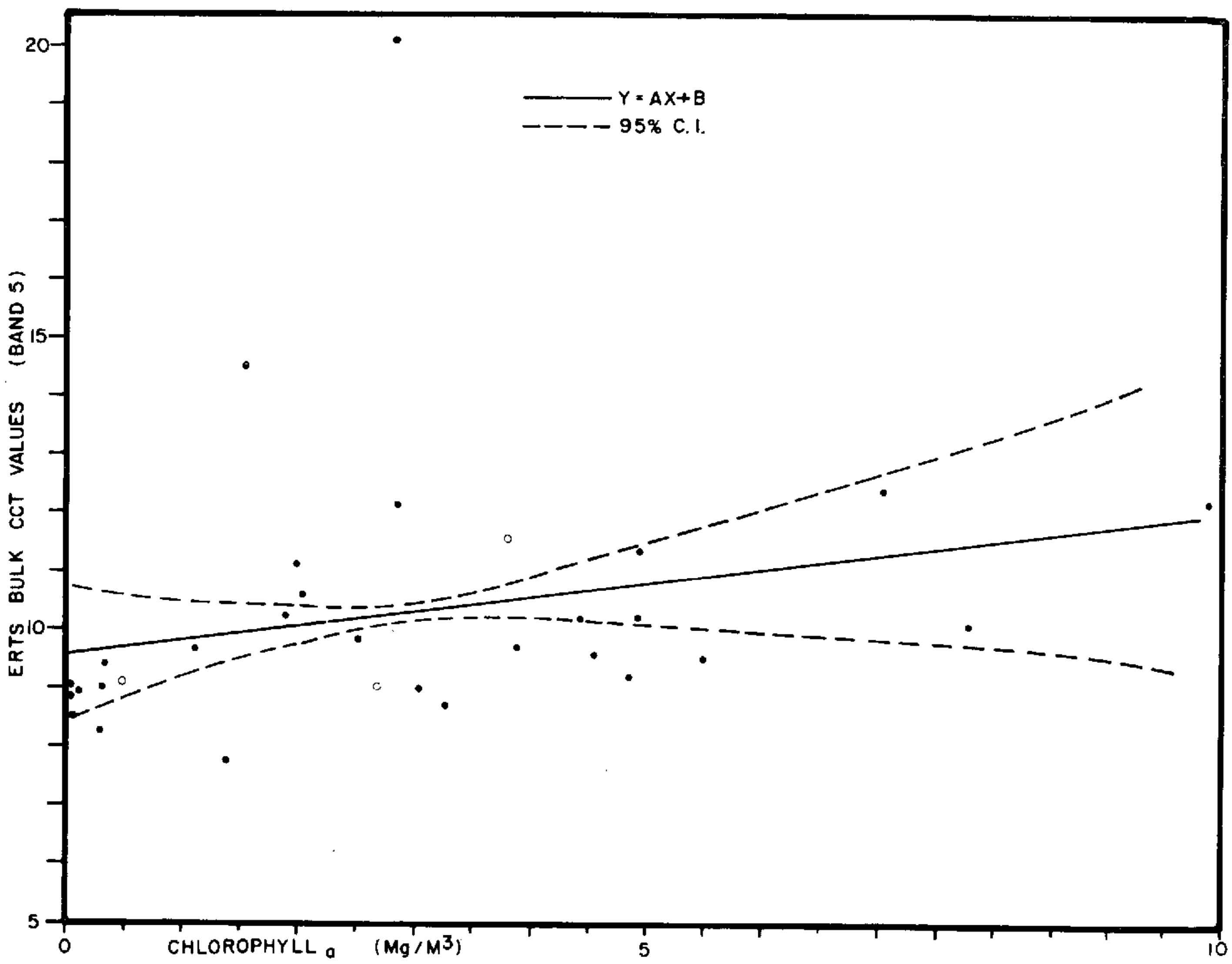

Figure 3-23. Regression of total Chlorophyll A (mg/M^3) pigment concentration on spectral reflectance measured by remote sensing (ERTS-1 MSS sensor, Band 5, Bulk CCT data) suggests the feasibility of satellite monitoring of water chemistry parameters. Open circles represent points where the ERTS data was affected by cloud cover. Solid line represents line of best fit while dashed line represents 95% Confidence Interval. A F-test of the significance of the slope was not significant.

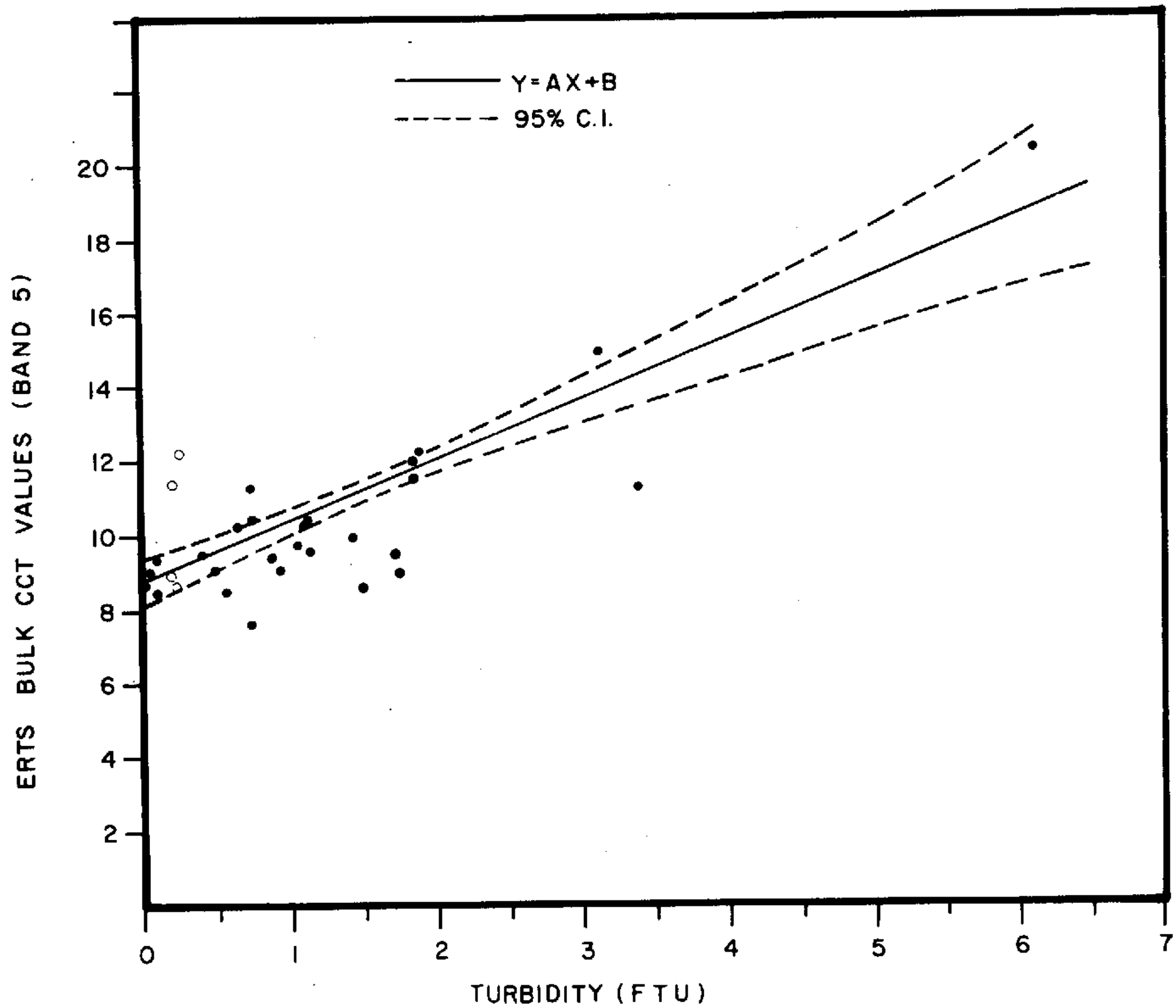

Figure 3-24. Regression of Turbidity (FTU) on spectral reflectance measured by remote sensing (ERTS-1 MSS sensor, Band 5, Bulk CCT data) suggests the feasibility of satellite monitoring of water chemistry parameters. Open circles represent points where the ERTS data was affected by cloud cover. Solid line represents line of best fit while dashed line represents 95% Confidence Interval. A F-test for the significance of the slope was highly significant.

since wide geographical areas can be compared instantaneously, thereby eliminating the temporal variable completely. Repeated coverage of the same site should demonstrate temporal changes occurring between satellite passes.

Temporal variability analyses were conducted seeking trends in "predictability". Weather effects dominated these analyses and significant correlations applicable to predictability were not realized.

The results of the oceanographic parameter sampling supported the findings of Precious et al (1972) in many ways. We noted the interaction between bottom topography, wind and tidal currents in determining current direction and velocity. The current within the inner harbor is low and the waters are generally higher in salinity and temperature. Within the inner harbor there is greater variability in the water column than in the offshore waters. The general current trends indicate that these offshore waters are divided by the harbor entrance and Hassell Island. The water mass is funnelled through the Gregerie Channel and normally flows southwest until it rejoins the oceanic water mass. In the area south of Lindbergh Bay the inshore waters effect variable water conditions throughout large area.

Twice during the course of the study (during maximum tidal flow) this general trend was reversed and the offshore current flowed from the southwest instead of the southeast. The cause of this reversal was not further investigated but the effects should be taken into consideration in any ocean dumping plans by the Virgin Islands' government. At present this reversal carries much of the loose garbage from the solid waste disposal site at Harry S. Truman Airport back into the Gregerie Channels. This unfortunate consequence could be rectified by regulating dumping during these periods. Waste from the new sewage outfall could be affected during reversal periods.

Benthic sampling indicates that the waters of the inner harbor have effected changes in the benthic communities adjacent to the harbor and extending from at least Rupert Rock (Station 13) and southwest to the airport. The inner harbor and Crown Bay is almost devoid of life. Although circulation from the waters of the Gregarie Channel may result in a "return" to a diverse community type, the inner harbor will certainly lag behind since there is little circulation.

The ERTS MSS Band 5 appears capable of monitoring turbidity, which is one of the water quality parameters measured in the "Ground Truth" program. Turbidity is also one of the best indicators of water quality and correlates with benthic diversity.

Benthic diversity is the best indicator of the long term water quality conditions existing within the study area. The reason for this was simply that water chemistry parameters are very dynamic and instantaneous measurements are stochastically unrepresentative of parametric conditions. We observed a significant correlation between benthic diversity and turbidity. The inferential web that is being woven is that the satellite appears to have the capability of sensing turbidity which suggests benthic diversity which is indicative of long term water quality conditions. Changes in turbidity are complex and our attempts to relate turbidity and ERTS data to two possible sources of increased turbidity (Chlorophyll a and Total Carotenoids) were somewhat hampered by the small sample size.

Turbidity is a complex parameter and changes in any of a number of oceanographic parameters can effect changes in it. Certainly phytoplankton blooms as well as sedimentation in the highly euthrophicated waters of Charlotte Amalie Harbor and Crown Bay should show up as increases in turbidity.

The results of this analysis suggest positive areas of application for the satellite in water quality monitoring. The study task attempted to define areas of similar "water quality" through the analysis of a broad spectrum of parameters generally considered to be indicative of variability in this condition.(1)

----

(1)The correlation of "water quality" and marin biology data with satellite data is treated further in Sections II and IV.

ACKNOWLEDGEMENTS

As in all field operations, any success is due to the cooperation and assistance of many people. The present project was particularly fortunate in that the field team was made up of people that were both highly skilled and cooperative. I think that one of the greatest achievements of the field operations is that we all parted friends. Below are listed most of the people who either worked on the project or aided it through advice and expedition of our interests in the vagaries of the field situation.

Ian Koblick, MRDF president, was responsible for much of the planning during proposal preparation.

Field Data Acquisition

Paul Blackwell - Diver - Research Assistant (MRDF)
Tom Conway - Field Instrumentation Technician - Grumman Aerospace
Dick Cutler - Field Research Assistant - Grumman Ecosystems
Arthur Dammann - Oceanographic consultation - V.I. Dept. of Conservation and Cultural Affairs
Jack Ebert - Field Instrumentation Technician - Grumman Aerospace
Bruce Glanville - Diver - Research Assistant (MRDF)
Victor Greenberg - Research Assistant (MRDF)
John Hees - Data Analysis (MRDF)
Larry Liddle - Pigment Analysis - Univ. of Puerto Rico
Anthony J. Massanet - Business Manager (MRDF)
Eben Medlicott - V.I. Coordination (MRDF)
David A. Olsen - Director of in situ data acquisition (MRDF)
Susan Olsen - Project Coordinator in November (MRDF)
Bill Perl - Oceanographic Consultant - Puerto Rico Dept. of Natural Resources
Dick Pratt - Director Boat Operations (MRDF)
Marty Pratt - Secretary - Research Assistant (MRDF)
Maria de los A. Ramirez Irizarry - Secretary - (MRDF)
Rolf Schaub - Boat Operations (MRDF)
Michael O. Sheen - Research Coordinator (MRDF)
Jane Snyder - Technical writer - (MRDF)
Vance Vicente - Research Assistant (MRDF)

LITERATURE CITED

Colwell, R. N. 1973. Remote sensing as an aid to the management of Earth Resources. American Scientist 61 (2): 175-183.

Dammann, A. E. 1969. Study of the fisheries potential of the Virgin Islands. Virgin Islands Ecological Research Station Contribution No. 1, Special Reports, Caribbean Research Institute, College of the Virgin Islands.

Donnelly, T., and Whetten, J. 1968. Field guide to the geology of the Virgin Islands. Fifth Caribbean Geological Conference. Dept. of Geology, State Univ. of New York, Binghampton.

Finch, W. A. (ed.) 1973. Earth Resources Technology Satellite-1. Symposium Proceedings. NASA publications X-650-73-10. Goddard Space Flight Center.

Garrison, L. E., Holmes, C. W., and Trumball, J. Y. A. 1971. Geology of the insular shelf south of St. Thomas & St. John, U. S. Virgin Islands. U. S. Dept. of the Interior, Geological Survey.

Hutchinson, G. E. 1969. Euthrophication past and present. (In) Euthrophication (N. A. S. Symposium) National Academy of Science. U. S. Goot Printing Office, Wash., D. C.

Nagle, F. 1971. Caribbean geology, 1970. Bull of Marine Science, 21(2): 375-439.

Olsen, D. A., Wells, J. M., and Sheen, M. O. 1972. Quick Look Report, Mission No. 1, Puerto Rico Inter-National Undersea Laboratory.

Percious, D. J., vanEepoel, R. P., and Grigg, D. I. 1972. Water Pollution Report No. 18, Reconnaissance survey of St. Thomas harbor and Crown Bay, St. Thomas, Virgin Islands. Government of the Virgin Islands, Dept. of Health, Division of Environmental Health.

Randall, J. E. 1965. Grazing effect on sea grasses by herbivorous reef fishes in the West Indies. Ecol. 46 (3).

Spearman, C. 1927. The abilities of man: Their nature and measurement. Macmillan, London.

Steel, R. G. D., and Torrie, J. H. 1960. Principles and procedures of statistics. McGraw Hill, New York.

Strickland, J. D. H., and Parsons, T. R. 1968. A practical handbook of seawater analysis. Fisheries Research Board of Canada, Ottawa.

Tabb, D. C., and Michael, J.F., 1968. A study of the biological and coastal engineering aspects of the proposed jet airstrip at Jersey Bay, St. Thomas, U. S. Virgin Islands. Inst. of Marine Sciences, Univ. of Miami.

Wenner, A. M., Wells, P. A., and Rohlf, F. J. 1967. An analysis of the waggle dance of honey bees. J. Physiol Zool. 40(4): 317-340.

N74-15005

SECTION IV

DATA PROCESSING FOR THE ERTS-1 VIRGIN ISLANDS EXPERIMENT #589

acknowledgement

This section has been prepared by:

GEORGE B. HEASLIP

GRUMMAN DATA SYSTEMS CORP

under subcontract to

GRUMMAN ECOSYSTEMS CORPORATION

Bethpage, N.Y. 11714

I

4.0 INTRODUCTION

Initial data handling for the NASA/Grumman St. Thomas program consisted of:

(1) Computer processing of optical, biological, chemical and physical data for over 50 water quality sample stations within the 3-1/4 mile wide study area and for the Brewers Beach area northwest of Harry S. Truman Airport.

(2) Conversion of analog current meter microfilm to time versus current characteristics displays.

(3) Conversion of analog aircraft thermal infrared scanner data to black and white imagery.

(4) Computer processing of ERTS bulk and precision computer compatible digital tapes (CCT's).

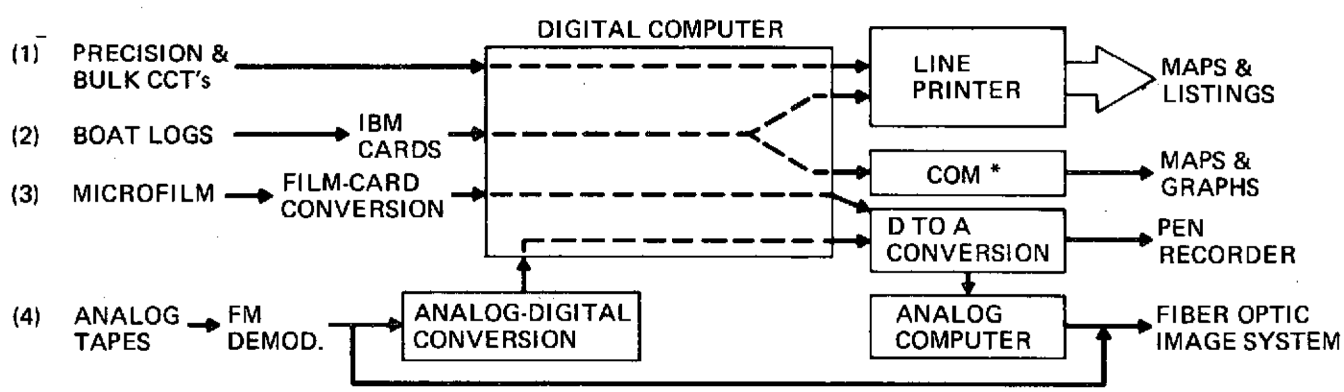

Figure 4-1. Data Processing Hardware Configurations

Utilization of graphical data summaries was extensive. This enabled both "first look" anomaly detection, parameter correlation and the specification of final data handling steps required to assess the applicability of ERTS data for monitoring water quality.

Paragraphs 4.2 and 4.3 of this report discuss input data and automatic data handling. Each of the major analog and digital data products utilized to initially ascertain satellite-to-aircraft correlation, and satellite/aircraft-to-water quality relationships are discussed in paragraph 4.4. These initial data handling results, both by Grumman Data Systems (ERTS &

IN SITU) and Dr. W. Egan of Grumman Aerospace Corporation (Optical and Aircraft) together suggested a strong ERTS-to-optical data and ERTS-to-turbidity correlation. The latter correlation was also deduced following analysis performed by Dr. D. Olsen of the Marine Resources Development Foundation.

Grumman computers were employed subsequently to test these findings. Following conversion of MSS quantum data to radiance values and the elimination of cloud affected data points, automated statistical analysis techniques confirmed these initial deductions. Results are contained in paragraph 4.4.

Also discussed in paragraph 4.4 are observations made by the writer during the course of this project. Summary conclusions, including one related to the application of ERTS data in visible sea bottom mapping will, we believe, be of use in future studies related to water quality.

4.1 INPUT DATA FORMATS

4.1.1 Computer Base Map

The Department of Commerce C & GS Map #933 served as the base map for this study. Each data station was defined as the area contained in a 1-second longitude by 1-second latitude (1" x 1") cell. Map #933 was digitized and a computer program enabled the production of the base map illustrated in Figure 4-2. Each computer line printer character corresponded to a unique 1" x 1" cell.

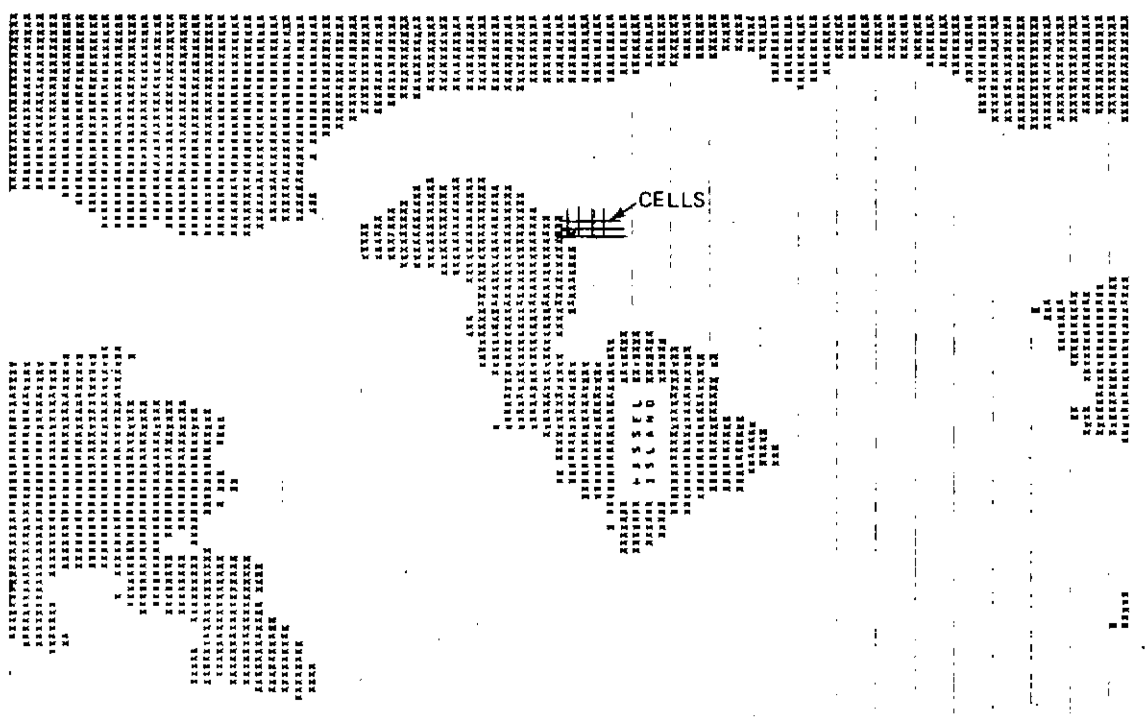

Figure 4-2. Computer Base Map - St. Thomas Harbor

4.1.2 In Situ Logs

All boat collected in situ data were either directly entered onto or finally transferred to Grumman 80 column Field Data Report forms. Utilization of keypunch compatible log sheets facilitated entering data into the data base (and improved accuracy). Each data station # (on the log sheet) corresponded to a unique character location space on the computer base map illustrated in Figure 4-2. Appendix 1 contains a sample in situ log sheet. Specific measurements recorded on "computer compatible logs" included:

1	Wind Speed	MPH	11	Conductivity	MHO/CM2
2	Wind Directn	DEG/10	12	Salinity	PPT
3	Colud Cover	PERCENT	13	Water Temp.	DEG. C
4	Ambient Temp	DEG. C	14	Turbidity	F. T. U.
5	Swell Height	FEET	15	Secchi Avg	FEET
6	Swell Dirctn	DEG/10	16	Sea Photomtr	MICAMPS
7	Water Depth	FEET	17	Dek Photomtr	MILAMPS
8	Sample Depth	FEET	18	Curnt. Speed	KNOTS
9	Dis. Oxygen	PPM	19	Curnt. Dirct	DEG/10
10	---pH---	NONE	20	Plankton Vol	CC. S

Data related to species diversity was received on keypunch cards following initial calculations made by Dr. Olsen of the Marine Resources Development Foundation (MRDF). These together with bottom type data (on keypunch cards) and biological species data for 170 species (on coding forms) were converted to keypunch cards for computer entry.

4.1.3 Satellite Data

ERTS-1 data, for one scene only (# 1086-14162-17 Oct., 1972) included Imagery and CCT's both precision and bulk CCT's. Processing the 7 track computer tapes is discussed in paragraph 4.3.

4.1.4 Aircraft Data

A single channel, 8 to 14 micron, thermal line scanner recorded data on 1/4" wide-band FM tapes. Processing of these tapes included geometric corrections which eliminated the typical "S" curve and rectilinearized the data.

4.1.5 Current Meter Data

Current Meter Data, consisting of velocity, magnetic direction and time were recorded on 34 reels of 16MM microfilm. See Figure 4-3 for format. Trace lengths and positions related to current velocity (in knots) and magnetic direction in degrees.

These data were converted via a LARR 29E film to-card system to a computer compatible format.

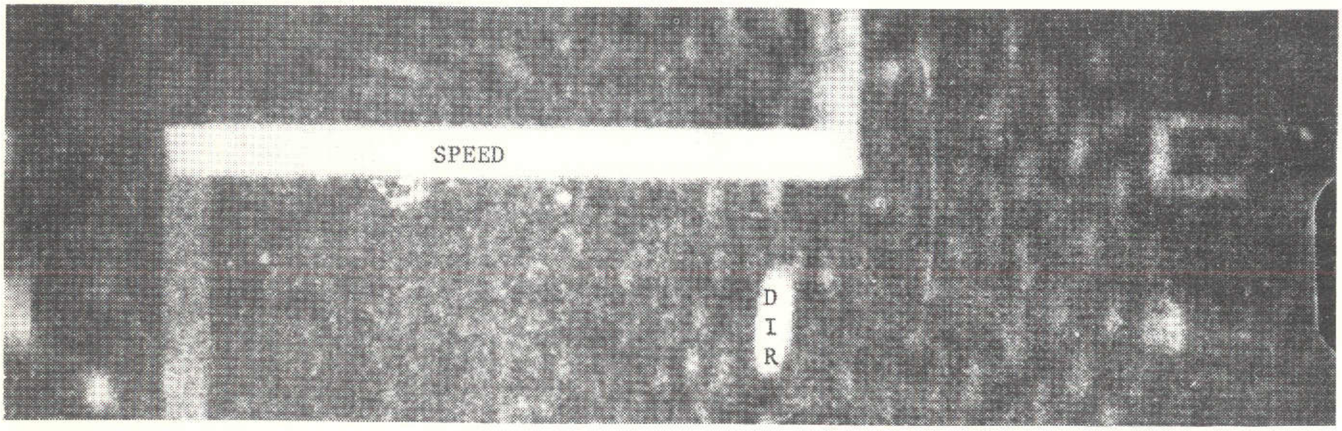

Figure 4-3. 16MM Microfilm. Current Velocity & Direction vs Time

4.2 ANALOG & DIGITAL TECHNIQUES

Summary of Primary Data Processing Hardware, Software Employed.

- Hardware utilized in performing those data processing operations shown in Figure 4-1 and statistical analysis and computer automated simulation included:
  - CDC 3200, PDP-10 and IBM 360/67 computers
  - CDC Model DD80 Computer Output Microfilm System
  - Calcomp Plotter
  - LARR Model 29E Film to Card Converter
  - PACE Model TR 10 Analog Computer
  - Astrodata Analog to Digital Converter
  - Astrodata Digital to Analog Converter
  - Brush Pen Recorder
  - Honeywell Fiber Optics Oscillograph Recorder
  - Astrodata Wideband FM Discriminators

These hardware sections are similar to those in standard test data processing facilities. The Fiber Optic Recorder, however, was configured utilizing both analog and digital systems and generated final data via a Grumman modified image recording system.

- The computer mapping scheme for precision CCT's assigned the nearest CCT pixel (resolution element) to the 1 second by 1 second latitude by longitude water quality station. All land areas were represented by X's. Additionally, each in situ data map was configured to provide a computer listing of:

  - Measurement Name
  - Water Depth Range
  - Test Data Range
  - Minimum Value Recorded
  - Statistical Distribution Curve
  - Statistics
  - Maximum Value Recorded
  - Average Value Recorded
  - Per cent Deviations of Min. & Max. from Average

Examples of map annotation are shown in Figures 4-7 and 4-8. Paragraph 4-3 - Data Products. A computer generated map was made for each of the 4 zones listed below.

	CORNER COORDINATES			
ZONE #	NW	NE	SW	SE
01	Lat 18°20'38" Lon 64°58'48"	Lat 18°20'38" Lon 64°57'49"	Lat 18°18'30" Lon 64°58'48"	Lat 18°18'30" Lon 64°57'49"
02	Lat (as 01) Lon 64°57'50"	Lat (as 01) Lon 64°56'51"	Lat (as 01) Lon 64°57'50"	Lat (as 01) Lon 64°56'51"
03	Lat (as 01) Lon 64°56'51"	Lat (as 01) Lon 64°55'52"	Lat (as 01) Lon 64°56'51"	Lat (as 01) Lon 64°55'52"
04	Lat (as 01) Lon 64°55'53"	Lat (as 01) Lon 64°54'54"	Lat (as 01) Lon 64°55'53"	Lat (as 01) Lon 64°54'54"

The basic mapping program is expandable to permit the addition of more zones, should this become necessary in follow-on investigations. In situ data, orginally recorded on log sheets (sample in Appendix 1) were keypunched and automatically averaged (over a desired time span) with resultant values appearing as a numeric character ranging between

0 and 9 - (minimum and maximum ranges, respectively). These averages (scaled) were printed in the 1 second by 1 second map cell associated with each water quality station.

- Current meter data was converted from microfilm to keypunch cards. A computer program enabled an analog strip chart display of current velocity, direction, east-west and north-south components, predicted tide curves, and time data. Corrections for magnetic deviation were applied through a least square's third order calibration curve computed from Endeco supplied calibration data. Also magnetic variation correction was incorporated for true north output. Figure 4-6 illustrates the strip chart output record.

- Data listings, through utilization of the Grumman DEPRINTER program, were made available in four formats (listed below).
  DEPRINTER sorts and tabulates user specified parameters stored in the blocks of data resident in the mass storage data base. (CDC 854 disk).

  Available Listings

  1. Format A - Lists the station, location, acquisition data and data value for each in situ measurement recorded.
  2. Format B - Lists the station, depth, acquisition data and data value for a maximum of 4 user-specified measurements.
  3. Format C - Lists the weather conditions for a user-specified station.
  4. Format D - Lists all data parameters acquired at a user-specified station. (A message is printed if no data is available for a particular station. Further, this type of tabulation sorted the data first by sampling type* and then by station number and lastly listed in chronological order.)

- Measurement value vs time graphs were created via the Grumman DEPICTUR program which sorts and arranges data in a chronological order on a selective basis. (User specifies starting and end time, station number, sample depth, and parameter ID). Resultant outputs are graphs displayed on CRT and transferrable to 35 and 16 mm microfilm. Paragraph 4.3.4 contains sample outputs of the DEPICTUR PROGRAM.

- Thermal IR data was rectilinearized with S-curve corrections applied through utilization of the system depicted in Figure 4-4. Although not shown, final conditioning of digital/analog outputs was achieved through use of an analog computer.

*Repetitive, benthic, diurnal or photometer samplings.

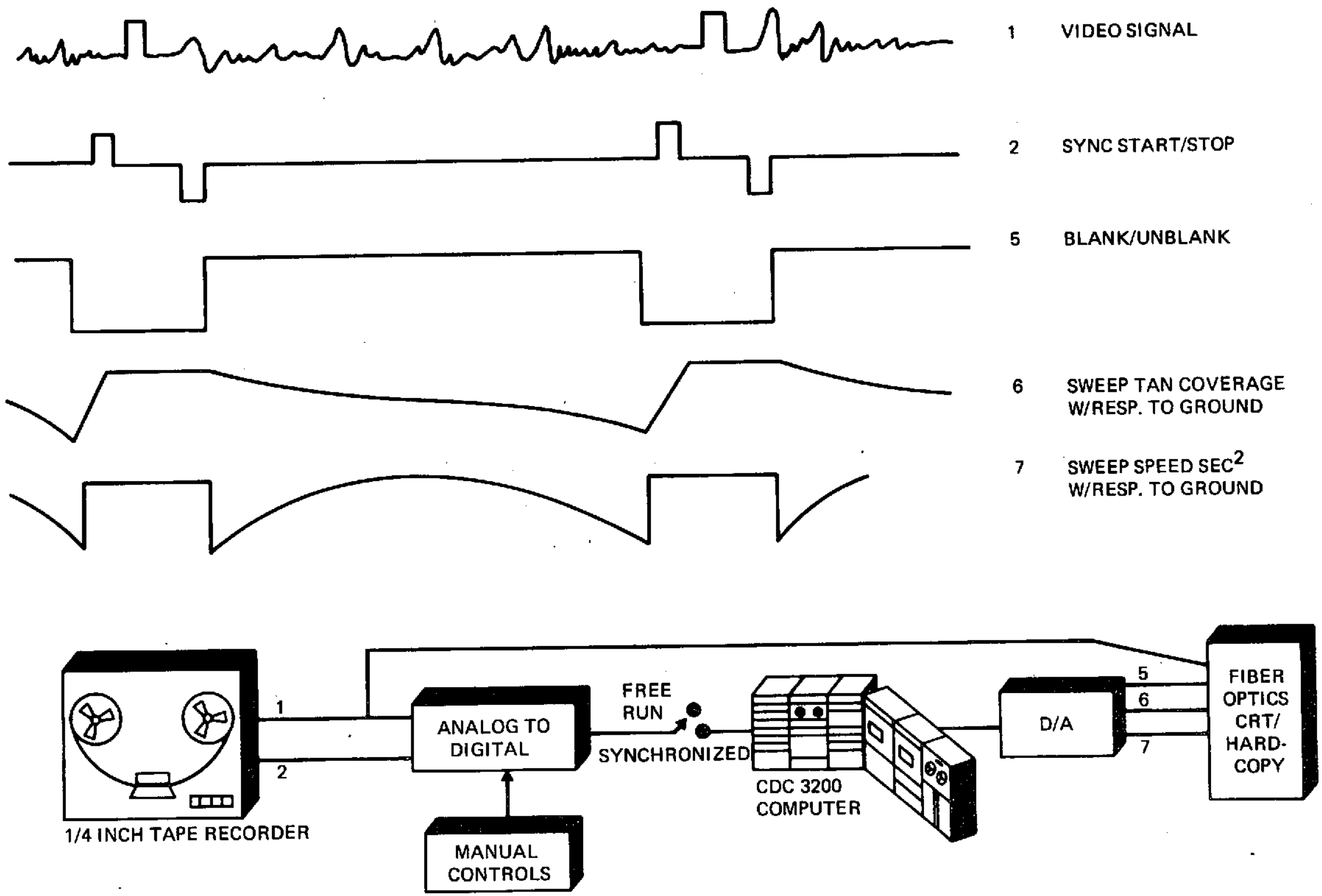

Figure 4-4. Aircraft Thermal IR Data Processing Configuration

Paragraph 4.4.1 contains seven output images created from 5" film utilized in the Fiber optics recording system.

4.3 DATA PRODUCTS

Data products were generated in nine classifications:

1. IR Imagery
2. Current Meter Time Histories
3. Parameter Summary Maps - Scaled
4. Boat Measured Parameter Time Histories
5. In Situ Measurement Listings Per Data Section
6. Scaled Computer Maps - Precision and Bulk CCT Data
7. MSS Value Listings Per Data Station
8. Tubidity vs MSS Displays
9. MSS Overlays - To 1:10,000 C & GS Map #933

Samples and discussions pertaining to each data product are contained in paragraphs 4.3.1 through 4.3.9.

Special analysis, of selected primary products, was performed through use of Grumman software operating in PDP and IBM computers. Results are summarized in paragraph 4.4 - Final Analysis Results.

4.3.1 Analog Thermal IR Line Scanner Imagery

Initial imagery, was produced from magnetic tapes containing approximately 250 line miles of single channel 8.0-14.0 micron line scanner data. Imagery of the desalinization/power plant located on Lindbergh Bay is shown in Figure 4-5.

The demonstrated ability of the ERTS MSS system to provide over 100 computer resolution elements in the approximately 700 x 900 meter bay suggests that a future ERTS containing the NASA planned 10.4 to 12.6 nanometer thermal IR band with an instantaneous field of view of $\leq$ 3 times that of bands 1-4, and thermal resolution better than 1.2°C will be capable of monitoring the subject thermal plume (28-31°C range).

ERTS MSS band 7 was used together with easily recognizable land water interface points to compare charted land mass-to-land mass distances (water separated). Computer

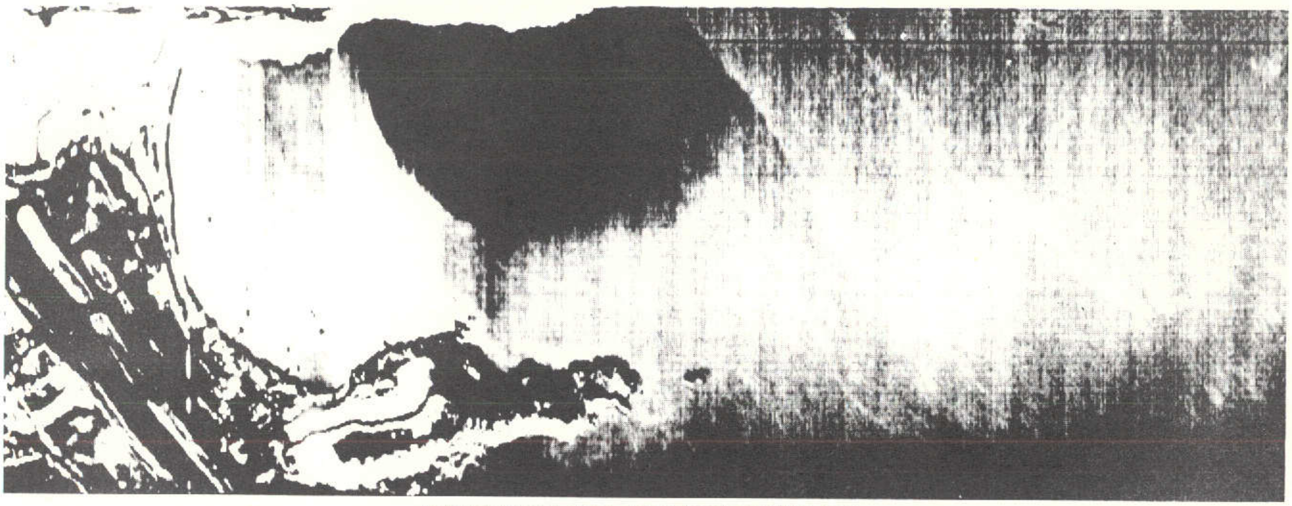

INTENSITY 1.94 BACKGROUND 2.6

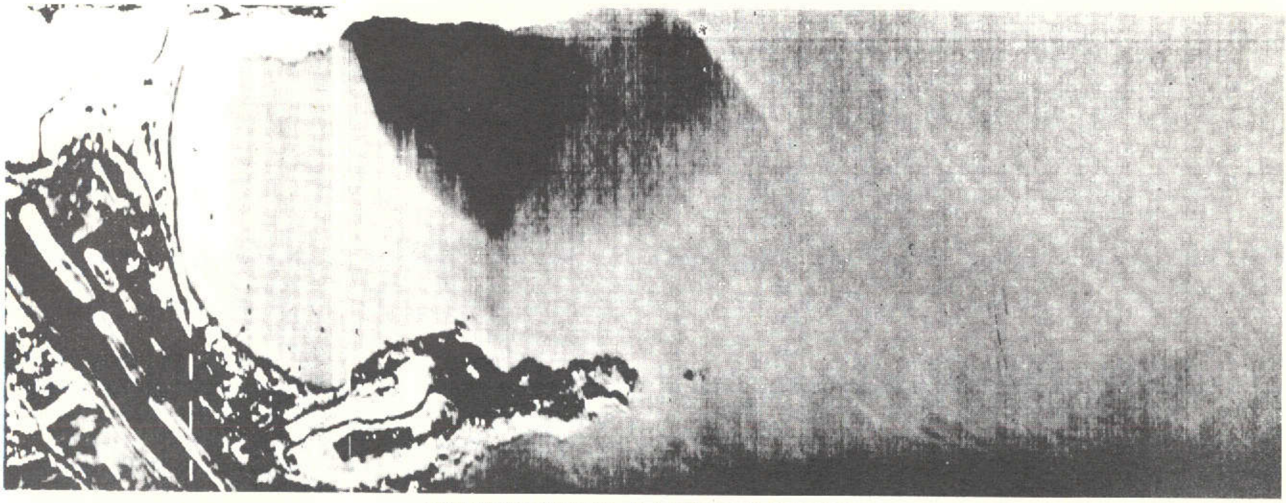

INTENSITY 2.04 BACKGROUND 2.8

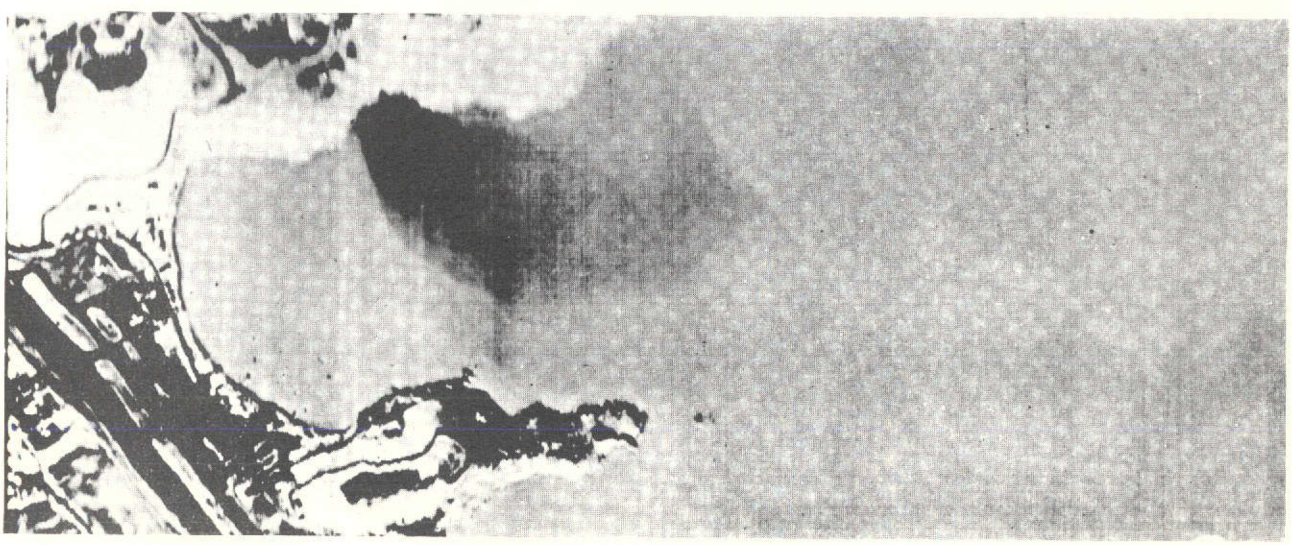

INTENSITY 2.14 BACKGROUND 3.0

Figure 4-5. Lindbergh Bay Saint Thomas, V.I. 8.0-14.0 Micrometer Thermal IR printouts revealed an accuracy of between 1/2 and 1.0 the area represented by each printout character (pixel) of approximately 57 meters by 79 meters.

CCT data from band 7 enabled mapping of land/water boundaries to within a 1-2 pixel accuracy.

4.3.2 Analog Current Meter Measurement Time Histories

Raw data (16 MM microfilm) was processed on a semi-automatic reader-recorder with valid data segments being converted to keypunch cards for computer entry.

A digital program effected the transfer of time of day, current speed, and current direction data to an analog pen recorder. Resultant strip charts were utilized to record current velocity and direction vs time for each Endeco Type 105 current meter.

Strip charts generated through utilization of a digital-to-analog converter, were formatted as shown below in Figure 4-6.

4.3.3 Scaled In Situ Data Summary Maps

Following entry of all in situ data into the computer data base, selected water quality parameters were plotted on the scaled computer maps utilizing the following criteria:

DEPTH: Selectable, Number of feet ± tolerance in feet or midpoint ± tolerance in %.

TIME: Selectable, user specifies single day, or, if an average over more than one day is required, start and stop days.

Resultant map printouts show averaged parameter values per station at a scale of 0 to 9. 0 pertains to lowest value recorded and 9 the maximum value recorded for the selected test period. Additionally, the minimum, maximum and average values over the entire test period are displayed.

Figures 4-7 and 4-8 are segments of actual maps generated during the study program. Each depicts scaled values (Salinity and Water Temperature) during an 11 day span at a depth of 5 ± 2 feet.

Figure 4-9 illustrates a mid depth temperature summary for the six week test period.

Figure 4-6. Computer Generated Current Velocity and Direction vs Time

Figure 4-7. Salinity (11 day average) - St. Thomas Harbor

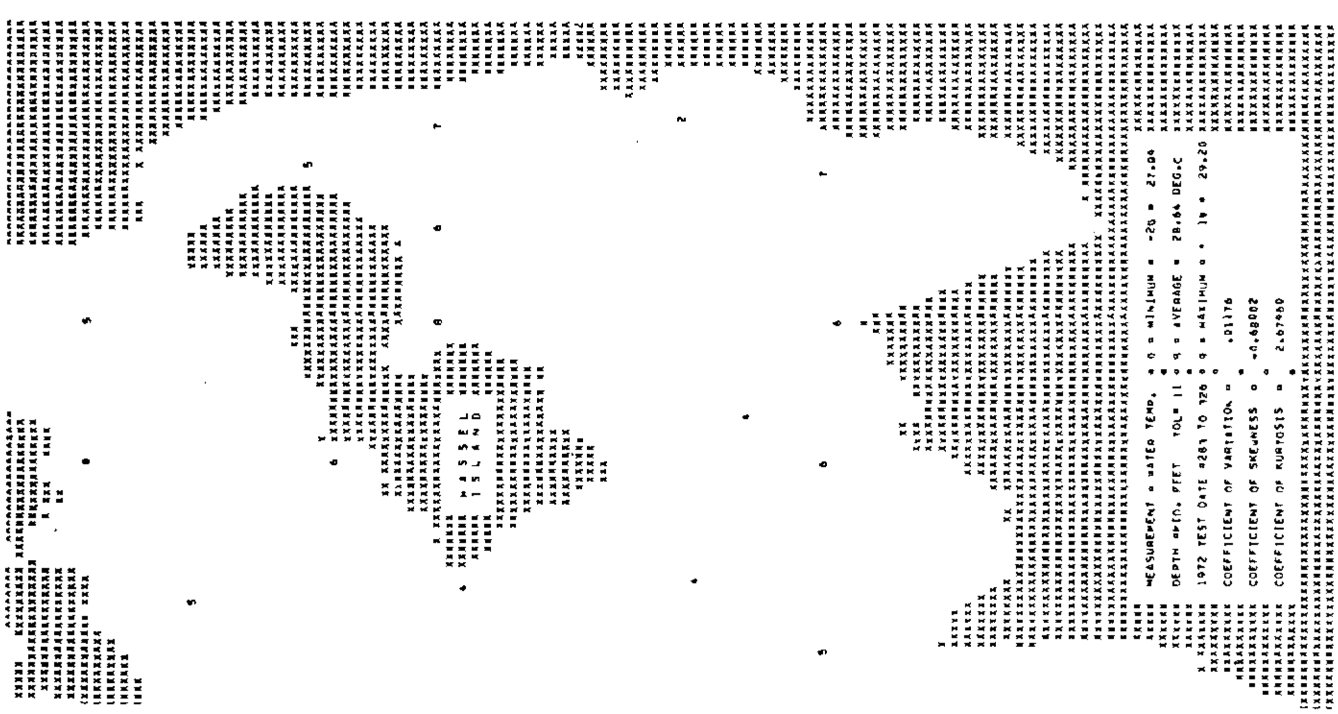

Figure 4-8. Water Temperature (11 day average) - St. Thomas Harbor

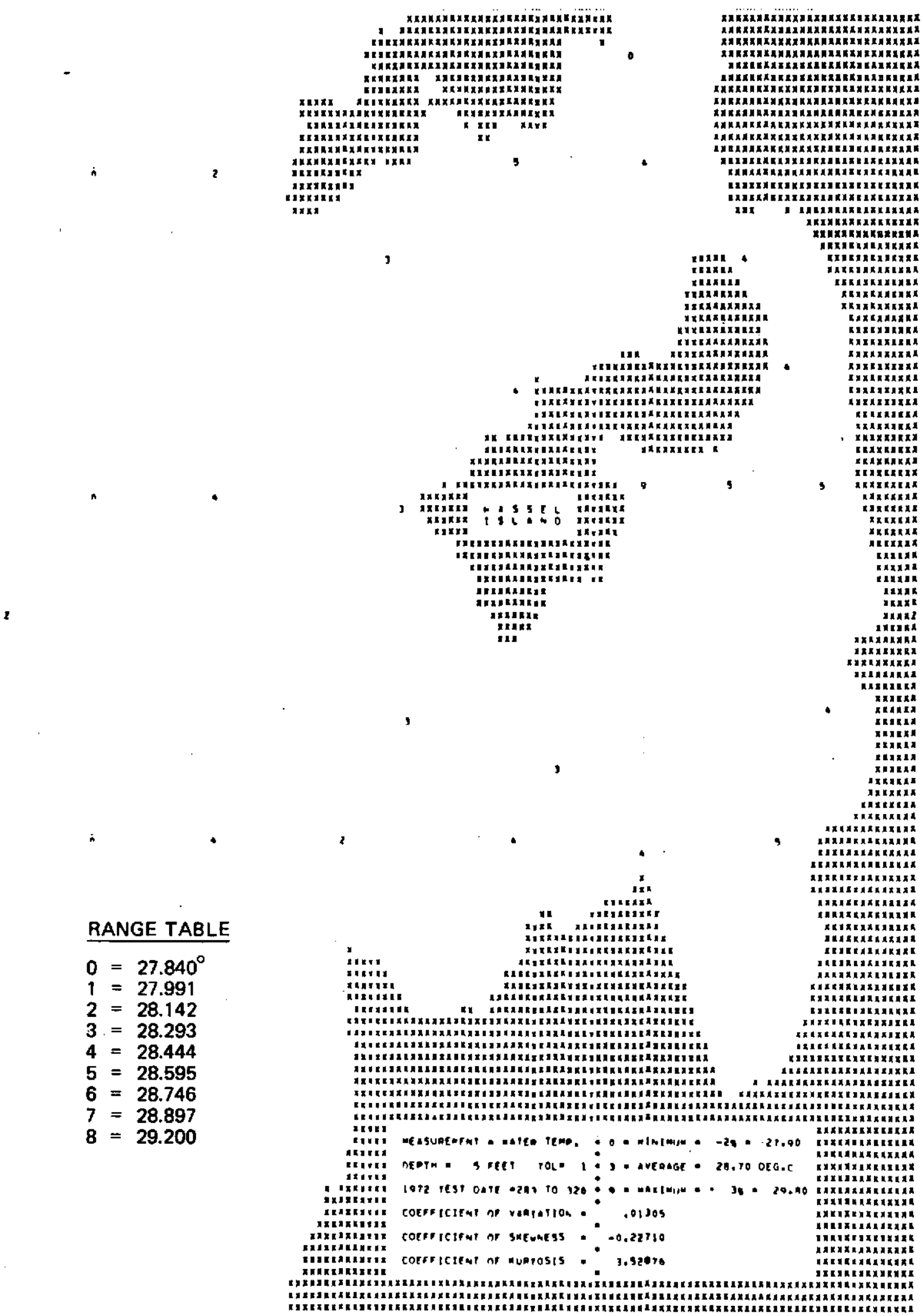

RANGE TABLE

0 = 27.840°
1 = 27.991
2 = 28.142
3 = 28.293
4 = 28.444
5 = 28.595
6 = 28.746
7 = 28.897
8 = 29.200

Figure 4-9. Averaged and Scaled Quantitative Summary-Water Temperature

In addition to numerical scaled maps, a series of maps was generated utilizing shaded circles in lieu of numeric values; these displays were extremely useful in "first look" analysis and in determining those harbor areas and/or parameters requiring more detailed data processing.

Figures 4-10 and 4-11 are representative samples. Also shown, in Figure 4-12 is a measurement summary map for turbidity. Circle sizes vary (in ten steps) from minimum turbidity (outer harbor) to maximum turbidity (inner harbor).

Maximum turbidity readings occur in the northern St. Thomas Harbor. High bottom turbidity (with respect to surface and mid depth) occurs at point A.

4.3.4 Boat Measured Parameter Time Histories

The alphanumeric/graphic computer output microfilm system provided graphs (up to two per page) of measurement time histories for each sample station. These graphs included sample station number, start date, end date and parameter name and depth. The computer program also enabled recording measurement graphs on 35 mm and 16 mm microfilm. Film products were read on a roll film reader with key data areas being converted to hard copy. Examples are contained in Figures 4-13 and 4-14.

4.3.5 In Situ Measurement Listings

In situ measurement listings are available, in the formats indicated in Figures 4-15a and 4-15b, and constitute complete data listings per data station. These are in chronological order, indicating measurement values - with up to four selectable parameters permissible per page. These listings comprise the bulk of status data for St. Thomas Harbor.

Additionally, the analyst can also obtain data printouts sorted by measurement name and by weather conditions.

Measurement listings were useful in extracting weather and boat mounted current meter data and serving as the detailed reference manual from which measurement summary maps were created.

4.3.6 Scaled Computer Maps - Precision & Bulk CCT Data

Computer aided graphics were employed to facilitate both understanding the variance in "water quality" with location, and also correlation of in situ, aircraft and spacecraft data. In each case, satellite computer maps were accompanied with listings of MSS data values at and surrounding each data station. Figure 4-16 for example, indicates a scaled map and MSS values for each subject station.

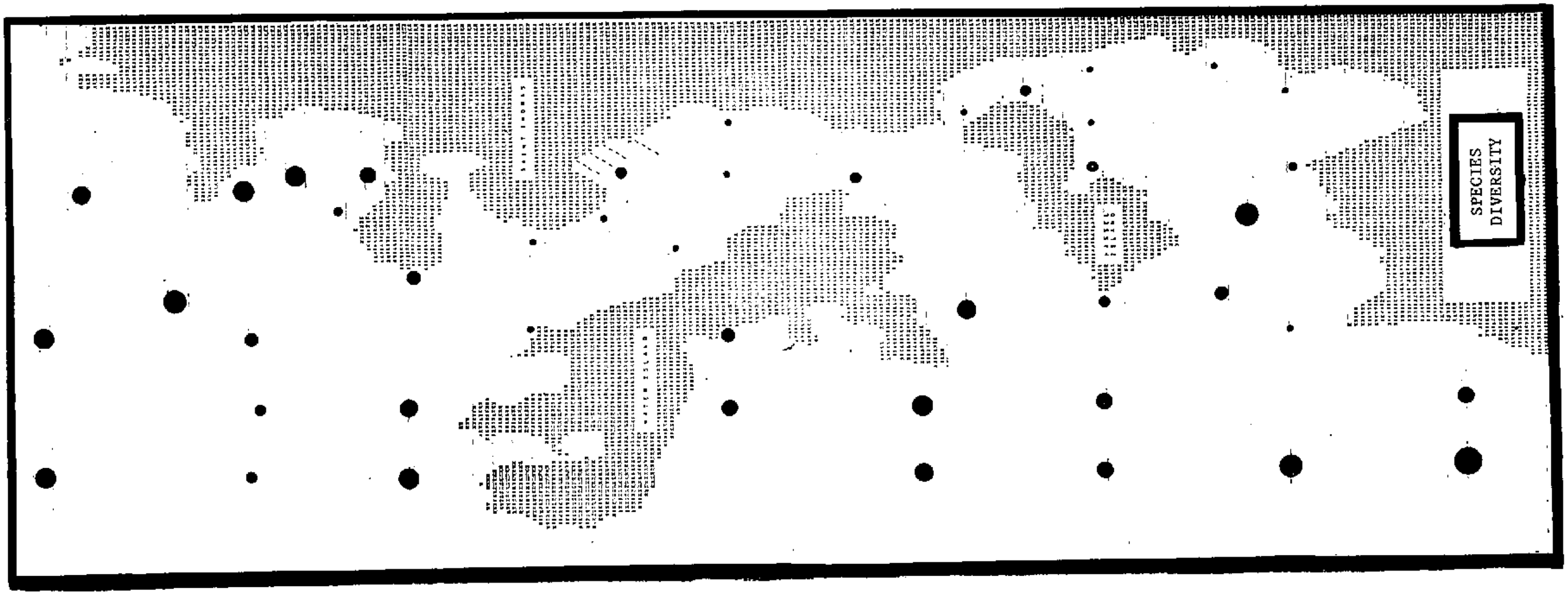

SPECIES DIVERSITY
Range: 0.00 NITS to 2.56 NITS
Average: 0.96 NITS
Test Duration: Day 283 to 326, 1972
Scaled: • Min., ● Max.

Figure 4-10. Species Diversity - 6 Week Average

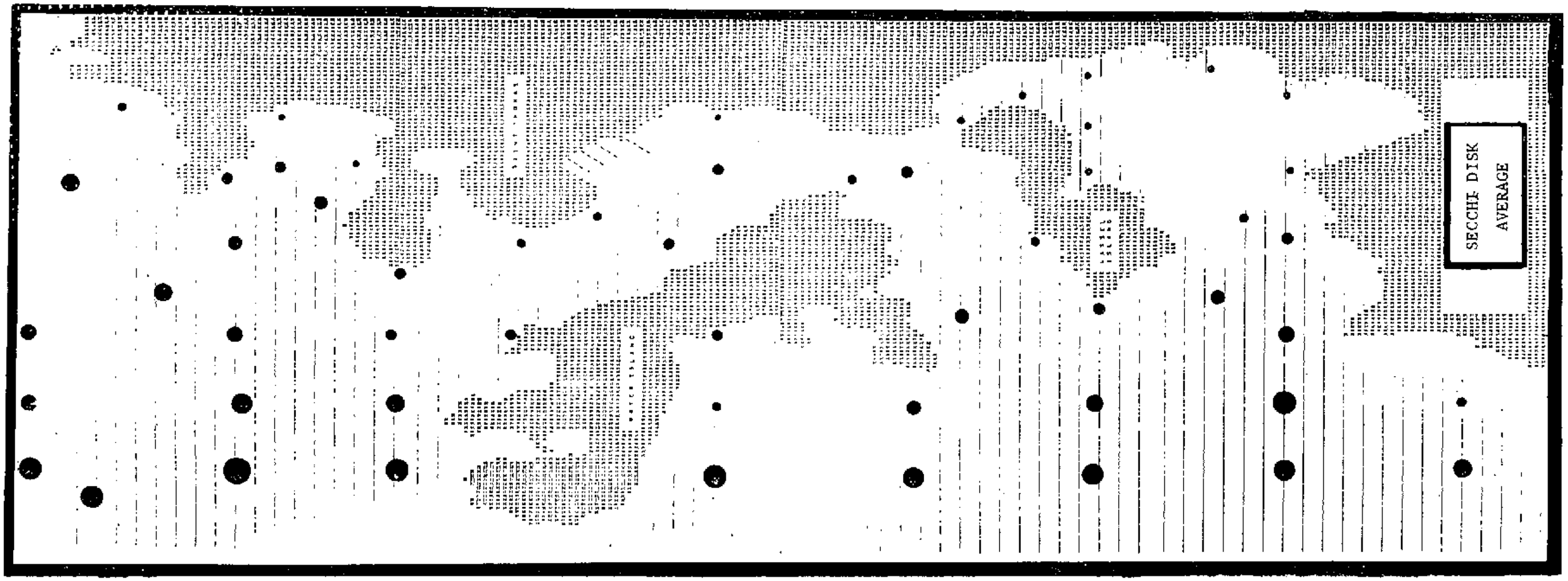

SECCHI DISK AVERAGE
Range: 21.00 Ft. to 171.00 Ft.
Average: 75.27 Feet
Test Duration: Day 283 to 326, 1972
Scaled: • Min., ● Max.

Figure 4-11. Secchi Disk - 6 Week Average

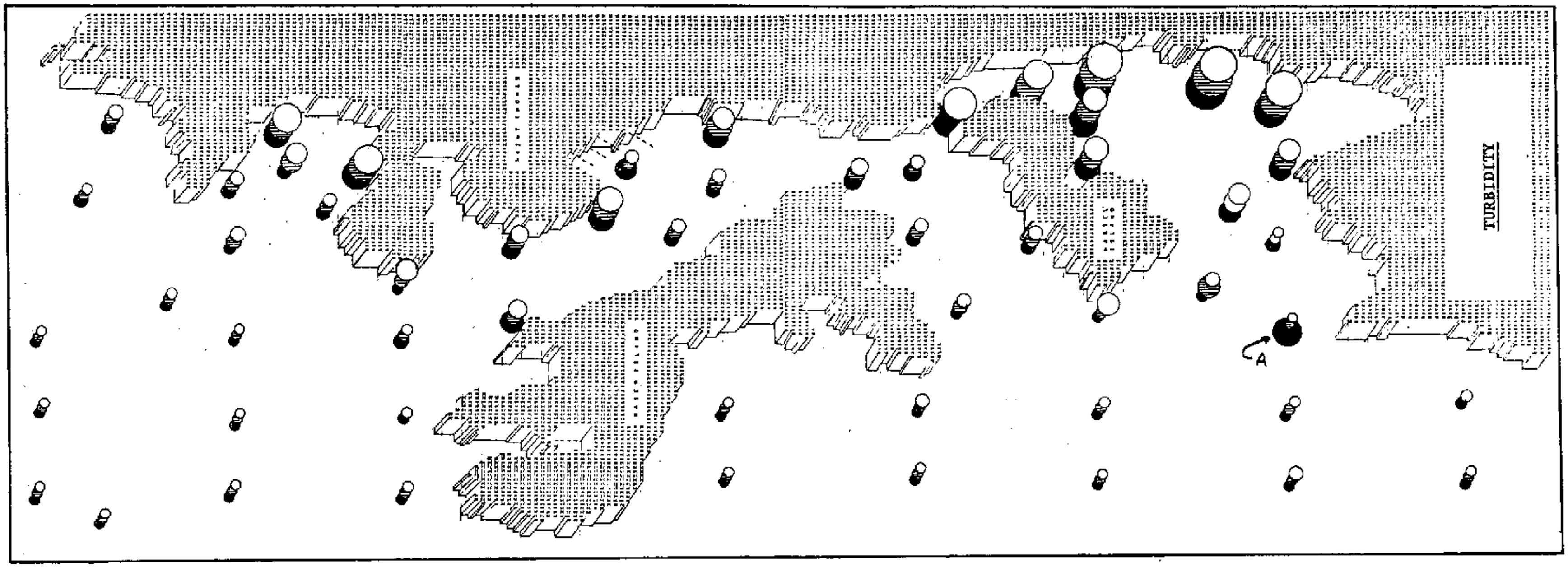

TURBIDITY (F.T.U.)
DEPTHS: 5' (±1'), MIDPOINT (±15%) & BOTTOM (to + 6')
RECORDED MIN./MAX. = 0.12/3.58; AVERAGE + 0.96
TEST PERIOD: Day 283 to Day 326, 1972
SCALED: • Min., ● Max.

Figure 4-12. Turbidity-6 Week Average At Surface, Midpoint & Bottom

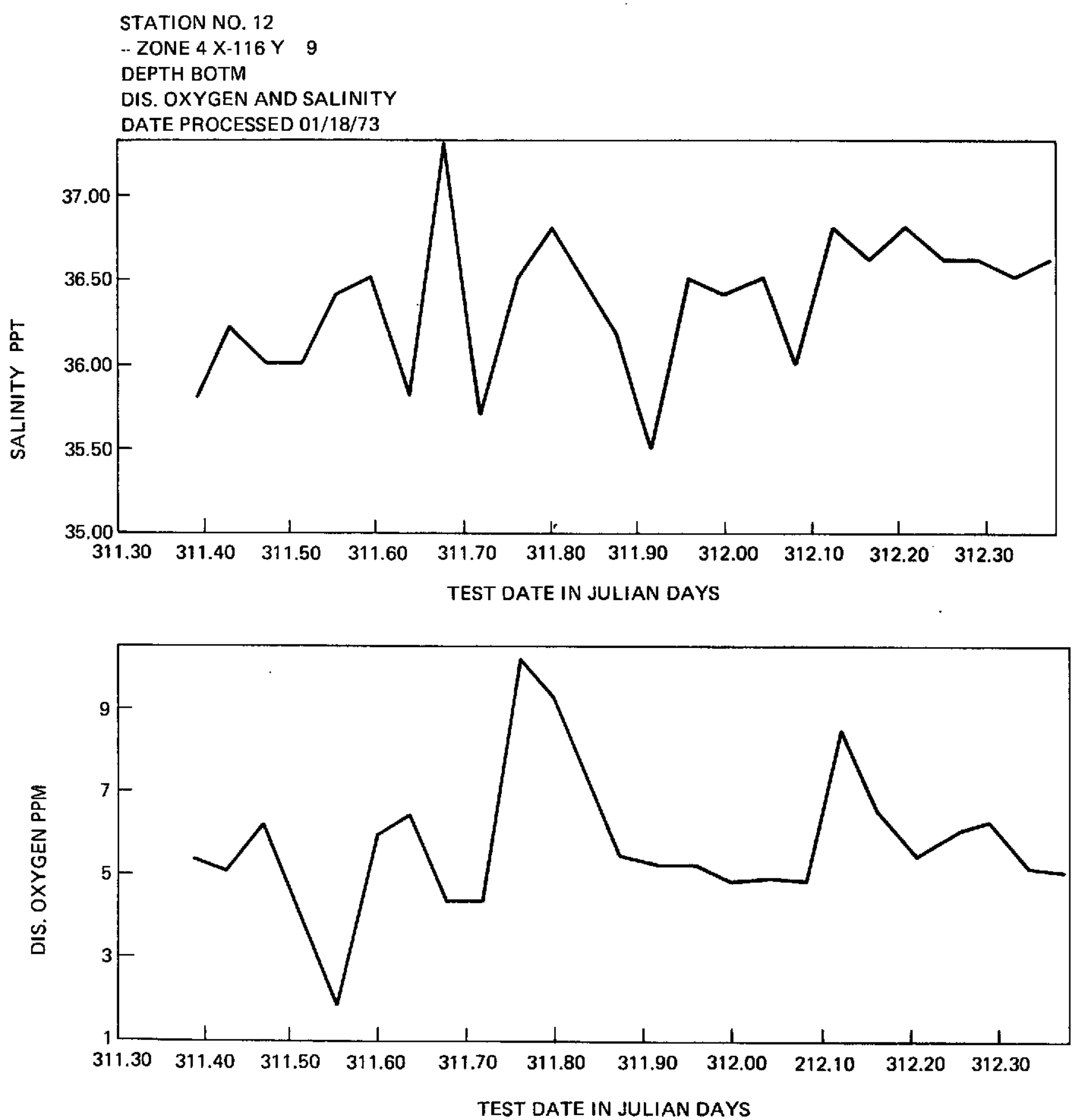

Figure 4-13. Dissolved Oxygen and Salinity vs Time - Station 12, Depth Bottom

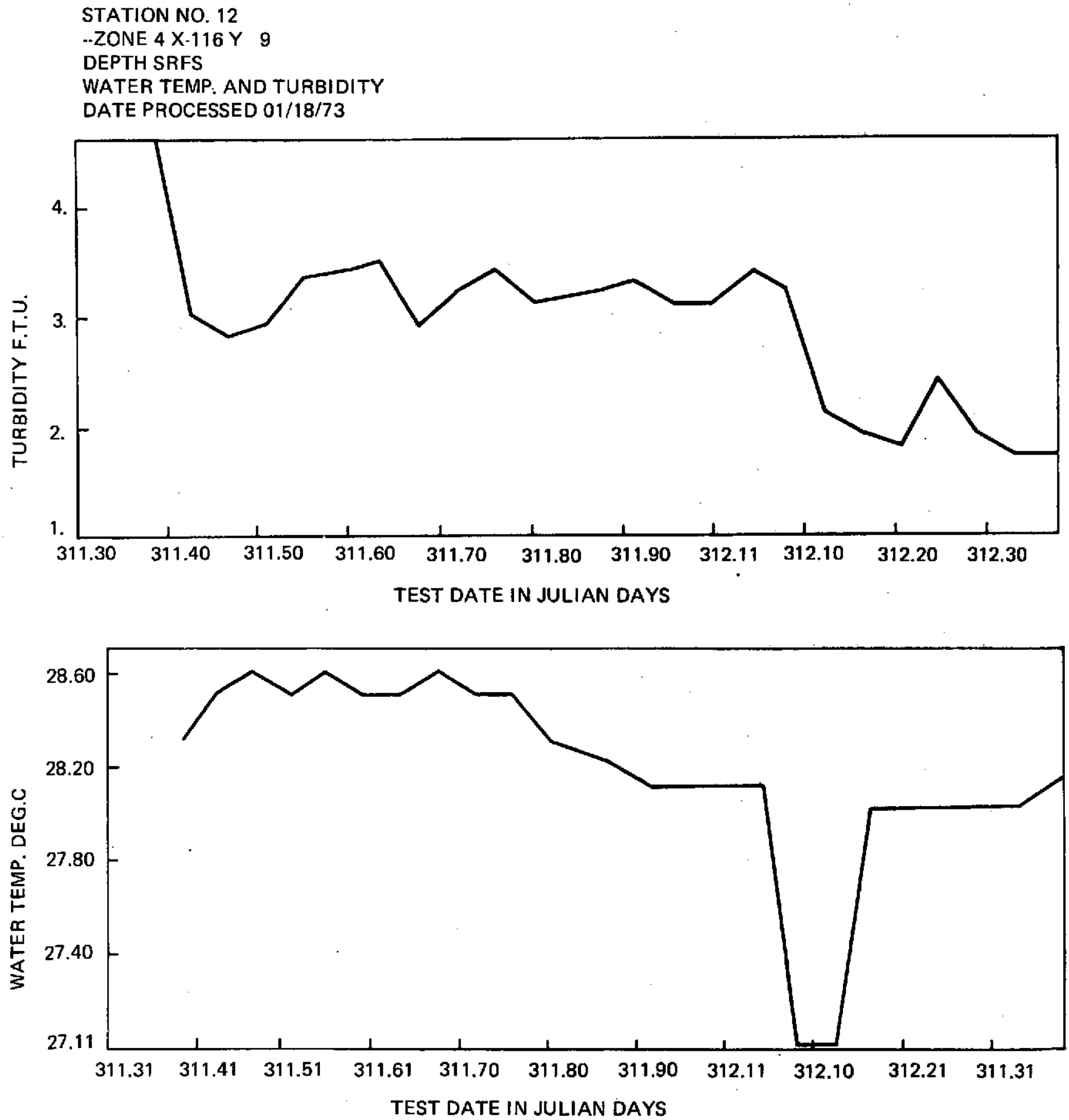

Figure 4-14. Turbidity and Water Temperature vs Time - Station 12, Depth: Surface

PAGE NO. 92

VIRGIN ISLANDS TEST SITE PROGRAM

ST. THOMAS HARBORS WATER QUALITY DETERMINANTS STUDY

STATION NO. 6 ZONE2 ROW 31 COLUMN 79

ACQUISITION DATE	TIME	WIND SPEED	WIND DIR.	% CLOUD COVER	SWELL HEIGHT	SWELL DIR.	MATH. DEPTH
287	1437	6	15	15	1	25	25
290	1210	8	5	50	1	5	25
299	1120	5	23	90	1	23	25
306	1300	15	2	50	0	0	23

DATE PROCESSED 01/22/73 PAGE NO. 73

VIRGIN ISLANDS TEST SITE PROGRAM

ST. THOMAS HARBORS WATER QUALITY DETERMINANTS STUDY

STATION = 12
TYPE = 3

BLOCK	DATE	TIME	WIND SPEED MPH	WIND DIRECTN DEG/10	CLOUD COVER PERCENT	AMBIENT TEMP DEG.C	SWELL HEIGHT FEET	SWELL DIRCTN DEG/10	WATER DEPTH FEET
657	311	2300	12.00000	6.00000	2.00000	26.60000	1.00000	19.00000	18.00000
658	311	2300	12.00000	6.00000	2.00000	26.60000	1.00000	19.00000	18.00000
660	311	2400	8.00000	7.00000	10.00000	26.40000	1.00000	19.00000	18.00000
661	311	2400	8.00000	7.00000	10.00000	26.40000	1.00000	19.00000	18.00000
662	311	2400	8.00000	7.00000	10.00000	26.40000	1.00000	19.00000	18.00000
664	312	100	7.00000	11.00000	0	26.30000	1.00000	19.00000	18.00000
665	312	100	7.00000	11.00000	0	26.30000	1.00000	19.00000	18.00000
666	312	100	7.00000	11.00000	0	26.30000	1.00000	19.00000	18.00000
668	312	200	8.00000	7.00000	0	26.00000	1.00000	19.00000	18.00000
669	312	200	8.00000	7.00000	0	26.00000	1.00000	19.00000	18.00000
670	312	200	8.00000	7.00000	0	26.00000	1.00000	19.00000	18.00000
672	312	300	9.00000	7.00000	1.00000	26.10000	1.00000	19.00000	18.00000
673	312	300	9.00000	7.00000	1.00000	26.10000	1.00000	19.00000	18.00000
674	312	300	9.00000	7.00000	1.00000	26.10000	1.00000	19.00000	18.00000
676	312	400	6.00000	8.00000	0	26.20000	1.00000	12.00000	18.00000
677	312	400	6.00000	8.00000	0	26.20000	1.00000	12.00000	18.00000
678	312	400	6.00000	8.00000	0	26.20000	1.00000	12.00000	18.00000
680	312	500	7.00000	12.00000	0	26.30000	1.00000	18.00000	18.00000
681	312	500	7.00000	12.00000	0	26.30000	1.00000	18.00000	18.00000
682	312	500	7.00000	12.00000	0	26.30000	1.00000	18.00000	18.00000
684	312	600	2.00000	6.00000	30.00000	26.30000	1.00000	15.00000	18.00000
685	312	600	2.00000	6.00000	30.00000	26.30000	1.00000	15.00000	18.00000
686	312	600	2.00000	6.00000	30.00000	26.30000	1.00000	15.00000	18.00000
688	312	700	3.00000	12.00000	35.00000	27.90000	1.00000	19.00000	18.00000
689	312	700	3.00000	12.00000	35.00000	27.90000	1.00000	19.00000	18.00000
690	312	700	3.00000	12.00000	35.00000	27.90000	1.00000	19.00000	18.00000
697	312	800	8.00000	11.00000	21.00000	28.60000	1.00000	16.00000	16.00000
698	312	800	8.00000	11.00000	21.00000	28.60000	1.00000	16.00000	18.00000
699	312	800	8.00000	11.00000	21.00000	28.60000	1.00000	16.00000	18.00000
706	312	900	6.00000	8.00000	40.00000	28.70000	1.00000	19.00000	18.00000
707	312	900	6.00000	8.00000	40.00000	28.70000	1.00000	19.00000	18.00000
708	312	900	6.00000	8.00000	40.00000	28.70000	1.00000	19.00000	18.00000

• • • • • • • • • • NO DATA AVAILABLE • • • • • • • • • • STN= 13 TYPE= 3

• • • • • • • • • • NO DATA AVAILABLE • • • • • • • • • • STN= 14 TYPE= 3

• • • • • • • • • • NO DATA AVAILABLE • • • • • • • • • • STN= 15 TYPE= 3

• • • • • • • • • • NO DATA AVAILABLE • • • • • • • • • • STN= 16 TYPE= 3

• • • • • • • • • • NO DATA AVAILABLE • • • • • • • • • • STN= 17 TYPE= 3

Figure 4-15a. In Situ Measurement Listings

PAGE NO. 3

VIRGIN ISLANDS TEST SITE PROGRAM

ST. THOMAS HARBORS WATER QUALITY DETERMINANTS STUDY

SALINITY PPT

STATION NO.	ZONE	X	Y	DEPTH--FEET	ACQUISITION DATE	ACQUISITION TIME	VALUE	INSTR.CODE	TYPE	COMMENTS
4	1	58	24	2	285	1520	34.900	0	3	
4	1	58	24	4	285	1520	34.950	0	3	
4	1	58	24	8	285	1520	34.900	0	3	
4	1	58	24	12	285	1520	34.900	0	3	
4	1	58	24	16	285	1520	34.900	0	3	
6	1	81	48	5	285	1450	34.800	0	1	
6	1	81	48	12	285	1450	34.700	0	1	
6	1	81	48	18	285	1450	34.800	0	1	
6	1	81	48	2	285	1450	34.900	0	3	
6	1	81	48	4	285	1450	34.800	0	3	
6	1	81	48	5	285	1450	34.830	0	3	
6	1	81	48	6	285	1450	34.900	0	3	
6	1	81	48	7	285	1450	34.800	0	3	
6	1	81	48	8	285	1450	34.800	0	3	
5	1	87	34	5	285	1400	34.900	0	1	
5	1	87	34	9	285	1400	34.900	0	1	
5	1	87	34	17	285	1400	34.890	0	1	
5	1	87	34	2	285	1400	34.800	0	3	
5	1	87	34	4	285	1400	34.900	0	3	
5	1	87	34	6	285	1400	34.830	0	3	

PAGE NO. 26

VIRGIN ISLANDS TEST SITE PROGRAM

ST. THOMAS HARBORS WATER QUALITY DETERMINANTS STUDY

STATION	DEPTH FEET	ACQUISITION DATE	ACQUISITION TIME	SALINITY PPT	IC	WATER TEMP. DEG.C	IC	TURBIDITY F.T.U.	IC	CURNT.SPEED KNOTS	TYPE IC	COMMENTS
4	5	285	1520	34.700		28.800		.460		.500	1	
4	25	285	1520	34.900		28.800		.470		.350	1	
4	45	285	1520	34.900		28.500		.560		.350	1	
4	2	285	1520	34.900		28.500		.550		.350	3	
4	4	285	1520	34.900		28.500		.550		.350	3	
4	8	285	1520	34.900		28.500		.560		.350	3	
4	12	285	1520	34.900		28.500		.560		.350	3	
4	16	285	1520	34.900		28.500		.560		.350	3	
4	5	292	1050	35.300		28.800		.150		.550	1	
4	25	292	1050	34.900		28.900		.320		.400	1	
4	45	292	1050	35.300		28.700		.420		.450	1	
4	2	292	1050	35.300		28.700		.420		.450	3	
4	4	292	1050	35.300		28.700		.420		.450	3	
4	8	292	1050	35.300		28.700		.420		.450	3	
4	10	292	1050	35.300		28.700		.420		.450	3	
4	12	292	1050	35.300		28.700		.420		.450	3	
4	5	298	1110	35.000		28.900		.350		.250	1	
4	25	298	1110	35.000		27.900		.310		.250	1	
4	45	298	1110	35.000		27.900		.350		.400	1	
4	5	307	1030	35.000		29.500		.490		.250	1	

Figure 4-15b. In Situ Measurement Listings

STA	LATITUDE	LONGTITUDE	VALUES		
1	.0000000	.0000000	-1	-1	-1
			-1	-1	-1
			-1	-1	-1
2	18.3318504	-64.9775136	25	23	23
			26	26	24
			27	29	25
3	18.3091732	-64.9766809	24	24	24
			22	23	23
			23	23	23
4	18.3242913	-64.9736363	26	25	28
			24	25	26
			25	24	26
5	18.33[illegible]	-64.97[illegible]723	[illegible]	32	28
			32	31	27
			33	29	28
6	18.33[illegible]	-64.967[illegible]	30	28	27
			28	26	2[illegible]
			30	29	2[illegible]
7	18.322[illegible]516	-64.9584255	24	25	25
			24	2[illegible]	26
			2[illegible]	28	26
8	18.32[illegible]	-64.9553836	33	32	34
			29	3[illegible]	38
			29	34	3[illegible]
9	18.33269[illegible]	-64.9443191	30	30	30
			29	31	30
			31	31	31
10	18.3231715	-64.9396176	25	27	27
			26	26	28
			31	28	28
11	18.33[illegible]495	-64.9371277	36	35	42
			36	35	41
			36	38	3[illegible]
12	18.3405293	-64.9288298	37	38	[illegible]
			36	35	3[illegible]
			34	37	40

Figure 4-16. Computer Processed Precision MSS Data

Figure 4-17 illustrates precision tape MSS quantum values (0-127) transferred to the standard harbor chart utilized in this experiment.

4.3.7 MSS Listings Per Data Station

Both Bulk and Precision CCT's were processed to extract MSS values for each sample station, and for water areas (computer cells) immediately surrounding the subject area.

Where the average value of a group of cells differed sharply (e.g. 20%) from the individual value of any single cell within the group, further analysis was performed.

Example: Station 53, for MSS Bulk Band 5 was found to contain data as follows:

	10	
16	9	8
	9	

9 = cell at sample sta.

The value 16 to the west of station 53 was suspect; subsequent analysis revealed a cloud in that area.

Example: Station 81, for Precision MSS Band 4 was found to contain data as follows:

28-26-26
26-26-26
27-90-26

The value 90 was rejected. It could have been caused by a ship, several of which frequently visit St. Thomas.

Small clouds (and shadows) were difficult to precisely locate by viewing 70 mm images (with a microscope) and with photo enlargements. However, through the use of computer processed MSS data which was transferred to the standard harbor map (C & GS #933) cloud locations were established, and provided to Dr. Egan. Refer to Figure II - 26.

Approximately 10% of all water quality stations were determined to be cloud or cloud shadow affected.

Figure 4-22 illustrates St. Thomas Harbor; C represents cloud areas. (Mapping based on MSS quantum levels ranging from 0 to 127).

Precision CCT and Bulk CCT values at and surrounding sample stations were computed for precision MSS Bands 4-6 and for bulk MSS Bands 4-7. Appendix 2 contains a listing of station vs MSS values and averages for both bulk and precision products.

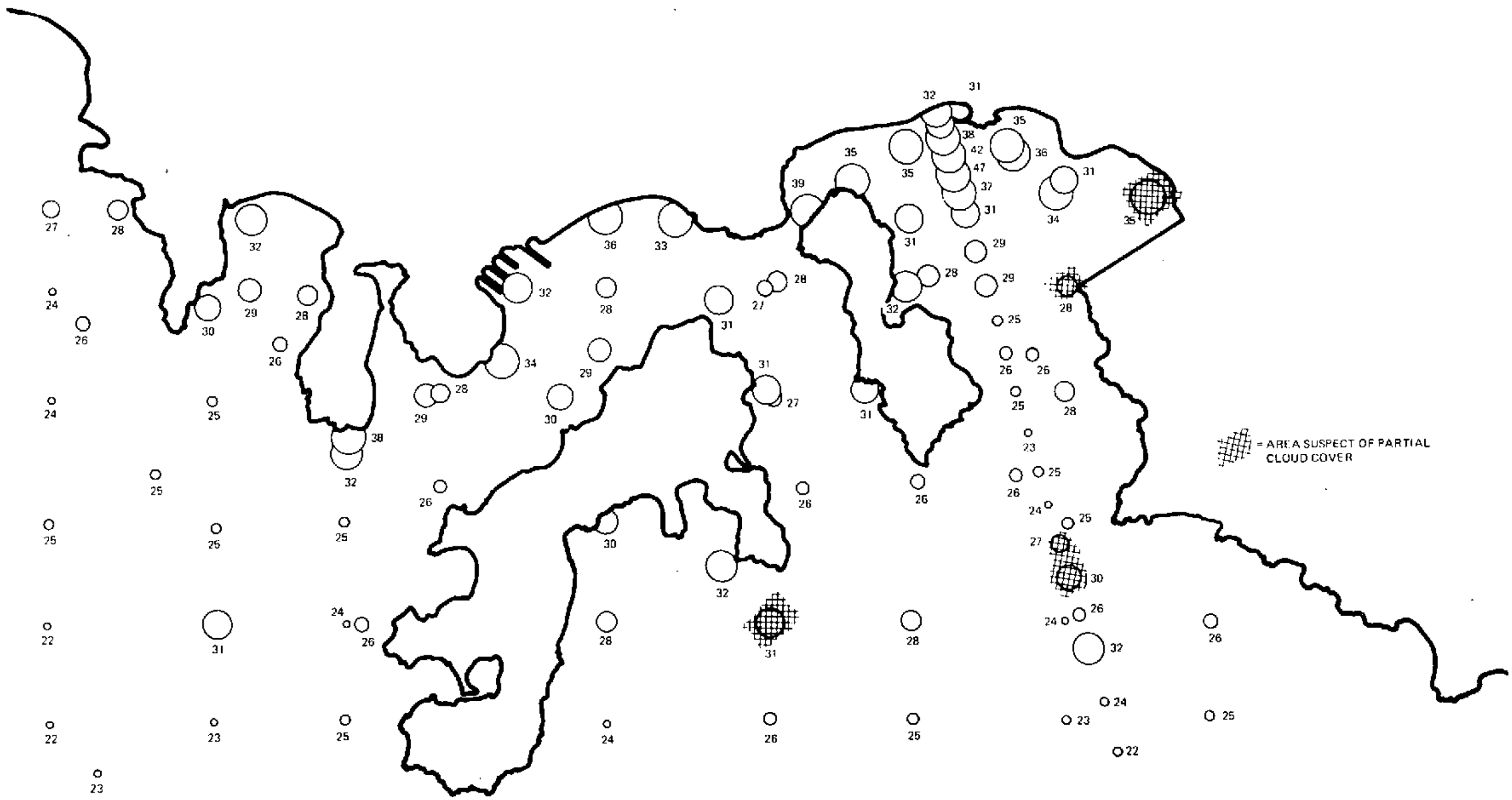

Figure 4-17. ERTS Precision CCT Data

4.3.8 Turbidity vs MSS Value Displays

In situ computer maps revealed highest turbidity values occurring in Northern Charlotte Amalie Harbor (the inner harbor), in Lindbergh Bay and north of Water Island. (Refer to Figure 4-18.)

To facilitate qualitative correlation between turbidity and MSS data, three map overlays were generated from original computer maps:

1. Precision MSS Band 4 vs Surface Turbidity, Figure 4-20.
2. Bulk MSS Band 4 vs Surface Turbidity, Figure 4-21.
3. Bulk MSS Band 5 vs Surface Turbidity, Figure 4-19.

Computer correlation was also performed, results are listed in paragraph 4.5.9.

4.3.9 MSS Overlays - To 1:10,000 Scale C & GS Map #933 (Refer to Figure 4-22)

MSS Bulk CCT print-out data (Band 5) was transferred manually to an overlay of C & GS Harbor Chart #933. Each cell was shaded according to its MSS quantum value, based upon 127 counts. Utilization of the resultant maps enabled rapid determination of overall MSS ranges within the study area, was useful in establishing the geographic location of clouds, and demonstrated the ability of ERTS to provide acceptable resolution within the narrow channels and bays of St. Thomas Harbor.

Although the MSS harbor map was manually generated* future programs calling for repetitive (i.e. 18 day) CCT's should take advantage of computer plotters which can provide maps much more efficiently. Either the computer output microfilm system or the computer output plotter could be used for bulk CCT-to-map overlay generation.

4.4 FINAL ANALYSIS RESULTS

Data handling for the St. Thomas Program was comprised of the subject matter discussed in Sections 1-4 of this report. Preliminary statistical analyses were discussed with Dr. Egan, Dr. Olsen and coordinated by W. Coulbourn. Finally, computer processing was tailored to achieve three goals:

1) Determination of degrees of correlation of in situ acquired data with aircraft and satellite data.
2) Determination of the applicability of computer automated simulation techniques to future investigations.
3) Utilization of CCT data for sea bottom mapping.

*The limited quantity of satellite data received did not warrant software modification.

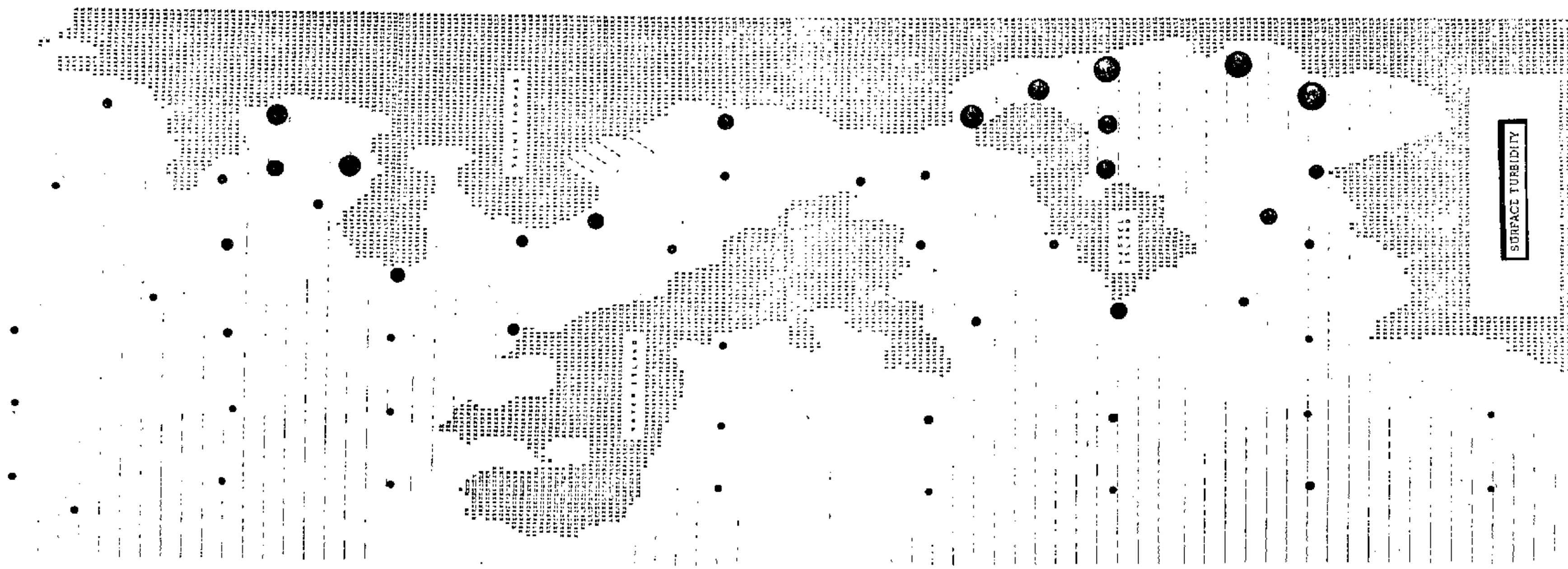

TURBIDITY (Surface)
Range: 0.12 F.T.U. to 3.10 F.T.U.
Average: 0.94 F.T.U.
Test Duration: Day 283 to 326, 1972
Scaled: • Min., ● Max.

Figure 4-18. Average Surface Turbidity Per Data Station (over 6 weeks)

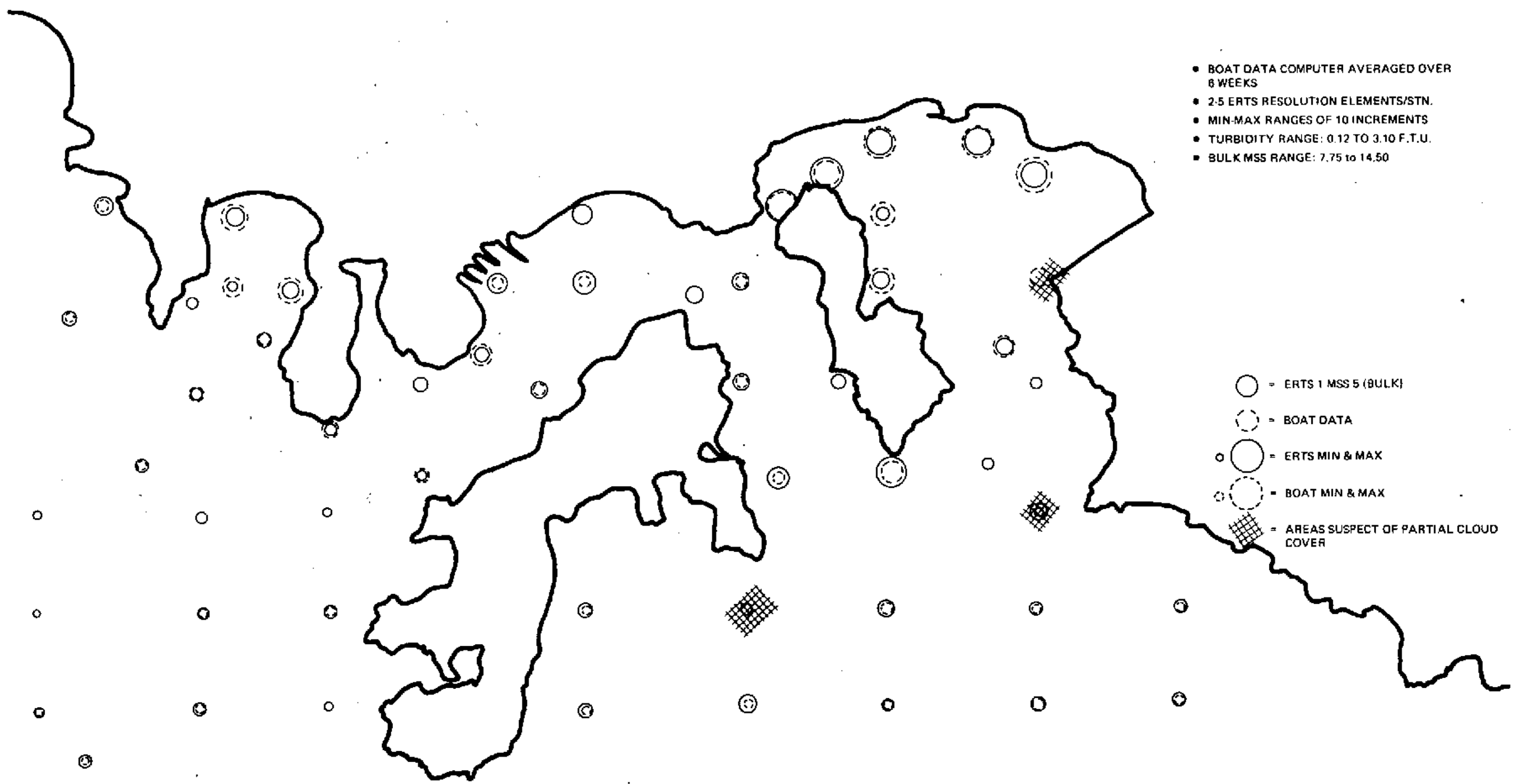

Figure 4-19. ERTS 1 Computer Tape Data (Bulk MSS Band 5) vs Boat Measured Surface Turbidity

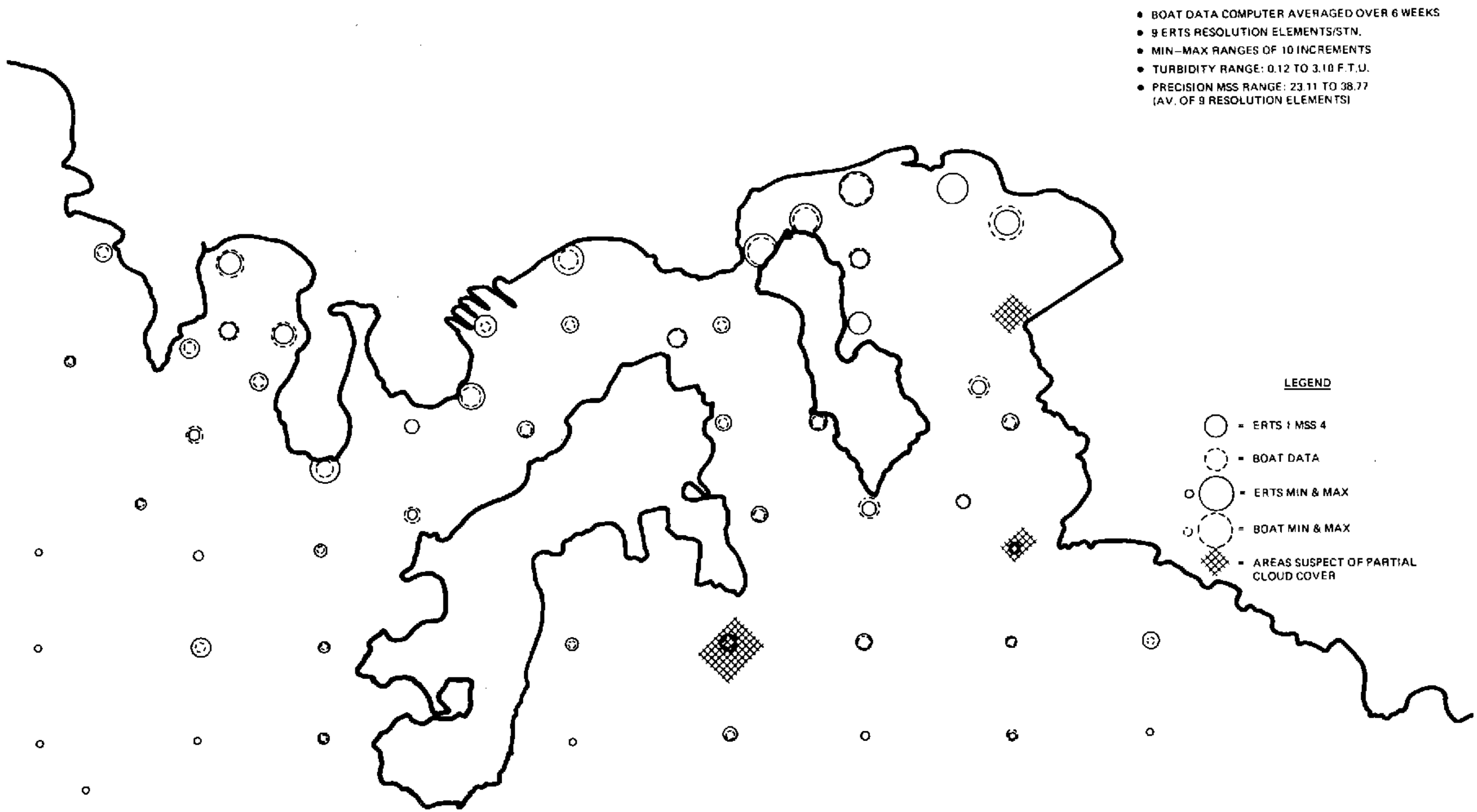

Figure 4-20. ERTS 1 Computer Tape Data (Precision MSS Band 4) vs Boat Measured Surface Turbidity

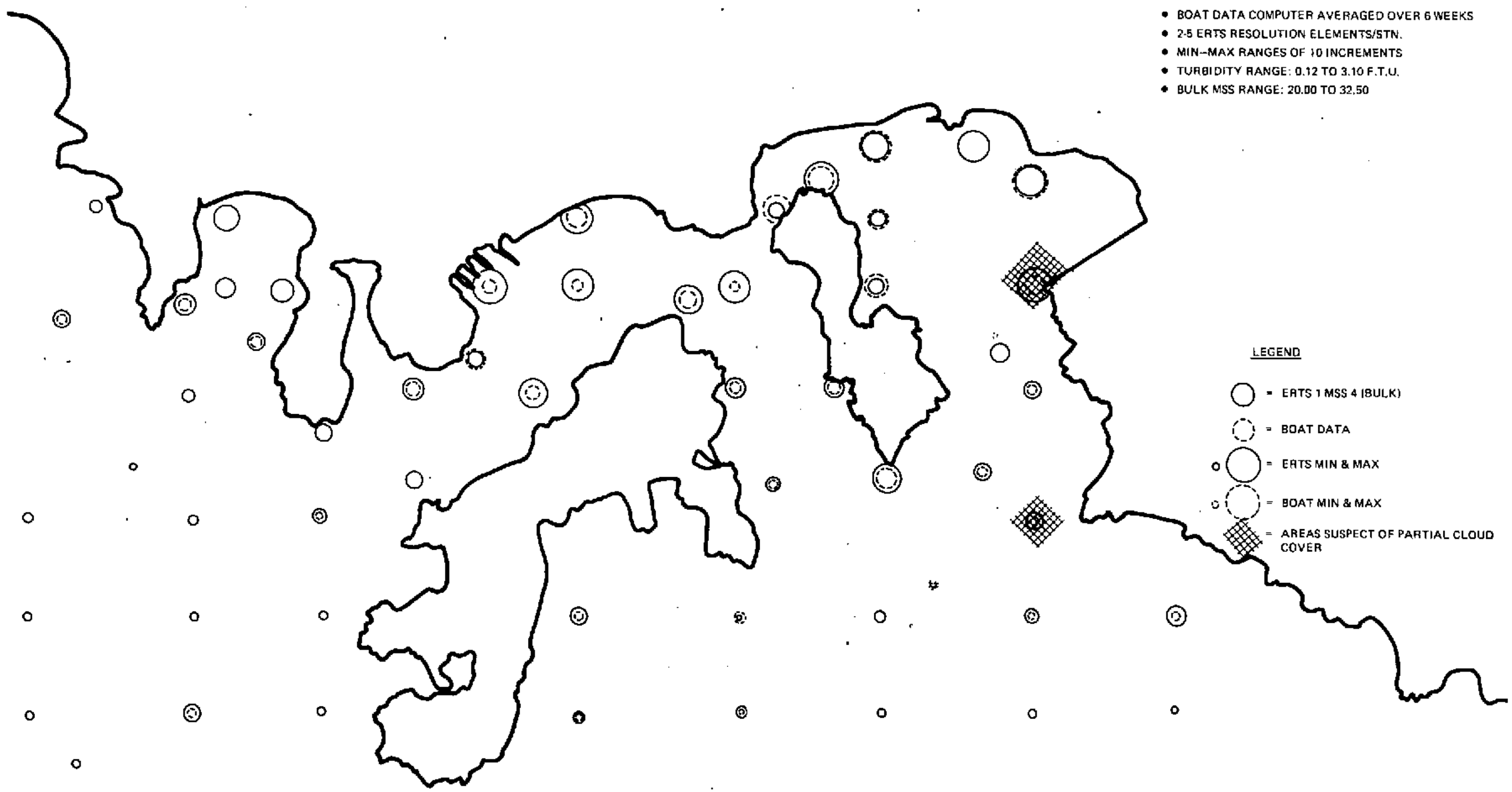

Figure 4-21. ERTS 1 Computer Tape Data (Bulk MSS Band 4) vs Boat Measured Surface Turbidity

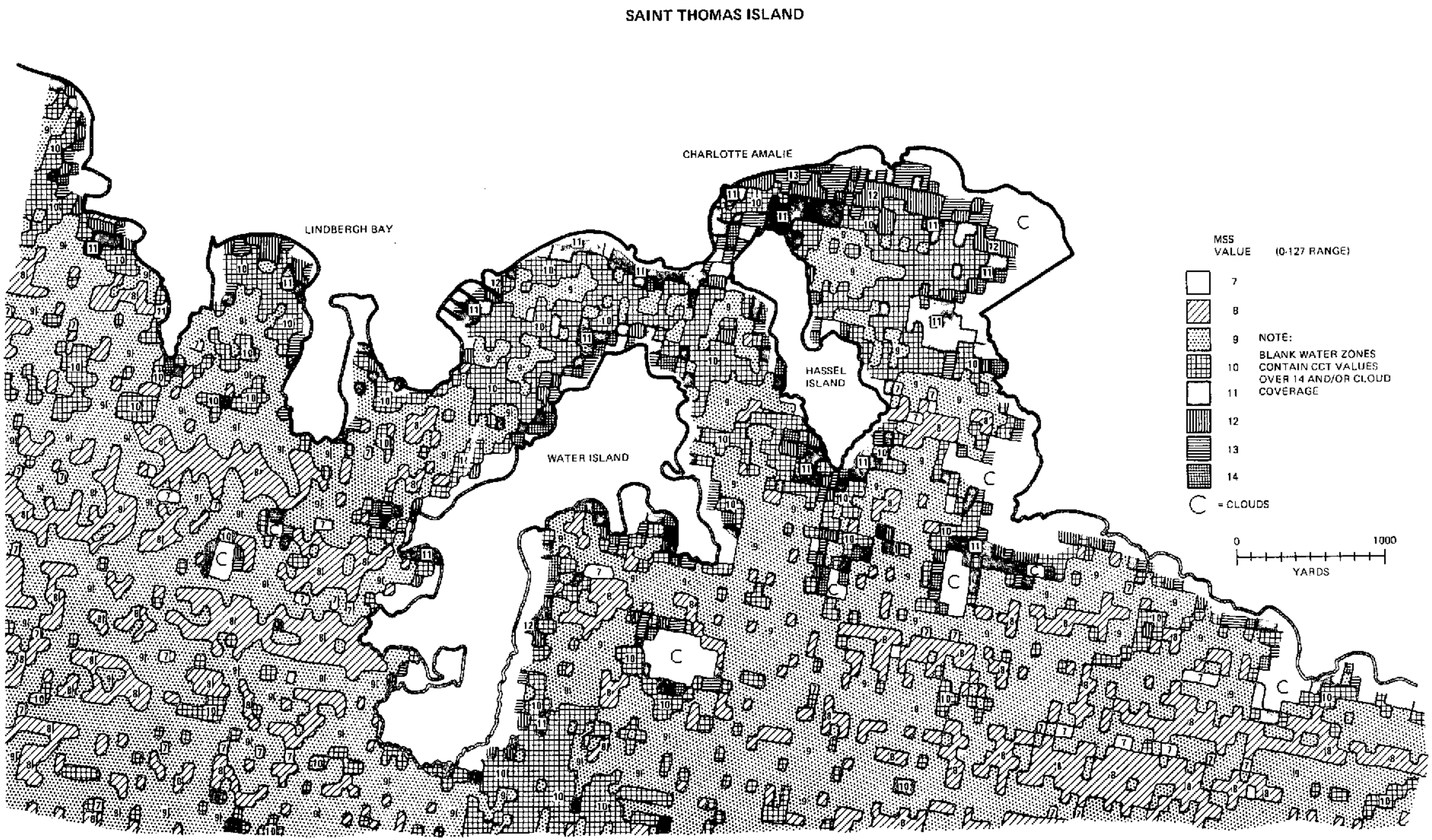

Figure 4-22. Charlotte Amalie Harbor St. Thomas, V.I. EPTS Bulk CCT Printout, MSS Band 5 Coded

Results are discussed in paragraphs 4.5.1 through 4.5.4. Also included (paragraph 4.4.5) are summary notes based on an overview of the entire data handling effort.

4.4.1 Correlation of Satellite and Aircraft Data with In Situ Data Acquired Along A North-South Transect in St. Thomas Harbor

4.4.1.1 Determination of Correlation Coefficients*

Computer correlation was performed on twenty-two separate transect parameters. Five groups of data were processed:

(1) All transect data stations (#102-#120)

(2) Station #'s 102, 104 & 106/107

(3) Station #'s 104, 106/107 & 109/110

(4) Station #'s 109/110, 112 & 115

(5) Station #'s 112, 115 & 119/120

Group (2) contains data stations in a polluted region; Group (5) contains stations in zones of high water clarity.

For each case, conversion of MSS quantum data to radiance was performed. Cloud shadows affected Station 112 and a cloud partially obscured Station 115. High energy readings, from the harbor sea wall affected Station 102 MSS quantum values, due to MSS detector response characteristics.

Bulk MSS clusters, for Stations 102, 112 and 115 were carefully selected so as not to include points (pixels) affected by high energy readings or shadow.

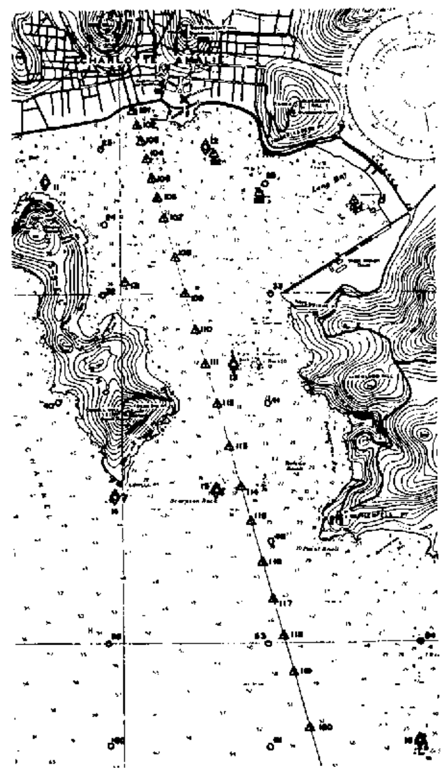

*Correlation coefficients (r_{jk}) obtained via Grumman Data Systems STATPAK software.

$$r_{jk} = s_{jk}/\sqrt{s_{jj}}\sqrt{s_{kk}}, \text{ where } s_{jk} = \sum_{i=1}^{n} (x_{ij}-x_{1j})(x_{ik}px_{1k}) - \frac{\sum_{i=1}^{n}(x_{ij}-x_{1j})\sum_{i=1}^{n}(x_{ik}-x_{1k})}{n}$$

x(ij) denote input data, i=1, . . . , n are observations and j=1, . . . , m are variables.

An exceptionally high degree of correlation is indicated, in Table 4-1, between bulk MSS bands 4 and 5 and turbidity (i.e., 91 and 96%, respectively). Aircraft, satellite, and in situ optical measurements also exhibited strong correlations.

In situ measurements, as reported by Dr. Egan, were known to be less accurate in shore (i.e., Stations 102, 104) than further south on the transect. Correlation runs 3 and 4 (Tables 4-2 through 4-5) agree, in that a stronger in situ to aircraft and satellite correlation was recorded in outer waters.

Also indicated in the correlation tables is a strong ERTS-to-carotenoids* correlation in-shore but a negative correlation in outer harbor waters. (r_{jk} = -.90 (MSS4), -.69 (MSS5) in Run 2 and +.88 (MSS4), +.84 (MSS5) in Run 5. Similarly, ERTS-to-Chlorophylls a, b, c, comparisons show negative correlation in-shore and strong positive correlation in outer waters.

*Plant & Animal Pigments

Table 4-1 indicates that ERTS MSS Bands 4 and 5 are useful for monitoring harbor turbidity.

The known link between benthic diversity and turbidity and the indicated strong ERTS-to-turbidity correlation is indeed promising from a standpoint of developing a method of applying ERTS data. Correlation tables, however show only weak ERTS to biological data correlations. Additional satellite and in situ data are required to establish with certainty if, and to what extent biological parameter status can be related to turbidity and thence to ERTS data.

Precision MSS 4 values showed weaker correlation with aircraft and turbidity data. Note however, that cloud shadow corrections were not employed. Although a bulk CCT vs precision CCT evaluation was not part of this program, favorable precision-to-turbidity results were shown in cloud free areas. (Paragraph 4.4.2.1). A comparison of Figures 4.20 and 4.21 (shown in paragraph 4.4) suggests that additional data is needed in order to specify the overall merits of precision vs bulk CCT's. Geometric correction of the bulk digital data without degradation in radiometric fidelity is of course desired.

Table 4-1. All Transect Data Stations (#102-#120)

	In Situ Red	Aircraft Green	Aircraft Red	Prec. MSS 4	Bulk MSS 4	Bulk MSS 5	Turbidity	Chlorophyll a	Total Chlorophyll	Pigment Diversity	Total Carotenoids	Bulk MSS 4 UC*	Bulk MSS 5 UC*	Bulk 4 MUC*	Bulk 5 MUC*	Chlorophyll C	Bulk MSS 6
In Situ Green	99.9	83	85	86	78	64	79	62	40	18	13	57	65	76	62	31	47
In Situ Red		82	83	86	78	64	79	60	38	49	41	56	65	75	62	29	51
Aircraft Green			97	69	98		94	17	23	68	28	82	84	96	79	11	16
Aircraft Red				78	90	74	88	61	35	54	41	70	72	90	66	27	28
Precision MSS 4					63	44	64	47	15	25	19	20	15	57	38	5	21
Bulk MSS 4						83	91	12	17	80	22	86	83	97	79	8	60
Bulk MSS 5							96	3	-11	19	-6	81	100	82	99.4	-16	53
Turbidity								26	5	53	10	80	96	90	9	-2	47
Chlorophyll A									93	38	94	34	4	49	1	88	11
Total Chlorophyll										23	99.8	26	-11	29	-11	99.4	5
Diversity (NITS)											25	78	50	78	48	17	81
Total Carotenoids												30	-6	34	-7	99	46
Bulk MSS 4 UC*													81	86	82	22	60
Bulk MSS 5 UC*														83	99.3	-15	53
Bulk MSS 4 MUC**															78	23	60
Bulk MSS 5 MUC**																-15	55
Chlorophyll C																	0

*MSS quantum value (0-127) uncorrected for atmospheric attenuation

**Midpoint pixel MSS quantum value (0-127) uncorrected for atmospheric attenuation

Table 4-2. Run 2 Stations 102, 104, and 106/107

	In Situ Red	Aircraft Green	Aircraft Red	Prec. MSS 4	Bulk MSS 4	Bulk MSS 5	Turbidity	Chlorophyll a	Total Chlorophyll	Pigment Diversity	Total Carotenoids	Bulk MSS 4 UC*	Bulk MSS 5 UC*	Bulk 4 MUC*	Bulk 5 MUC*	Chlorophyll C	Bulk MSS 6
In Situ Green																	
In Situ Red																	
Aircraft Green			93.7	6	100	94	98	-99.6	-90	90	-89	65	94	99	89	-88	68
Aircraft Red				40	94	76	85	-97	-99.6	69	-99.5	34	77	88	68	-99	38
Precision MSS 4					7	-28	-14	-15	-48	39	-49	-72	-28	-8	-40	-53	-69
Bulk MSS 4						94	98	-99.7	-90	90	-90	64	94	99	89	-88	67
Bulk MSS 5							99	-91	-70	99	-69	87	100	99	99	-66	89
Turbidity								-96	-80	97	-80	78	99	99.8	96	-76	81
Chlorophyll A									94	-86	94	-58	-91	-97	-85	92	-61
Total Chlorophyll										-62	100	-25	-71	-83	-61	99.8	-30
Diversity (NITS)											-62	92	99.3	95	100	-57	93
Total Carotenoids												-25	-70	-83	-61	99.9	-29
Bulk MSS 4 UC*													86	75	92	-20	99.9
Bulk MSS 5 UC*														98	99	-66	89
Bulk MSS 4 MUC**															95	-80	78
Bulk MSS 5 MUC**																-58	94
Chlorophyll C																	-24

*MSS quantum value (0-127) uncorrected for atmospheric attenuation

**Midpoint pixel MSS quantum value (0-127) uncorrected for atmospheric attenuation

Table 4-3. Run 3 Stations 104, 106/107 and 109/110

	In Situ Red	Aircraft Green	Aircraft Red	Prec. MSS 4	Bulk MSS 4	Bulk MSS 5	Turbidity	Chlorophyll a	Total Chlorophyll	Pigment Diversity	Total Carotenoids	Bulk MSS 4 UC*	Bulk MSS 5 UC*	Bulk 4 MUC*	Bulk 5 MUC*	Chlorophyll C	Bulk MSS 6
In Situ Green	100	59	52	80	63	50	63	17	-21	99	-25	-29	50	0	87	-31	97.5
In Situ Red		59	52	80	63	50	63	17	-21	99	-25	-29	50	0	87	-31	97.5
Aircraft Green			99.7	95	99.9	99.5	99.0	-69	-92	70	-93	-94	99.4	81	91	-95	40
Aircraft Red				93	99	100	99	-75	-94	64	-95	-97	100	85	88	-97	33
Precision MSS 4					97	92	97	-44	-75	88	-77	-80	92	59	99	-81	65
Bulk MSS 4						99	100	-66	-89	74	-91	-93	99	78	93	-93	45
Bulk MSS 5							99	-76	-95	62	-96	-97	100	86	87	-98	30
Turbidity								-66	-89	73	-91	-93	99	78	93	-93	44
Chlorophyll A									93	3	91	89	-76	-99	-34	98	39
Total Chlorophyll										35	99.9	99.7	-95	-98	-67	99.5	1
Diversity (KITS)											-38	-42	62	14	93	-44	93
Total Carotenoids												99.9	-96	-97	-69	99.8	-3
Bulk MSS 4 UC*													-97	-96	-73	100	-7
Bulk MSS 5 UC*														87	87	-98	30
Bulk MSS 4 MUC**															50	-95	-22
Bulk MSS 5 MUC**																-74	74
Chlorophyll C																	-9

*MSS quantum value (0-127) uncorrected for atmospheric attenuation
**Midpoint pixel MSS quantum value (0-127) uncorrected for atmospheric attenuation

Table 4-4. Run 4 Stations 109/110, 112 and 115

	In Situ Red	Aircraft Green	Aircraft Red	Prec. MSS 4	Bulk MSS 4	Bulk MSS 5	Turbidity	Chlorophyll a	Total Chlorophyll	Pigment Diversity	Total Carotenoids	Bulk MSS 4 UC*	Bulk MSS 5 UC*	Bulk 4 MUC*	Bulk 5 MUC*	Chlorophyll C	Bulk MSS 6
In Situ Green	98	91	95	91	82	99	95	99	93	92	95	82	96	90	0	92	-79
In Situ Red		80	88	81	69.4	99.9	87	99.8	99	82	99	69	99.8	97	0	98	-65
Aircraft Green			99	100	99	83	99	84	69	99.9	72	99	84	63	0	66	-98
Aircraft Red				99	96	89	100	90	78	99.5	81	95	90	73	0	75	-94
Precision MSS 4					99	83	99	84	69	100	73	99	84	63	0	66	-98
Bulk MSS 4						72	96	73	56	-98	60	100	71	49	0	52	-100
Bulk MSS 5							88	100	98	-84	99	72	100	96	0	97	-68
Turbidity								90	77.2	99.6	80	96	90	72	0	74	-94
Chlorophyll A									98	-85	98	73	100	95	0	96	-70
Total Chlorophyll										-71	99.9	56	99.5	99.6	0	99.9	-52
Diversity (NITS)											-74	-98	-85	-65	0	-68	97
Total Carotenoids												59	98	.99	0	99.6	-55
Bulk MSS 4 UC*													73	49	0	52	-100
Bulk MSS 5 UC*														95	0	96	-70
Bulk MSS 4 MUC**															0	99.9	-44
Bulk MSS 5 MUC**																-	-
Chlorophyll C																	-47

*MSS quantum value (0-127) uncorrected for atmospheric attenuation

**Midpoint pixel MSS quantum value (0-127) uncorrected for atmospheric attenuation

Table 4-5. Run 5 Stations 112, 115, and 119/120

	In Situ Red	Aircraft Green	Aircraft Red	Prec. MSS 4	Bulk MSS 4	Bulk MSS 5	Turbidity	Chlorophyll A	Total Chlorophyll	Pigment Diversity	Total Carotenoids	Bulk MSS 4 UC*	Bulk MSS 5 UC*	Bulk 4 MUC*	Bulk 5 MUC*	Chlorophyll C	Bulk MSS 6
In Situ Green	84	**92.6**	**99.8**	26	72	65	**99.8**	**96**	**90**	34	**96**	71	66	50	50	86	-30
In Situ Red		**98**	80	-30	**98**	**96**	87	**96**	**99.4**	79	**96**	**98**	**96**	89	89	**99.9**	27
Aircraft Green			**90**	-13	**93**	89	**95**	**99.4**	**98**	67	**99**	92	**90**	79	79	**99**	85
Aircraft Red				32	67	60	**99**	**94**	86	27	**94**	66	61	44	44	82	-36
Precision MSS 4					-49	-56	20	-1	-20	-82	-1	-50	-55	-71	-71	-27	**-99.9**
Bulk MSS 4						**99.7**	76	88	**95**	**90**	88	**100**	**99.8**	**96**	**96**	**97**	46
Bulk MSS 5							70	84	**92**	**93**	84	**99.8**	**100**	**98**	**98**	**95**	53
Turbidity								**98**	**92**	40	**98**	74	75	71	55	89	-24
Chlorophyll A									**98**	58	**100**	87	84	72	72	**97**	-3
Total Chlorophyll										72	**98**	**95**	**93**	83	83	**99.7**	16
Diversity (NITS)											58	**90**	**93**	**98**	**98**	77	80
Total Carotenoids												87	84	72	72	**97**	-3
Bulk MSS 4 UC*														**99.8**	**97**	**97**	46
Bulk MSS 5 UC*														**98**	**98**	**95**	52
Bulk MSS 4 MUC**															**100**	87	68
Bulk MSS 5 MUC**																87	68
Chlorophyll C																	22

*MSS quantum value (0-127) uncorrected for atmospheric attenuation
**Midpoint pixel MSS quantum value (0-127) uncorrected for atmospheric attenuation

4.4.2 Correlation of Data Acquired During Similar Tidal Periods

4.4.2.1 Correlation of Satellite Data With In Situ Turbidity Data. During the six-week in situ data collection period, many turbidity measurements were taken during tidal periods similar to the one which occurred during the time of the ERTS-1 overpass on 17 October 1972.

The strong degree of correlation between ERTS MSS bands 4 and 5 and turbidity, as reported in paragraph 4.4.1.1, suggested that an additional correlation be performed, namely ERTS-1, 17 October data vs turbidity data acquired over the 6-week test period but only within the ERTS-1 overpass tidal window. (Tidal windows are listed in paragraph 4.5.4.)

Three sets of correlation were performed:

1) St. Thomas Harbor Only (Stas. 9-16 & 69)

2) Total Test Site (Stas. 2-16 & 69)

3) Total Test Site Minus Stas. 7, 8, 9 in West Gregerie Channel

The validity of tidal window data for West Gregerie Channel was not considered reliable due to the rapid changes in current direction. Resultant improved correlation for set 3 substantiates this deletion.

The selected tidal window was 1 hour before to 2 hours following low water slack.

Resultant correlation coefficients (r_{jk}) were as follows:

Set 1) .706 vs Precision MSS Band 4
.660 vs Bulk MSS Band 5
.638 vs Bulk MSS Band 4

Set 2) .645 vs Precision MSS Band 4
.514 vs Bulk MSS Band 4
.399 vs Bulk MSS Band 5

Set 3) .657 vs Bulk MSS Band 5
.626 vs Bulk MSS Band 4
.610 vs Precision MSS Band 4

An original intent of the St. Thomas data handling program was to compare three sets of ERTS data (i.e., three separate overpasses) with harbor data. Although data from only one overpass was available, coefficients shown above are based on 6 week data, when combined with the results of the transect data study (paragraph 4.5.1), establishes that MSS bands 4 and 5 strongly correlate with turbidity.

Six week in situ data was also compared to ERTS MSS band 6. No significant correlation was recorded. (Bands 6 and 7 penetrate the water only very slightly.)

4.4.2.2 Analysis of Harbor Data in "Tidal Window" Time Frames. A statistical analysis of data collected throughout the program, but selected from only those time periods which corresponded closest with tidal conditions existing at the time of the ERTS overpass, or "Tidal Windows", was made. Further, the data was segregated into four distinct groups (see Chart Figure I-1).

- Inner harbor data (Sample stations No.: 7, 8, 9, 11, 12, 13)
- Intermediate harbor data (Sample stations No.: 2, 4, 5, 6)
- Outer harbor data (Sample Stations No.: 3, 10, 13, 15, 16, 17)
- Repetitive Sample Station Data (Sample Stations 2 through 17)

The first three areas, above, were selected on the basis of their spatial similarity relative to harbor topography while the last set was selected to check use of data from all stations during the same tidal window. Data acquired in the satellite tidal window was used to improve homogeneity of samples by providing information which should be more representative of the conditions of the harbor during the satellite overpass, although acquired on different days. Additionally, these results were used to compare general harbor conditions, as explained by Olsen (page 3-19) to those at the time of satellite overpass.

The objective of using tidal window data was to relate in situ turbidity data to other water quality parameters. If positive results were obtained then ERTS detectability of turbidity, determined by the transect data, could be utilized as an inferential indicator of these parameters. Generally, by inspection of the correlation tables this hypothesis was not supported (see correlation table, keyed to harbor maps).

As a further test insofar as data collected allows, the underlying determinants of water quality were investigated by use of factor analysis. The accuracy of factor analysis is dependent upon a linear relationship between variables and normal multivariate distributions. The aim in factor analysis is to account for, or explain, the matrix of covariance by a minimum, or at least a small number, of hypothetical variates, or 'factors'. Here we attempt to assign determinants of conditions affecting the defined harbor areas, whatever their basic nature, in terms of a relatively small role in determining the other water quality parameters. However, the importance of turbidity is at a maximum in the inner harbor areas, Tables 4-6, 7, 8, 9). Inasmuch as this experiment was directed at determining the application of the ERTS in harbor areas, and the coastal zone, and the primary detectable parameter was turbidity, this is an encouraging qualitative, if not overpowering quantitative finding. Comparison of the Tidal Window factor tables with the conclusions of Dr. Olsen, show that the role turbidity plays during the ERTS Tidal Window is very low compared to its role in Dr. Olsen's analysis. (Olsen's results based on use of all data showed a turbidity role of -.77 in Table 3-8 VIII page 3-26, whereas much lower numbers (8 to 29) were calculated when using only the tidal window data, Tables 4-6, 7, 8, 9. The availability of only a single ERTS overpass has disallowed comparison with other tidal conditions to see if better correlation with turbidity would occur during other tidal windows. It is recommended that repetitive coverage to establish chronistic data acquisition parameters related to turbidity and other ERTS detectable measures and harbor tidal conditions be made in the future.

4.4.3 Application of Computer Automated Simulation Software to ERTS CCT Data

It has been stated earlier that either the computer output microfilm system and/or the computer output plotter could be of valuable assistance to investigators requiring a "contour view" of ERTS computer data for geographical areas under study.

Still another meaningful application of ERTS data is the conversion of CCT values to a graphics format enabling the investigator to obtain perspective views over a fixed geographical area. Figures 4-23 and 4-24 show plots generated via the simulation technique. Two separate viewing angles are shown.

Table 4-6. Intermediate Harbor Sample Stations No's 2, 4-6 (Satellite Tidal Windows)

	CORRELATION MATRIX												ROTATED FACTOR MATRIX			
	Wind Speed	Cloud Cover	Amb. Temp.	Swell Ht.	Depth	Turbidity	Water Temp.	D. O.	pH	Conductivity	Salinity	Plankton Den.	A	B	C	D
Wind Speed	100	13	-14	24	-28	10	-10	-17	-19	-14	25	26	-10	-14	13	-91
Cloud Cover		100	74	-14	-19	-23	79	-6	72	79	-67	-75	86	-1	-10	-34
Ambient Temp.			100	-21	6	-24	97	-26	92	81	-80	-94	96	9	-6	9
Swell Height				100	20	8	-1	-23	-48	-3	39	16	-21	25	.71	-32
Water Depth					100	-60	11	2	-10	-20	3	-24	-5	87	20	31
Turbidity						100	-30	-30	-12	13	18	37	-19	-87	27	10
Water Temp.							100	-22	84	85	-78	-95	95	19	14	-2
Dissolved Oxygen								100	-16	-35	-23	18	-20	25	-83	-5
pH									100	82	-89	-88	94	-11	-16	17
Conductivity										100	-72	-82	91	-23	22	6
Salinity											100	82	-86	-1	38	14
Plankton Density												100	-94	-26	-5	-15

Table 4-7. Outer Harbor Repetitive Sample Stations No.'s 3, 30, 14-17

CORRELATION MATRIX / ROTATED FACTOR MATRIX

	Wind Speed	Cloud Cover	Amb. Temp.	Swell Ht.	Depth	Turbidity	Water Temp.	D. O.	pH	Conductivity	Salinity	Plankton Den.	A	B	C	D
Wind Speed	100	8	5	61	-9	-34	-3	-64	-6	-13	5	15	1	70	4	69
Cloud Cover		100	75	-28	-40	36	82	33	79	84	-62	-76	80	-19	-32	32
Ambient Temp.			100	-8	-17	17	92	14	93	65	-89	-91	97	3	-4	3
Swell Height				100	60	-52	-12	-67	-29	-38	13	16	-6	74	53	15
Water Depth					100	-64	-30	-18	-24	-52	1	9	-8	15	89	-31
Turbidity						100	35	14	24	55	-14	-22	17	-6	-88	-38
Water Temp.							100	24	85	84	-76	-89	93	-5	-22	6
Dissolved Oxygen								100	26	36	-9	-30	16	-96	-3	4
pH									100	72	-93	-86	94	-14	-12	1
Conductivity										100	-54	-70	72	-22	-51	12
Salinity											100	83	-92	-3	-6	18
Plankton Density												100	-94	13	2	8

Table 4-8. Repetitive Sample Stations No.'s 2-17 (Satellite Tidal Windows)

CORRELATION MATRIX

	Wind Speed	Cloud Cover	Amb. Temp.	Swell Ht.	Depth	Turbidity	Water Temp.	D. O.	pH	Conductivity	Salinity	Plankton Den.
Wind Speed	100	-15	-47	29	-6	-21	-37	-19	-47	-44	34	39
Cloud Cover		100	65	-8	-18	23	78	17	70	72	-64	-73
Ambient Temp.			100	67	15	-3	81	-16	86	71	-71	77
Swell Height				100	52	-46	7	-23	-11	-22	7	7
Water Depth					100	-53	3	-11	-1	-31	-7	13
Turbidity						100	7	20	6	26	-10	-3
Water Temp.							100	-10	80	81	-74	-92
Dissolved Oxygen								100	-9	-14	-2	11
pH									100	76	-86	-78
Conductivity										100	-58	-72
Salinity											100	79
Plankton Density												100

ROTATED FACTOR MATRIX

	A	B	C	D
Wind Speed	32	10	-89	-10
Cloud Cover	-87	-21	-23	24
Ambient Temp.	-87	-14	25	13
Swell Height	-3	74	-39	-10
Water Depth	-1	-89	21	4
Turbidity	-8	-78	8	15
Water Temp.	-95	2	4	-6
Dissolved Oxygen	6	-15	9	97
pH	-90	-3	24	-7
Conductivity	-81	-36	-13	-20
Salinity	84	-3	-14	-11
Plankton Density	91	-5	- 14	4

Table 4-9. Inner Harbor Repetitive Sample Stations No.'s 7, 8, 9. 11, 12, 13 (Satellite Tidal Windows)

CORRELATION MATRIX / ROTATED FACTOR MATRIX

	Wind Speed	Cloud Cover	Amb. Temp.	Swell Ht.	Depth	Turbidity	Water Temp.	D. O.	pH	Conductivity	Salinity	Plankton Den.	A	B	C	D
Wind Speed	100	-4	-58	20	-53	11	-42	-31	-50	-35	48	44	40	86	14	-14
Cloud Cover		100	63	-16	-17	-18	69	1	68	64	-66	-71	-82	31	8	9
Ambient Temp.			100	-10	7	-20	77	-5	85	77	-70	-68	-84	-30	3	-14
Swell Height				100	45	-43	-3	-5	-30	-24	44	33	27	-9	87	-19
Water Depth						-30	5	40	-15	-18	6	-5	12	-77	45	22
Turbidity						100	-41	-26	-19	-11	14	25	29	1	-78	-29
Water Temp.							100	-13	79	85	-78	-90	-93	-12	22	-12
Dissolved Oxygen								100	6	-46	-21	1	4	-23	05	96
pH									100	81	-91	-74	-92	-10	-13	6
Conductivity										100	-70	-79	-88	5	-7	-43
Salinity											100	87	90	10	22	-26
Plankton Density												100	91	11	4	-5

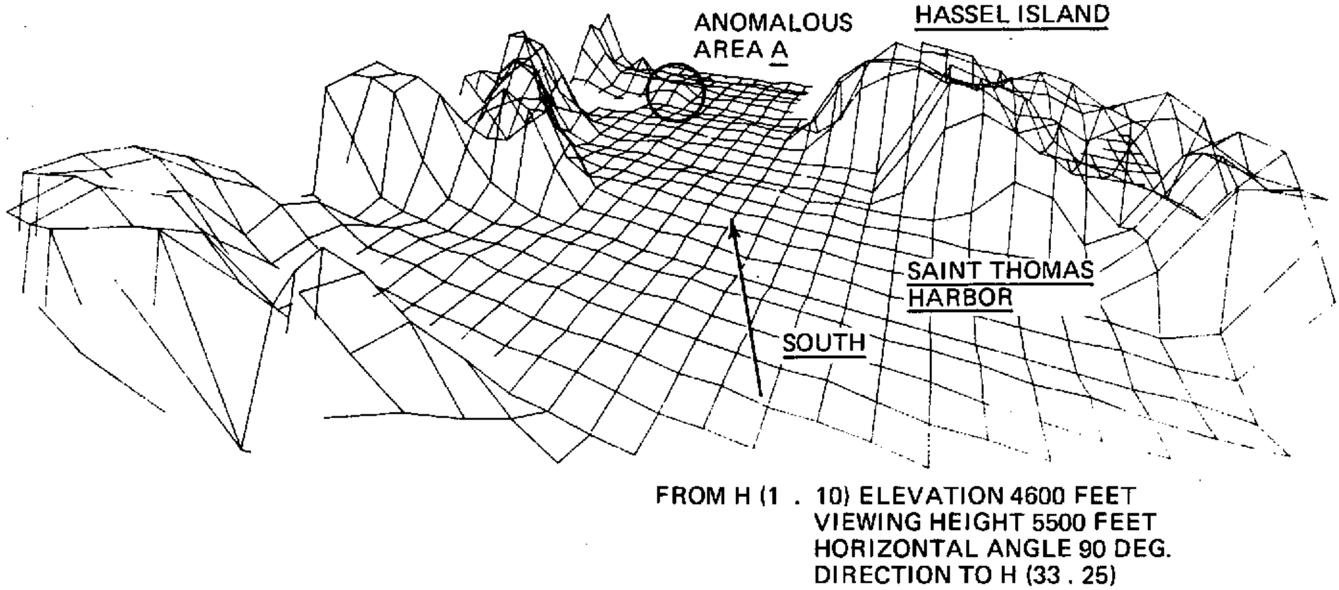

Figure 4-23. ERTS MSS CCT Data (Viewing Angle: North to South)

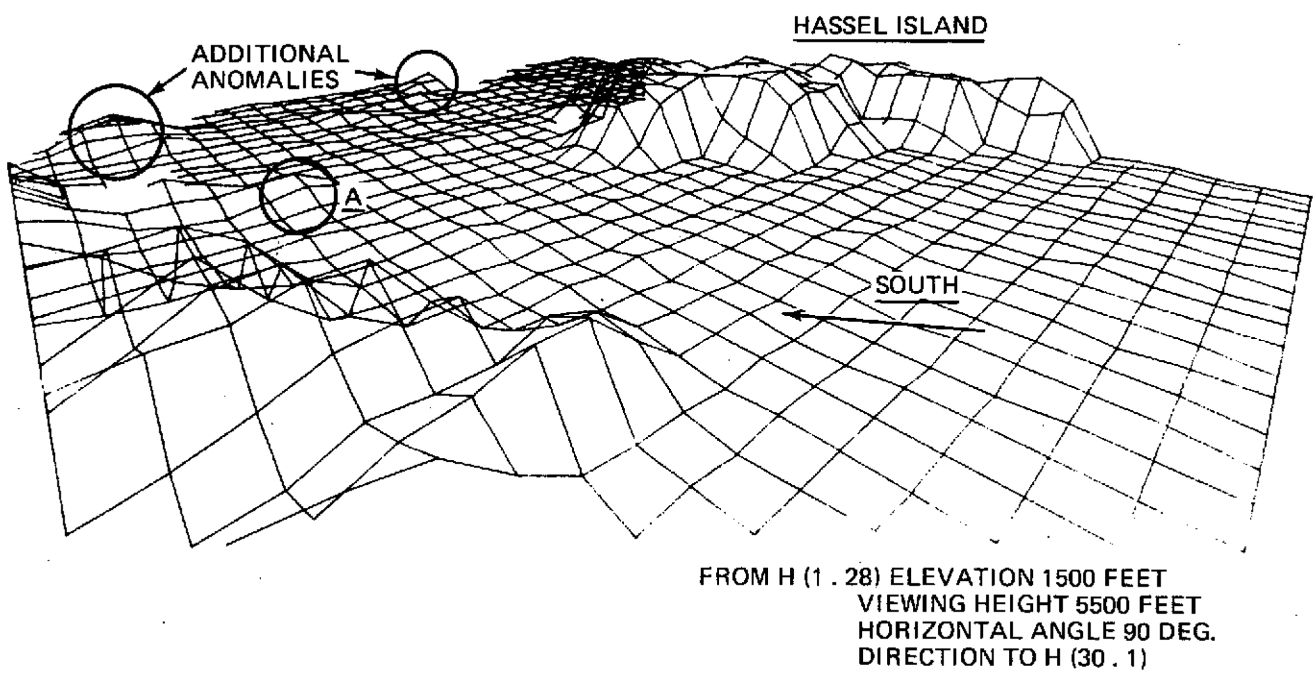

Figure 4-24. ERTS MSS CCT Data (Viewing Angle: East to West)

In generating the figures shown on the preceding page, Grumman "Automated Simulation of Terrain" software was utilized. Formerly, the simulation technique was employed to aid in landscape management via computer-generated views of large landscapes from selected ground sites and altitudes.

In adapting this software for use with ERTS data, each bulk MSS CCT pixel became an intersection point on a grid overlaying St. Thomas Harbor. The "height" or "z" value at intersect points was directly related to pixel (or MSS computer printout) values.

With MSS CCT values entered into computer storage, a variety of output graphics displays can be generated from a single matrix of values by varying look directions (i.e., one point in a grid to another) and by varying the vertical height above the grid. Output was generated via a Calcomp plotter.

MSS graphics presentations, in this format, possess several advantages:

1. Conceptualization of MSS values, per band, in x, y, and z values.
2. Comparison of bands via plot overlays.
3. Coordination with topographic overlays.
4. Simulation of in situ data, along a transect, with ERTS values.
5. Anomaly detection.
6. Presents intensity as a third dimension (vertical) on a large scale horizontal plot, and facilitates rapid comprehension by the human eye.

Among other applications is the presentation of sets of data taken over time from sampling stations on a transect. Final presentations enable combination of spectral, spatial and temporal aspects of in situ, satellite, and aircraft data in a single format.

Graphics overlays of three or more MSS bands, presented with identical look angle and viewing height, present the data interpretor with a valuable tool in studies related to determining land/water boundaries and misalignment of data points (pixels) between bands due to sensor error.

Finally, the utilization of MSS-to-x,y,z plotting technique, when applied for specific areas and for each ERTS overpass, offers a practical and valuable tool for displaying trends and cause and effect relationships.

Figure 4-32 (Page 4-69) is a further example of MSS-to-simulation plotting.

4.4.4 Mapping of Visible Sea Bottom

In order to determine the usefulness of ERTS CCT data for bottom mapping of high clarity water areas, a study of St. James Bay (Ref. Figure 4-25) on Eastern St. Thomas was undertaken. Data utilized consisted of Bulk CCT MSS bands 4 and 7, and multiband

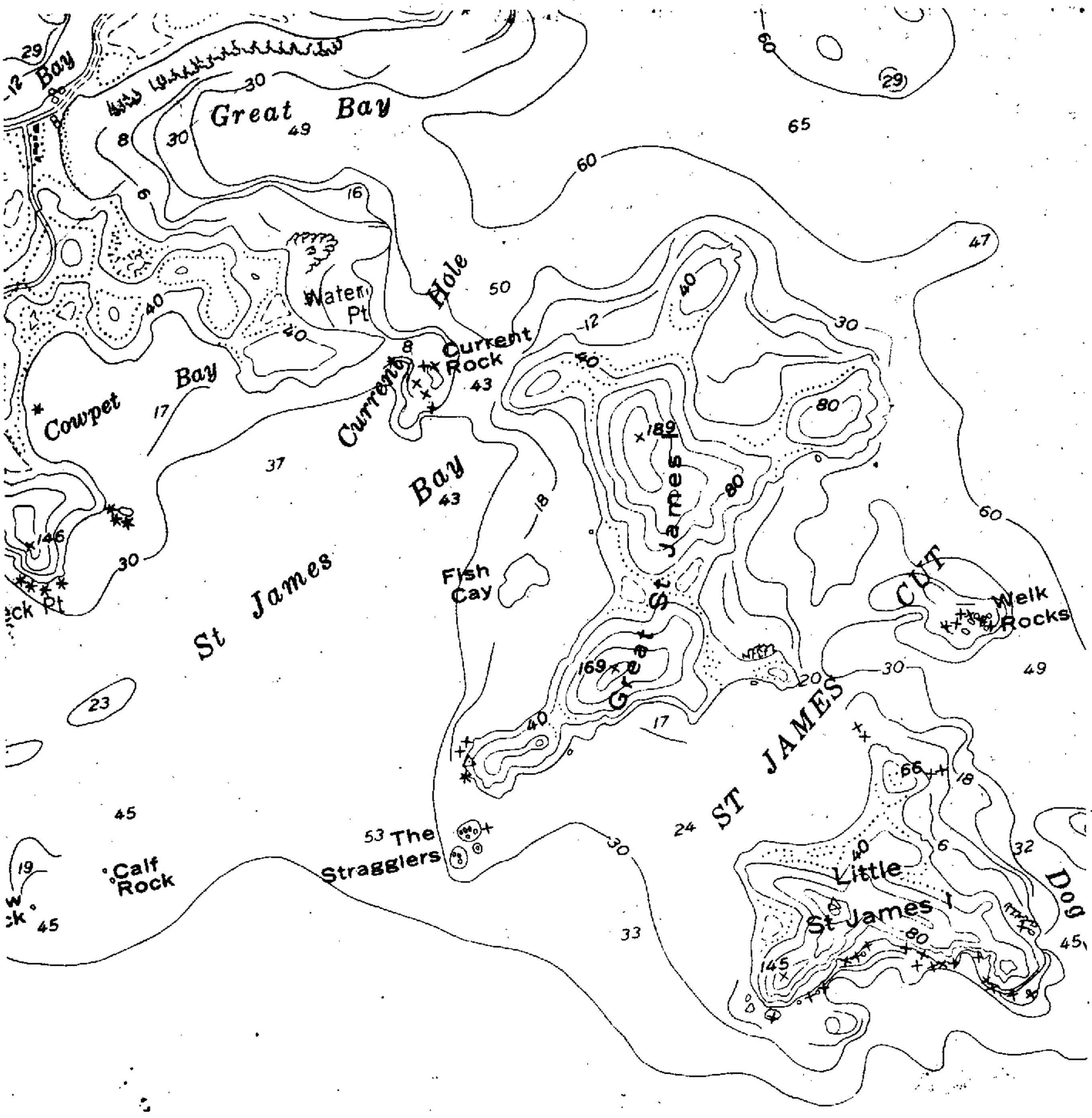

Figure 4-25. USGS Quadrangle St. James Bay Area

The initial step taken was the initilization of MSS band 7 CCT data to determine land/water interface areas. Findings, namely island boundaries, were superimposed onto a data printout generated from CCT MSS band 4. Figure 4-26 shows the MSS 4/MSS 7 combination.

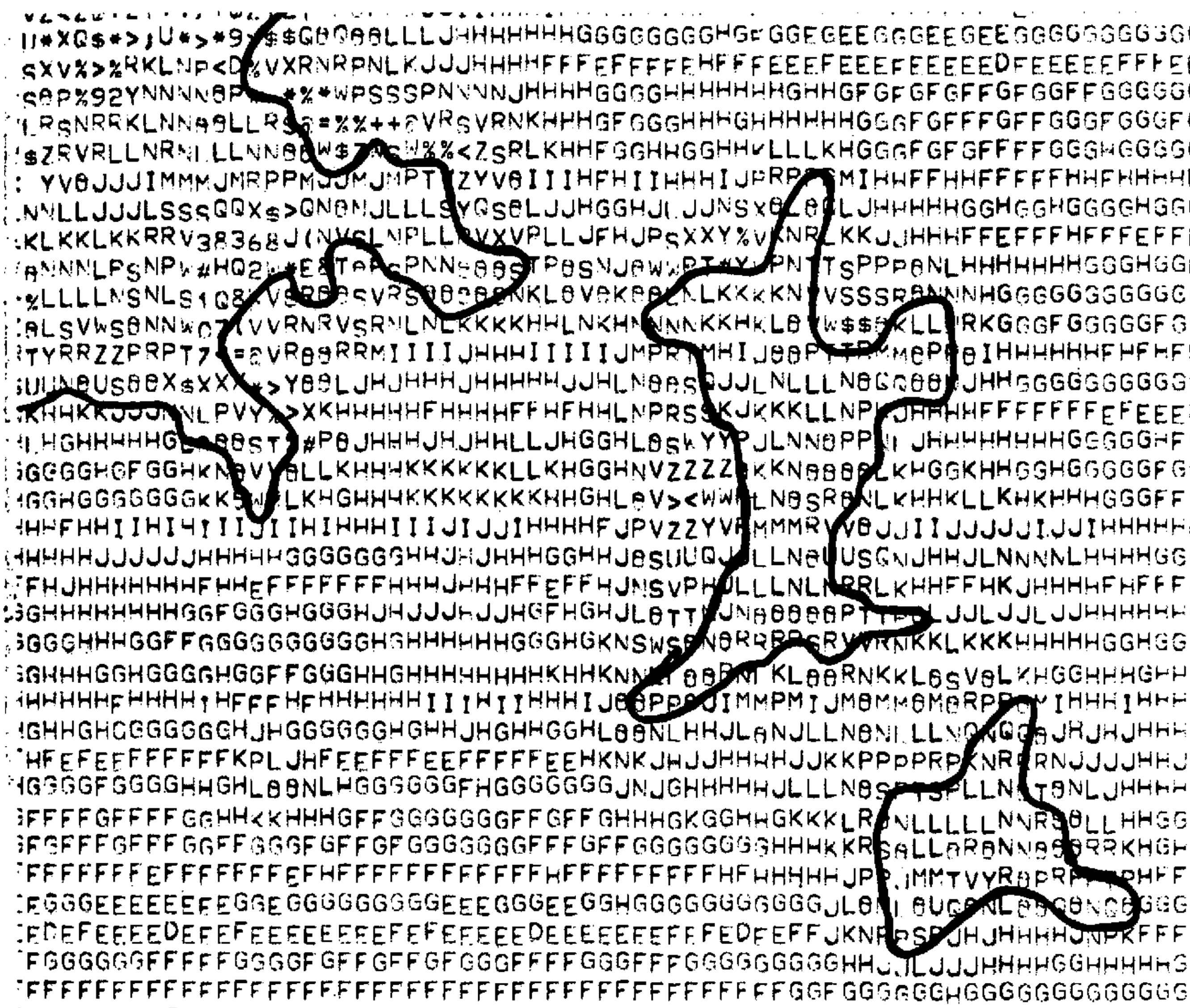

Figure 4-26. Bulk MSS Band 4 Data Containing Land/Water Boundaries Derived from Bulk MSS Band 7

Within water areas, MSS 4 radiance value contours were drawn for:

1) MSS values E through J

2) MSS values of K and greater

Lines of separation were generated; resultant mapping is shown in Figure 4-27.

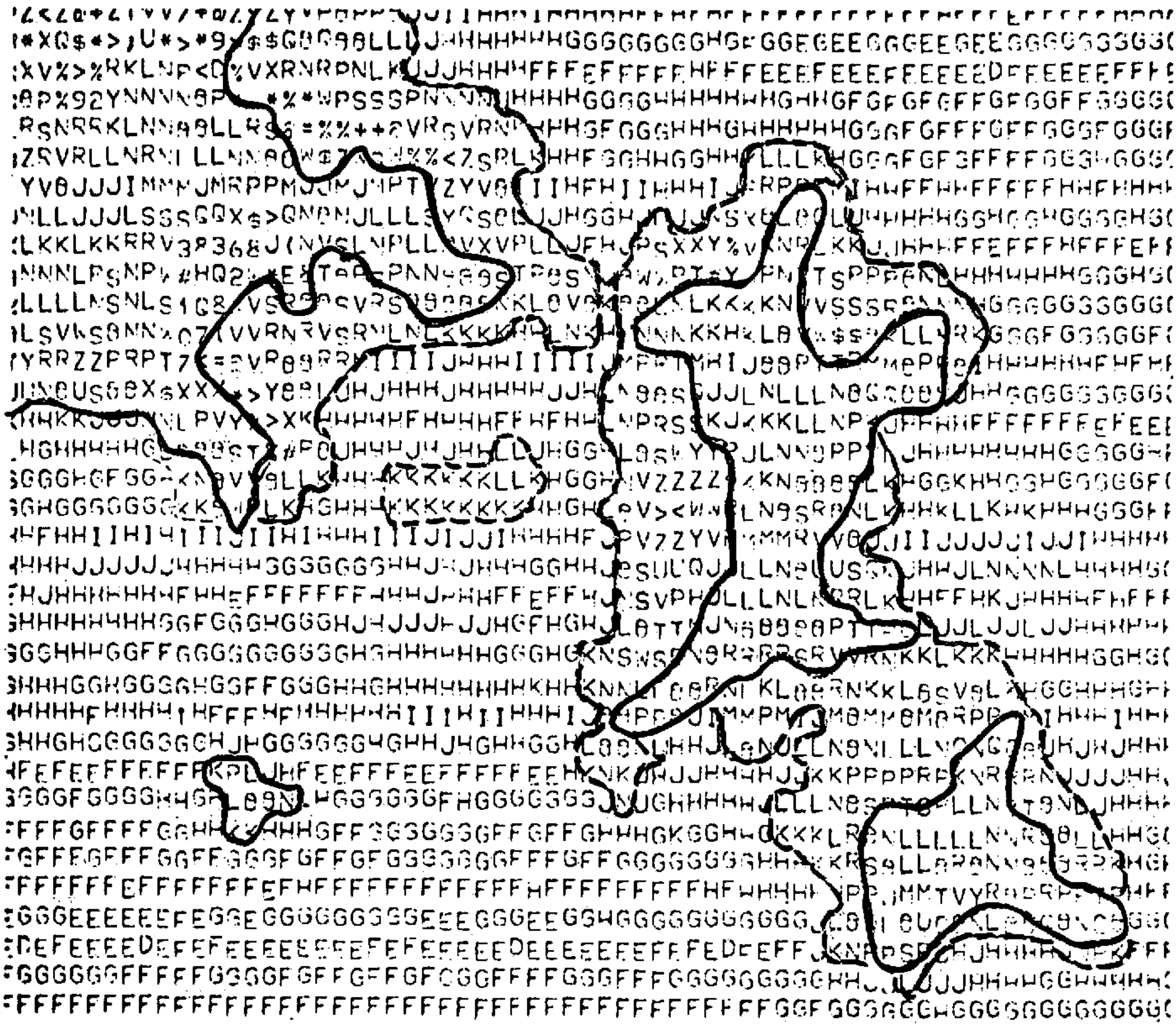

Figure 4-27. Bulk MSS Band 4 Data Land/Water Boundary Derived from Band 7, Contour Lines Separate MSS Values ≤ J from Values ≥ K

Significant findings were:

1) The MSS Band 4 contour line closely follows the 30' contour line shown on the USGS Quadrangle.

2) The contoured area in the lower left portion of Figure 4-27 falls geographically in the same location that water in St. James Bay rises from 45' to 19'.

3) Subsurface features were detectable. Figure 4-28 illustrates a reef area in Great Bay.

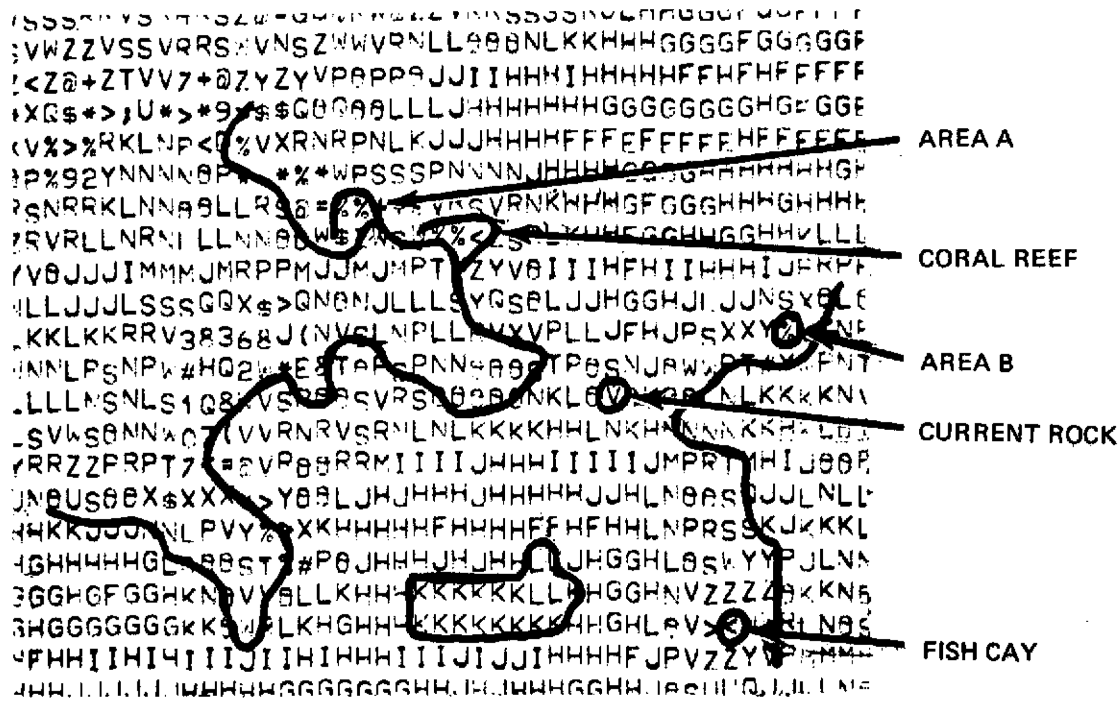

Figure 4-28. Subsurface Anomalies

Although no ground truth was taken for this area, comparison of MSS Band 4 data with aircraft multiband photography (Figures 4-29 and 4-30) indicates that ERTS band 4 offers immense potential for bottom mapping in high clarity areas of water depths ≤ 30 feet, and for revealing anomalous areas suitable for field check. Areas A & B in Figure 4-28 are examples of visible sea bottom features not shown on the 1954 U.S.G.S. quadrangle map.

Areas A, B and the indicated coral reef are not visible on the 0.74 - 0.90 micron photo, thus indicating their being subsurface features:

4.4.5 Final Notes

As a result of the data handling activities carried out during this program several points, which are briefly mentioned below, are believed worth highlighting-

1) Satellite CCT Printouts, when compared to C & GS charts showed an accuracy within the instantaneous field of view of approximately 80 meters. (i.e., ± one computer printout pixel)

2) Land/Water Interfaces were most easily determined through the use of MSS band 7, as expected

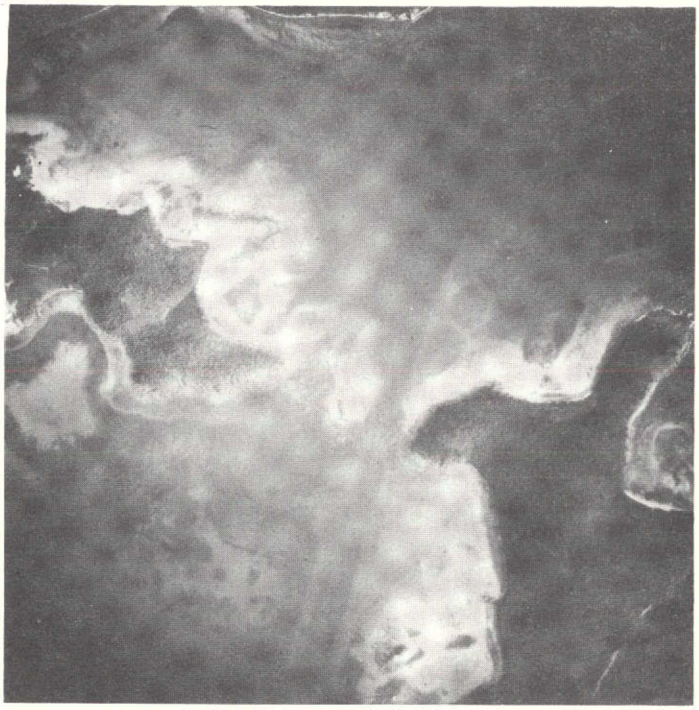

Figure 4-29. 0.41 - 0.47 micron Aircraft Photography
St. James Bay

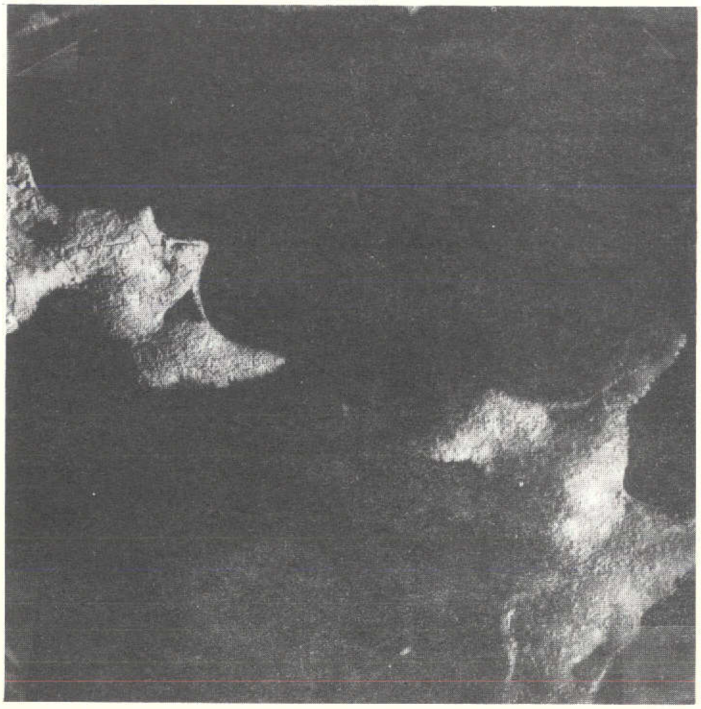

Figure 4-30. 0.74 - .90 micron Aircraft Photography
St. James Bay

3) Cloud Location was best determined through use of CCT computer dumps of MSS band 5

4) Determination of CCT MSS Values from Computer Printouts required blanking out of all values from 53 to 127 and printing only values from 0 to 52. Where resultant printouts showed blank areas, those areas were classified as being in the higher energy range and examined in detail where necessary (i.e., Brewers Beach). This process was mandatory since, for example, under the NASA mapping scheme on "E" could represent either 18 or 67. If blanking out of upper level showed no "E's" these were read as 18.

5) ERTS-1 Imagery was used for reference primarily.* MSS data was extracted from the CCT tape by computer for correlation with in situ and aircraft data.

6) Comparison of Precision and Bulk CCT Data revealed precision data to be significantly superior in terms of local geographical resolution. (i.e., a ± 1 element positional, error in Bulk CCT's was observed). Use of Bulk CCT's necessitated cluster averaging; namely, determining the average radiance of a group of cells in the subject area. Care, however, must be exercised when the value of one element varied sharply from the value of other group cells. (See discussion in Section 4.3.7).

7) Graphics Data Summaries for both satellite and in situ data played the major role in data handling. Measurement listings were utilized primarily to extract data points to be utilized in performing correlations.

8) Utilization of 80 Column In Situ Logs are recommended. Their use prevents the necessity of having to transfer boat data listings to 80 column computer keypunch forms.

9) Determination of bulk MSS CCT values for specific geographical areas may be achieved via construction of a transparent grid overlay to a standard map. (Reference Figure 4-31).

   The overlay shown was generated through use of band 7 computer printouts to locate sharp land-water interface points with respect to satellite track and cross track CCT printout lines. The number of pixels versus ground distance, as measured on a map, yielded the ground distance per pixel and permitted construction of an overlay with grid lines that correlated directly to computer print lines.

*Discussed in Report Section II by Dr. Egan.

4.5 DATA TABULATION

4.5.1 In Situ Boat Data Log-Keypunch Compatible

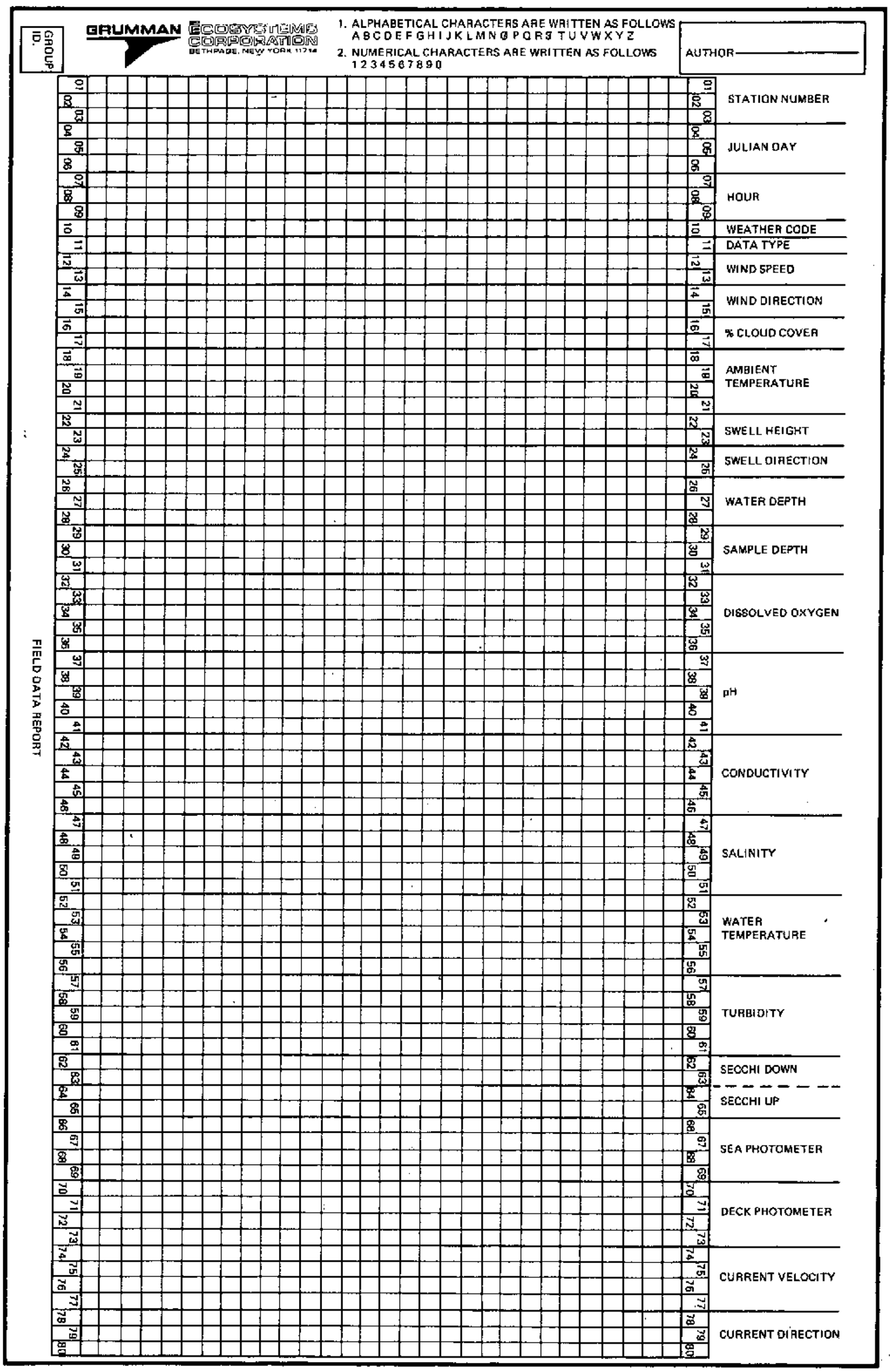

GROUP ID.

GRUMMAN ECOSYSTEMS CORPORATION
BETHPAGE, NEW YORK 11714

1. ALPHABETICAL CHARACTERS ARE WRITTEN AS FOLLOWS
A B C D E F G H I J K L M N O P Q R S T U V W X Y Z
2. NUMERICAL CHARACTERS ARE WRITTEN AS FOLLOWS
1 2 3 4 5 6 7 8 9 0

AUTHOR

FIELD DATA REPORT

STATION NUMBER
JULIAN DAY
HOUR
WEATHER CODE
DATA TYPE
WIND SPEED
WIND DIRECTION
% CLOUD COVER
AMBIENT TEMPERATURE
SWELL HEIGHT
SWELL DIRECTION
WATER DEPTH
SAMPLE DEPTH
DISSOLVED OXYGEN
pH
CONDUCTIVITY
SALINITY
WATER TEMPERATURE
TURBIDITY
SECCHI DOWN
SECCHI UP
SEA PHOTOMETER
DECK PHOTOMETER
CURRENT VELOCITY
CURRENT DIRECTION

4.5.2 Computed MSS Values Per Water Quality Station

PRECISION TAPE VALUES MSS BAND 4

STATION NUMBER	CLUSTER AV.	CENTER ELEMENT	STATION NUMBER	CLUSTER AV.	CENTER ELEMENT
2	25.33	26	34	25.00	24
3	23.22	23	35	25.66	25
4	25.22	25	36	35.44	38
5	30.11	30	37	27.77	28
6	28.00	26	38	29.11	30
7	25.55	26	39	28.22	31
8	33.44	34	40	29.11	31
9	30.33	31	41	28.11	28
10	27.33	26	42	24.11	25
11	37.44	35	43	25.11	25
12	36.33	35	44	26.88	25
13	26.88	26	45	28.66	30
14	26.66	26	46	25.00	25
15	26.55	26	47	23.44	22
16	24.44	25	48	29.11	31
18	26.66	27	49	25.11	24
19	28.77	28	50	27.33	28
20	32.22	32	51	30.00	31
21	36.22	36	52	27.55	28
22	38.77	39	53	25.44	24
23	37.33	35	54	28.22	26
24	30.88	31	55	23.88	22
25	32.66	31	56	23.11	23
26	23.88	24	57	24.88	25
27	28.22	29	58	24.55	24
28	29.88	28	59	27.22	26
29	32.11	32	60	24.66	25
30	29.00	28	61	24.33	23
31	28.77	27	101	31.77	32
32	31.22	32	102	34.00	31
33	28.33	28	103	37.22	38

PRECISION TAPE VALUES MSS BAND 4 (Continued)

STATION NUMBER	CLUSTER AV.	CENTER ELEMENT	STATION NUMBER	CLUSTER AV.	CENTER ELEMENT
104	44.33	42	119	30.44	32
105	43.44	47	120	24.88	24
106	37.88	37	121	23.44	22
107	32.22	31	123	29.22	27
108	29.33	29	124	28.44	28
109	28.77	29	125	33.44	33
110	25.55	25	126	29.55	29
111	26.62	26	127	28.22	29
112	26.55	25	128	31.55	32
113	24.33	23	129	27.33	26
114	24.88	25	130	31.00	32
115	23.44	24	131	28.44	28
116	27.11	27	132	36.88	36
117	26.88	30	133	33.00	34
118	26.22	26	134	34.55	35

STATION # vs COMPUTER PRINTOUT LOCATION
BULK PROCESSED CCT DATA (BANDS 4, 5, 6, & 7)

STN.	COMPUTER AREA	STN.	COMPUTER AREA
2	1605--852	31	1594--917
3	1635--861	32	1592--930/31 (centroid of 2 horiz. elements)
4	1614--861/862 (centroid of 2 horiz. elements)	33	1590--946/47 (centroid of 2 horiz. elements)
5	1602--863/64 (centroid of 2 elements)	34	1610/11--850/51 (centroid of 4 elements)
6	1604--871	35	1608/09--865/66 (centroid of 4 elements)
7	1611--889	36	1609/10--879/80 (centroid of 4 elements)
8	1602--893	37	1605--887
9	1595/96--912/13 (centroid of 4 elements)	38	1604--899
10	1607--924	39	1601--919
11	1585/86--923/924 (centroid of 4 elements)	40	1600--928
12	1581--938	41	1597--948
13	1595--944	42	1619--852
14	1605--935	43	1617--868
15	1604--945	44	1615/16--880/81 (centroid of 4 elements)
16	1618--968	45	1612--906
18	1597--847	46	1606/07--950/951
19	1597--853	47	1626--854
20	1596--866	48	1624--870
21	1591--900	49	1622--882/83 (centroid of 2 horiz. elements)
22	1588--920	50	1618/19--907/08 (centroid of 4 elements)
23	1583--928	51	1617--923
24	1587/88--929/30 (centroid of 4 elements)	52	1615--937
25	1583--944	53	1613--952
26	1603--848	54	1611--966
27	1601--867	55	1632--856
28	1600--873	56	1630--872
29	1597--893		
30	1596--902		

STATION # vs COMPUTER PRINTOUT LOCATION BULK PROCESSED CCT DATA (BANDS 4, 5, 6, & 7) (Continued)

STN.	COMPUTER AREA	STN.	COMPUTER AREA
57	1628--884	60	1622--939
58	1626--909	61	1620--954
59	1623--925		

SATELLITE VALUES - PIGMENT SAMPLE STATIONS
(CLUSTER AVERAGES)

STATION NO.	MSS 4 BULK	MSS 5 BULK
123	25.00	9.20
124	31.00	9.80
125	29.00	9.00
126	32.00	10.40
127	28.00	9.50
128	23.50	8.75
129	20.40	8.40
130	23.00	9.50
131	25.00	10.00
132	30.00	12.20
133	27.50	11.25
135	CLOUDS	CLOUDS

ERTS 1 MSS BAND 4
(BULK CCT)

STN.		AV.
(2)	24 24-24-24 23	23.8
(3)	20 21-20-20 21	20.2
(4)	19-21	20.0
(5)	27-24	25.5
(6)	25 25-25-25 25	25.0
(7)	24 24-24-25 23	24.0
(8)	27 27-25-25 25	24.8
(9)	29-31 32-28	30.0
(10)	23 25-25-21 24	23.6
(11)	31-32 28-29	32.5
(12)	32 32-31-31 29	31.0

ERTS 1 MSS BAND 4

(BULK CCT) (Continued)

STN.		AV.
(13)	28 27-25-27 24	26.2
(14)	28 32-31-28 26	29.0
(15)	21 24-24-25 25	23.8
(16)	21 21-21-19 20	20.4
(18)	21 21-21-21 20	20.8
(19)	24 25-25-23 21	23.6
(20)	30 27-27-25 30	27.8
(21)	31 32-29-29 31	30.4
(22)	27 26-23-23 25	24.8
(23)	31 28-30-30 27	29.2
(24)	25 24 23 26	24.5
(25)	31 30-28-28 27	28.8

STN.		AV.
(26)	21 21-21-23 20	21.2
(27)	26 27-25-27 24	25.8
(28)	27 26-26-29 28	27.2
(29)	31 33-32-32 31	31.8
(30)	30 31-31-31 33	31.2
(31)	31 31-31-29 30	30.4
(32)	25-24	24.5
(33)	32	
(34)	24 21 24 24	23.25
(35)	24 23 23 23	23.25
(36)	25 25 25 25	25.0
(37)	31 28-27-25 23	26.8
(38)	29 31-28-28 28	28.8
(39)	26 28-25-25 25	25.8

ERTS 1 MSS BAND 4
(BULK CCT) (Continued)

STN.		AV.	STN.		AV
(40)	27 23-26-26 27	25.8	(52)	21 23-21-21 21	21.4
(41)	21 25-25-21 27	23.8	(53)	23 28-21-21 21	22.8
(42)	22 21-21-23 21	21.6	(54)	28 25-27-24 23	25.4
(43)	24 21-21-21 22	21.8	(55)	20 21-19-21 20	20.2
(44)	23-23 21-24	22.75	(56)	22 26-26-23 25	24.4
(45)	32 31-29-28 30	30.0	(57)	21 20-21-20 22	20.8
(46)	26-26 25-23	25.0	(58)	21 21-23-21 21	21.4
(47)	21 19-21-21 21	20.6	(59)	24 22-22-22 22	22.4
(48)	22 21-21-21 20	21.0	(60)	23 20-21-20 20	20.8
(49)	21-21	21.0	(61)	20 19-19-21 21	20.0
(50)	26-26 25-23	25.0			
(51)	21 21-21-21 21	21.0			

BULK CCT VALUES
MSS 4, 5, 6, 7, - 17 OCTOBER

STATION NO.	MSS 7	MSS 6	MSS 5	MSS 4
	16	7	26	40
101	8-6-9	9-8-7	17-22-23	35-39-39
	4	7	14	32
	6	8		
102*	3-4-5	7-7-7	17-22-23	32-32-32
	1	5	14	31
	5	7	13	32
103	1-0-1	5-5-5	12-13-12	31-31-29
	1	5	12	28
	0	5	13-11-13	32-31-31
104*	0-1-1	5-5-5	13-12-12	31-29-28
	1	5	12-12-12	28-28-27
	1	5	12	28
105	1-0-1	5-6-5	11-10-10	25-25-27
	1	6	10	27
	1	5	10-11-11	27-27-27
106*	1-1-1	6-6-6	10-11-11	27-27-27
	1	5	10-10- 9	27-27-25
	1	6	10-11-11	27-27-27
107*	1-1-1	5-6-5	10-11-11	27-27-27
	1	3	10-11- 9	27-27-25
	1	3	9	28
108	0-0-0	5-4-5	10-10-10	25-27-27
	1	5	10	27
	1	6	10-10-11	25-25-25
109*	0-1-0	7-7-7	10-10-11	27-28-27
	1	5	10-10-11	25-27-27
	1	5	10-10-11	25-25-25
110*	1-1-1	5-6-6	10-10-11	27-28-27
	0	6	10-10-11	25-27-27
	1	4	10	28
111	0-1-0	5-4-5	10-10-10	25-27-27
	0	4	9	19
	1	6	9-9-9	19-21-24
112*	0-0-1	5-6-5	9-9-7	19-19-20
	1	6	9-8-6	19-20-19
	1	5	8	19
113	0-0-0	5-5-8	9-9-10	20-20-21
	1	13	9	19

*In situ optical data available for these stations. Ref: Section 4.5.3

BULK CCT VALUES
MSS 4, 5, 6, 7, - 17 OCTOBER (Continued)

STATION NO.	MSS 7	MSS 6	MSS 5	MSS 4
	4	24	17	31
114	1-5-4	13-16-35	10-11-10	21-27-28
	2	19	9	25
	1	43	11-10-15	27-28-32
115*	1-2-2	9-22-43	9-10-12	25-25-25
	1	21	9- 8-10	25-24-24
	1	40	10	25
116	1-1-1	10-9-8	11-11-11	24-25-24
	1	7	15	32
	1	8	10	25
117	1-2-1	7-9-9	20-11-9	36-27-24
	2	6	11	27
	1	6	9	24
118	2-0-0	3-3-4	10-9-9	23-21-21
	1	3	8	21
	0	4	9-9-8	19-19-19
119*	0-0-1	6-5-5	9-9-9	21-21-23
	0	6	8-9-10	20-21-20
	0	6	9-9-8	19-19-19
120*	0-0-0	3-4-4	9-9-9	21-21-23
	0	4	8-9-10	20-21-20
	1	4	9	21
121	0-1-0	5-5-5	9-9-9	20-20-20
	1	4	9	20
	1	4	8	20
122	1-0-0	4-5-4	9-9-9	18-18-18
	0	4	9	20

*In situ optical data available for these stations. Ref: Section 4.5.3

ERTS 1 MSS BAND 5
(BAND CCT)

STN.		AV.	STN.		AV.	STN.		AV.
(2)	9 10-10-8 10	9.40	(18)	9 9-9-9 9	9.00	(32)	10-10	10.0
(3)	8 9-9-9 10	9.00	(19)	11 10-10-10 11	10.4	(33)	28-43	N/A
(4)	9-8	8.50	(20)	9 10-10-10 10	9.80	(34)	10-10 9-9	9.50
(5)	9-9	9.00	(21)	11 12-11-11 10	11.00	(35)	9-9 9-9	9.00
(6)	9 9-9-9 10	9.20	(22)	15 14-13-13 14	13.80	(36)	9-9 8-10	9.00
(7)	9 9-8-8 9	8.60	(23)	13 12-12-13 11	12.20	(37)	10 10-9-9 9	9.40
(8)	8 10-9-10 9	9.20	(24)	9-10 9-9	9.25	(38)	10 9-9-10 9	9.40
(9)	10-10 11-10	10.22	(25)	13 12-12-13 11	12.20	(39)	10 10-10-9 9	9.60
(10)	9 10-10-10 14	10.60	(26)	8 10-10-9 9	9.20	(40)	11 9-9-9 10	9.60
(11)	11-11 18-18	14.50	(27)	9 9-9-9 9	9.00	(41)	9 9-9-9 9	9.00
(12)	13 13-11-13 12	12.40	(28)	10 10-10-10 10	10.00	(42)	8 8-9-8 9	8.40
(13)	10 10-10-13 9	10.40	(29)	11 11-11-10 10	10.60	(43)	8 8-9-9 9	8.60
(14)	13 15-13-11 12	12.80	(30)	10 10-11-10 11	10.40	(44)	7-7 8-9	7.75
(15)	9 9-9-9 8	8.80	(31)	10 9-10-10 10	9.80	(45)	15 14-9-8 9	11.00
(16)	9 9-9-9 9	9.00				(46)	10-10 10-10	10.00
						(47)	8 8-8-9 9	8.40

NOTE: Underlined elements suspect of cloud interference. Not utilized in average calculations.

ERTS 1 MSS BAND 5
(BULK CCT) (Continued)

STN.		AV.	STN.		AV.
(48)	9 9-9-8 8	8.60	(55)	8 9-9-9 9	8.80
(49)	9-8	8.50	(56)	8 9-10-10 10	9.40
(50)	9-9 9-8	8.75	(57)	9 8-8-8 9	8.40
(51)	9 8-9-9 8	8.60	(58)	9 10-9-10 10	9.60
(52)	10 9-10-10 9	9.60	(59)	13 9-9-9 9	9.80
(53)	10 16-9-8 9	9.00	(60)	9 9-8-9 8	8.60
(54)	9 9-9-8 8	8.60	(61)	9 9-10-9 9	9.20

NOTE: Underlined elements suspect of cloud interference. Not utilized in average calculations.

4.5.3 Transect Data (Boat, Aircraft, Satellite)

	1) In-Situ GREEN cm^{-1}	2) In-Situ RED cm^{-1}	3) Aircraft GREEN ∝ brightness	4) Aircraft RED ∝ brightness	5) Precision MSS 4 (low) $MW/cm^2 - S R$	6) Bulk MSS 4 (low) $MW/cm^2 - S R$	7) Bulk MSS4 (mid) $MW/cm^2 - S R$	8) Bulk MSS 4 (high) $MW/cm^2 - S R$	9) Bulk MSS 5 (low) $MW/cm^2 - S R$	10) Bulk MSS 5 (mid) $MW/cm^2 - S R$	11) Bulk MSS 5 (high) $MW/cm^2 - S R$	12) TURBIDITY FTU*	13) CHLOROPHYLL A MC/M^3	14) TOTAL CHLOROPHYLL MC/M^3	15) PIGMENT DIVERSITY (NITS)****	16) TOTAL CAROTENOIDS MSPU**	17) Bulk MSS 4 Uncorrected (QV)***	18) Bulk MSS 5 Uncorrected (QV)***	19) Bulk MSS 4 Centroid, Uncorrected (QV)***	20) Bulk MSS 5 Centroid, Uncorrected (QV)***	21) Chlorophyll C	22) Bulk MSS 6 (QV)***
102	.0140	.0190	.1550	.200	.2293	.1924	.2060	17.2197	.1313	.1426	.1533	3.20	1.565	44.094	1.529	1.963	31.75	19.00	32	22	1.5793	6.25
104	.0140	.0190	.1340	.195	.3603	.1620	.1754	.1885	.0613	.0708	.0803	1.80	2.830	5.249	1.468	2.281	29.44	12.22	29	12	1.4714	5.0
106/107	.0140	.0190	.1110	.167	.2238	.1274	.1403	.1531	.0416	.0515	.0613	1.050	4.732	23.715	1.462	8.338	26.78	10.33	27	11	14.0874	5.78
109/110	.0044	.0066	.1080	.166	.1323	.1205	.1332	.1459	.0416	.0514	.0613	.90	3.4915	17.964	1.429	6.645	26.22	10.33	28	10	11.3267	5.0
112	.0030	.0052	.1030	.149	.1245	.1208	.1335	.1463	.03715	.04692	.05692	.70	1.376	2.886	1.443	1.310	26.25	9.88	25	10	1.0224	4.89
115	.0019	.0047	.0073	.108	.0860	.1013	.1135	.1260	.03524	.04499	.05474	.18	.409	1.308	1.501	.446	24.67	9.67	25	10	.5237	6.39
119/120	.0019	.0041	.0615	.111	.1386	.04907	.0609	.0728	.0277	.0374	.0470	.14	.0342	.034	1.199	.110	20.33	8.89	21	9	.000	4.44

*FORMAZIN TURBIDITY UNIT
**MILLI SPECIAL PIGMENT UNIT
***QUANTUM VALUE (0-127)
****NATURAL LOG BASE

FOLDOUT FRAME 1

FOLDOUT FRAME 2

4.5.4 Similar Tidal Periods - St. Thomas Harbor

Julian Day	Time
284	1500-2000
285	1800-2300
289	0500-1000
290	0700-1200
291*	0800-1300
292	0800-1300
293	0900-1400
294	1000-1500
295	0400-1000
296	0800-1200
297	0000-1200
298	0200-1300
299	0200-1400
300	0800-1600
304	0800-1200
305	0800-1300
306	1000-1400
307	1100-1400
308	1200-1600
309	1200-1600
310	1200-1800
311	1400-1800
312	1400-1800
313	1000-2000
318	0700-1000
319	0700-1100
320	0800-1200
321	0900-1300
322	1000-1400
323	1100-1600
324	1200-1700

*Day of ERTS 1 Overpass

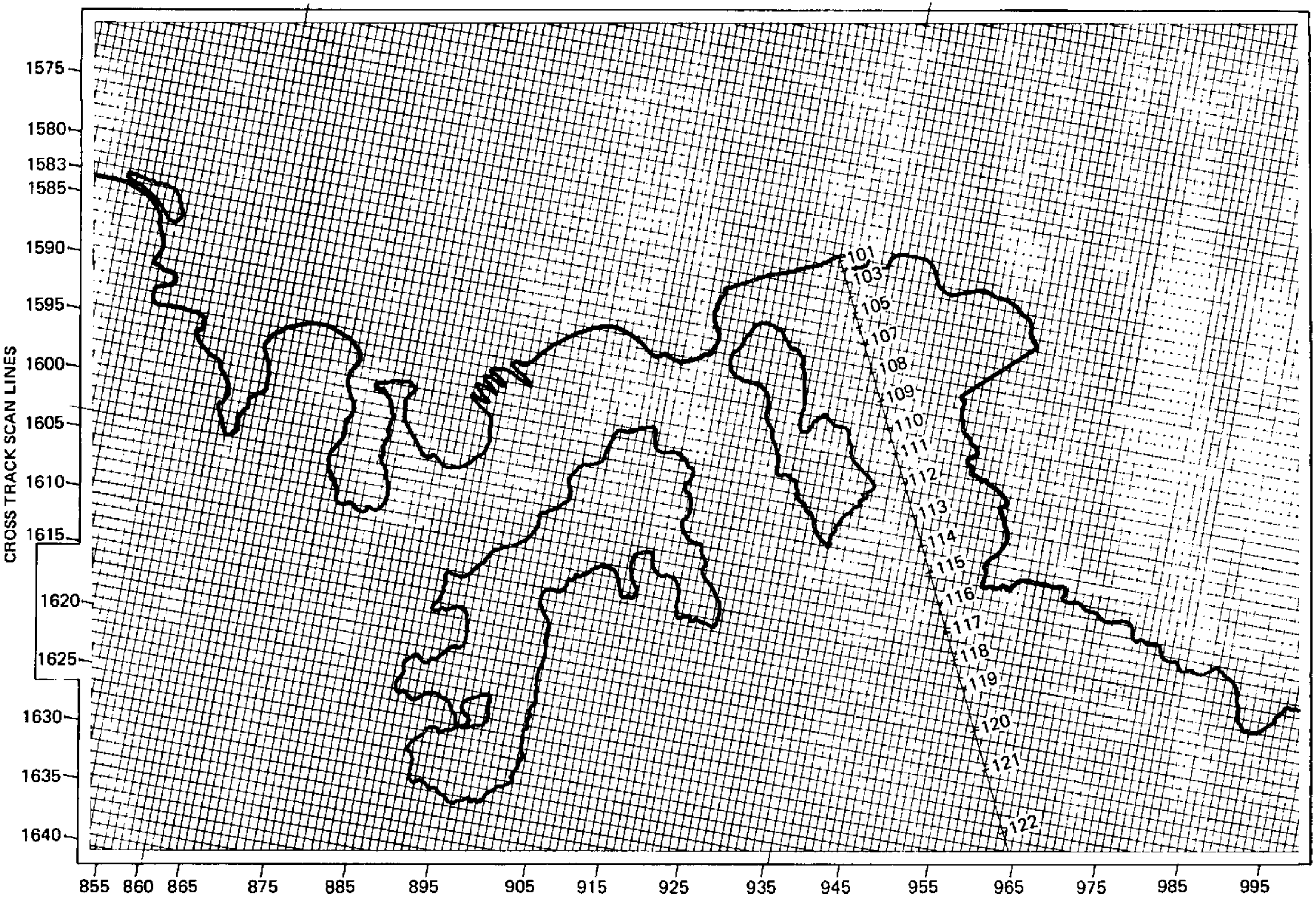

Figure 4.31. Along Track Scan Lines Bulk CCT Computer Printout Grid, Scene 1086-14162 Scaled to Match C&GS Chart 933, St. Thomas, V.I.

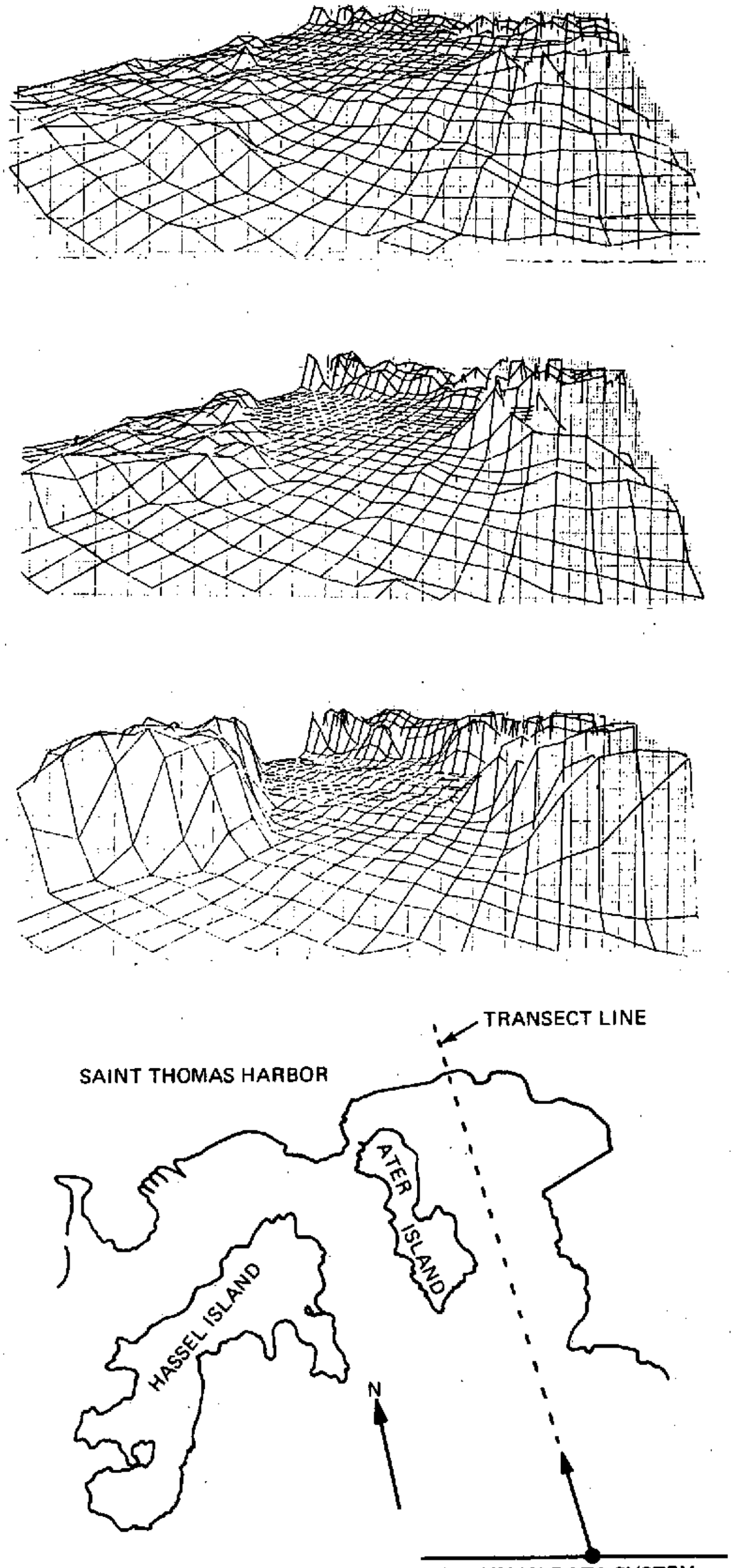

Figure 4-32. Saint Thomas Harbor ERTS 'A' Bulk Computer Data Viewing Angle From South to North Along Transect

ACKNOWLEDGEMENTS

Grateful thanks to all those participating individuals whose sincere interest, and personal contributions to this project have resulted in the development of data handling procedures and techniques which, we believe, will be useful to future investigators is hereby acknowledged. In particular, Mr. Richard Quinn (Senior Systems Programmer) responsible for boat in situ and ERTS CCT Processing, and Mr. Thomas Gilmartin (Applications Programmer), responsible for current meter and thermal line scanner data handling, jointly have enabled the production of those primary data products discussed in this report. Also, Mr. Robert Skirkanich (Senior Science System Analyst) with assistance from Mr. Joseph Trubisz (Associate Programmer) applied special computer analysis techniques to primary analog and digital products. Mr. Skirkanich also assisted in the original proposal effort.

Mr. William Ratchford (Assistant Director - Applications Software Development Department for assistance in both obtaining and scheduling the manpower and computer resolution utilized for this ERTS-1 Experiment.